UNIVERSITÉ DE STRASBOURG

THÈSE présentée par :

Christian LANSHOEFT

soutenue le : **08 Décembre 2017**

pour obtenir le grade de : **Docteur de l'université de Strasbourg**

Discipline / Spécialité : Chimie Analytique

Generic mass spectrometric workflows for mAb-related therapeutic protein quantification in pre-clinical species

Développement de nouvelles approches génériques de spectrométrie de masse pour la quantification de protéines thérapeutiques dans des études précliniques

THÈSE dirigée par :

Dr. CIANFÉRANI Sarah   Directrice de Recherche, CNRS, Université de Strasbourg

RAPPORTEURS :

Pr. Dr. BISCHOFF Rainer   Professeur des universités, Université de Groningue

Pr. Dr. HUBER Christian G.   Professeur des universités, Université de Salzbourg

AUTRES MEMBRES DU JURY :

Dr. BRUN Virginie   Principle Investigator, CEA Grenoble

Dr. BECK Alain   Senior Director, Centre d'Immunologie Pierre Fabre

Dr. HEUDI Olivier   Senior Investigator, Novartis Institutes for Biomedical Research

"Nothing has such power to broaden the mind as the ability to investigate systematically and truly all that comes under thy observation in life."

- Marcus Aurelius

Abbreviations

ACN	acetonitrile
ADA	anti-drug antibody
ADC	antibody-drug conjugate
ADCC	antibody-dependent cell-mediated cytotoxicity
ADCP	antibody-dependent cell-mediated phagocytosis
ASMS	American Society for Mass Spectrometry
(b)-mAb$_{capture}$	(biotinylated) mouse anti-hIgG Fc capture antibody
BSA	bovine serum albumin
bsAb	bispecific antibody
C1q	complex of complement system
CDC	complement-dependent cytotoxicity
CDR	complementarity-determining region
C_H	constant domain of heavy chain
C_L	constant domain of light chain
Cs	calibration standards
CV	coefficient of variance
D	deglycosylation
D.A.R.T.'S	disposable automated research tips
DAR	drug-to-antibody ratio
DLD	drug load distribution
DTT	dithiothreitol
E	elution
e.g.	*exempli gratia*
ELISA	enzyme-linked immunosorbent assay
EMA	European Medicines Agency
EU	European Union
FA	formic acid
Fab	fragment antigen binding

Fc	fragment crystallizable
FcRn	neonatal fragment crystallizable receptor
FcγR	fragment crystallizable gamma receptor
FDA	Food and Drug Administration
FNW	FNWYVDGVEVHNAK (tryptic peptide)
FNWd	deamidated FNW peptide
GlcNac	N-acetylglucosamine
GLP	good laboratory practice
GPS	GPSVFPLAPSSK (tryptic peptide)
H	heavy chain
hIgG	human immunoglobulin G
HRMS	high-resolution mass spectrometry
i.e.	*id est*
IAA	iodoacetamide
IC	immuno-capture
Ig	immunoglobulin
IG	immunogenicity
IgG	immunoglobulin G
ISTD	internal standard
LBA	ligand binding assay
L	light chain
LC	liquid chromatography
LLOQ	lower limit of quantification
m/z	mass-to-charge ratio
mAb	monoclonal antibody
MRM	multiple reaction monitoring
MS	mass spectrometry
MS/MS	tandem mass spectrometry
MSIA	mass spectrometric immunoassay
MXW	mass extraction window

PBS	phosphate buffered saline
PD	pharmacodynamic
PK	pharmacokinetic
PNGase F	N-glycosidase F
Q	quadrupole
QC	quality control
qHRMS	quantitative high-resolution mass spectrometry
QqQ	triple quadrupole
QTRAP	quadrupole linear ion trap
r^2	coefficient of determination
scFv	single chain variable fragment
SIL	stable isotope labeled
SISCAPA	stable isotope standards and capture by anti-peptide antibodies
S/N	signal-to-noise
SRM	selected reaction monitoring
SPE	solid phase extraction
TFA	trifluoroacetic acid
TOF	time-of-flight
TTP	TTPPVLDSDGSFFLYSK (tryptic peptide)
ULOQ	upper limit of quantification
US	United States of America
V_H	variable domain of heavy chain
V_L	variable domain of light chain
VVS	VVSVLTVLHQDWLNGK (tryptic peptide)
VVSd	VVSVLTVLHQDWLDGK (deamidated VVS peptide)
XIC	extracted ion chromatogram

Acknowledgements

Table of contents

Résumé de la thèse

Introduction

Parmi les protéines thérapeutiques, les anticorps monoclonaux (mAbs) et leurs produits dérivés, tels que les immuno-conjugués (ADCs, *antibody-drug conjugates*) ou les anticorps bispécifiques (bsAbs) se sont imposés comme l'une des classes de molécules thérapeutiques à croissance rapide, représentant un chiffre d'affaire global de 107 milliards de dollars US en 2016 (Figure 1).[1] Afin de soutenir le développement de ces molécules très complexes, des outils analytiques quantitatifs, robustes et validés sont nécessaires pour l'évaluation de leur pharmacocinétique (PK), pharmacodynamique et immunogénicité. La spectrométrie de masse (MS) a évolué au cours de la dernière décennie et se positionne maintenant comme technologie analytique complémentaire aux tests immuno-enzymatiques (ELISA, *enzyme-linked immunosorbent assay*) pour la quantification de mAb dans des matrices biologiques complexes.[2] En raison de la taille des mAbs et de leurs produits dérivés (approximatif 150 kDa) et des exigences de sensibilité des méthodes analytiques à développer, des peptides de substitution (*surrogate peptides*), résultant de la digestion protéolytique des mAbs, sont classiquement utilisés pour la quantification de mAbs par chromatographie en phase liquide couplée à la spectrométrie de masse en tandem MS (LC-MS/MS). Ces surrogate peptides sont souvent choisis dans la région complémentaire (CDR, *complementarity-determining region*) des mAbs et lui sont donc très spécifiques, mais imposent un nouveau développement de méthode pour chaque nouveau mAb. Afin de contourner cette limitation, des méthodes génériques basées sur des approches LC-MS/MS utilisant des peptides de la région constante (C_L, C_H1, C_H2 et C_H3) ont récemment été rapportées pour la quantification de mAbs dans des études précliniques.[3,4] Le but de ce travail de thèse a été de développer de
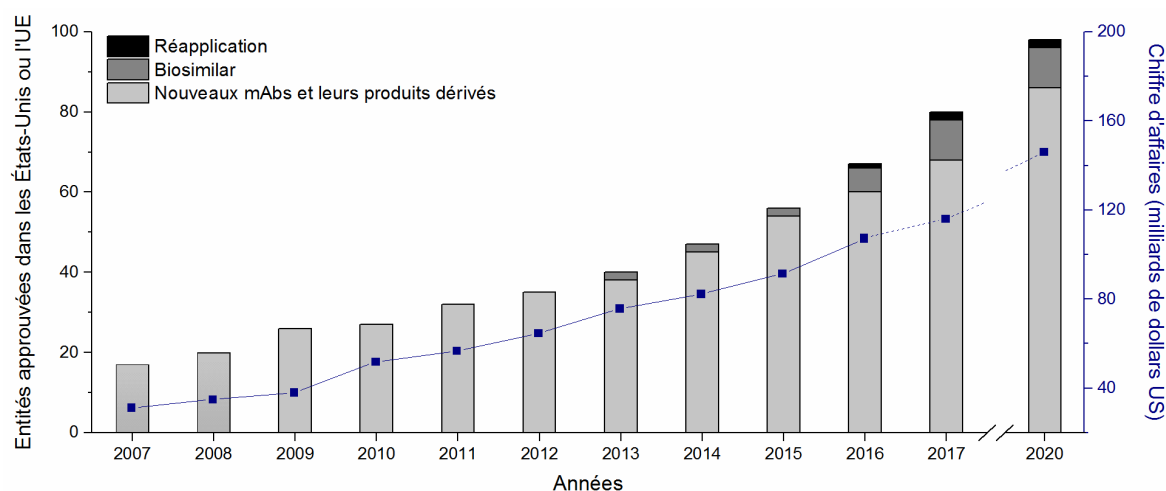
Figure 1 Évolution du marché des mAbs et leurs produits dérivés aux États-Unis et dans l'UE au cours de la dernière décennie et chiffre d'affaires global déclaré.

nouvelles approches de MS quantitatives plus génériques pour la quantification d'immuno-globulines (Igs) chimériques, humanisées et humaines (hIgG) ainsi que des anticorps de nouvelle génération de type bispécifiques et immuno-conjugués dans des échantillons précliniques (Figure 2).
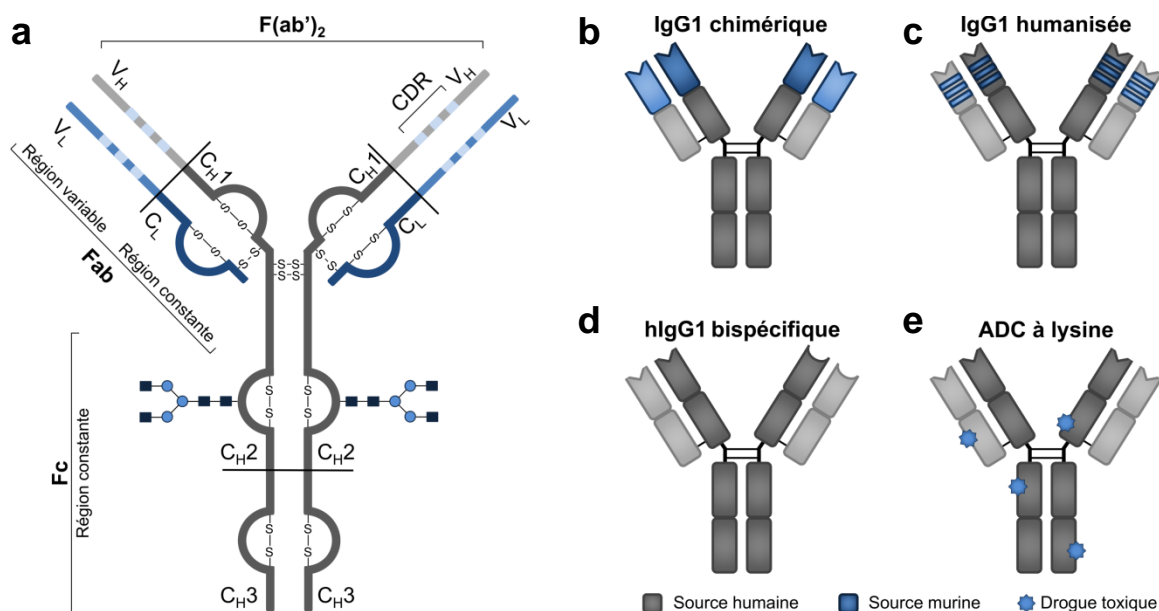
Figure 2 Représentation de différentes protéines thérapeutiques liées aux anticorps monoclonaux. (**a**) Structure détaillée d'une hIgG1 et autres formats dérivés tel que: (**b**) une IgG1 chimérique, (**c**) une IgG1 humanisée, (**d**) une hIgG1 bispécifique, (**e**) un ADC à lysine.

Première partie - Bibliographie

La première partie de cette thèse est un travail bibliographique qui fournit une brève introduction sur les IgGs, y compris leurs structures, leurs glycanes et leurs fonctions effectrices. De plus, la diversité des mAbs et leurs produits dérivés sont présentés ainsi que leur enjeu socio-économique dans le monde au cours de ces dix dernières années. Cette partie bibliographique présente également les diverses techniques biophysiques et approches analytiques qui sont implémentées tout au long du processus de développement de ces molécules. Les méthodes quantitatives de type ELISA ou celles basées sur la MS sont décrites ainsi que les exigences des institutions de régulation pour la validation d'une méthode analytique. Les chapitres suivants sont consacrés aux principaux résultats obtenus avec une discussion propre à chaque chapitre.

Deuxième partie - Développement des méthodologies LC-MS/MS bottom-up quantitatives et polyvalentes pour la quantification de mAbs et produits dérivés dans des sérums

Dans la deuxième partie de la thèse, on s'est d'abord attelé à améliorer les protocoles de préparation d'échantillons, en amont de l'analyse *"bottom-up"* (après digestion enzymatique) MS quantitative, à partir de sérum dans un contexte d'études précliniques. Dans le cadre de la thèse, trois axes d'amélioration ou de développement pour la préparation d'échantillon ont été étudiés: (i) une méthode de préparation d'échantillon basée sur la digestion directe de culots protéiques à partir de sérum, (ii) l'utilisation de kits de digestion permettant d'envisager une standardisation de cette étape cruciale et (iii) le développement d'une méthode de préparation d'échantillon basée sur une étape d'immuno-précipitation spécifique par anticorps (IC, *immuno-capture*).

Mise au point de la méthode LC-MS/MS générique à partir de digestion directe du culot protéique de sérum

Une méthode LC-MS/MS basée sur une digestion directe du culot de sérum (Figure 3a) et la quantification à partir de quatre surrogate peptides trypsiques génériques, à savoir FNWYVDGVEVHNAK (FNW), GPSVFPLAPSSK (GPS), TTPPVLDSDGSFFLYSK (TTP) et VVSVLTVLHQDWLNGK (VVS), provenant de différentes parties de la région constante du mAb a d'abord été développée et validée. Cette méthode a permis la quantification d'un mAb de type hIgG1 dans du sérum de rat sur la gamme dynamique de 1.00 à 1000 µg/mL. Des échantillons de sérum de singe dopés avec cet hIgG1 ont ensuite été quantifiés à partir d'une courbe d'étalonnage préparée avec l'hIgG1 dans le sérum de rat avec une justesse (±20.0% de biais) et
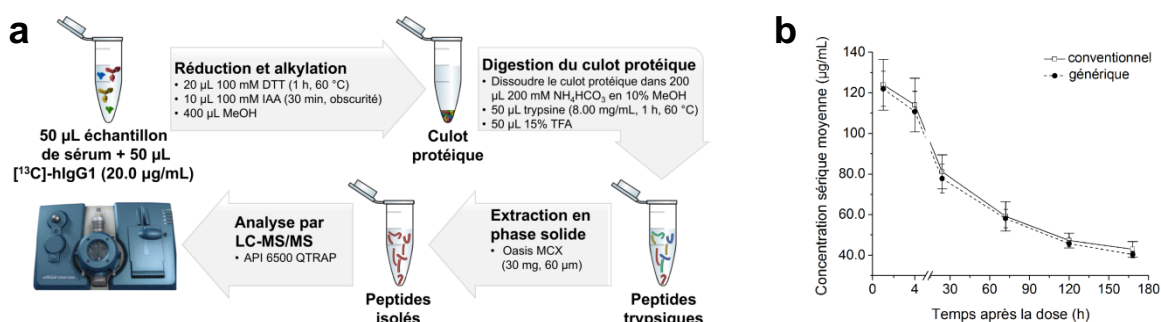
Figure 3 Les différentes étapes de la méthode LC-MS/MS générique. (**a**) Description de la préparation des échantillons. (**b**) Evolution de la concentration sérique moyenne déterminée à partir d'échantillons provenant de trois singes ayant reçus une dose d'ADC. Les mesures ont été réalisées soit avec la méthode conventionnelle (ADC dans sérum de singe), soit avec la méthode générique (hIgG1 dans sérum de rat).

une précision [≤20.0% de coefficient de variation (CV)] en accord avec les exigences des instances réglementaires. L'incorporation d'une protéine marquée ([^{13}C]-hIgG1) comme étalon interne au début de la préparation d'échantillon a permis d'atténuer l'effet matrice ainsi que l'interchangeabilité du sérum (rat/singe). La polyvalence et la robustesse de la méthode LC-MS/MS quantitative ainsi développée sur un sérum de rat a été illustrée par la quantification dans des sérums de singe pour différents types de mAbs (deux autres hIgG1, une hIgG4, un bsAb et deux ADC à lysine). Il a ensuite été démontré que la méthodologie ainsi développée permet l'analyse d'échantillons PK *in vivo* (Figure 3b), du fait de la conservation des peptides génériques dans les différents formats de mAbs étudiés. Par conséquent, ce travail de thèse a permis de mettre en évidence le fort degré de flexibilité/polyvalence de la méthode développée, permettant non seulement le passage d'une espèce à l'autre mais aussi d'un type de molécule à l'autre.

Evaluation de la standardisation de l'étape de digestion trypsique par l'utilisation de kits commerciaux

Étant donné que les réactifs et les différentes étapes de préparation des échantillons peuvent influencer la performance globale d'une analyse bottom-up, des kits de digestion ont été développés, afin de permettre une standardisation de la préparation des échantillons. Dans le cadre de cette thèse, deux kits, à savoir le *SMART Digest Kit* (Thermo Fisher Scientific) et le *ProteinWorks eXpress Digest Kit* (Waters), ont été comparés au protocole de digestion à partir du culot protéique pour la quantification d'hIgG1 sur des échantillons de sérum de rat. Des résultats très similaires ont été obtenus en termes de sélectivité, de sensibilité, de justesse et de précision indépendamment du peptide générique sélectionné et du kit testé (Tableau 1).

Tableau 1 Comparaison (linéarité, rapport signal/bruit, justesse et précision) entre digestion directe du culot de sérum et deux kits de digestion pour la quantification d'hIgG1 dans de sérum de rat.

Peptide	Paramètres	Digestion du culot protéique	SMART Digest Kit	ProteinWorks eXpress Digest Kit
FNW	Gamme (µg/mL), r^2-valeur (n=3)	1.00-1000, 0.9929	5.00-1000, 0.9898	5.00-1000, 0.9941
	Rapport signal/bruit (n=3)	8.3±1.1	4.8±0.8	13.0±0.6
	Inter-essais justesse (% de biais, n=9)	de -2.4 à 4.3	de -3.4 à 0.6	de -5.9 à -2.5
	Inter-essais précision (% de CV, n=9)	de 6.6 à 9.9	de 4.6 à 11.3	de 3.5 à 6.6
GPS	Gamme (µg/mL), r^2-valeur (n=3)	1.00-1000, 0.9940	1.00-1000, 0.9970	1.00-1000, 0.9921
	Rapport signal/bruit (n=3)	3.5±0.2	3.3±0.1	3.8±0.6
	Inter-essais justesse (% de biais, n=9)	de -8.3 à 4.6	de -6.6 à 2.0	de -9.9 à -2.2
	Inter-essais précision (% de CV, n=9)	de 4.7 à 5.4	de 6.1 à 7.7	de 5.4 à 8.8
TTP	Gamme (µg/mL), r^2-valeur (n=3)	1.00-1000, 0.9945	1.00-1000, 0.9935	1.00-1000, 0.9960
	Rapport signal/bruit (n=3)	11.3±3.0	9.7±0.8	10.1±7.9
	Inter-essais justesse (% de biais, n=9)	de -2.2 à 0.3	de -7.6 à 1.3	de -8.1 à -1.4
	Inter-essais précision (% de CV, n=9)	de 5.7 à 7.2	de 3.9 à 6.5	de 4.0 à 6.3
VVS	Gamme (µg/mL), r^2-valeur (n=3)	1.00-1000, 0.9917	1.00-1000, 0.9955	1.00-1000, 0.9929
	Rapport signal/bruit (n=3)	16.8±4.0	5.9±0.2	35.3±9.3
	Inter-essais justesse (% de biais, n=9)	de -6.1 à 3.8	de -7.3 à 0.7	de -11.6 à 1.8
	Inter-essais précision (% de CV, n=9)	de 8.0 à 14.5	de 4.3 à 18.7	de 3.0 à 8.4

Parmi les avantages de l'utilisation de kits, on peut mentionner un temps de développement de méthode réduit, une optimisation facilitée de la digestion et l'emploi de moins de réactifs. Néanmoins, l'utilisation de ces kits présente également un certain nombre d'inconvénients, notamment l'augmentation du nombre de peptides déamidés observés avec le *SMART Digest Kit* pour les peptides génériques contenant une asparagine (FNW et VVS) à une température de digestion élevée (Figure 4). Ainsi, même si les deux kits ont permis une préparation plus rapide et plus facile des échantillons, la probabilité de générer des peptides modifiés de manière artéfactuelle a été augmentée, ce qui affecte la sensibilité et la robustesse de la méthode.
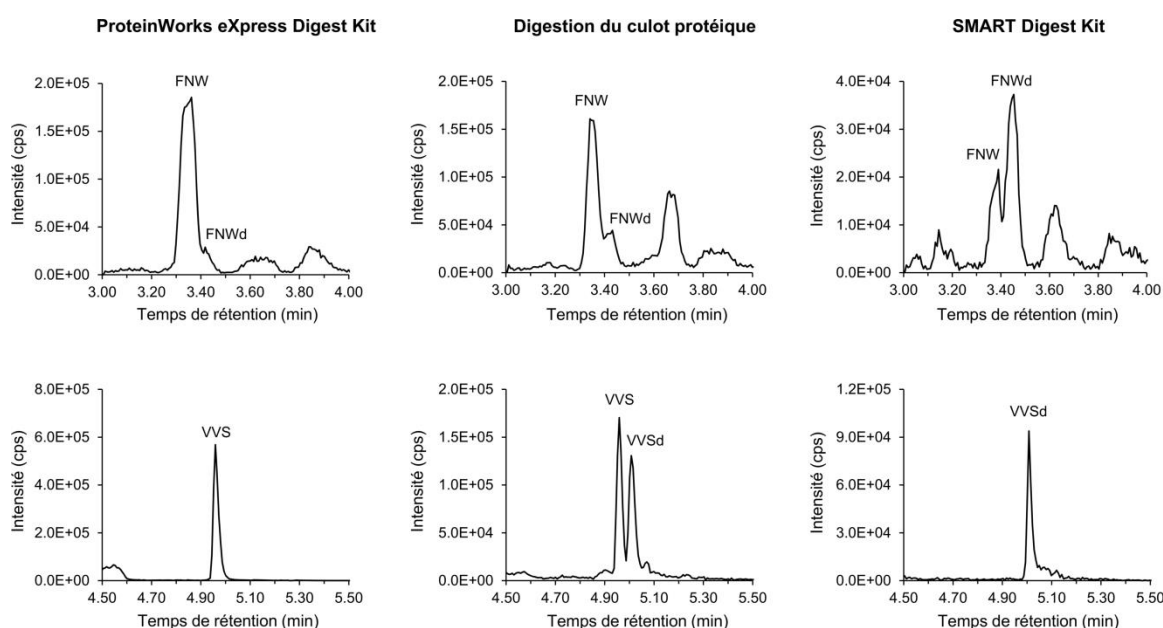
Figure 4 Chromatogrammes obtenus à partir de l'analyse d'échantillon de sérum de rat dopé avec l'hIgG1 à 10.0 µg/mL après digestion avec le *ProteinWorks eXpress Digest Kit* (45 °C), digestion du culot protéique (60 °C) et digestion avec le *SMART Digest Kit* (70 °C). Les chromatogrammes du haut illustrent le peptide FNW et les chromatogrammes du bas illustrent le peptide VVS.

Développement d'une méthode de préparation d'échantillon basée sur une étape d'IC pour l'amélioration de sensibilité d'une méthode LC-MS/MS générique

Bien que les approches de digestion directe du sérum, avec ou sans utilisation de kits, offrent une sensibilité suffisante pour la plupart des études précliniques de PK, des méthodes plus sensibles sont nécessaires dans certains cas, en particulier pour les mAbs très puissants nécessitant une administration à des doses très faibles.[5,6] Dans ce travail de thèse, une méthodologie d'IC automatisée utilisant des pointes de cônes a été développée pour l'enrichissement en hIgG1 et pour réduire la complexité des échantillons de sérum (Figure 5). Trois paramètres essentiels, à savoir la quantité d'anticorps anti-hIgG Fc biotinylé à fixer sur les pointes de cône enduites de
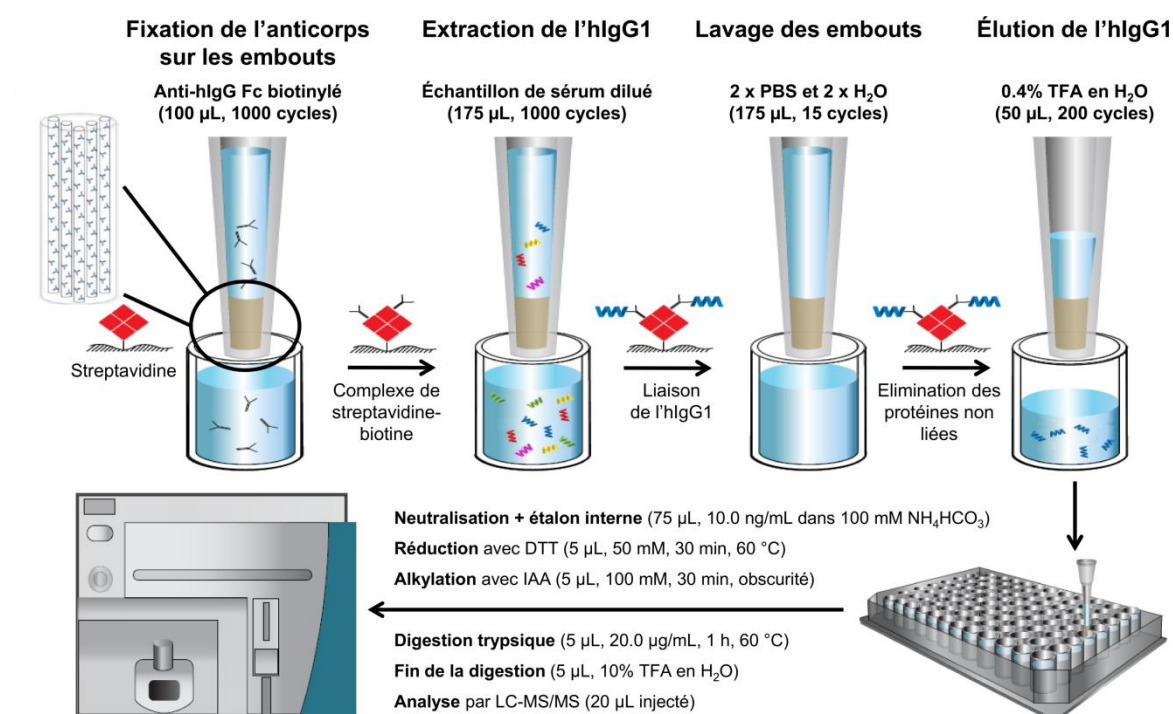
Figure 5 Description de la préparation des échantillons pour la quantification d'hIgG1 dans le sérum de singe par IC-LC-MS/MS.

streptavidine, le nombre de cycles d'aspiration/distribution ainsi que l'élution de l'hIgG1 ont été optimisés. La méthode finale d'IC couplée à la LC-MS/MS a permis d'obtenir un gain en sensibilité de facteur 100 pour la quantification d'hIgG1 dans le sérum de singe avec une limite de quantification inférieure validée de 10.0 ng/mL (Tableau 2). L'applicabilité de cette approche générique de type IC-LC-MS/MS a encore été démontrée lors de l'analyse d'échantillons de PK *in vivo* de deux singes, dosés par voie intravitale.

Tableau 2 Résultats de validation de la méthode de quantification d'hIgG1 dans le sérum de singe.

Paramètre	Résultat
Sélectivité: trois lots de sérum vierge (n=3)	TTP: ≤7.4%, ISTD: ≤0.1%
Contribution du signal	TTP à ISTD: 0.1%, ISTD à TTP: 19.0%
Linéarité (n=3), $y=ax^2+bx+c$, facteur de pondération: 1/x	10.0-1000 ng/mL, $r^2=0.9938\pm0.0014$
Effets de report	TTP: <60.2% de la limite inférieure de quantification ISTD: 0.1% de la réponse de l'étalon interne
Justesse (% de biais) et précision (% de CV), QCs à 10.0, 25.0, 400 et 800 ng/mL	Intra-essai (n=3): de -6.9 à 19.9% de biais, de 1.2 à 14.3% de CV Inter-essais (n=9): de -3.1 à 8.9% de biais, de 7.4 à 10.3% de CV
Dilution (50.0 µg/mL, 500-fois, n=5)	Biais moyen de 12.8% avec une précision de 7.3% de CV
Stabilité du peptide trypsique à 10 °C (n=3)[a] QCs à 25.0 et 800 ng/mL	24 h: 2.1% de biais (800 ng/mL), ≤14.4% de CV (25.0 ng/mL) 72 h: -15.2% de biais (25.0 ng/mL), ≤24.7% de CV[b] (25.0 ng/mL)

[a] Seulement les valeurs maximales sont rapportées, [b] hors critère d'acceptation ≤20.0% de CV.
QCs: échantillons de contrôle de la qualité (*quality control samples*)

Troisième partie - Développement des approches par spectrométrie de masse à haute résolution (HRMS) pour la quantification de mAbs et produits dérivés dans des études précliniques

La troisième partie de la thèse est concentrée sur l'évaluation de l'apport de la HRMS en tant qu'alternative aux spectromètres de masse de type triple quadripôle (QqQ) traditionnellement utilisés pour le développement des méthodes LC-MS/MS quantitatives.

Développement d'une méthodologie LC-HRMS bottom-up quantitative

Différents modes d'acquisition d'un instrument hybride de type quadripôle - temps de vol (QTOF), à savoir les modes TOF-MS, TOF-MS/MS et TOF-MRM, ont été testés. Les modes d'acquisitions TOF-MS/MS et TOF-MRM ont été identifiés comme les plus appropriés pour des approches quantitatives. Le mode TOF-MRM a été utilisé pour la quantification d'hIgG1 dans la gamme 1.00-1000 µg/mL à la fois dans le sérum de rat et de singe en utilisant la digestion directe de culots de sérum comme préparation d'échantillon. Des profils de PK similaires et un accord parfait entre les méthodes LC-HRMS et génériques LC-MS/MS ont été obtenus sur des échantillons *in vivo* (Figure 6a). En outre, il a été démontré avec succès avec le peptide VVS que, dans certains cas, des interférences endogènes dans la matrice pouvaient être éliminées en raison du haut pouvoir
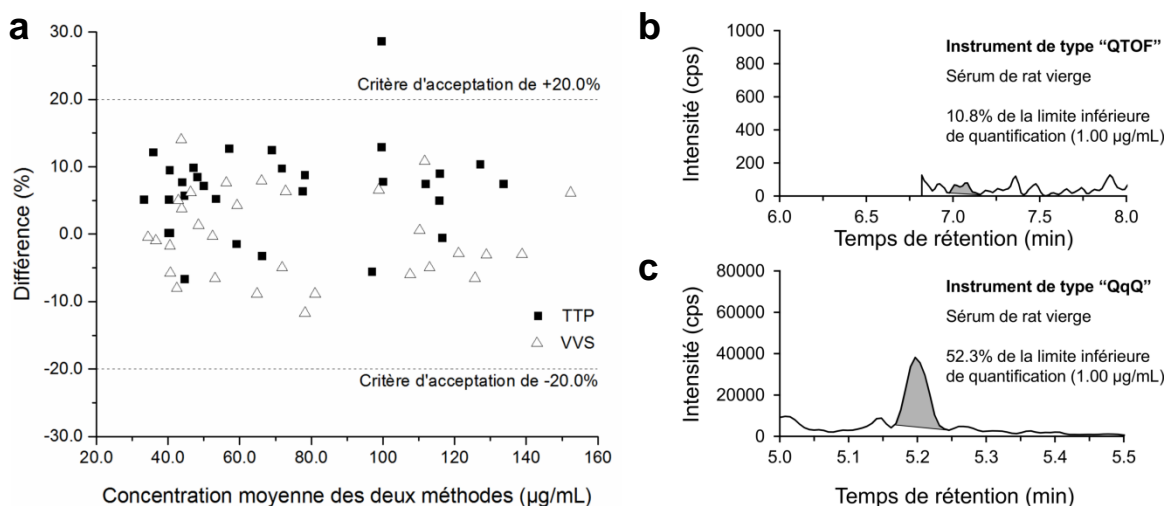
Figure 6 Comparaison entre LC-HRMS et LC-MS/MS pour la quantification d'hIgG dans les espèces précliniques. (**a**) Analyse de Bland-Altman basé sur deux peptides trypsiques génériques (TTP et VVS) lors de l'analyse d'échantillons *in vivo* de cinq singes cynomolgus après administration par voie intraveineuse d'un ADC à lysine (5.00 mg/kg). Amélioration de la sélectivité par utilisation d'un instrument haute résolution: chromatogramme ionique extrait (peptide VVS) dans le sérum de rat vierge en utilisant (**b**) un QTOF et (**c**) un QqQ.

résolutif du TOF et de la possibilité de sélectionner des isotopes individuels pour la quantification. Par conséquent, une sélectivité et une sensibilité améliorées sont associées aux approches basées sur la HRMS pour ce peptide (Figure 6b) par rapport à l'analyse QqQ (Figure 6c). Les données ont également indiqué que l'utilisation de la LC-HRMS peut être avantageuse pour le développement de la méthode bottom-up, comme en témoigne l'élucidation du site de déamidation pour deux peptides sur quatre (FNW et VVS).

Approche quantitative au niveau d'hIgG1 intacte par IC-LC-HRMS

Les sections suivantes de la troisième partie de la thèse concernent le développement d'une méthode de spectrométrie de masse quantitative se basant non plus sur la quantification des peptides de digestion issus des mAbs, mais directement des protéines intactes. En effet, il demeure un problème principal avec les approches de quantification au niveau peptidique (bottom-up), indépendant de l'analyseur de masse choisi, à savoir la perte de l'information au niveau du mAb intact, ce qui peut induire une sous-estimation de la concentration de la substance active.[7,8] Par conséquent, disposer d'approches quantitatives basées sur la MS au niveau des protéines intactes et non plus des peptides serait bénéfique. Afin de développer une méthode générique de MS basée sur la quantification d'hIgG1 intacte dans le sérum de rat, les avantages de l'IC, décrits précédemment pour l'enrichissement sélectif et les performances accrues des instruments de type HRMS ont été combinés (Figure 7). La méthode développée repose sur
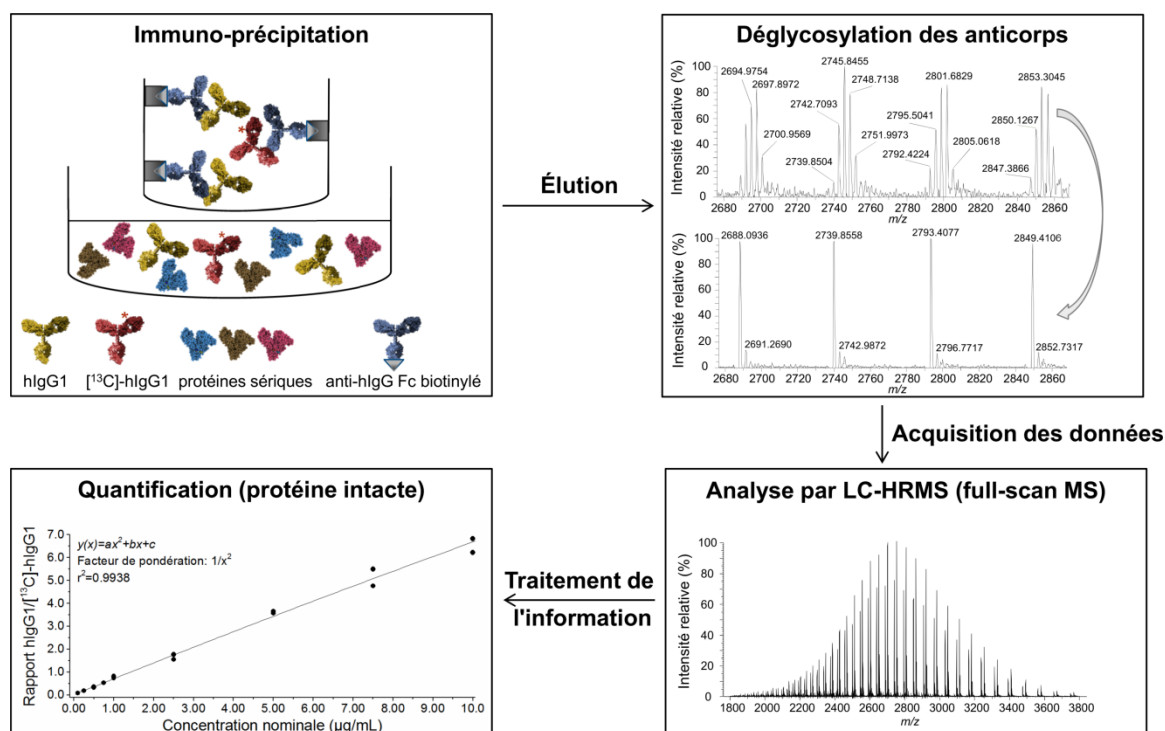
Figure 7 Présentation de la méthode de quantification d'hIgG1 dans les espèces précliniques au niveau des protéines intactes par IC-LC-HRMS.

l'utilisation d'une protéine en tant qu'étalon interne marqué au ^{13}C ($[^{13}$C]-hIgG1) qui est ajoutée dans l'échantillon à doser. L'étalon interne est ensuite co-extrait avec l'hIgG1 à partir d'échantillons de sérum de rat, en utilisant un anticorps ciblant la région Fc (anti-hIgG Fc). De plus, une étape de déglycosylation a été incorporée pour réduire l'hétérogénéité de l'hIgG1 à analyser, en simplifier l'interprétation au niveau du spectre de masse et tenir une sensibilité acceptable pour les études de PK. Pour la quantification hIgG1 intacte, le signal des six états de charge les plus abondants a été utilisé pour la quantification, avec une fenêtre d'extraction de masse de 2 *m/z*. Après addition des chromatogrammes individuels ioniques extraits (XICs, *extracted ion chromatograms*) et de leur intégration, une courbe d'étalonnage a été réalisée en reportant le rapport hIgG1/$[^{13}$C]-hIgG1 en fonction de la concentration nominale en hIgG1. Cette approche IC-LC-HRMS a été validée par la suite (de 0.100 à 10.0 µg/mL) conformément aux directives internationales (Tableau 3).[9,10]

Tableau 3 Résultats de validation de la méthode quantitative d'hIgG1 au niveau des protéines intactes.

Paramètre	Résultat
Sélectivité: trois lots de sérum vierge (n=3)	hIgG1: ≤3.0%, $[^{13}$C]-hIgG1: ≤0.3%
Contribution du signal	$[^{13}$C]-hIgG1 à hIgG1: 12.8%, hIgG1 à $[^{13}$C]-hIgG1: 13.0%
Linéarité (n=3), $y=ax^2+bx+c$, facteur de pondération: $1/x^2$	0.100-10.0 µg/mL, $r^2=0.9919\pm0.0027$
Effets de report	hIgG1:< de la limite inférieure de quantification $[^{13}$C]-hIgG1: 0.0% de la réponse de l'étalon interne
Justesse (% de biais) et précision (% de CV) QCs à 0.100, 0.250, 5.00 et 8.00 µg/mL	Intra-essai (n=3): de -2.7 à 16.0% de biais, de 1.3 à 11.7% de CV Inter-essais (n=9): de -0.1 à 9.3% de biais, de 6.1 à 8.7% de CV
Dilution (300 µg/mL, 50-fois, n=5)	Biais moyen de 2.9% avec une précision de 8.6% de CV
Reproductibilité	Le biais de concentration est compris entre ±20.0% pour 97% des échantillons

QCs : échantillons de contrôle de la qualité (*quality control samples*)

La méthode développée a ensuite été appliquée avec succès pour la quantification d'hIgG1 intacte dans des échantillons de sérum de rat et comparée aux résultats obtenus pour une méthode classique de quantification au niveau peptidique de type bottom-up, ceci à la fois pour des analyses des échantillons de sérum de rat dopés avec l'hIgG1 (Figure 8a) et *in vivo* (Figure 8b). En outre, il a été démontré que l'approche développée au niveau de la protéine entière permettait la quantification simultanée de deux hIgGs de la même sous-classe d'isotypes (hIgG1), ce qui est n'est pas possible aisément par une approche quantitative bottom-up générique. De plus, cette approche de quantification au niveau du mAb intact élimine la génération artéfactuelle de modifications telles que les déamidations ainsi qu'une fastidieuse optimisation de paramètres pour la méthode en MS.
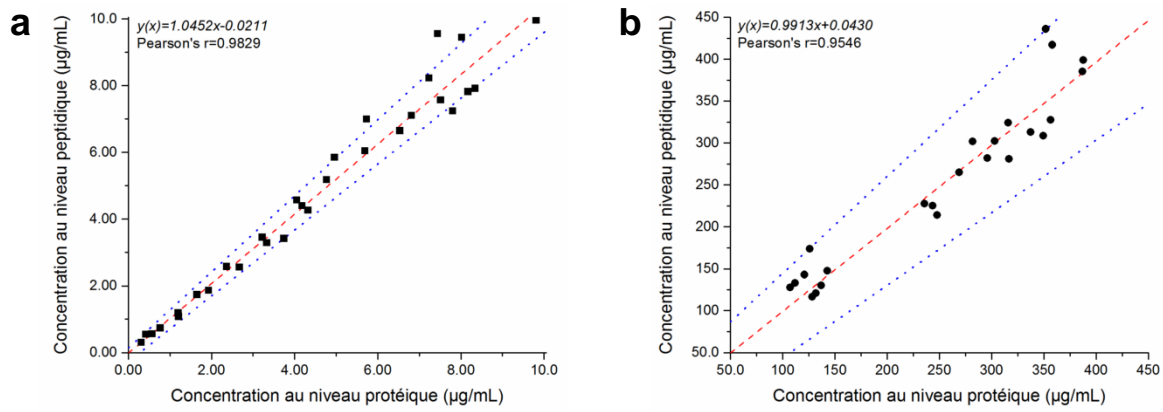
Figure 8 Comparaison de la concentration en hIgG1 par la méthode de quantification des protéines intactes ou par approche bottom-up quantitative. Le graphique (**a**) représente les concentrations mesurées dans les échantillons de sérum de rat dopés avec l'hIgG1 (n=30) et le graphique (**b**) les résultats obtenus dans les échantillons *in vivo* issus d'une étude PK de rat (n=24). En pointillé rouge, la droite de régression linéaire calculée et en bleu l'intervalle de confiance de 95% selon la méthode de régression de Passing-Bablok.

Analyse qualitative et quantitative combinée d'ADC intacte

Cette approche de quantification d'hIgG1 intacte a ensuite été étendue à la quantification d'ADC à lysine dans un sérum de rat. Une préparation d'échantillon dédiée a été développée, consistant en une immuno-précipitation sur billes IC-LC-HRMS. Cette approche permet de fournir des informations qualitatives sur le profil de conjugaison de l'ADC (DLD, *drug load distribution*) ainsi que le nombre moyen de molécules conjuguées par anticorps (DAR, *drug-to-antibody ratio*) parallèlement aux données quantitatives *in vivo* (Figure 9a+b). Ces dernières incluent non seulement la détermination de la concentration totale d'ADC (concentration totale d'espèces portant le cytotoxique) et du mAb total (en utilisant le spectre de masse déconvolué), mais a
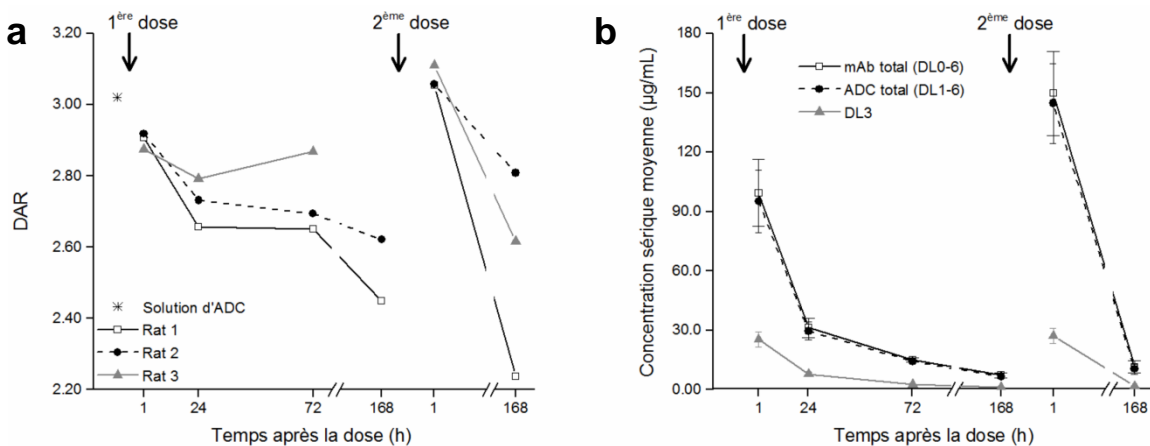
Figure 9 Données *in vivo* provenant de trois rats après administration de deux doses (jour 1 et 8) par voie intraveineuse d'un ADC à lysine (5.00 mg/kg). (**a**) Profils individuels de DAR et (**b**) concentration sérique moyenne.

également permis de quantifier les principales espèces conjuguées individuellement (DL, *drug load*) de l'ADC, ce qui est impossible avec les approches ELISA et LC-MS/MS bottom-up. Dans l'ensemble, le principal avantage de cette approche est de combiner des informations qualitatives et quantitatives à trois niveaux (ADC, mAb et DL) en une seule méthode tout en utilisant un seul anticorps pour l'IC par opposition aux méthodologies actuellement appliquées.[11,12]

Conclusion générale

Les différentes méthodes de quantification des mAbs basées sur MS développées tout au long de ce travail de thèse ont considérablement étendu le nombre d'approches disponibles pour la quantification de mAbs et de leurs produits dérivés dans des espèces précliniques. Une large gamme d'étalonnage de cinq ordres de grandeur a été couverte pour la quantification de protéines thérapeutiques par une approche bottom-up soit à partir de digestion du culot protéique (de 1.00 à 1000 µg/mL), ou après immuno-précipitation (de 10.0 à 1000 ng/mL). Étant donné qu'un anticorps anti-hIgG Fc générique a été utilisé pour la capture, la méthodologie développée permet la quantification dans un échantillon préclinique de sérum de toute protéine thérapeutique présentant une région Fc reconnue par l'anticorps. Bien que les approches bottom-up génériques offrent une grande flexibilité grâce aux peptides génériques conservés dans la région constante, une certaine connaissance des modifications ou des sites de conjugaison des mAb reste un prérequis. Par conséquent, il serait souhaitable d'incorporer au moins deux peptides provenant de différentes régions constantes afin de gagner en confiance dans les données quantitatives et d'améliorer ainsi la flexibilité de la méthode.

L'apport de la HRMS utilisant un analyseur de type QTOF a clairement été démontré dans cette thèse pour l'analyse qualitative et quantitative des protéines thérapeutiques de type mAbs et produits associés. Sur la base des progrès récents de l'instrumentation HRMS, les précédentes limitations associées aux analyses quantitatives peuvent maintenant être surmontées. En effet, des données quantitatives équivalentes entre les instruments QTOF et QqQ ont été obtenues pour la quantification de mAbs dans le cas d'approches bottom-up. Un avantage majeur de l'intégration des analyseurs de masse QTOF ou orbitrap dans le développement de méthodes génériques a été montré dans ce travail de thèse. Ainsi la quantification de mAbs et produits associés directement au niveau de la protéine entière a été possible, fournissant un niveau d'informations bien au-delà de celui obtenu avec des approches bottom-up. Il est cependant nécessaire de préciser que le plus important aspect est la possibilité de quantifier individuellement chaque espèce conjuguée des ADCs. Le développement d'approches IC-LC-HRMS entièrement automatisées permettrait d'envisager l'utilisation de la quantification au niveau des protéines entières en routine. Cependant, pour que cette transition s'opère, de nouveaux verrous liés à la taille des fichiers de données et à l'automatisation du traitement des données doivent être levés. Bien que les méthodes quantitatives génériques basées sur la MS développées dans ce travail de thèse aient démontré leur potentiel pour la quantification des mAbs et de leurs produits

dérivés, leur application reste toutefois limitée aux échantillons d'études précliniques. Ceci est notamment lié à la présence de hIgGs endogènes dans les échantillons cliniques qui peuvent interférer avec l'hIgG à analyser. Dans le futur, il serait souhaitable de voir comment appliquer l'approche générique développée au cours de ce travail de thèse pour la quantification de protéines thérapeutiques sous forme intacte dans les études cliniques.

Références

1.   La Merie Publishing. 2016 Sales of Recombinant Therapeutic Antibodies & Proteins. Mar 2017, www.pipelinereview.com.

2.   van den Broek I, Niessen WM, van Dongen WD. Bioanalytical LC-MS/MS of protein-based biopharmaceuticals. *J Chromatogr B*, 2013, 929, 161-179.

3.   Furlong MT *et al*. A universal surrogate peptide to enable LC-MS/MS bioanalysis of a diversity of human monoclonal antibody and human Fc-fusion protein drug candidates in pre-clinical animal studies. *Biomed Chromatogr*, 2012, 26(8), 1024-1032.

4.   Li H *et al*. General LC-MS/MS method approach to quantify therapeutic monoclonal antibodies using a common whole antibody internal standard with application to preclinical studies. *Anal Chem*, 2012, 84(3), 1267-1273.

5.   Chan AC, Carter PJ. Therapeutic antibodies for autoimmunity and inflammation. *Nat Rev Immunol*, 2010, 10(5), 301-316.

6.   Qu M *et al*. Qualitative and quantitative characterization of protein biotherapeutics with liquid chromatography mass spectrometry. *Mass Spectrom Rev*, 2016, 36(6), 734-754.

7.   Jian W, Kang L, Burton L, Weng N. A workflow for absolute quantitation of large therapeutic proteins in biological samples at intact level using LC-HRMS. *Bioanalysis*, 2016, 8(16), 1679-1691.

8.   Kellie JF, Kehler JR, Mencken TJ, Snell RJ, Hottenstein CS. A whole-molecule immunocapture LC-MS approach for the in vivo quantitation of biotherapeutics. *Bioanalysis*, 2016, 8(20), 2103-2114.

9.   U.S. Food and Drug Administration. Guidance for Industry: Bioanalytical Method Validation. May 2001, www.fda.gov.

10.   European Medicine Agency. Guideline on Bioanalytical Method Validation. Jul 2011, www.ema.europa.eu.

11.   Myler H *et al*. An integrated multiplatform bioanalytical strategy for antibody-drug conjugates: a novel case study. *Bioanalysis*, 2015, 7(13), 1569-1582.

12.   Kaur S, Xu K, Saad OM, Dere RC, Carrasco-Triguero M. Bioanalytical assay strategies for the development of antibody-drug conjugate biotherapeutics. *Bioanalysis*, 2013, 5(2), 201-226.

General introduction

Monoclonal antibody (mAb)-related therapeutic proteins including immunoglobulin Gs (IgGs), bispecific antibodies (bsAbs), antibody-drug conjugates (ADCs), and their truncated versions such as fragment crystallizable (Fc) fusion proteins are one of the fastest growing therapeutic classes throughout the last decade. As of Nov 14th 2017, 81 mAb-related therapeutic proteins (*i.e.* originators and their biosimilars) were granted approval by the Food and Drug Administration (FDA) and European Medicines Agency (EMA) for marketing in the United States of America (US) and European Union (EU), respectively. The compound annual growth rate in sales of mAb-related therapeutic proteins has been estimated to be approximately 8.0% (2014-2019) and the latest publicly available marketing data reported a global sales revenue of 107 billion US$. Considering a mean annual approval rate of 5.9 mAb-related therapeutic proteins per year (2007-2017), almost 100 mAb-related modalities will be marketed in the US and EU by 2020 with an estimated global sales revenue of 145 billion US$. Based on these data, it is not surprising that pharmaceutical companies invest notable resources in the development of such entities.

During the whole development process, ranging from candidate selection in an early-stage to late-stage support of pre-clinical and clinical pharmacokinetic (PK), pharmacodynamic (PD), and immunogenicity (IG) studies, robust and validated quantitative assays are required. In the last few years, mass spectrometry (MS) has evolved as a complementary analytical technology to ligand binding assays (LBAs) for mAb quantification in complex biological matrices. Major benefits of liquid chromatography tandem MS (LC-MS/MS) over LBA-based assays include an increased selectivity due to specific mass-to-charge (*m/z*) ratios of the precursor and product ion(s), a wider linear dynamic range as well as less cross-reactivity, matrix effects, and assay-specific interferences caused by *in vivo* generated anti-drug antibodies (ADAs). Although no expensive and time-consuming production of specific capture antibodies is required for MS-based approaches employing direct digestion of the biological sample, the identification of the most appropriate surrogate peptide and optimization of the mass transition used for quantitative purposes can still be challenging and tedious. Even though peptides from the complementarity-determining region (CDR) of the mAb are highly specific, a novel assay has to be developed for each mAb-related therapeutic protein. In order to circumvent this issue, conserved generic peptides from the constant region of the mAb were lately reported. Hence, the aim of this PhD thesis was to design and implement generic MS-based workflows for chimeric, humanized, and human IgG (hIgG) quantification in pre-clinical species and extend their applicability to related entities from the next-generation (*i.e.* bsAbs and ADCs).

The **first part** of this doctoral work provides a brief introduction to IgGs including their structure, glycans, and effector function. Moreover, the diversity of mAb-related therapeutic proteins is presented and their therapeutic uses are summarized after which the market development over

the last decade is displayed. In addition, the variety of required qualitative methods during the drug development process, conventional quantitative LBA and MS-based assays as well as regulatory considerations regarding method validation are introduced.

The **second part** discusses the development of bottom-up LC-MS/MS methodologies for generic and versatile mAb-related therapeutic protein quantification in pre-clinical serum samples.

- The first chapter illustrates the development of a generic pellet digestion-based LC-MS/MS assay for hIgG1 and hIgG4 quantification in rat serum, utilizing four conserved tryptic surrogate peptides from different parts of the constant region. Moreover, the versatility of such a generic approach is explored in spiked serum and pre-clinical study samples by (i) interchanging the serum of animal species (rat with monkey), while keeping the same analyte (hIgG1) and (ii) measuring different hIgGs and related modalities (two additional hIgG1s, one hIgG4, one bsAb, and two lysine-conjugated ADCs) against the initially selected hIgG1.

- In the second chapter, two commercially available digestion kits, namely the SMART Digest Kit (Thermo Fisher Scientific) and ProteinWorks eXpress Digest Kit (Waters) are evaluated and compared to the developed pellet digestion protocol using spiked rat serum samples in order to standardize the sample preparation for generic hIgG1 quantification.

- The third chapter describes the development of a generic tip-based immuno-capture (IC)-LC-MS/MS methodology in order to improve the method sensitivity for hIgG1 quantification in cynomolgus monkey serum and the optimization of critical IC parameters is presented.

The **third part** focuses on the development and evaluation of high-resolution mass spectrometry (HRMS)-based approaches as an alternative to traditional triple quadrupole (QqQ) mass analyzers for mAb-related therapeutic protein quantification.

- In the first chapter, the implementation of a generic LC-HRMS assay using a Synapt G2-Si quadrupole time-of-flight (QTOF) mass spectrometer is described for targeted bottom-up hIgG1 quantification in rat and cynomolgus monkey serum.

- The second chapter describes the development of a generic IC-LC-HRMS approach, using a quadrupole orbitrap mass spectrometer (Q-Exactive), in order to conduct hIgG1 quantification in rat serum at an intact level.

- The last chapter illustrates the implementation of an IC-LC-HRMS-based methodology (Synapt G2-Si QTOF) for a combined analysis of intact lysine-conjugated ADCs in spiked rat serum and pre-clinical study samples in order to obtain qualitative information about the drug load distribution (DLD) and drug-to-antibody ratio (DAR), while simultaneously providing quantitative data (total mAb, total ADC, and individual ADC drug load species).

Part 1 - Introduction to mAb-related therapeutic proteins and their quantification in biological fluids

The first part provides a brief general introduction to immunoglobulins before structural differences between the IgG isotype subclasses, leading to various Fc receptor-mediated effector functions, are succinctly discussed. Furthermore, the diversity of mAb-related therapeutic proteins and their market development over the last decade are displayed. After a short excursion to qualitative assays required during the drug development process of such modalities, analytical platforms for their quantification in biological fluids are described in more detail with a focus on mass spectrometry. The last chapter summarizes regulatory considerations from the US FDA and EMA related to analytical method validation.

Chapters

1.1   Structure and physiological functions of immunoglobulins

1.2   Diversity of mAb-related therapeutic proteins

1.3   Market development of mAb-related therapeutic proteins

1.4   Required assays for the development of mAb-related entities

1.5   Analytical platforms for PK, PD, and IG assessments

1.6   Regulatory considerations for method validation

1.1 Structure and physiological functions of immunoglobulins

The class of mAb-related therapeutic proteins covers a broad range of high-molecular weighted modalities, which are derived from immunoglobulins (Igs).[1] Naturally occurring Igs are involved in humoral immune responses by the adaptive immune system of vertebrates.[2] Igs are expressed by B lymphocytes (B cells) and are able to bind principally any foreign antigen whereby each individual B cell bears Igs of single specificity.[3,4] Naive B cells express Igs in form of membrane-bound antigen receptors (B cell receptor).[5,6] The binding of the B cell receptor to its unique antigen induces the differentiation of the naive B cell into an effector cell (plasma cell) that subsequently secretes soluble Igs (antibodies) in order to protect the body from pathogens and toxins *via* neutralization, opsonization to facilitate phagocytosis or antibody-dependent cell-mediated cytotoxicity (ADCC) by additional leucocytes of the innate immune system, and activation of the complement system.[4,7]

1.1.1 Structure

Igs are Y-shaped glycoproteins, which consist of four polypeptide chains, more precisely two identical light (L) and two identical heavy (H) chains linked through various inter-chain disulfide bonds (Figure 1.1a). The structure of each L and H chain can be further divided into variable (V_L and V_H) and constant (C_L and C_H) regions, whereby C_H is composed of up to four distinct domains entitled C_H1, C_H2, C_H3, and C_H4. Each of the individual L and H chain domains is composed of 110-130 amino acids and exhibits a molecular weight of approximately 12.5 kDa.[8] The 25 kDa
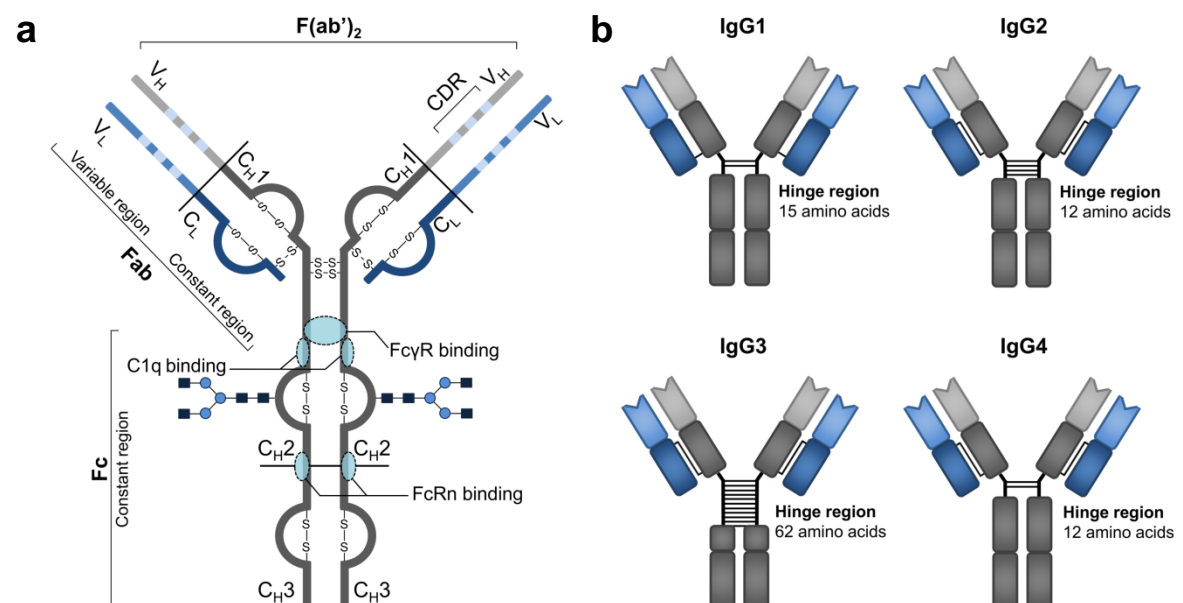
Figure 1.1 Schematic illustration of an Ig. (**a**) Detailed Ig structure exemplified with an IgG1 and (**b**) structural differences between the four IgG isotype subclasses. Fab: fragment antigen binding, C1q: C1 complex of complement system, FcγR: Fc gamma receptor, FcRn: neonatal Fc receptor

either kappa or lambda-based L chain, the V_H, and the C_H1 domain form a flexible Y arm, namely the fragment antigen binding (Fab) region. The dimeric structure of two flexible Fab arms tethered through the hinge region is referred to as F(ab')$_2$. The broad diversity of Igs is generated by hypervariable regions in form of three loops of ß-strands from the V_H and V_L (CDRs), which determine the antigen specificity and represent the antigen-binding site.[9] The remaining C_H domains (C_H2-C_H4) form the stem of the Y (Fc region), which mediates the Ig effector function and define the Ig isotype. In placental mammals, five different Ig isotypes exist: IgG (75%), IgA (15%), IgM (10%), IgD (<0.5%), and IgE (<0.01%).[8] Since the mAb-related therapeutic proteins investigated in this work were based on the IgG scaffold, its structure is discussed in more detail in the following.

The basic structural unit for one IgG H chain (50 kDa) relies on one N-terminal variable and three C_H domains (Figure 1.1a).[8] Hence, the IgG Fc region is constituted out of the C_H2 and C_H3 domain. A complete IgG molecule (approximately 150 kDa) is formed by inter-H chain disulfide bonds, linking two covalently paired L/H constructs. Depending on the number and position of the inter-chain linkages, the IgG isotype can be further categorized into four subclasses, namely IgG1, IgG2, IgG3, and IgG4, which display a 90-95% similiarity in amino acid sequence (Figure 1.1b).[10,11] The position of the cysteine in the L chain responsible for L/H linkage represents one structural difference between individual IgG isotype subclasses and is either located at position 220 (IgG1) or 131 (IgG2, IgG3, and IgG4).[10] The number of cysteine residues in each H chain necesarry for the formation of inter-H chain disulfide bonds likewise depends on the IgG subclass with two for IgG1 and IgG4, four for IgG2, and eleven for IgG3. As a result of alternative disulfide bond formation, IgG2 and IgG4 exist in several isomers, respectively.[12,13] The IgG4 isotype subclass particularly displays a high variablity as an inter-molecular exchange of Fab arms can occur *in vivo*, leading to monovalent bispecific IgG4 with a limited ability for effective antigen binding.[14] Another structural difference between the IgG isotype subclasses is reflected by the flexibility and length of the hinge region, varying between 12 and 62 amino acids.

1.1.2 Fc receptor-mediated effector functions

Subclass-dependent differences in the hinge region impact epitopal antigen binding due to the relative conformation of Fab arms. Furthermore, the IgG binding to the complement system and Fc gamma receptor (FcγR) is affected as a result of partially or completely shielded binding sites.[10] Binding of the IgG Fc region to the complement system, more precisely to C1q of the C1 complex, mediates complement-dependent cytotoxicity (CDC).[15] This process involves a cytolytic cascade of several complement proteins causing membrane attack complex formation and target cell lysis after disruption of the bilipid target cell membrane (Figure 1.2).[16] Destruction of the target cell can also be initiated by natural killer cells through interaction of the IgG Fc region with one of the five activiting FcγRs (FcγRI, FcγRIIa, FcγRIIc, FcγRIIIa, and FcγRIIIb).[17] Subsequent mediation of intracellular signaling pathways *via* phosphorylation of the immunoreceptor tyrosine-based activation motif leads to pro-inflammatory activities and antigen clearance by ADCC.[17,18] In case of
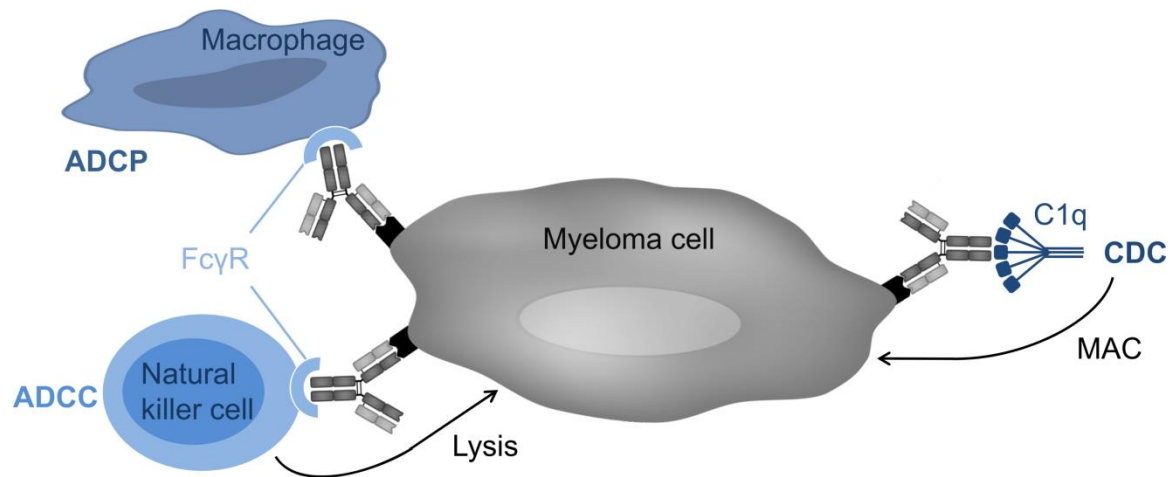
Figure 1.2 Schematic illustration of Fc receptor-mediated effector functions causing death of target cell by ADCP, ADCC, and CDC. MAC: membrane attack complex

antibody-dependent cell-mediated phagocytosis (ADCP), removal of the target cell is mediated by macrophages.[19,20] In contrast to hIgG2 and hIgG4, hIgG1 and hIgG3 exhibit a high ADCC effector function and can efficiently trigger CDC (Table 1.1). Another intracellular interaction is caused following IgG binding to the neonatal Fc receptor (FcRn). Besides facilitating the transcytosis of IgG in FcRn-expressing epithelial cells such as in the placenta or mucosal surfaces, the FcRn mediates intracellular recycling of the IgG and prevents its lysosomal degradation.[10,21,22] The FcRn is located in the endosomes and binds under acidic conditions (pH 6.0-6.5) to the endocytosed IgG.[23] Upon formation of the IgG-FcRn complex, which is redirected to the cell membrane surface, the IgG dissociates at physiological pH from the IgG-FcRn complex and is released into the systemic circulation.[10] Histidine residues at position 310 and 435 within the C_H2/C_H3 domains are likely responsible for the pH-dependent binding to the FcRn.[24] A lower binding affinity of the IgG3 to the FcRn is caused by the histidine-arginine replacement at position 435, resulting in an accelerated clearance and relative short serum half-life of one week compared to other IgG isotype subclasses with a half-life of three weeks (Table 1.1).[10,25]

Table 1.1 Fc receptor-mediated effector functions listed for each IgG isotype subclass. Adapted from Irani V *et al.* (2015)[24] and Vidarsson G, Dekkers G, and Rispens T (2014).[10]

	IgG1	IgG2	IgG3	IgG4
C1q binding	++	+	+++	-
FcγRI binding	+++	-	++++	++
FcγRIIa binding	++++	+	+++	+
FcγRIIb binding	+++	+	++++	++++
FcγRIIIa binding	+++	+	++++	++
FcγRIIIb binding	++	-	++++	-
FcRn binding	+++	+++	++	+++
Serum half-life	3 weeks	3 weeks	1 week	3 weeks

1.1.3 The effect of IgG glycans on Fc receptor-mediated effector functions

The glycosylation profile significantly affects the quaternary structure of the C_H2 domain in IgGs, which is crucial for Fc receptor binding through glycan-protein and glycan-glycan interactions.[10,17,18] Regardless of the IgG isotype subclass, a conserved glycan structures is attached to the asparagine residue at position 297, maintaining the IgG in an open conformation.[10] In contrast, carbohydrate removal results in a rather closed structure, abolishing binding to FcγR and C1q.[26] The heptasaccharides biantennary glycan core structure (G0) contains four N-acetylglucosamine (GlcNac) and three mannose moieties, forming the α1,3 or the α1,6 arm (Figure 1.3). The glycan core structure of most IgGs is further extended with various monosaccharides. The addition of galactose through a β1,4-linkage on the α1,6 arm (G1) results in an increased binding affinity to the C1q, whereas the removal of galactose is associated with decreased CDC.[18] The addition of a second galactose residue on the α1,3 arm results in the G2 form. Moreover, 92% of IgGs are further fucosylated at the core GlcNac.[27] As a key regulator of ADCC, fucose controls the FcγRIIIa-mediated IgG response either towards pro or anti-inflammatory effects.[10,28,29] A minor fraction of IgGs are mono (<10.0%) or disialylated (<1.0%), resulting in the A1 or A2 glycan forms, respectively.[17,30,31] Terminal sialic acids decrease the binding affinity to the FcγRIIIa, leading to a reduction of ADCC.[32] Furthermore, FcγRIIb-mediated anti-inflammatory properties are only associated with α2,6-linked sialylated N-glycans, whereas α2,3-terminal sialic acids do not demonstrate any anti-inflammatory effects.[33,34] Besides the herein briefly discussed major glycan forms and their effect on Fc receptor-mediated effector functions, additional glycans or glycosylation sites (*i.e.* in the Fab region) have been identified.[10,27]
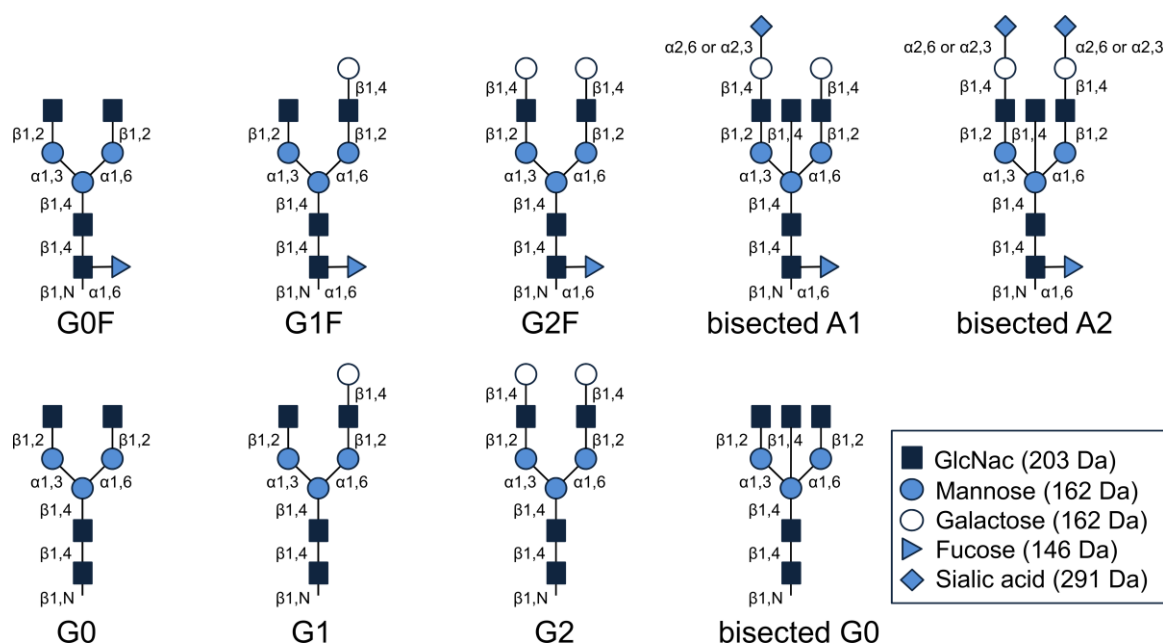
Figure 1.3 Examples of IgG glycans, which are attached to the C_H2 asparagine residue at position 297.

1.2 Diversity of mAb-related therapeutic proteins

IgGs are effective therapeutic agents due to their ability to simultaneously bind antigens *via* the Fab region and stimulate the immune system through Fc-mediated effector functions.[35,36] Throughout the last years, a broad diversity of mAb-related therapeutic proteins has emerged as important therapeutic class for the treatment of various types of cancer,[37-39] chronic inflammatory disorders,[40-42] and cardiovascular,[43,44] auto-immune,[45,46] or infectious diseases.[47-49] In addition, mAbs were successfully employed upon tissue, cell, or organ transplantation in order to prevent their rejection.[50-52]

1.2.1 Unconjugated mAbs

1.2.1.1 Sources

In contrast to polyclonal antibodies, recognizing multiple epitopes of a specific antigen, mAbs exhibit a monovalent affinity to one particular epitope of an antigen.[53] These highly specific antibodies are derived from different sources (Figure 1.4). The origin of the mAb can be identified from its international nonproprietary name with a general "*-mab*" suffix. The first mAbs were of murine origin ("*-omab*"), which were produced with the hydridoma technology proposed by Köhler and Milstein.[54] Major limitations of murine mAbs for therapeutic use result from their inability to properly induce an effector function and the increased formation of human anti-mouse antibodies, leading to adverse events in patients as well as rapid clearance.[55,56] In order to overcome these drawbacks, mAbs were gradually humanized. Chimeric mAbs ("*-ximab*") consist of a variable murine and constant human region. Consequently, 75% of the amino acid sequence of chimeric mAbs are of human origin.[35] Humanized mAbs ("*-zumab*") have 95% similarity to human mAbs and are composed of human variable as well as constant regions with grafted CDR regions of murine origin.[57] The last mAb source are fully human mAbs ("*-umab*").

Murine	Chimeric	Humanized	Human
e.g. catumaxomab	*e.g. infliximab*	*e.g. trastuzumab*	*e.g. adalimumab*

■ murine   ■ human
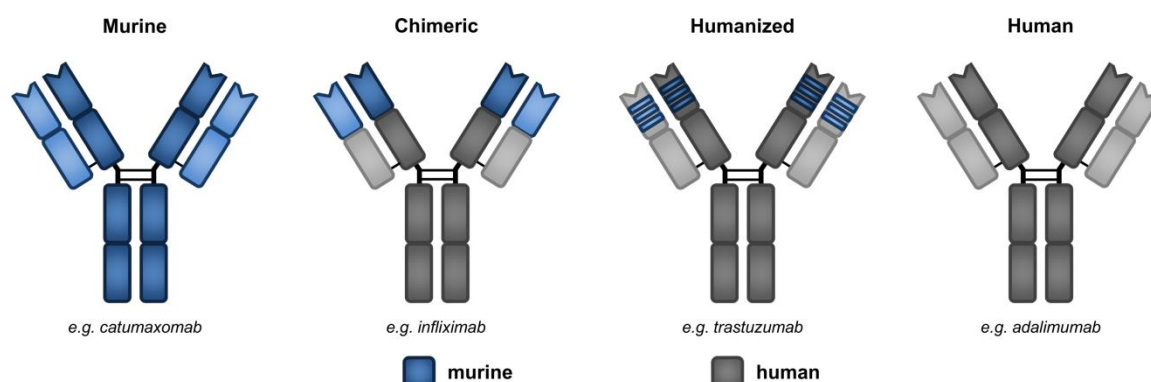
Figure 1.4 Schematic illustration of mAbs from different sources.

1.2.1.2 Mechanism of action

A therapeutic effect of mAbs results from (i) neutralization of soluble antigens, (ii) blocking or stimulation of intracellular signal pathways, (iii) activation of cellular and complement-mediated mechanisms (ADCC, ADCP, and CDC), and (iv) targeted delivery of various components.[58,59]

Many mAbs bind to a specific epitope in the binding domain of their antigen and prevent ligand-receptor interactions. For instance, *bevacizumab*, a humanized IgG1, exhibits a strong binding affinity to the vascular endothelial growth factor and hinders its binding to the vascular endothelial growth factor receptor-1 and vascular endothelial growth factor receptor-2, leading to an inhibition of tumor cell proliferation.[60,61] The prevention of ligand-receptor interaction can likewise occur through blocking of the receptor by the mAb: *cetuximab*, a chimeric IgG1, demonstrates such an antagonistic mechanism, which exhibits a 5 to 10-fold higher affinity to the epidermal growth factor receptor compared to its natural occurring ligands.[62] Binding of the mAb to a receptor expressed on the target cell can additionally activate intracellular pathways promoting apoptosis.[59] For instance, *rituximab*, a CD20-targeting chimeric IgG1, demonstrated pro-apoptotic effects *in vivo* by activation of the mitochondrial pathway, resulting in apoptosis of the target cell.[63] In addition, *rituximab*'s mechanism of action involves ADCP, ADCC, and CDC.[64] As mentioned already in section 1.1.2, ADCC, ADCP, and CDC are mediated by the complement and immune effector cells. Due to advancements in antibody-engineering, mAbs with customized effector functions can nowadays be developed. For instance, enhanced ADCC or CDC can be achieved through glycoengineering or Fc mutagenesis, whereas extended half-lives of histidine-rich IgG3s and Fc-modified IgG1s were reported.[65-67] On the other hand, for mAbs, whose mechanism of action is rather Fab region-mediated or rely on receptor blocking, "Fc-silent" variants were designed in order to reduce activation of the FcγR and decrease Fc receptor-mediated toxicity.[68,69] Finally, the mAb can act as carrier for the targeted delivery of radionuclides for radioimmuno-therapy,[70,71] immunocytokines (*e.g.* for the treatment of neuroblastoma),[72,73] or highly potent cytotoxic drugs in order to induce apoptosis of the target cell as discussed in the next section.[74-79]

1.2.2 Antibody-drug conjugates

As outlined in the previous section, targeted delivery of highly potent cytotoxic drugs is an important mechanism of action for mAb-related therapeutic proteins. ADCs play a remarkable role in the treatment of solid tumors, leukemias, and lymphomas.[80] The rational for the design of ADCs follows Paul Ehrlich's vision of a "magic bullet" for the targeted treatment of diseases by combining the selectivity of a mAb with the cytotoxic potency of a small molecule drug (payload), which is covalently conjugated by a linker/spacer.[81] The conjugation of the payload masks its hydrophobicity and prevents its renal clearance, resulting in an increased half-life in the systemic circulation.[82]

1.2.2.1 Mechanism of action

The ADC recognizes a tumor-specific antigen expressed on the cell surface, *e.g.* the human epidermal growth factor receptor-2.[83,84] Following internalization by receptor-mediated endocytosis, the ADC can undergo FcRn-mediated recycling (section 1.1.2) or lysosomal degradation, releasing the cytotoxic payload into the cytoplasm.[85] Subsequent interaction between the payload and its intracellular target (*e.g.* microtubules or deoxyribonucleic acid) causes tumor cell apoptosis through various mechanisms (Figure 1.5). In addition, the released cytotoxic payload can diffuse out of antigen-positive tumor cells and enter surrounding antigen-negative tumor cells to induce their apoptosis (bystander effect).[80,86] The targeted payload delivery to tumor cells by highly specific mAbs is associated with less off-target toxicity and hence enlarge the therapeutic window for cancer treatment compared to conventional chemotherapeutic treatments.[86]
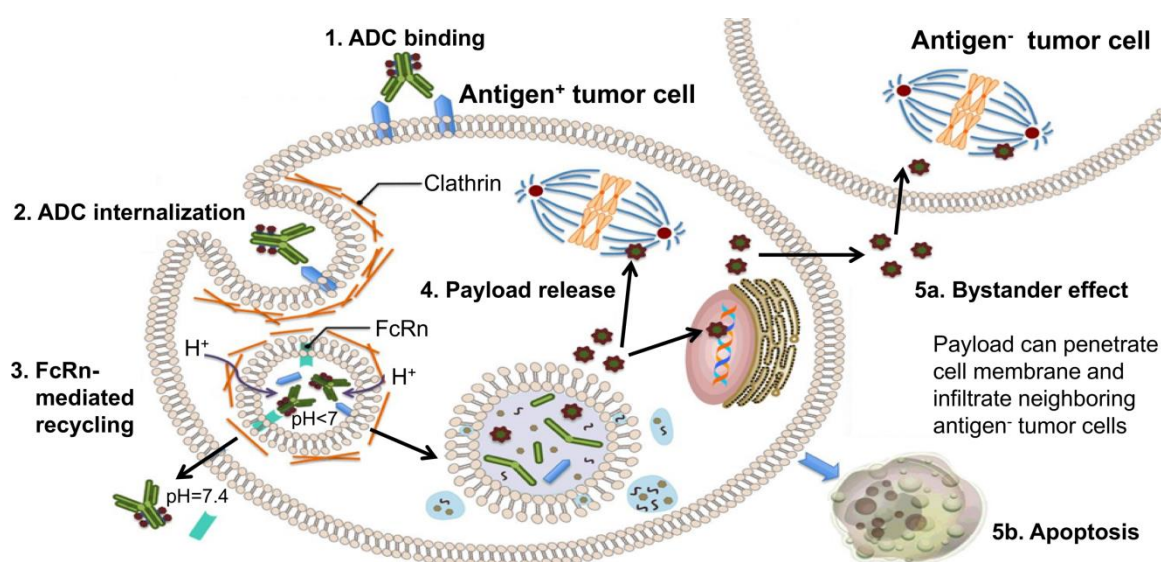
Figure 1.5 Mechanism of action for an ADC. Adapted from Peters C and Brown S (2015).[85]

1.2.2.2 ADC structure

Depending on the conjugation site, ADCs can be classified into lysine, cysteine, and site specific-conjugated ADCs (Figure 1.6). Although a mAb contains approximately 90 lysine residues, only the ones exposed to the surface can be randomly conjugated with the payload, which results in a heterogeneous mixture of different ADC species. On the other hand, selective reduction and payload conjugation to inter-chain cysteine residues decrease the heterogeneity, resulting in ADC constructs with an even number of payloads attached (n=0, 2, 4, 6, 8).[87] The latest generation of ADCs, however, utilizes specific conjugation sites through the incorporation of additional cysteine residues,[88] unnatural amino acids,[89] specific tags,[90] or glycoengineering,[91] allowing the production of homogenous ADCs with an almost uniform number of payloads. This additionally reduces off-
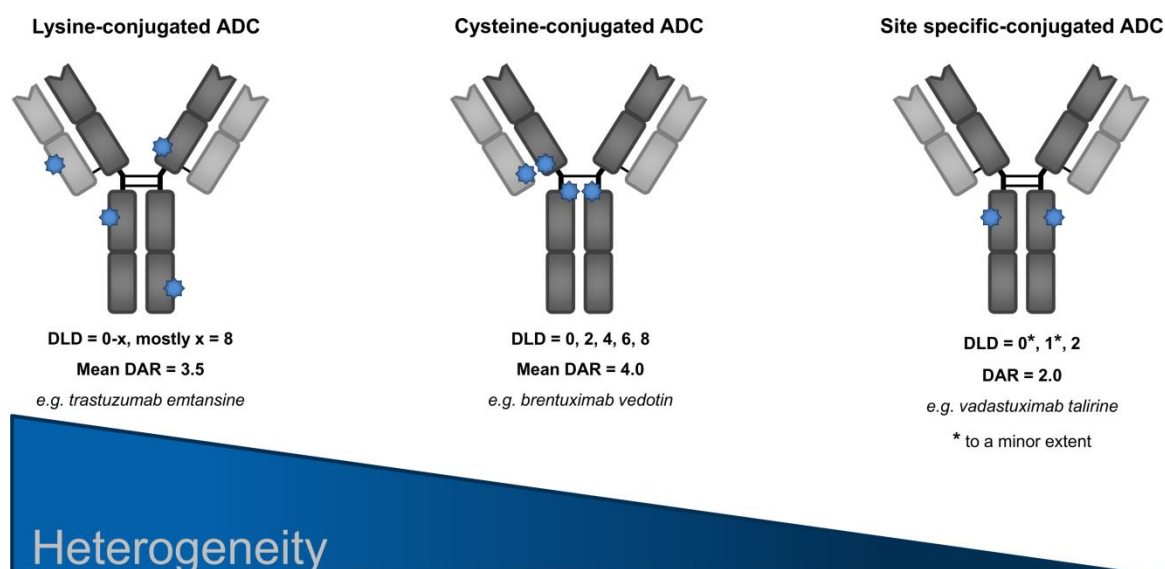
Figure 1.6 Schematic illustration of different types of ADCs.

target toxicity due to less payload deconjugation, widening the therapeutic window of ADCs even further.[88] All IgG isotype subclasses with their respective effector function (section 1.1.2) can act as carrier for the payload whereby humanized or human IgGs are preferred due to the already mentioned reduced formation of human anti-mouse antibodies.[55] The selected mAb should further demonstrate a high degree of specificity and affinity to a certain antigen expressed exclusively on the surface of tumor cells and should exhibit minimal immunogenic effects.[92]

The linker is crucial for the safety and efficacy of ADCs, as premature payload release in the blood stream due to linker instability results in increased systemic exposure of the payload (*i.e.* increased off-target toxicity) and reduces the amount of payload reaching its target (*i.e.* reduced efficacy), narrowing the therapeutic index.[80,93] On the other hand, the payload should be efficiently released upon endocytosis into the target cell.[94] Moreover, the hydrophobicity of the linker determines the potential for aggregation, which subsequently lead to the formation of immune complexes and increased ADC clearance.[95] Nonpolar drug-linker metabolites or ADC constructs with reducible disulfide bonds are able to enhance the bystander effect, whereas charged linker-drug metabolites or non-reducible thioether-conjugated ADCs exhibit a decreased bystander effect.[80] Consequently, the development of a proper ADC linker chemistry is challenging and a broad variety of different ADC linker is currently under development.[92] In general, two categories of ADC linker exist. Non-cleavable linkers release the biological active payload/linker catabolite including the last amino acid from the mAb after lysosomal degradation *e.g.* Lys-MCC-DM1.[96-98] In contrast, cleavable linker release the cytotoxic payload by three distinct mechanisms: (i) hydrolysis of an acid-labile hydrazone linker in the lysosome or endosome, (ii) dipeptide cleavage through lysosomal proteases, or (iii) linker reduction through glutathione.[80,99]

The cytotoxic payload determines the efficacy of ADCs and has to fulfill certain criteria. First of all, payloads must exhibit a high potency with half-maximal inhibitory concentration (IC_{50}) values in the picomolar range as only 1-2% of administrated ADC reach the intracellular drug target.[100] Another important aspect is the amount of cytotoxins attached to the mAb as antibodies with a low payload exhibit lower efficacies.[94] On the other hand, large amounts of toxins are associated with the likelihood for systemic toxicity and enhanced hydrophobicity, leading to aggregate formation and hence faster clearance, reduced half and shelf-life, and insolubility.[80] Lastly, the synthesis should be straightforward and the cytotoxin should retain its potency after introduction of reactive groups for linker conjugation.[80] Besides commonly used microtubuline-inhibiting or deoxyribonucleic acid-damaging payloads, α-aminitin (riboinucleic acid polymerase II inhibitor), rhizoxin (tubuline inhibitor), or spliceostatin and thailanstatin (both riboinucleic acid splicing inhibitors) are currently in development (Table 1.2).[80,101]

Table 1.2 Common linker and cytotoxic payloads used in ADC constructs.

Linker		Payload	Action
Cleavable	vc	Auristatin *e.g.* MMAE, MMAF	Tubuline inhibitor
	va	Maytansinoid *e.g.* DM1, DM4	Tubuline inhibitor
	SPDB	Calicheamicin *e.g.* ozogamicin	DNA cleaving agent
	sulfo-SPDB	Duocarmycin *e.g.* rachelmycin	DNA alkylation agent
	SPP	Doxorubicin	DNA intercalating agent
	Hydrazone	Benzodiazepine *e.g.* tesirine, talirine	DNA cross-linking agent
Non-cleavable	MCC	Tubulysin	Microtubule polymerization inhibitor
	mc	Camptothecin	Topoisomerase I inhibitor

vc: valine-citrulline, va: valine-alanine, SPDB: N-hydroxysuccinimidyl-4-(2-pyridyldithio)butanoate, sulfo-SPDB: N-hydroxysuccinimidyl-4-(2-pyridyldithio)-2-sulfobutanoate, SPP: N-succinimidyl-4-(2-pyridyldithio)pentanoate, MCC: maleimidomethyl cyclohexane-1-carboxylate, mc: maleimidocaproic acid, MMAE: monomethyl auristatin E, MMAF: monomethyl auristatin F, DM1: emtansine, DM4: ravtasine, DNA: deoxyribonucleic acid

1.2.3 Bispecific antibodies and truncated mAb-related modalities

Treatment with monospecific mAbs may cause drug resistance, leading to an inefficient therapeutic effect such as the inability to induce tumor cell destruction.[102] An advanced therapeutic effect can be induced with bsAbs due to their ability to bind multiple targets, antigens, or epitopes on the same antigen. Bispecific mAbs, can trigger the same mechanism of actions compared to mAbs.[103-105] In addition, bsAbs can force the formation of protein complexes by Fab arm binding to different proteins *e.g.* Factor IXa and X in order to mimic Factor VIIIa.[106] Depending on the mechanism of action and intended therapeutic application, a plethora of bispecific constructs with varying valence, size, flexibility, half-life, and biodistribution properties were developed throughout recent years, which can be mainly classified into five categories (Figure 1.7).[107-109] The production of bsAb generally relies on quadroma cell lines (fusion of two Ig-producing myeloma cells), which secrete a heterogeneous bsAb population including the desired hetero bsAb as well as nine additional variants due to random pairing of L and H chains.[108-110] In order to force the heterodimerization of H chains, the knob-into-hole technology is commonly applied for bsAb
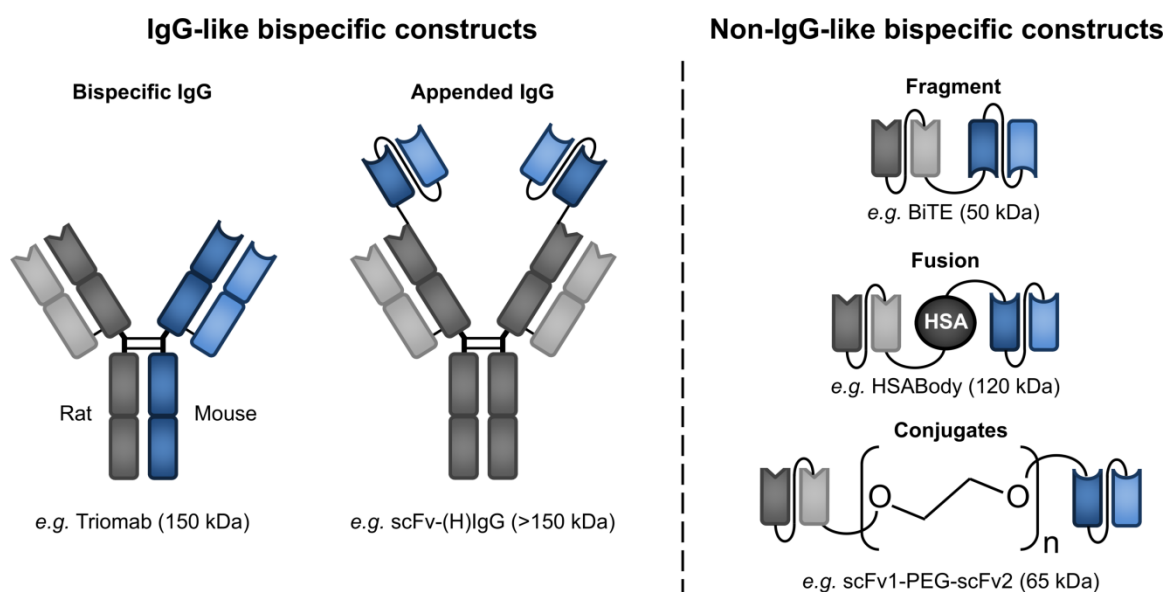
Figure 1.7 Examples of bispecific formats from each of the five major classes (bispecific IgGs, appended IgGs, bsAb fragments, bispecific fusion proteins, and bsAb conjugates). scFv: single chain variable fragment, BiTE: bispecific T cell engager, HSA: human serum albumin, PEG: polyethylene glycol

production.[111,112] This technology is based on creation of an artificial "knob" in the C_H3 domain of one H chain by replacing one amino acid with a larger one, whereas on the partner H chain a "hole" is designed by inserting a smaller amino acid instead of a larger one. The bispecificity can readily be introduced by adding a second antigen-binding unit to the N or C-terminus of the L or H chain as illustrated with the appended IgG (Figure 1.7).

Truncated bispecific formats such as the bispecific T cell engager are less immunogenic, exhibit enhanced tissue penetration, and bind epitopes that are sterically inaccessible for full-length mAbs.[107,108] Size reduction of mAb-related therapeutic proteins potentially alters their physicochemical properties and causes considerable changes in their biological activity.[113] On the other hand, truncated formats lacking the Fc region cannot induce Fc receptor-mediated processes and hence have a relatively short serum half-life.[108,114] In order to modulate PK properties including half-life extension by FcRn-mediated recycling, small-sized formats can be fused to Fc fragments, other proteins such as human serum albumin, or can be conjugated to polyethylene glycol.[107,108] Hence, the pharmacological properties can be customized for specific applications to improve the safety and efficacy.[114] Thus, various truncated (bispecific) Fc and variable region-containing mAb-related formats were developed for research and therapeutic purposes (Figure 1.8). The largest Fc region-containing truncated mAb format, namely camelid antibodies, lacks the L chain and the C_H1 domain (similar to shark antibodies) and uses only the V_H domain of camelids (referred to as V_HH) for antigen binding. Fc fusion proteins represent another important subclass of truncated mAb-related formats. This class of mAb-related therapeutic proteins consists of a Fc region fused to therapeutic ligands such as peptides, extracellular receptors, cytokines, or enzymes, which exhibit in this format a prolonged serum half-

life through interactions with the FcRn receptor.[115] The most advanced variable region-containing truncated mAb-related therapeutic proteins are F(ab')$_2$ and Fab fragments.[116] Nevertheless, the development of single chain variable fragments (scFv) has significantly progressed, accounting for up to 40% of clinically evaluated mAb fragments.[114] The range of scFv constructs includes simple formats (V_H and V_L linkage *via* flexible synthetic peptide), non-covalent scFv dimers (dia, tria, or tetrabodies) with an increased target affinity, and covalently linked tandem scFv.[117] Single domain antibodies, also referred to as Nanobodies, present the smallest version of truncated IgG-derived formats, containing only the V_H domain, which binds to specific antigens with a pico to nanomolar affinity.[118,119] General advantages of truncated mAb formats include a straightforward and cost-effective manufacturing process of a less heterogeneous mixture using prokaryotic systems, increased solubility, better stability, heat-resistance, and the aforementioned enhanced tissue penetration, while maintaining the selectivity for antigen binding.[113,114,120,121] On the other hand, truncated mAb-related formats bear the risk to cross-react with endogenous antibodies, which specifically recognize antibody fragments but not their full-length counterparts, resulting in negative biological effects through cytokine release or liver toxicity.[122-124] Besides their use as affinity capture antibodies, potential diagnostic applications of truncated mAb-related constructs include their use as chromobodies for intracellular target identification and non-invasive *in vivo* imaging with radionuclides.[125-128] Therapeutic applications involve the treatment of various forms of cancer, rheumatoid arthritis, acute lymphoblastic leukemia, or scorpion/snake envenomation.[117,129-132]
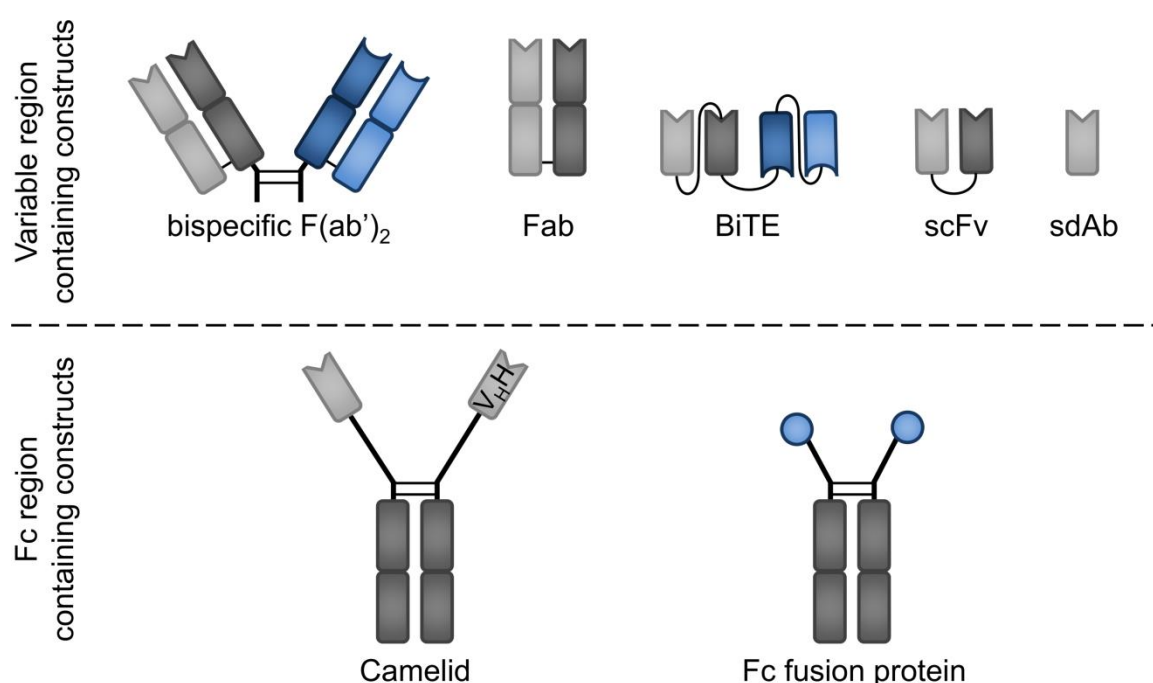
Figure 1.8 Schematic illustration of various truncated mAb-related therapeutic proteins. V_HH: variable region of camelid antibodies, BiTE: bispecific T cell engager, sdAb: single domain antibodies

1.3 Market development of mAb-related therapeutic proteins

The number of new molecular entities and biological license agreements, which were granted first marketing approval, dropped in 2016 compared to the previous year from 45 to 22 and from 39 to 27 as reported by the US FDA and EMA, respectively.[133-135] Seven out of the 22 novel drug approvals for the US market were mAb-related therapeutic proteins, whereas only three of them namely *olaratumab*, *reslizumab*, and *ixekizumab* were approved in the EU.[136] Considering the latest publicly available sales revenue data, an increase by 16.9% was reported in 2016, which resulted in a global sales revenue of 107 billion US$.[137] Twenty five mAb-related therapeutic proteins reached blockbuster status with a sales revenue over 1 billion US$, whereas seven out of them (*i.e. adalimumab*, *etanercept*, *infliximab*, *rituximab*, *trastuzumab*, *bevacizumab*, and *aflibercept*) exceeded a threshold of five billion US$.[137] Additionally, >300 mAb-related therapeutic proteins were estimated to be in early-stage development, >230 mAb-related modalities were reported in clinical phase II, 52 mAb-related entities were listed in late-stage clinical trials, and eleven constructs were under regulatory review by the US FDA and EMA as of Dec 2016.[136,138]

Similar to previous years,[139] the majority of novel drug approvals in the first three quarters of 2017 can be assigned to low-molecular weighted chemical entities. Nevertheless, the number of approved mAb-related therapeutic proteins as of Nov 14th 2017 has reached its maximum throughout the last decade (n=17). In terms of originator drugs, five novel IgGs (*avelumab*, *dupilumab*, *ocrelizumab*, *durvalumab*, and *guselkumab*) were exclusively licensed for the US market, whereas *bezlotoxumab* and *atezolizumab* were approved in the EU after receiving US approval already in 2016. *Brodalumab*, *sarilumab*, and *inotuzumab ozogamicin* (Besponsa, a novel calicheamicin-based ADC) were granted market approval on both markets. Additionally, *gemtuzumab ozogamicin* (Mylotarg) received approval for its relaunch by the US FDA early in Sep 2017 after it has been withdrawn from the market in 2010.[140] Consequently, together with *brentuximab vedotin* (Adcetris) and *trastuzumab emtansine* (Kadcyla), which received EU approval in 2012 and 2013, respectively, four ADCs are currently licensed for marketing in the US and EU.

The remaining six approved mAb-related therapeutic proteins were copies of already licensed blockbuster biologics, so called biosimilars, which demonstrated comparable physicochemical characteristics, quality, purity, (non-)clinical efficacy and safety in biosimilarity studies.[141-143] Novartis' Erelzi and Amgen's Solymbic/Amjevita, were approved in EU, but received US approval already in 2016. The remaining biosimilars were copies of *adalimumab* (Biogen's Imraldi) and *rituximab* (Novartis/Sandoz' Rixathon and Celltrion's Truxima), whose patents in the US and EU will expire in 2018.[144] In addition, Pfizer's Lifmior was approved, copying *etanercept*, whose EU patent already expired in 2015, while its US patent will last until 2028.[145,146] Hence, in total 10 mAb biosimilars have received marketing approval since their first introduction in 2013 (Figure 1.9).
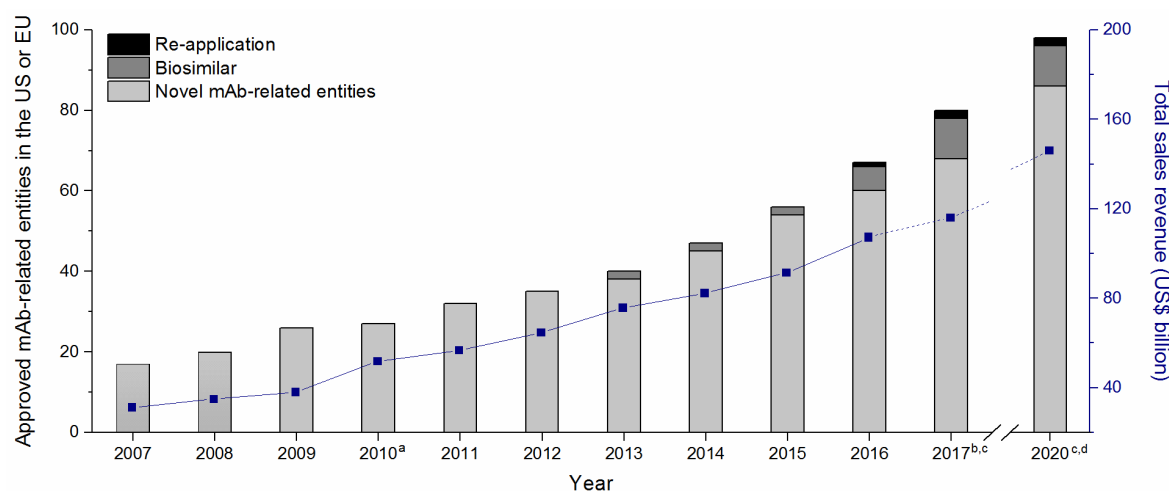
Figure 1.9 Trend of mAb-related therapeutic proteins granted marketing approval in the US or EU and reported sales revenue. Sales revenue data were extracted from publicly available financial reports or scientific articles.[137,138,147-150] Notes: [a] Prolia and Xgeva (both *denosumab*) were approved in 2010, but were counted as single entity, [b] number of approved mAbs as of Nov 14th 2017, [c] estimated sales revenue based on a compound annual growth rate in sales of 8.0%, [d] estimated number of approved mAb-related entities using a mean annual approval rate of 5.9 mAbs per year (2007-2017)

As of Nov 14th 2017, the majority of the 81 marketed mAb-related therapeutic proteins rely on full-length mAbs followed by Fc fusion proteins, while only a minor portion is based on mAb fragments (Figure 1.10a). This distribution is related to an improved effector function, extended serum half-life, and better neutralization effects in presence of the Fc region.[24,151] The class of full-length mAbs is further composed of 59 first-generation mAb-related therapeutic proteins (unconjugated mAbs and their biosimilars), whereas the bsAb and the four ADCs belong to next-generation mAb-related constructs (inlet Figure 1.10a). Since murine and chimeric mAbs feature an increased risk to induce the formation of human anti-mouse antibodies,[55] 77% of licensed full-
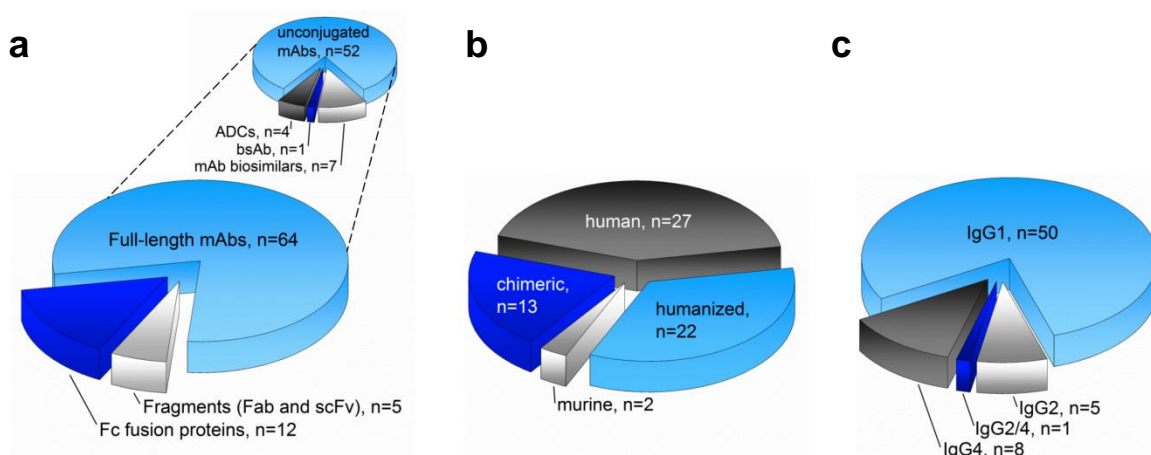
Figure 1.10 Distribution of licensed mAb-related therapeutic proteins according to their (**a**) format, (**b**) source of full-length mAbs, and (**c**) isotype subclass of full-length mAbs.

length mAbs are nowadays of human or humanized origin (Figure 1.10b). Due to their potency to effectively induce effector functions, most of the marketed full-length mAbs belong to the IgG1 isotype subclass followed by the IgG4 and IgG2 isotype subclasses with *eculizumab* representing the only hIgG2/4 isotype subclass hybrid (Figure 1.10c). Although the IgG3 isotype subclass exhibits among all IgG isotype subclasses the highest affinity to various Fc receptors (Table 1.1), no therapeutic protein related to this subclass is currently licensed due to its relatively short serum half-life, increased likelihood for proteolysis due to the prolonged hinge region, and the existence of several allotypes.[24,152] A similar distribution in terms of format, source, and isotype subclass is also reflected by the constructs currently in development.[136,139,153] Taking the mean annual approval rate of 5.9±4.0 mAbs per year (2007-2017) and the estimated five-years compound annual growth rate of 8.0% (2014-2019) into account,[138,154] almost 100 mAb-related therapeutic proteins will be marketed in the US or EU by 2020, resulting in a forecasted global sales revenue of 145 billion US$ (Figure 1.9). Consequently, mAb-related therapeutic proteins represent one of the fastest growing therapeutic classes and pharmaceutical companies invest notable resources in the development of such constructs.

1.4 Required assays for the development of mAb-related entities

Not only the diversity of mAb-related therapeutic proteins, but also the implementation of a variety of required assays represents a tremendous analytical challenge during their drug development. Mandatory assays can be divided into two categories: (i) qualitative assays for mAb-related therapeutic protein characterization and (ii) bioanalytical assays for PK, PD, and IG assessments.

1.4.1 Qualitative assays for mAb-related therapeutic protein characterization

In order to ensure high product quality, safety, and efficacy of mAb-related therapeutic proteins, a multitude of mostly MS-based analytical tools is employed for batch-to-batch control analysis, structural characterization, and comparability studies (Figure 1.11).[87,155,156] Characterization of structural conformation, epitope mapping, aggregate analysis, or protein-ligand interactions are commonly investigated at higher order structure, utilizing hydrogen/deuterium exchange MS,[157,158] chemical cross-linking MS,[159] or native MS either as stand-alone technology[160-162] or with ion mobility.[163-166] Top-down analysis provides important information about the intact mass, major modifications, and charge/size variants of mAbs.[162,167-173] Moreover, the DLD and DAR of ADCs can readily be assessed at the intact level.[174-176] Middle-up approaches enable the detection of positional isomers and mAb truncations or extensions in addition to the previously mentioned modifications.[177] The most detailed information about the primary amino acid sequence,[155,178] potential conjugation sites,[177,179,180] and post-translational modifications[181-185] are provided with bottom-up approaches. Transitioning from intact to peptide level further allows the refinement of structural modifications and the exact location can be identified (*e.g.* mAb oxidation site).[169,181,186]
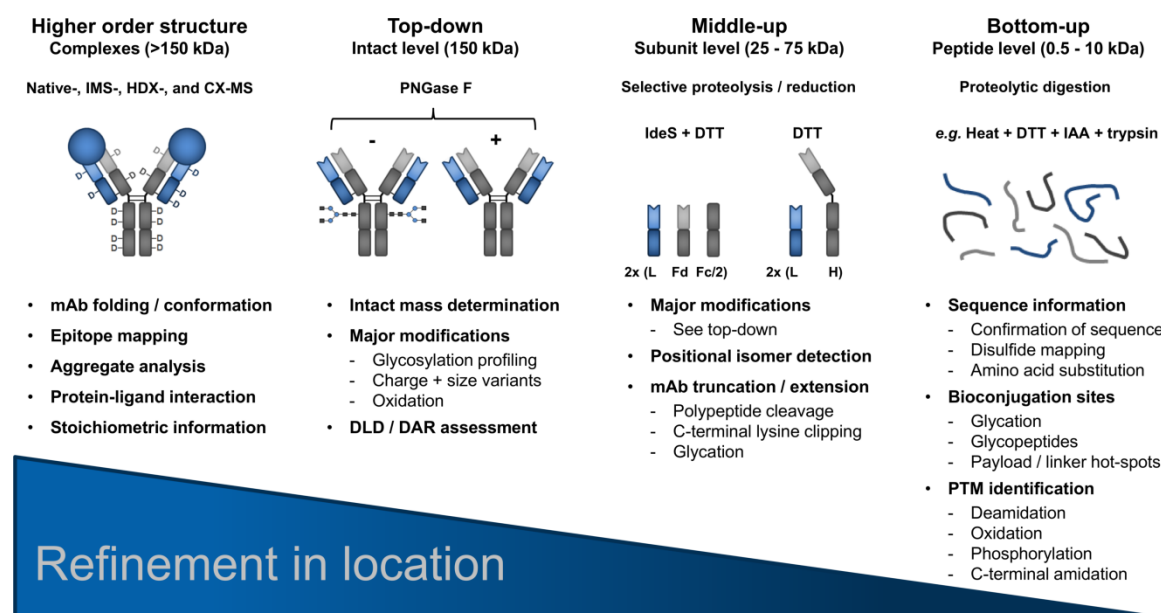
Figure 1.11 Qualitative assessment of mAb-related therapeutic proteins at different structure levels. IMS: ion mobility, HDX: hydrogen/deuterium exchange, CX: cross-linking, PNGase F: N-glycosidase F, IdeS: IgG-degrading enzyme of *S. pyogenes*, DTT: dithiothreitol, Fd: Fab H chain, IAA: iodoacetamide, PTM: post-translational modifications

1.4.2 Bioanalytical assays for PK, PD, and IG assessments

During the drug discovery and development process, several reliable and robust bioanalytical assays have to be implemented for PK, PD, and IG assessments in order to investigate the exposure-response relationships between mAb-related therapeutic proteins and their target(s), to evaluate safety margins, and to select the proper dosing regimen.[187] At pre-clinical stage, quantitative assays are required for exploratory non-good laboratory practice (GLP) dose range finding studies and GLP toxicity studies in one rodent and one non-rodent species in order to design an appropriate first-in-human GLP study.[188] However, pre-clinical studies using only one relevant species may be sufficient in certain justified cases, if the biology of the mAb-related therapeutic protein is well understood and characterized.[189] In addition to the *in vivo* generated mAb catabolites and metabolites, the variable region of the mAb-related therapeutic protein with its binding site(s) further complicates quantitative assessment due to antigen interaction.[190] Consequently, the administrated mAb-related therapeutic protein and its soluble target exist in different binding states (Figure 1.12). However, only the free mAb-related therapeutic protein species has target-binding potential and is able to induce pharmacological effects.[191,192] Consequently, bioanalytical assays have to be developed, which are capable to discriminate between free and bound species in order to estimate the efficacious mAb concentration.[190] In contrast, information about the total mAb concentration provides insights into the dynamic relationship with the target, allowing the determination of on and off-target toxicological effects.[187]
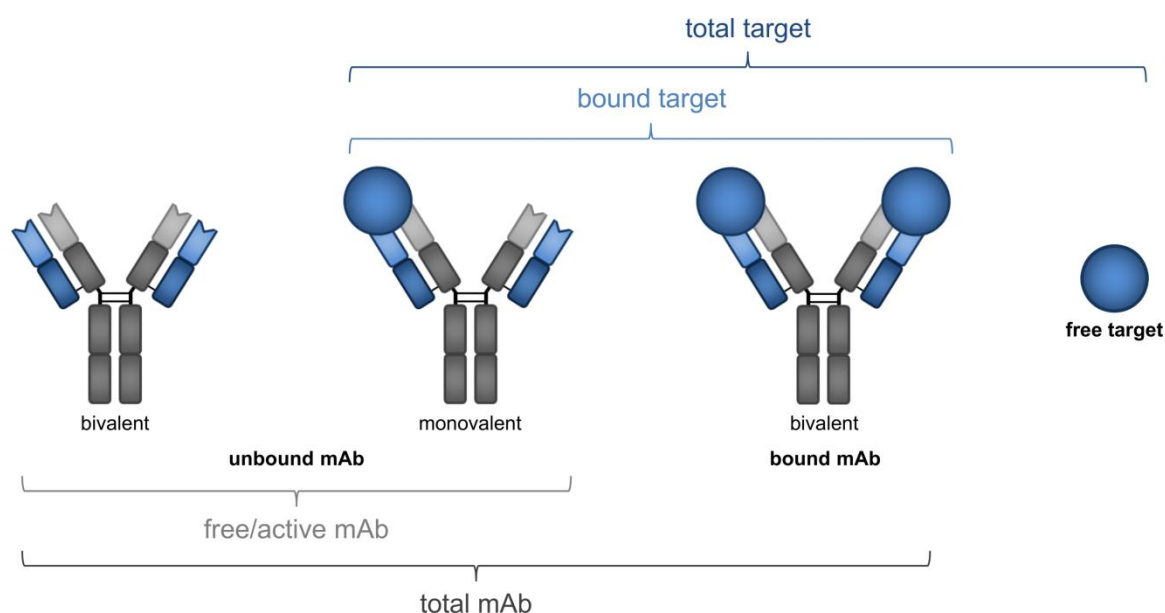
Figure 1.12 Schematic illustration of potential mAb and target species present *in vivo*.

Besides PK/PD assays, additional analytical methods for IG assessments are required as the presence of exogenous modalities *in vivo* triggers the formation of endogenous ADAs, which alter the PK, PD, and safety profiles.[193] The formation of ADAs strongly depends on the proportion of foreign amino acids and post-translational modifications in the administered mAb, administration route, dosing regimen, and the duration of exposure.[55] The resulting immune complexes decrease the half-life of the administered mAb-related therapeutic protein due to enhanced clearance, which is indicated by a fast concentration drop in the PK profile.[23] Lastly, the number of required bioanalytical assays is further increased, if bioconjugated therapeutic proteins such as ADCs have to be analyzed (Table 1.3).

Table 1.3 Assays required for ADC PK, PD, and IG assessments. Adapted from Myler H *et al.* (2015)[194]

Assessment	Analyte	Information / physiological effect
PK	Total mAb	Clearance
	Total ADC	Total mAb > total ADC = deconjugation of payload
	Active ADC	Total ADC > active ADC = inactivation through metabolism
	Conjugated active payload	Similar to active ADC assay
	Metabolized conjugated payload	Indication for inactivation of ADC
	Unconjugated payload	Deconjugation and off-target toxicity
PD	Total target	Effect of mAb / ADC on target accumulation
	Bound target	Therapeutic efficacy
	Free target	Therapeutic efficacy
	Cytotoxic biomarker	Apoptosis, lysis
IG	mAb / ADC-specific ADA	Accelerated clearance / neutralization
	Payload-specific ADA	Accelerated ADC clearance and potential decelerated clearance of unconjugated payload

1.5 Analytical platforms for PK, PD, and IG assessments

1.5.1 Ligand binding assays

LBAs with the enzyme-linked immunosorbent assay (ELISA) as most prominent format are conventionally employed for PK, PD, and IG assessments of mAb-related therapeutic proteins.[187,195,196] Depending on the ELISA design, these assays measure indirectly specific mAb and target species either in their free or bound form through reversible non-covalent interactions with an antigen or detection antibody. The sandwich ELISA exhibits the highest selectivity among the existing ELISA formats due to the use of two different epitope-recognizing antibodies as exemplified with a possible format for total PD assessment (Figure 1.13a). A fixed amount of anti-target capture antibody is immobilized on the plate surface. This capture antibody must be non-cross reactive to the mAb in order to avoid binding competition. In a next step, a diluted biological serum sample is added to the plate, followed by an enzyme-linked detection antibody (direct sandwich ELISA). If the primary detection antibody is unlabeled, a secondary enzyme-linked detection antibody has to be subsequently introduced (indirect sandwich ELISA). Binding of the detection antibody (*e.g.* anti-hIgG Fc peroxidase) to the target conjugated-mAb is indicated by a change in color induced by the reaction of the detection antibody-linked enzyme with its substrate (*e.g.* horseradish peroxidase and tetramethylbenzidin). Following termination of the enzymatic reaction and colorimetric read-out at a specific wavelength, the concentration of the mAb-conjugated target can be determined. By replacing the anti-target capture antibody with the target itself, the free mAb concentration can be determined for PK assessment (Figure 1.13b). In contrast, the bridging ELISA utilizes only one antigen/antibody for capture and detection as exemplified with one possible format for the determination of the total mAb (Figure 1.13c) and bivalent unbound mAb (Figure 1.13d) concentration.
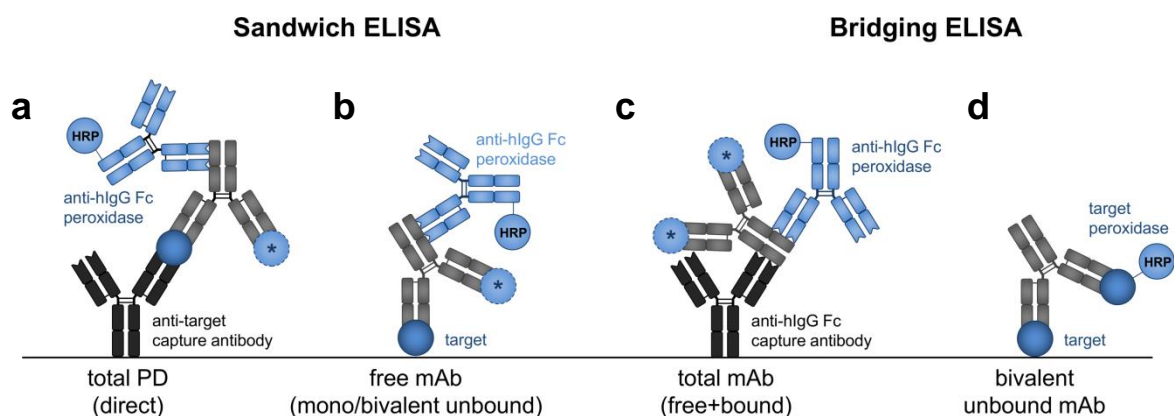
Figure 1.13 Possible sandwich and bridging ELISA formats for the determination of (**a**) total PD, (**b**) free mAb, (**c**) total mAb, and (**d**) bivalent unbound mAb for PK assessment. The asterisks indicate optional target conjugation to the mAb. HRP: horseradish peroxidase

Based on the three proposed PK assays, the concentration of bivalent bound mAb (total minus free), mono and bivalent bound mAb (total minus bivalent unbound) as well as the monovalent bound mAb (free minus bivalent unbound) can be derived. Despite of minimal requirements in sample preparation, high sensitivity (pg/mL to ng/mL range), relatively low analytical costs per sample, and high sample throughput,[190,197-201] ELISA formats exhibit the following disadvantages:

- Robustness, sensitivity, and specificity depend on the quality of capture and detection antibodies[190,202,203]

- Expensive and time-consuming development of specific capture antibodies with optimal binding properties[197,204]

- Difficult method transfer as the specificity is strongly affected by the sample matrix with varying extent of interferences and cross-reactivity[205]

- No discrimination between the parent mAb and generated catabolites or metabolites

- Analytical bias from the sample preparation and analysis cannot be corrected as no internal standard (ISTD) is employed[199,206]

1.5.2 Mass spectrometry-based assays

In order to overcome disadvantages associated with LBAs, MS-based assays have evolved in the recent years as a complementary analytical technology for PK, PD, and IG assessments of mAb-related therapeutic proteins in complex matrices.[207-217] In contrast to LBAs, MS-based assays offer an increased specificity and robustness, a wider linear dynamic range, shorter method development time, ability to multiplex, and the possibility to implement an ISTD to minimize matrix effects, which facilitates method transfer between biological matrices.[200-202,218-222] The majority of MS-based assays utilizes proteolytic peptides as surrogates for an indirect quantification of the parent mAb-related therapeutic protein (bottom-up approach) due to the following reasons:

- Superior sensitivity compared to the analysis at the intact protein level[223]

- Less analytical variability is generated at the peptide level in comparison to the intact protein as surrogate peptides are usually selected from a domain where post-translational modifications unlikely occur[202,224]

1.5.2.1 Selection of surrogate peptide

The selection of the most appropriate surrogate peptide is critical and affects the assay specificity, sensitivity, and robustness.[201,218,224,225] Several *in silico* software tools such as Skyline, PeptideAtlas, PeptideSieve, MRMaid, MRMer, or MaRiMba assist in the selection of surrogate peptides.[226-231] The ideal surrogate peptide should be rapidly and reproducibly generated during proteolytic digestion, should be stable, and should exhibit a unique amino acid sequence based on the following criteria:

- No methionine, cysteine (Cys), or tryptophan (Trp) included to avoid peptide oxidation[218]

- No glycosylation sites on asparagine [Asn-x-Ser and Asn-x-Thr whereby x can be any amino acid except for proline, serine (Ser), or threonine (Thr)], on hydroxyl groups (Ser and Thr rich regions), or on other motifs known to be glycosylated (Trp-x-x-Trp, Trp-Ser/Thr-Cys)[232-235]

- Proline should be not located downstream of lysine or arginine and the location of two basic amino acids next to each other should be avoided to prevent peptide miscleavage[201,218]

- Peptide length should be 8-20 amino acids to guarantee adequate retention under reversed-phase chromatographic conditions and appropriate mass spectrometric properties in terms of ionization and fragmentation[218]

In order to verify the uniqueness of the surrogate peptide, proper bioinformatic software tools such as the *Basic Local Alignment Search Tool* (BLAST) are available, which compare the amino acid sequence of a peptide with protein sequences entered in databases.[236] In general, surrogate peptides from the CDR region are highly specific for each individual mAb and less susceptible for interferences from endogenous IgGs.[207,237,238] However, a novel assay has to be developed for each new construct. In order to circumvent this issue and accelerate method development, generic surrogate peptides from the constant region (C_L, C_H1, C_H2, and C_H3) were proposed for the quantitative analysis at pre-clinical stage. These peptides are conserved throughout chimeric, humanized, and human IgGs as well as in any mAb-related construct bearing the human constant region (*e.g.* Fc fusion proteins), but they are absent in IgGs from animal species.[239-243] Hence, only a single generic bottom-up MS-based assay has to be implemented to generate quantitative data for a multitude of mAb-related therapeutic proteins in pre-clinical species as recently demonstrated and successfully validated.[244]

1.5.2.2 Bottom-up sample preparation approaches

Mainly two different sample preparation approaches are applied to generate surrogate peptides, which are required for bottom-up mAb-related therapeutic protein quantification (Figure 1.14). The first approach employs direct digestion of the untreated sample. Beneficial features of this approach include rapid method development, no requirement for target specific reagents (important for candidate screening), multiplexing capabilities, and small sample volume consumption (≤25 µL).[245-247] Furthermore, no assay-specific interferences are caused from ADAs and bound endogenous proteins or soluble targets.[248] In contrast to the quantitative analysis of small molecules by LC-MS/MS or mAb quantification by LBAs, the sample complexity is significantly increased following digestion, generating peptides with similar physicochemical properties.[248,249] Due to co-eluting and interfering compounds,[250] direct serum digestion approaches exhibit a limited sensitivity.[238,251,252] In order to reduce the amount of interfering background peptides, clean-up strategies such as solid phase extraction (SPE) or enrichment of specific peptides using *stable isotope standards and capture by anti-peptide antibodies* (SISCAPA) can be incorporated.[253-255] The second approach for bottom-up mAb quantification

utilizes protein-level IC with subsequent proteolytic digestion of the immuno-captured protein either directly on the solid support material or after elution.[256-259]

Regardless of the applied workflow, conventional digestion protocols for mAb-related therapeutic protein quantification contain four steps: (i) unfolding of the quaternary structure of the protein upon denaturation with heat,[260] chaotropic agents (urea, guanidine hydrochloride),[237,261] surfactants (sodium dodecyl sulphate, sodium deoxycholate),[242,262] or organic solvents (methanol, acetonitrile (ACN), and trifluoroethanol),[263,264] (ii) disulfide bond reduction with dithiothreitol (DTT) or tris(2-carboxyethyl)-phosphine,[238,265] (iii) alkylation of the generated reactive thiol groups with iodoacetamide (IAA) or N-ethylmaleimide,[238,266] and (iv) proteolytic digestion using trypsin, chymotrypsin,[267,268] Lys-C,[269,270] Glu-C,[271,272] Arg-C,[273] Asp-N,[274,275] or pepsin[276,277] with a recommended enzyme to protein ratio ranging from 1:20 to 1:100.[218] After proteolytic digestion, the peptides can be analyzed with a variety of different mass analyzers operating in different acquisition modes as described in section 1.5.2.4.
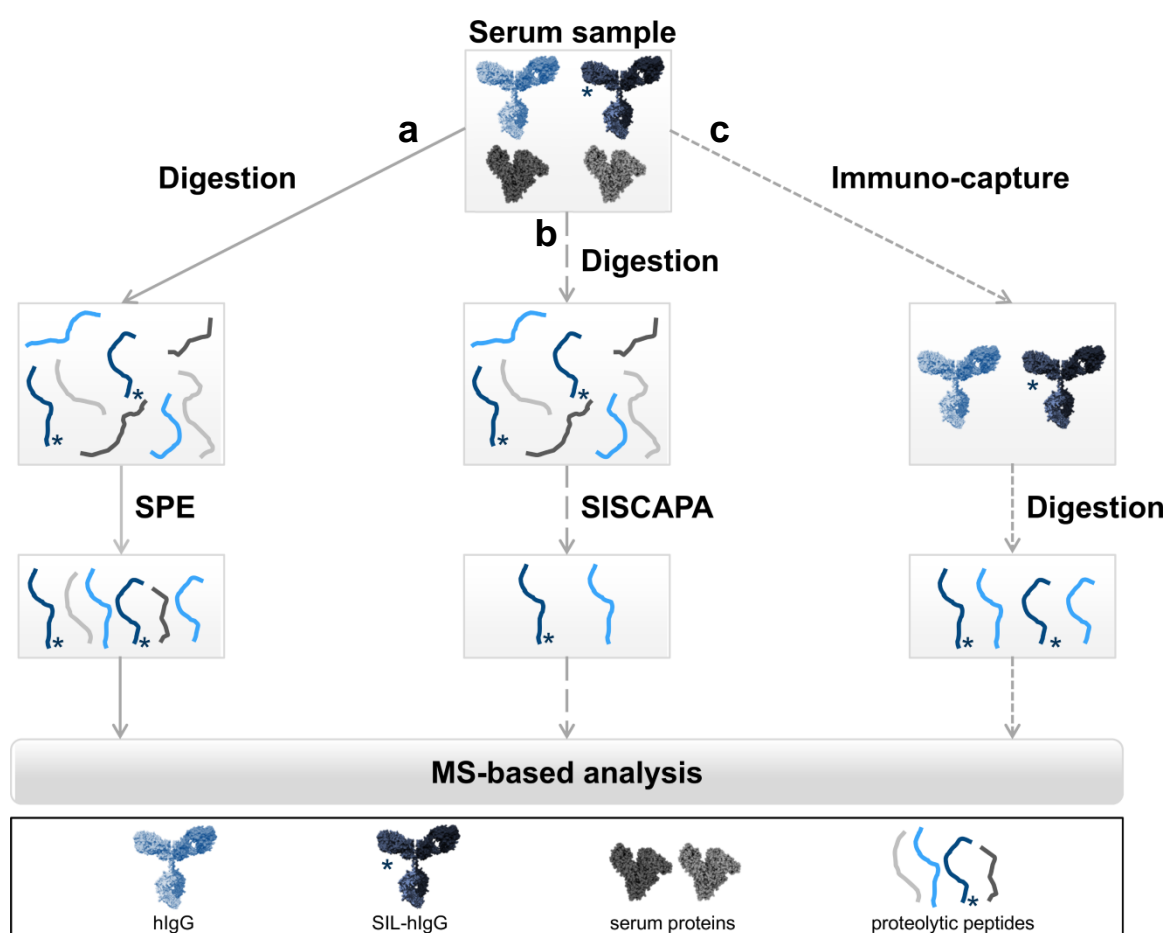
Figure 1.14 Commonly applied sample preparation procedures for bottom-up mAb-related therapeutic protein quantification by MS-based assays using (**a**) direct digestion approaches, (**b**) peptide-level, or (**c**) protein-level enrichment. SIL: stable isotope labeled

1.5.2.3 Internal standardization

Analytical variation originates either from the multistep bottom-up sample preparation, chromatographic separation (*i.e.* variability of injection volume or retention time), or MS analysis (*i.e.* matrix effects enhancing or suppressing the analyte signal).[278,279] As a consequence, the employment of a proper ISTD is essential for reproducible, precise, and accurate mAb-related therapeutic protein quantification. However, the format and introduction stage of the ISTD (Figure 1.15) can significantly impact the outcome of the quantitative data.[280-282]
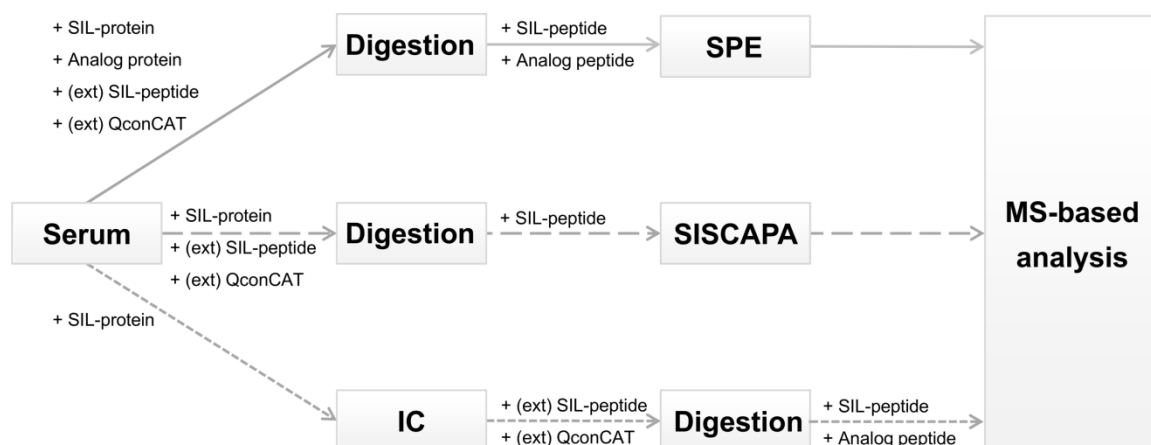
Figure 1.15 Overview of ISTD formats and possible introduction stages for bottom-up mAb-related therapeutic protein quantification by MS-based assays. SIL: stable isotope labeled, ext: extended, QconCAT: quantification concatemer

Peptide-level ISTD

Ideally, the ISTD is introduced at the earliest sample preparation stage and has similar physicochemical properties like the target analyte.[283] At the same time, it should exhibit a sufficient mass difference for its distinction from the target analyte by MS detection.[283] Hence, a stable isotope labeled (SIL) version (*i.e.* [^{13}C], [^{15}N], [^{2}H], or [^{18}O]) of the signature peptide, also referred to as *absolute quantification* (AQUA) peptide, is often utilized for protein quantification.[284-286] Differential labelling represents another simple and cost-effective possibility to generate SIL-peptides.[287] Alternatively, a structural analog peptide can be used which, however, might not correct as appropriate as SIL-peptides.[288-290] One advantage of peptide-level ISTDs relies on their faster and simplified production compared to protein-level ISTDs.[218] However, they can only compensate for variations induced post-digestion and hence correct only for peptide stability as well as for differences introduced upon LC-MS analysis.[218] Consequently, extended SIL-peptides with cleavable sequence tags were developed to partially compensate also for variations during proteolytic digestion.[291-293] The concatenation of several SIL-peptides, as employed with the

quantification concatemer (QconCAT) or *double standard concatemers* (DOSCAT) strategy,[294-297] creates an artificial protein-like construct, which can be selected as ISTD for multiplexed protein quantification.[298-300]

Protein-level ISTDs

Although structural analog proteins were applied for internal standardization, they cannot correct all induced variabilities similar to peptide-level ISTDs.[301-303] Hence, a SIL-variant of the whole protein would be the ideal ISTD to compensate for all introduced variabilities during the entire workflow.[283] However, their production is expensive and time-consuming.[218] SIL-whole protein ISTDs, also referred to as *protein standard absolute quantification* (PSAQ),[304-308] are produced in the same expression system or cell line as the mAb-related therapeutic protein with the difference that the medium contains SIL-amino acids for label incorporation.[309,310] By applying this *stable isotope labeling with amino acids in culture* (SILAC) approach, several SIL-whole protein ISTDs with different labeling strategies were successfully expressed, purified, and implemented for MS-based quantification of mAb-related therapeutic proteins.[238,240,311] Alternatively, universal SIL-whole protein ISTDs such as the *SILu™mAb* are nowadays commercially available, which likewise demonstrated the potential for mAb quantification.[243,312]

1.5.2.4 Mass analyzers for mAb-related therapeutic protein quantification

Various low and high-resolution mass analyzers operating in different acquisition modes have been applied for protein quantification.[218,224] The following section focuses on the mass analyzers utilized in this thesis and discusses the working principle of different acquisition modes suitable for mAb-related therapeutic protein quantification.

Triple quadrupole and quadrupole linear ion traps

The majority of bioanalytical MS-based assays for bottom-up mAb-related therapeutic protein quantification is conducted with tandem mass spectrometers either in the design of sequentially connected quadrupoles (QqQ) or hybrid quadrupole linear ion traps (QTRAPs).[224] QTRAP instruments operate either in the ion trapping mode to conduct multiple-stage fragmentation experiments (MS^n) or in the conventional QqQ mode.[313,314] For quantitative purposes, selected reaction monitoring (SRM), also partially referred to as multiple reaction monitoring (MRM), is the most appropriate acquisition mode providing high selectivity and sensitivity.[315] In SRM, a precursor ion with a specific *m/z* value is mass filtered from a complex mixture of ions in a first quadrupole Q1 (Figure 1.16). The detailed mathematical description of the exact quadrupole working principle is provided elsewhere and not discussed herein.[316,317] After precursor ion selection, its fragmentation in a serially connected second non-filtering quadrupole q2 is induced by collisional activation with neutral gas molecules or dissociation, where translational ion energy is converted into internal energy.[318] As a result of increased internal energy and unimolecular decomposition, charged and neutral product ions are formed. In a last step, the third quadrupole Q3 selects a

specific charged product ion for detection. By monitoring more than one transition for each peptide, the selectivity can be increased as the SRM acquisition mode allows sequential scanning of hundreds to thousands of transitions (Figure 1.16).[319,320] The most intense transition of a peptide is often selected as a quantifier, while the other transition(s) act as qualifier, confirming the analyte identity.[321,322] The cycle time is an important parameter, which requires consideration when monitoring several transitions.[225,315] The cycle time is defined as the product of the number of monitored transitions and the time spent at each transition (dwell time).[225,323] The dwell time affects the sensitivity [signal-to-noise (S/N) ratio], whereas the cycle time determines the sampling rate (number of data points across at the chromatographic peak) and subsequently the inter-run accuracy and reproducibility.[323] Consequently, all parameters have to be balanced and optimized for a SRM-based quantification. Despite the enhanced selectivity and sensitivity provided by the SRM acquisition mode, low-resolution mass analyzers such as QqQ or QTRAP cannot completely eliminate interfering signals from a complex sample. As a consequence, high-resolution mass analyzers such as the quadrupole orbitrap or QTOF were implemented, particularly in the field of targeted proteomics.[324-329]
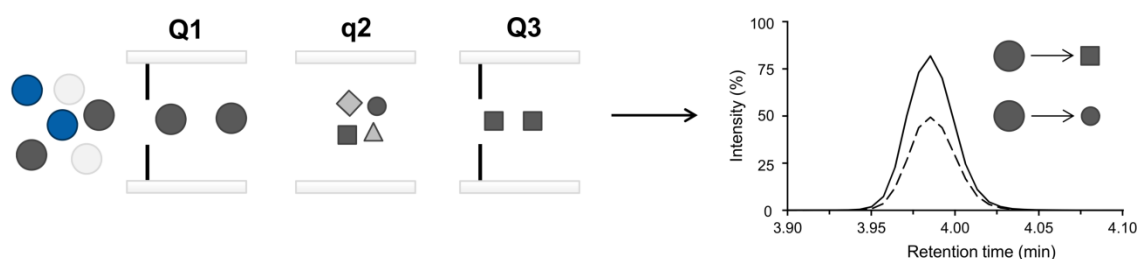
Figure 1.16 Working principle of the SRM acquisition mode. A precursor ion is mass filtered in the first quadrupole (Q1), fragmented in a serially connected non-filtering quadrupole (q2), and a specific product ion is selected in the third quadrupole (Q3) for detection. Multiple transitions of an analyte (precursor/product ion pairs) can be sequentially scanned to increase the selectivity.

Quadrupole orbitrap

Hybrid instruments, which are constituted of a quadrupole and an orbitrap mass analyzer such as the Q-Exactive orbitrap mass spectrometer from Thermo Fisher Scientific (Figure 1.17), combine the benefit of mass filtering, selective ion trapping, and analyte detection at high-resolution and mass accuracy.[330] Three different acquisition modes, namely full-scan MS,[331,332] single-ion monitoring,[333,334] and parallel reaction monitoring[331,335,336] were applied for quantitative analysis.

In the **full-scan MS** acquisition mode all charged ions are transmitted through the quadrupole and accumulate in a curved linear trap (C-Trap). The duration of accumulation is governed by a predefined maximum filling time and an automatic gain control setting (maximum number of ions entering the C-Trap). Following trapping, all accumulated ions are simultaneously injected into the orbitrap mass analyzer for detection, which is composed of a central spindle-like electrode and a
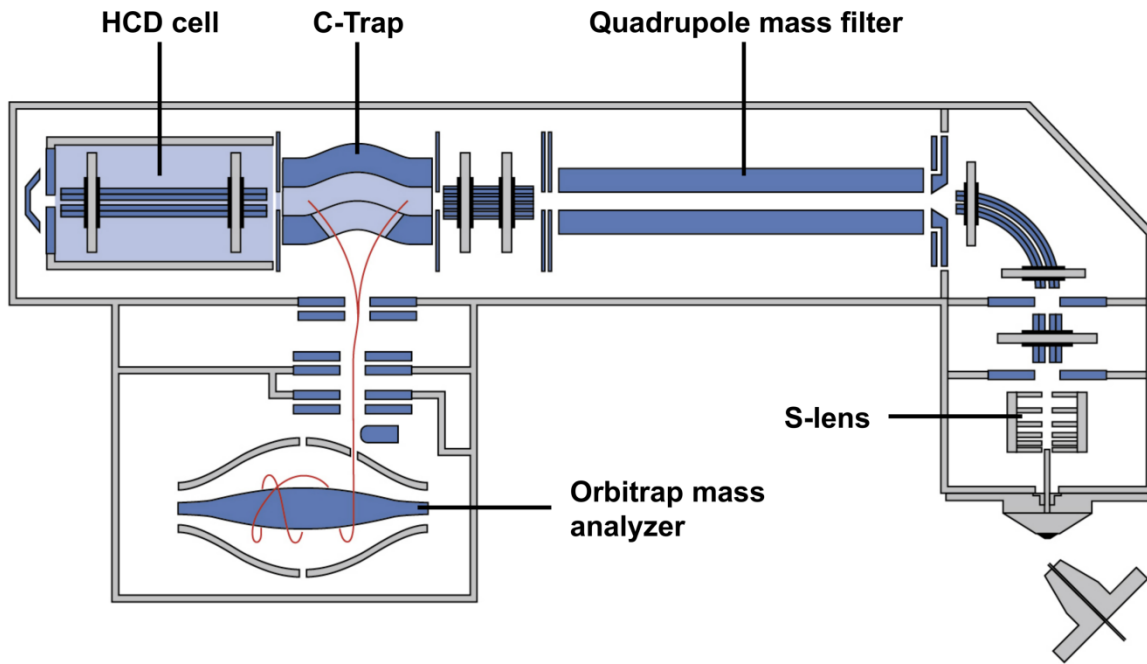
Figure 1.17 Schematic illustration of the Q-Exactive orbitrap mass spectrometer. Courtesy of Thermo Fisher Scientific. HCD: higher energy collisional dissociation

barrel-like outer electrode.[337] Injected ions rotate in orbital trajectories around the central electrode and simultaneously oscillate in horizontal direction, which describes a harmonic oscillator given by equation 1.1

$$z(t) = z_0 \cos(\omega t) + \sqrt{\frac{2E_z}{k}} \sin(\omega t) \qquad (1.1)$$

where z_0 is the initial axial amplitude, E_z the initial ion kinetic energy and

$$\omega = \sqrt{\frac{kz}{m}} \qquad (1.2)$$

is the frequency of axial oscillation with k as the constant potential between the electrodes, m the mass, and z the charge of the ion.[338,339] Based on the axial oscillation frequency, the m/z ratio of the ion can be determined following Fourier transformation.[340] As a result of an increased resolution compared to QqQ mass analyzers, the analyte can be discriminated to some extent from background ions by extracting its exact (theoretical) m/z value with a narrow mass extraction window (MXW) from the full-scan MS spectrum. For enhanced selectivity and sensitivity, targeted quantification approaches either at the precursor or product ion level can be employed.

Quantification based on the precursor is mostly conducted using **single-ion monitoring**. In this mode, a selected precursor ion is mass filtered in the quadrupole based on a predefined width of the isolation window, accumulated in the C-Trap, and transmitted to the orbitrap mass analyzer for

detection. An additional level of selectivity is introduced by conducting quantification at the product ion level using **parallel reaction monitoring**.[341] Instead of accumulation in the C-Trap, a mass filtered precursor ion is transmitted to the higher energy collisional dissociation cell. Following fragmentation, product ions are transmitted back to the C-Trap for accumulation with subsequent injection in the orbitrap. In contrast to SRM analysis, which acquires only one transition at a specific point of the cycle time, parallel reaction monitoring acquires all reactions and hence product ions from a given precursor ion.[342,343] This allows flexible selection and summation of different product ions in case of selectivity and sensitivity issues, respectively.[336] For both targeted quantification approaches, only two analyte-specific information (precursor ion *m/z* value and its retention time window) and three instrumental parameters (*i.e.* the resolution, the maximum filling time of the C-Trap, and the quadrupole mass isolation window) are necessary to implement sequential, simultaneous, or multiplexed targeted quantification experiments.[341]

Quadrupole time-of-flight

Similar to the mass analyzers discussed previously, QTOF instruments are composed of a mass filtering quadrupole and a serially connected collision cell whereby the last module is a TOF mass analyzer as illustrated with the Synapt G2-Si QTOF mass spectrometer from Waters (Figure 1.18). Similar to the quadrupole orbitrap mass analyzer, quantitative analysis can be conducted at the precursor (TOF-MS) or product ion level (TOF-MS/MS or TOF-MRM).[344-346]

When operated in the **TOF-MS** mode, charged ions are sampled, focused, and entirely transmitted through the quadrupole and collision cell.[347] Following transmission through the collision cell, the ion beam is refocused and accelerated into a modulator region. In this region, ions are orthogonally pushed by a pulsed electric field with an accelerating voltage *U* into a field-free
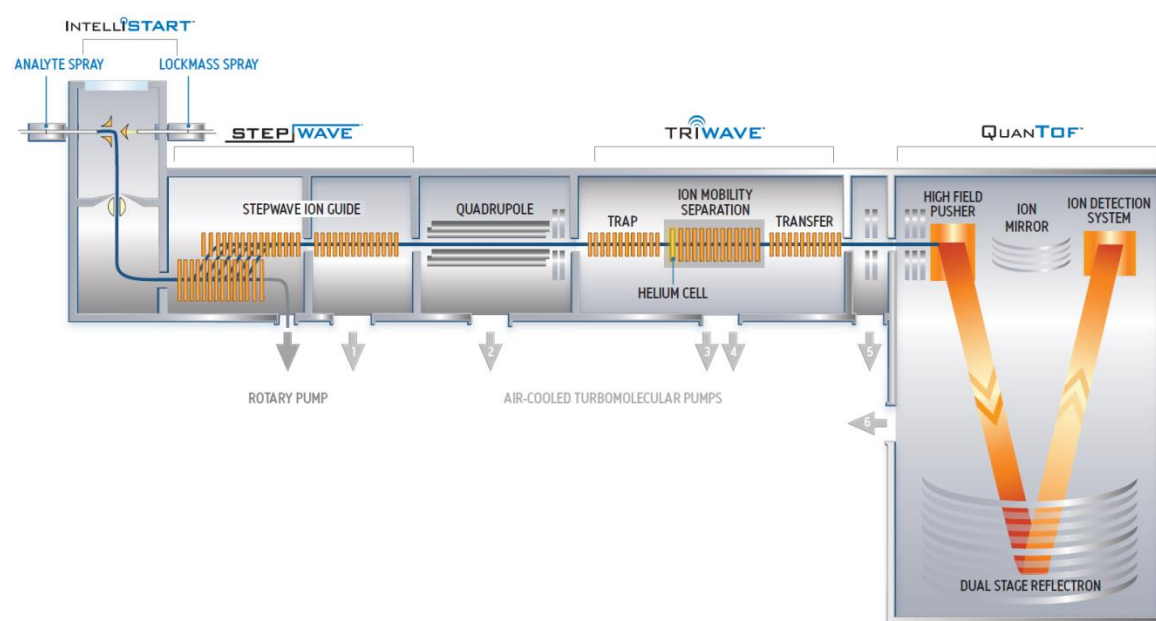
Figure 1.18 Schematic illustration of the Synapt G2-Si QTOF mass spectrometer. Courtesy of Waters.

drift tube with a fixed length l. Based on the time t required for a specific ion to traverse through the drift tube, its m/z value can be derived according to equation 1.3.

$$t = \frac{l}{\sqrt{2\,e\,U}} \sqrt{\frac{m}{z}} \tag{1.3}$$

In order to minimize ion spreading and maximize resolution, an ion mirror (reflectron) is utilized to compensate for initial energy differences of ions with similar m/z ratios during the push impulse.[348] If the Synapt G2-Si QTOF is operated in sensitivity mode, only one reflectron is employed, whereas a second reflectron can be utilized in resolution mode, doubling the flight path.

In **TOF-MS/MS**, the in unit resolution-operating quadrupole selects a specific precursor ion for subsequent fragmentation in the collision cell. Based on the design of the Synapt G2-Si QTOF TriWave collision cell, precursor ion fragmentation occurs either in the trapping or transfer cell. Following fragmentation, product ions are detected and their extracted ion chromatograms (XICs) can be used afterwards for quantification. **TOF-MRM**, a commercialized term from Waters, represents a third acquisition of the Synapt G2-Si QTOF for quantitative purposes, enabling duty cycle enhancement. In general, a duty cycle determines the amount of ions reaching the detector and hence the sensitivity of orthogonal acceleration TOF instruments as given by equation 1.4

$$Duty\ cycle = \frac{w_{ion\,beam}}{d} \sqrt{\frac{m/z}{m/z_{max}}} \tag{1.4}$$

where $w_{ion\,beam}$ is the width of the ion beam pushed into the TOF mass analyzer, d is the distance between high-field pusher and detector, and m/z and m/z_{max} are the m/z values for a particular ion and the upper limit of the m/z scan range, respectively. Since the first equation term is typically fixed to a value of 0.25 for most commercially available TOF instruments, maximum 25% of ions are accelerated by the pusher from a continuous beam into the orthogonal TOF mass analyzer.[349,350] In order to overcome significant ion losses between individual pushes, ion packages can be temporarily trapped and frequently ejected from the collision cell towards the pusher with a constant energy. Since the distance between pusher and collision cell exit is fixed, ions with different m/z values feature specific migration times due to different velocities and become separated. Knowledge about these migration times offers the possibility to adapt the pusher frequency in order to synchronize the release of a specific target ion from the collision cell with the push impulse for orthogonal acceleration. This duty cycle enhancement increases the amount of target ions hitting the detector and consequently boosts their signal intensity.

Regardless of the type of mass analyzer and acquisition mode, absolute quantification is conducted using the analyte to ISTD response ratio, either based on the peak area or height. The analyte concentration is derived by comparing the obtained response ratio against a calibration curve prepared with the analyte (spiked at different concentrations) and the ISTD (spiked at the fixed concentration) as depicted in Figure 1.19.
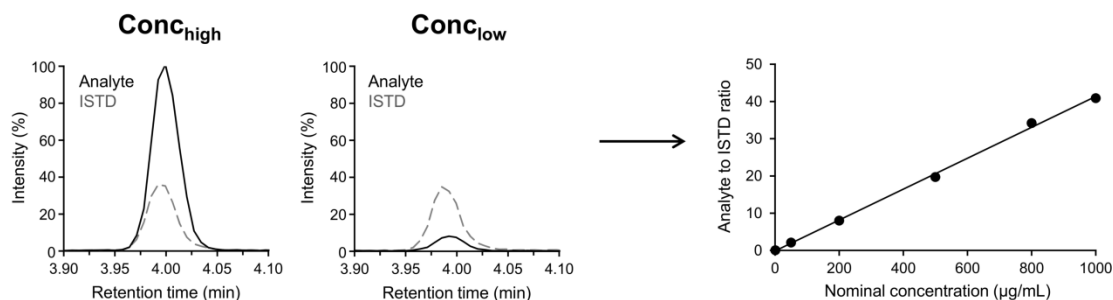
Figure 1.19 Principle of absolute quantification based on MS signal. The response ratio between the analyte at different concentrations and the ISTD spiked at a fixed concentration is used to construct a calibration curve for absolute quantification. Conc: concentration

1.6 Regulatory considerations for method validation

The performance of MS-based assays for the support of (pre-)clinical GLP studies has to be validated in accordance to industry-based recommendations[351] or regulatory guidelines from the US FDA and EMA.[352,353] This evaluation includes a variety of parameters such as selectivity, specificity, response contribution, sensitivity, linearity, carry-over, accuracy, precision, matrix effect, extraction recovery, dilution integrity, reproducibility, and various stability investigations. The latter include short and long-term storage of the lyophilizate, the reconstituted protein in neat solution and in the biological matrix at different temperatures, auto-sampler stability, and stability during freeze/thaw cycles. The next sections summarize the evaluated method validation parameters applied in this thesis and define their acceptance criteria.

1.6.1 Selectivity

The mean apparent analytical response (n=3) at the expected retention time in three different batches of blank biological matrix should be ≤20.0% for the analyte (either surrogate peptide or intact mAb-related therapeutic protein) compared to its response at the lower limit of quantification (LLOQ). The observed response of the peptide or protein-level ISTD in blank samples should be ≤5.0% relative to its zero sample response (blank sample spiked with ISTD).

1.6.2 Response contribution

The analyte to the ISTD response contribution was assessed by comparing the mean ISTD response (n=3) in a sample spiked only with the analyte at the upper limit of quantification (ULOQ) and the mean ISTD response in the zero sample (n=3). A potential contribution of the ISTD to the analyte was determined by comparing the analyte response in a zero sample (n=3) relative to its LLOQ response (n=3). The contribution should be ≤20.0% for the analyte, whereas the

acceptance criteria for the ISTD were set to ≤5.0% and ≤20.0% for a peptide or protein-level ISTD, respectively.

1.6.3 Linearity and sensitivity

Two individual sets of calibration standards (Cs), one located at the beginning and one at the end of each analytical run, were utilized to construct either linear $(y = ax + b)$ or quadratic $(y = ax^2 + bx + c)$ calibration curves, where y is the analyte to ISTD response ratio and x is the nominal concentration of the mAb-related therapeutic protein. The back-calculated concentrations should be within ±20.0% (±25.0% at the LLOQ and ULOQ) of the nominal concentration for at least 75.0% of Cs at minimum six non-zero concentration levels. Additionally, at least one replicate at each concentration should meet the stated acceptance criteria and the derived coefficient of determination (r^2) value should be at least 0.95. The lowest concentration meeting the acceptance criteria for selectivity, accuracy, and precision was defined as LLOQ.

1.6.4 Carry-over

The extent of carry-over within a series of up to four blank samples injected directly after the ULOQ sample should be ≤20.0% for the analyte compared to its LLOQ response and ≤5.0% for the ISTD signal relative to the zero sample response.

1.6.5 Accuracy, precision, and matrix effect

The accuracy was evaluated by the deviation (% bias) from the nominal concentration at four quality control (QC) concentration levels (LLOQ, 2-3 x LLOQ, around 50.0% of the ULOQ, and 80.0% of the ULOQ). The percentage of the coefficient of variation (% CV) determined the precision:

- *Accuracy (% bias) = 100% x (measured – nominal concentration) / nominal concentration*

- *Precision (% CV) = 100% x (standard deviation / mean concentration)*

Intra-day data (n=3) were generated on each validation day, whereas the inter-day performance was evaluated at a minimum of three non-consecutive days. Accuracy within ±20.0% bias (±25.0% bias at the LLOQ) and a precision of ≤20.0% CV (≤25.0% CV at the LLOQ) were set as acceptance criteria.

Due to peptide and protein absorption to various laboratory materials, conventional matrix effect investigations (analyte and ISTD response comparison in presence and absence of biological matrix) were replaced by comparing the accuracy and precision obtained on different days in different batches of blank biological matrix.

1.6.6 Dilution integrity

One additional QC exceeding the ULOQ of the method was prepared and diluted by a certain factor with blank biological matrix (n=5) using at least 10 µL of the original sample. The accuracy of the mean back-calculated concentration with the dilution factor incorporated should be within ±20.0% of the nominal concentration with a precision of ≤20.0% CV.

1.6.7 Reproducibility

Incurred study samples were analyzed on two different days. The concentration difference between individual measurements divided by the mean concentration should be within ±20.0% for at least 67.0% of investigated samples.

1.6.8 Stability of the mAb-related therapeutic protein

Short-term stability in blank biological matrix at room temperature (23±2 °C) and the stability of tryptic peptide(s) on the auto-sampler (≤10 °C) was assessed with two QC levels (n=3 each) for a predefined time. After storage, the samples were measured and compared to freshly prepared Cs and QCs. The stability was considered as acceptable, if the deviation from the initial concentration was ±20.0%.

Part 2 - Generic LC-MS/MS-based methods and their versatility for bottom-up mAb quantification

After a brief introduction to mAb-related therapeutic proteins, the diversity of qualitative and quantitative assays required during the drug development process, and regulatory considerations with respect to method validation, the second part will focus on the development of generic LC-MS/MS-based methods for bottom-up mAb-related therapeutic protein quantification in pre-clinical serum samples. Depending on the sensitivity requirement, two sample preparation routes either based on direct serum digestion or IC are presented throughout the next three chapters.

Chapters

2.1   Generic LC-MS/MS method based on pellet digestion

2.2   Evaluation of commercial digestion kits as standardized sample preparation for hIgG1 quantification in rat serum

2.3   Generic tip-based IC-LC-MS/MS method for sensitive bottom-up hIgG1 quantification in cynomolgus monkey serum

2.1 Generic LC-MS/MS method based on pellet digestion

2.1.1 Analytical context

The most straightforward LC-MS/MS-based approach for bottom-up mAb-related therapeutic protein quantification relies on direct serum digestion as outlined in the first part. Solvent-mediated protein precipitation with subsequent tryptic digestion of the protein pellet was reported as a promising direct digestion approach for reliable, reproducible, and high-throughput bottom-up mAb quantification in serum samples.[354-356] In comparison to whole serum digestion approaches, reduced matrix effects and better digestion efficiencies were obtained with the pellet digestion approach due to the removal of interfering compounds (*i.e.* small proteins, phospholipids, salts, and other low-molecular weighted entities).[357] In combination with generic surrogate peptides, a pellet digestion-based LC-MS/MS assay represents a simple and widely applicable approach to support the quantification of diverse mAb-related therapeutic proteins at pre-clinical stage. Despite of the time-saving benefit during method development, generic surrogate peptide-based LC-MS/MS methodologies possess the so far unexplored potential for analyte interchange. The use of conserved generic surrogate peptides theoretically allows the quantification of structurally identical mAb-related therapeutic proteins without the requirement for exact analyte matching. This concept would be comparable to the bicinchoninic acid assay in which an analogue protein (*e.g.* mouse IgG) is used to determine the concentration of other structurally identical proteins such as hIgGs.

2.1.2 Objectives

This project aimed to develop a generic LC-MS/MS method for hIgG1 quantification in rat serum and to evaluate its versatility in the following manner:

- Serum interchangeability by measuring cynomolgus monkey serum samples spiked with a hIgG1 (hIgG1A) against a calibration curve prepared with the same hIgG1 in rat serum

- Quantification of several hIgGs from the same (hIgG1) and another subclass (hIgG4) spiked in cynomolgus monkey and rat serum against Cs/QCs prepared with the hIgG1A in rat serum

- Application of the strategy to more complex biotherapeutics, namely a bispecific-bivalent hIgG1 and two lysine-conjugated ADCs (ADC1 and ADC2)

- Comparison of the mean ADC2 concentration-time profile after intravenous administration in three individual cynomolgus monkeys, which was determined with the proposed generic approach (Cs/QCs prepared with the hIgG1A in rat serum) or the conventional approach (Cs/QCs prepared with the ADC2 in cynomolgus monkey serum)

2.1.3 Results

2.1.3.1 Overview of the pellet digestion-based LC-MS/MS workflow

The pellet digestion protocol, previously reported by Zhang Q *et al.*,[243] was utilized as sample preparation in the generic LC-MS/MS workflow for bottom-up mAb-related therapeutic protein quantification in pre-clinical serum samples. Briefly, a fully SIL-hIgG1 ($[^{13}C]$-hIgG1) used as ISTD was spiked to serum samples in a first step (Figure 2.1). Since $[^{13}C_6]$-lysine and $[^{13}C_6]$-arginine were used for $[^{13}C]$-hIgG1 production, the $[^{13}C]$-hIgG1 could be deployed as generic ISTD for mAb-related therapeutic protein quantification as each tryptic peptide has the $[^{13}C]$-label incorporated.[309] The pellet digestion protocol consisted of four major steps: (i) reduction of the disulfide bonds with simultaneous denaturation at 60 °C, (ii) subsequent alkylation of the free thiol groups, (iii) generation and re-suspension of the protein pellet, and (iv) tryptic digestion. For the third step, a four-fold excess of organic solvent was utilized to achieve complete precipitation of the targeted mAb-related modalities along with other endogenous serum proteins. Although ACN was reported as more efficient protein precipitant, methanol was selected for pellet generation due to a facilitated pellet re-suspension prior to tryptic digestion.[243,357,358] The optimal digestion time was determined by kinetic investigations of the pellet digestion, which is further discussed in section 2.1.3.5. After quenching the enzymatic activity with trifluoroacetic acid (TFA), a SPE step was additionally incorporated prior to LC-MS/MS analysis. Separation of the tryptic peptides was conducted under standard reversed-phase conditions using an ACE C_{18} analytical column (150 x 4.6 mm, 3 µm) as well as 0.1% formic acid (FA) in water and ACN as mobile phase A and B, respectively. Following chromatographic separation, SRM transitions were acquired in positive ionization mode, utilizing a QTRAP instrument.
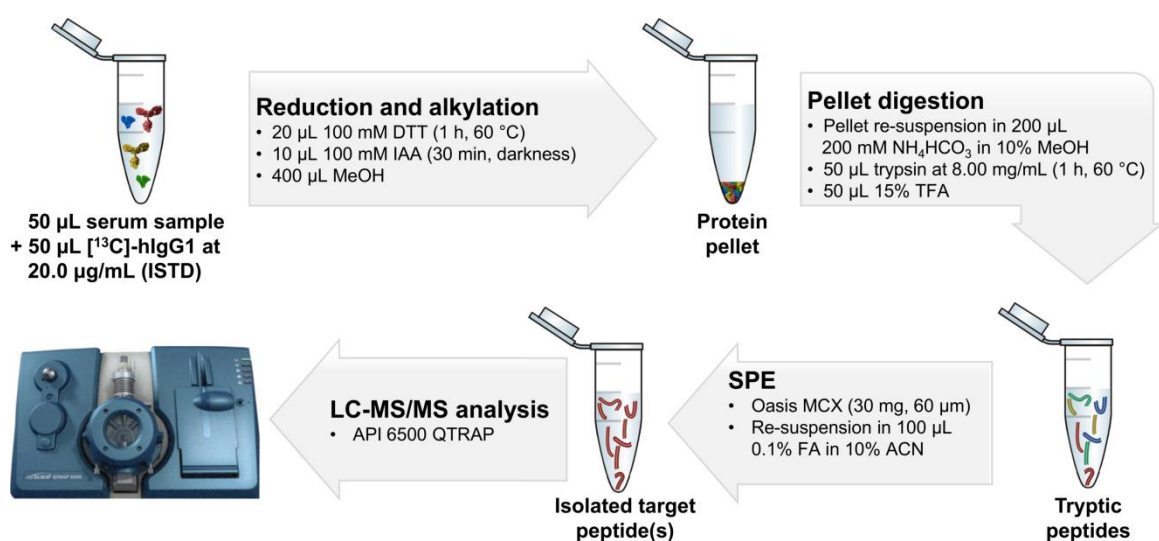
Figure 2.1 Pellet digestion protocol for bottom-up mAb-related therapeutic protein quantification by LC-MS/MS. MeOH: methanol, NH4HCO3: ammonium bicarbonate, MCX: mixed-mode cation exchange

2.1.3.2 Method development

Selection of generic surrogate peptides

Since the majority of currently marketed or developed full-length mAb-related therapeutic proteins is based on the hIgG1 isotype subclass (Figure 1.10c), a generic LC-MS/MS method was implemented for the quantitative assessment of this isotype subclass. The identification of the most appropriate generic surrogate peptides and the selection of their SRM transitions were conducted in three steps (Figure 2.2).
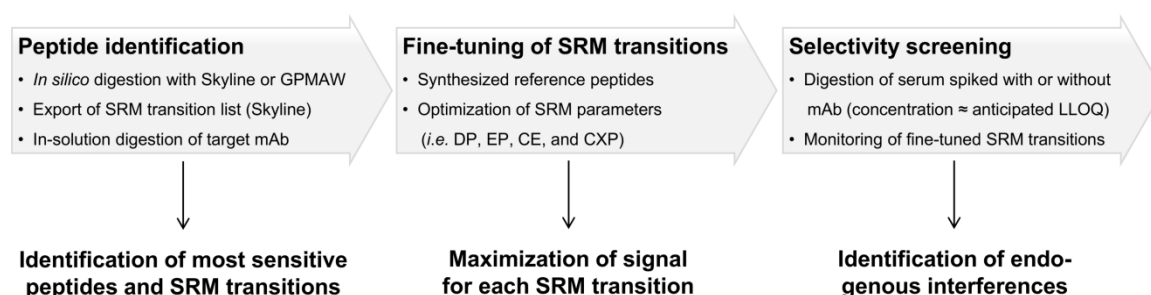
Figure 2.2 Workflow for generic surrogate peptide selection including *in silico* digestion, fine-tuning of SRM transitions, and selectivity screening of optimized SRM transitions in digested blank serum from pre-clinical species. DP: declustering potential, EP: entrance potential, CE: collision energy, and CXP: cell exit potential

In a first step, the amino acid sequence of a hIgG1 was imported into Skyline and GPMAW for *in silico* digestion. Skyline was mainly used to create and export SRM transition lists in order to identify the most intense SRM transitions for each generic peptide after in-solution digestion of the hIgG1. This first screening utilized standard values for the collision energy, declustering, entrance, and cell exit potential, which were proposed from Skyline for each peptide. On the other hand, GPMAW was employed to derive calculated hydrophobicity values in order to estimate potential peptide retention times. Out of 15 initially screened generic surrogate peptides, FNWYVDGVEVHNAK (FNW), GPSVFPLAPSSK (GPS), TTPPVLDSDGSFFLYSK (TTP), and VVSVLTVLHQDWLNGK (VVS) were identified as the most sensitive peptides, covering different parts of the constant region. The GPS and TTP peptides were located within the C_H1 and C_H3 domain, respectively. In contrast, the VVS and FNW peptides originated from the C_H2 domain. In a second step, the SRM transitions of the previously identified most intense generic surrogate peptides were fine-tuned to maximize signal intensity using a synthesized reference standard for each peptide. Due to the nature of electrospray ionization mostly doubly and triply charged peptide precursor ions are formed, while their product ions often exhibit less charges, resulting in increased *m/z* values. This property can be utilized to eliminate interferences from small molecules by exclusive selection of product ions with higher *m/z* values compared to the precursor ion.[224] For the generic LC-MS/MS method, up to three SRM transitions were optimized and monitored for each peptide. The optimized SRM transitions for each quantifier, which were used throughout the

thesis for bottom-up mAb-related therapeutic protein quantification in pre-clinical species by LC-MS/MS, are summarized in Table 2.1. Since deamidation was predicted for the VVS peptide, presenting a well-known modification of asparagine or glutamine-containing peptides, the corresponding SRM transition of the deamidated VVS (VVSd) was additionally included.[359-362] The last step of the generic surrogate peptide selection procedure identified potential interferences in blank serum from various pre-clinical species. Under the final chromatographic conditions, all four generic surrogate peptides were baseline separated with a resolution >1.5, resulting in a total sample run time of 8 min (Figure 2.3). During selectivity screening in mouse, rat, dog, cynomolgus, and marmoset monkey serum, the following interferences were observed at the expected retention time for each peptide: FNW none, GPS in dog and cynomolgus monkey, TTP in dog, and VVS in blank rat as well as marmoset monkey serum. For the corresponding isotopically labeled peptides, interferences were only caused by the $[^{13}C_6]$-TTP and $[^{13}C_6]$-VVS SRM transitions in blank rat and dog serum, respectively.

Table 2.1 Summary of optimized SRM transitions for each selected generic surrogate peptide and its ISTD (quantifier only) used in this thesis for bottom-up mAb-related therapeutic protein quantification in pre-clinical species by LC-MS/MS.

Peptide		Q1 *m/z*	Q3 *m/z*	DP	CE	CXP
Amino acid sequence	Abbreviation	(charge state / ion type)		(V)	(V)	(V)
FNWYVDGVEVHNAK	FNW	560.3 (3+)	709.3 (y_{12}^{2+})	48	20	15
FNWYVDGVEVHNAK[a]	$[^{13}C_6]$-FNW	562.3 (3+)	712.3 (y_{12}^{2+})	48	20	15
GPSVFPLAPSSK	GPS	594.2 (2+)	418.5 (y_4^+)	50	40	25
GPSVFPLAPSSK[a]	$[^{13}C_6]$-GPS	597.2 (2+)	424.4 (y_4^+)	50	40	25
TTPPVLDSDGSFFLYSK	TTP	938.1 (2+)	836.9 (y_{15}^{2+})	93	40	15
TTPPVLDSDGSFFLYSK[a]	$[^{13}C_6]$-TTP	941.0 (2+)	839.9 (y_{15}^{2+})	93	40	15
VVSVLTVLHQDWLNGK	VVS	603.7 (3+)	805.9 (y_{14}^{2+})	55	24	24
VVSVLTVLHQDWLNGK[a]	$[^{13}C_6]$-VVS	605.7 (3+)	808.9 (y_{14}^{2+})	55	24	24
VVSVLTVLHQDWLDGK	VVSd	604.0 (3+)	806.4 (y_{14}^{2+})	55	24	24
VVSVLTVLHQDWLDGK[a]	$[^{13}C_6]$-VVSd	606.0 (3+)	809.4 (y_{14}^{2+})	55	24	24

[a] Labeled with $[^{13}C_6]$-lysine. Q: quadrupole, DP: declustering potential, CE: collision energy, and CXP: cell exit potential

SPE optimization

The rationale for SPE incorporation was to introduce an additional clean-up step in order to remove interfering compounds to some extent prior to LC-MS/MS analysis. The mixed-mode cation exchange sorbent was selected as it was reported to be the most appropriate one for tryptic peptides, combining the mechanism of ion exchange with reversed-phase retention of the peptide.[363,364] Assuming a mean total serum protein concentration of 70.0 mg/mL and a 100% digestion efficiency, 50 µL of serum yields 3.5 mg of peptides.[365] Consequently, the mixed-mode cation exchange SPE plate with a sorbent amount of 30 mg was selected, which exhibits a
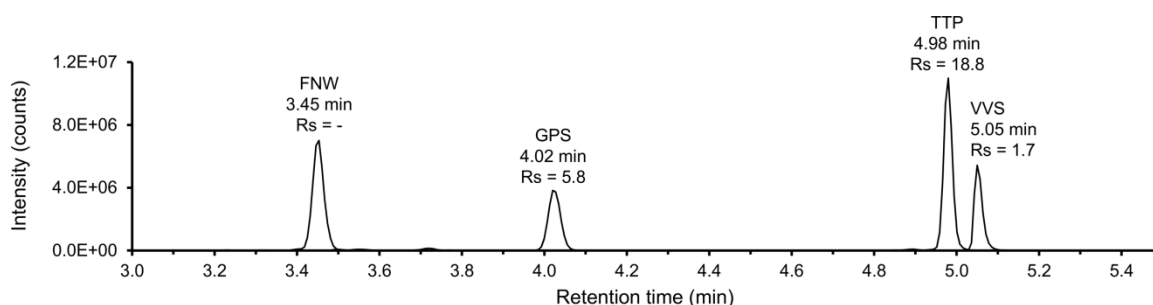
Figure 2.3 Overlaid extracted ion chromatograms of the four generic surrogate peptides obtained from a hIgG1-spiked rat serum sample (500 µg/mL) after pellet digestion and LC-MS/MS analysis. Rs: resolution

maximum mass loading capacity of 5.0 mg. After loading the acidified digested serum sample (250 µL), at least 91.3% of the generated four generic surrogate peptides were retained on the resin (Table 2.2). For the subsequent washing step, no significant peptide loss was observed using 1 mL of 1% acetic acid with an ACN fraction of up to 50.0%. Higher ratios of ACN were not utilized in order to avoid potential elution of the retained generic surrogate peptides from the sorbent. Efficient elution for all four generic surrogate peptides with recoveries ≥76.7% was only obtained when the fraction of ACN was at least 60.0% in the elution solvent. For the final elution solvent of the SPE protocol, the ACN fraction was increased to 70.0%.

Table 2.2 Optimization of SPE clean-up after pellet digestion using an Oasis MCX cartridge (30 mg, 60 µm).

SPE step	Solvent	Fraction of summed peak area (%)			
		FNW	GPS	TTP	VVS
Flow-through	-	4.1	8.7	3.6	2.2
Wash	1% acetic acid	2.1	1.8	2.7	2.7
	ACN/1% acetic acid (5/95, v/v)	<0.1	<0.1	0.7	10.2
	ACN/1% acetic acid (10/90, v/v)	<0.1	<0.1	<0.1	2.7
	ACN/1% acetic acid (20/80, v/v)	<0.1	<0.1	0.1	2.2
	ACN/1% acetic acid (30/70, v/v)	<0.1	<0.1	<0.1	0.4
	ACN/1% acetic acid (40/60, v/v)	<0.1	<0.1	<0.1	<0.1
	ACN/1% acetic acid (50/50, v/v)	<0.1	<0.1	<0.1	<0.1
Elution	NH₄OH (28%)/ACN/H₂O (1/2/7, v/v/v)	79.4	12.0	59.7	12.9
	NH₄OH (28%)/ACN/H₂O (1/4/5, v/v/v)	94.2	54.4	88.7	54.8
	NH₄OH (28%)/ACN/H₂O (1/6/3, v/v/v)	95.9	88.6	93.6	76.7

NH_4OH: ammonium hydroxide, MCX: mixed-mode cation exchange

2.1.3.3 Generic LC-MS/MS assay for hIgG1A quantification in rat serum

The pellet digestion-based generic LC-MS/MS method allowed hIgG1A quantification in rat serum using the GPS, TTP, or VVS peptides up to a concentration of 1.00 µg/mL, while the FNW peptide reached a LLOQ of 5.00 µg/mL (Table 2.3). The corresponding linearity for each peptide was excellent up to a concentration of 1000 µg/mL with r^2-values of ≥0.9913, using a linear (FNW, GPS, and VVS) or quadratic (TTP) regression model with a weighting of $1/x^2$. In terms of

Table 2.3 Method evaluation for hIgG1A quantification in rat serum with regard to linearity, accuracy, and precision (QCs at 3.00, 15.0, 450, and 750 µg/mL) for each generic surrogate peptide.

Peptide	Linearity		Accuracy (% bias)		Precision (% CV)	
	Range (µg/mL)	r^2-value (n=5)	Intra-day (n=3)	Inter-day (n=15)	Intra-day (n=3)	Inter-day (n=15)
FNW	5.00-1000	0.9927±0.0035	-9.5 to 17.8	-4.5 to 8.4	0.6 to 10.4	5.8 to 12.1
GPS	1.00-1000	0.9913±0.0057	-13.9 to 14.4	-5.0 to 6.2	2.0 to 17.3	7.2 to 9.4
TTP	1.00-1000	0.9961±0.0011	-10.6 to 13.0	-2.6 to 4.7	1.0 to 17.8	4.1 to 13.6
VVS	1.00-1000	0.9952±0.0024	-10.9 to 12.0	-3.1 to 8.5	1.6 to 17.2	6.7 to 14.8

selectivity, each peptide fulfilled the required acceptance criterion from US FDA and EMA guidances as the analytical response was ≤20.0% at the expected retention time compared to the response at their corresponding LLOQ (data not shown). Moreover, the intra and inter-day values obtained at four QC concentrations (3.00, 15.0, 450, and 750 µg/mL) also met the acceptance criteria regarding accuracy (±20.0% bias) and precision (≤20.0% CV). Furthermore, the variation between the obtained inter-peptide QC concentrations was ≤3.2%, indicating that the hIgG1A concentration was truly reflected by each generic surrogate peptide regardless of its origin.

2.1.3.4 Serum interchangeability between rat and cynomolgus monkey

The matrix of Cs/QCs is conventionally matched with the corresponding one from *in vivo* samples. However, due to impracticability of exact matrix matching with all pre-clinical samples, some uncertainties still remain. Moreover, if tissue or rare matrices (*e.g.* cerebrospinal fluid or tears) are analyzed, corresponding matrices are partially unavailable and surrogate matrices are used for Cs/QCs preparation.[366-368] However, this replacement, may impact the accuracy and precision in case of improper ISTD selection.[278,279] The incorporation of a [^{13}C]-hIgG1 as ISTD should theoretically compensate for any introduced variation and the resulting quantitative data should remain unaffected upon serum interchange. In order to examine this hypothesis, hIgG1-spiked cynomolgus monkey serum samples were quantified against Cs/QCs prepared with the same hIgG1 in rat serum. By monitoring the MS responses of the [^{13}C$_6$]-labeled peptides, only the [^{13}C$_6$]-FNW signal intensity was identical in both species (Figure 2.4a). In contrast, the other three generic peptides displayed a tendency towards ion suppression in cynomolgus monkey serum. Since the non-labeled surrogate peptides behaved accordingly (section 2.1.3.5), the MS response ratio between the surrogate peptide and its ISTD remained constant for each generic peptide regardless of the selected pre-clinical species (Figure 2.4b). Furthermore, the proportionality of individual MS response ratios at different QC concentrations was similar to the expected proportionality of nominal QC concentrations. For instance, the individual MS response ratios at 750 and 450 µg/mL were 39.7 and 23.3 as well as 43.4 and 26.4 in rat and cynomolgus monkey serum, respectively. This resulted in proportional ratios between both concentrations (1.7 for rat and 1.6 for cynomolgus monkey serum), which are in agreement with the expected ratio of 1.7 for
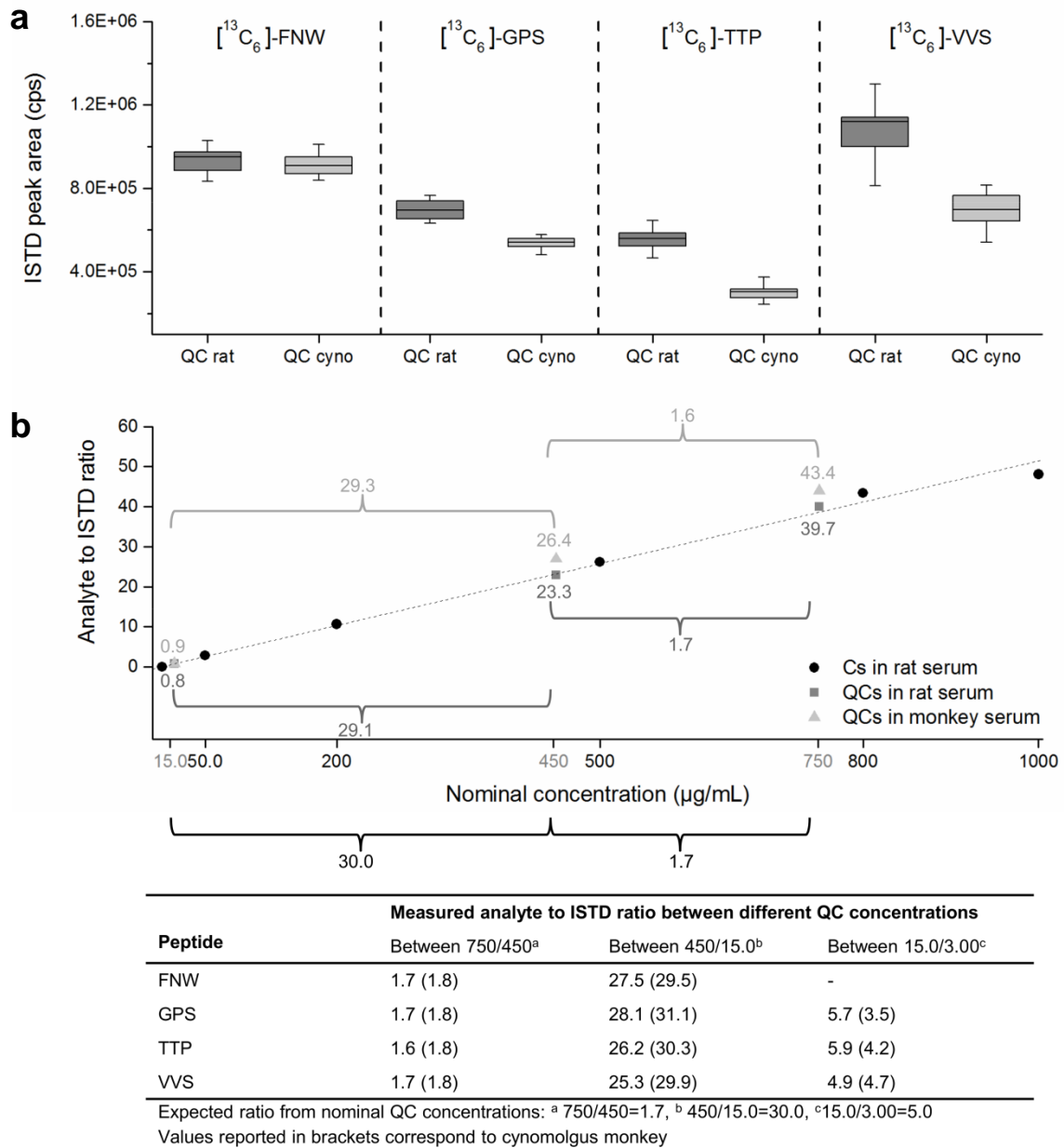
Figure 2.4 Interchangeability of rat and cynomolgus monkey serum spiked with the same hIgG1. (**a**) MS responses of [$^{13}C_6$]-labeled peptides in QCs (n=12), demonstrating tendency for ion suppression in cynomolgus monkey serum with the [$^{13}C_6$]-GPS, [$^{13}C_6$]-TTP, and [$^{13}C_6$]-VVS peptides. (**b**) Rationale for serum interchangeability between species: the proportionality of individual analyte to ISTD response ratios at different QC concentrations remained constant for each species, which was similar to the expected proportionality between nominal QC concentrations. Table displays measured values in QCs for each generic surrogate peptide, proving the validity of serum interchangeability.

both nominal QC concentrations. Since this consistent proportionality was observed for all peptides and concentrations (Table in Figure 2.4b), an interchange of serum between rat and cynomolgus monkey was possible without affecting the back-calculation of the hIgG1 concentration. The corresponding inter-day accuracy and precision values (n=9) of QCs spiked

with the hIgG1A in cynomolgus monkey serum ranged from -4.9 to 9.9% bias and 2.1 to 17.2% CV, respectively, when measured against Cs/QCs prepared with hIgG1A in rat serum. Inaccurate results exceeding the acceptance criterion of ±20.0% bias were only obtained for the GPS and VVS peptides at 3.00 µg/mL. By using the former peptide, the hIgG1 concentration was overestimated by 28.4%. This was related to an endogenous interference in blank cynomolgus monkey serum, which was in agreement with the results obtained upon selectivity screening and previously reported data.[243] However, the reason why only the low hIgG1 concentration was underestimated by -33.7% compared to the other remaining QC levels remains unknown, requiring further investigations and an extended data set based on several batches of blank rat and cynomolgus monkey sera.

2.1.3.5 Interchangeability of mAb-related therapeutic proteins

The prerequisite for a successful interchangeable quantification of different constant region-bearing mAb-related therapeutic proteins was an identical generic peptide formation upon pellet digestion. The kinetic profiles of the pellet digestion revealed that the TTP, FNW, and VVS peptides were equally generated from a hIgG1, [^{13}C]-hIgG1, or lysine-conjugated ADC (Figure 2.5a-c). The signal intensities of the FNW and VVS peptides decreased over time due to an increased deamidation (Figure 2.5b+c), which is illustrated by the increased VVSd formation over time (Figure 2.5c). The elucidation of peptide deamidation by HRMS is discussed in detail in section 3.1.3.2. The GPS peptide displayed comparable rapid peptide formation within 1 h (Figure 2.5d). However, the GPS signal obtained from the hIgG1 and ADC were significantly increased compared to the [^{13}C$_6$]-GPS following overnight digestion. Consequently, the [^{13}C$_6$]-GPS did not allow proper correction of introduced variations. Since the highest signal intensities were obtained after 1 h of digestion for most of the surrogate peptides and all [^{13}C$_6$]-labeled peptides behaved accordingly at this time point, interchangeable quantification of different mAb-related therapeutic proteins should be feasible. In order to prove this hypothesis, the assay complexity was gradually increased from unconjugated mAbs towards next-generation mAb-related therapeutic proteins.

hIgG1s

Similar to the results obtained with hIgG1A (section 2.1.3.4), two additional hIgG1s spiked in cynomolgus monkey serum were accurately and precisely quantified against Cs/QCs prepared with hIgG1A in rat serum over the whole concentration range with the TTP and FNW peptides, proving the proposed hypothesis of analyte interchangeability. For both hIgG1s and surrogate peptides, the accuracy ranged from -10.3 to 13.8% bias, while the corresponding precision was between 0.4 and 15.9% CV. Accurate and precise data (±20.0%, ≤20.0% CV), fulfilling the defined acceptance criteria, were also obtained with the VVS and GPS peptides for the QCs at 750, 450, and 15.0 µg/mL. Only the low QC concentration at 3.00 µg/mL was overestimated with the GPS peptide by maximal 24.4% (precision ≤15.4% CV) due to the selectivity issue or underestimated with the VVS peptide by maximal 49.3% with a precision of ≤4.6% CV.
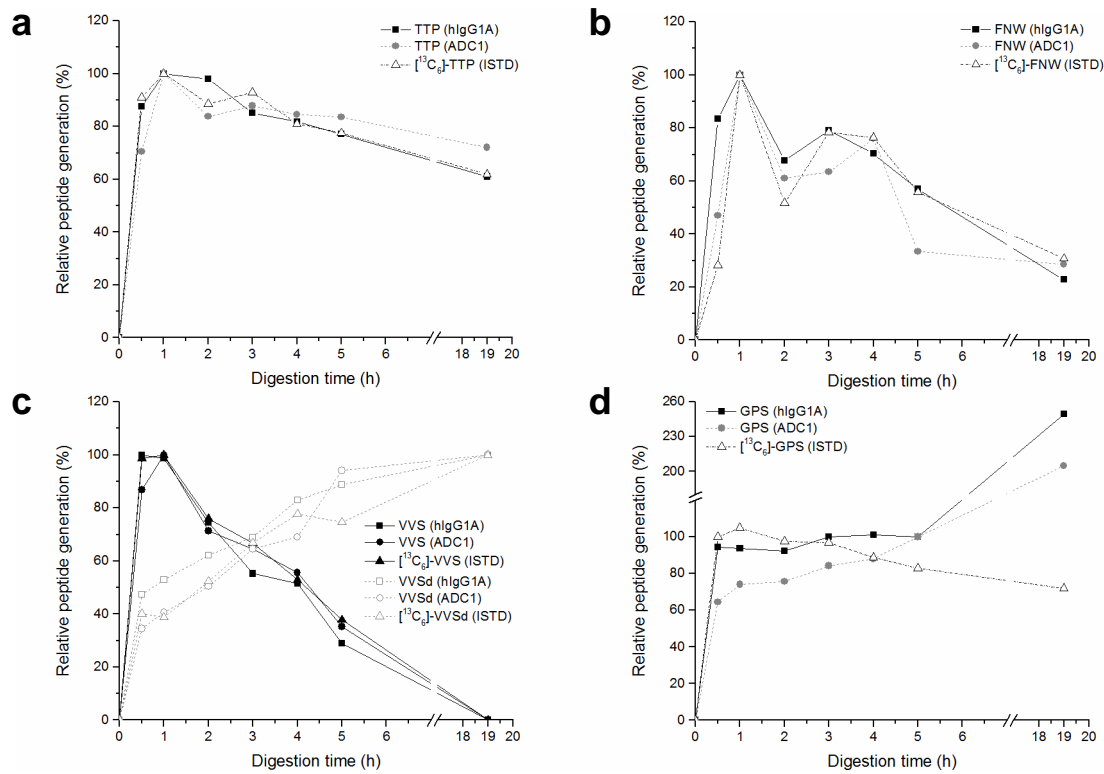
Figure 2.5 Kinetic for the (**a**) TTP, (**b**) FNW, (**c**) VVS (non-deamidated and deamidated form), and (**d**) GPS peptide following pellet digestion of hIgG1A, lysine-conjugated ADC1, or [^{13}C]-hIgG1 in serum.

hIgG4

In contrast to the remaining peptides, the VVS peptide can be used for the quantification of hIgG4-related therapeutic proteins as its amino acid sequence is also conserved in this isotype subclass. Of note, the amino acid sequence of the FNW peptide is highly conserved in hIgG2 and hIgG4, however, one missing C-terminal lysine or arginine residue hindered the release of the FNW peptide during tryptic digestion. In rat serum, the spiked hIgG4 was accurately (-17.9 to -11.1% bias) and precisely (≤2.5% CV) quantified at three out of four QC levels (750, 450, and 15.0 µg/mL). In contrast, the QC at 3.00 µg/mL exceeded the accuracy acceptance criterion by 5.2%, while the precision was 3.6% CV. Overall, the hIgG4 concentration in rat serum trended to be underestimated when determined against a calibration curve prepared with the hIgG1A in rat serum. This was likely attributed to the different amount of released peptides, resulting from the core-hinge stabilization of the hIgG4 to avoid Fab arm exchange.[369,370] The hIgG4 spiked in cynomolgus monkey serum was likewise accurately (-9.3 to 7.3% bias) and precisely (≤13.2% CV) quantified at 750, 450, and 15.0 µg/mL, whereas the low QC concentrations was overestimated by 48.2% with a precision ≤19.1% CV.

Bispecific-bivalent hIgG1

The bispecific-bivalent hIgG1 concentration was only accurately (-2.2 to 15.8% bias) and precisely (2.4-6.3% CV) determined with the GPS peptide from the C_H1 domain, which was not affected by the applied knob-into-hole technology and introduction of additional stabilizing disulfide bridges. The remaining three peptides significantly underestimated the concentration (-76.6 to -17.7% bias). This was once more related to the unequal amount of released surrogate peptides during digestion of the bispecific-bivalent hIgG1 compared to the hIgG1A used for Cs/QCs preparation.

Lysine-conjugated ADCs

The first ADC (MCC-DM1 construct) displayed a tendency towards underestimation ranging from -25.1% (GPS, 750 µg/mL) to -6.9% (FNW, 15.0 µg/mL). Following payload/linker conjugation, peptide miscleavage can occur due to steric hindrance and the inability of trypsin to recognize a payload/linker-conjugated lysine residue.[371] Consequently, the amount of correctly released tryptic peptides from the ADC1 did not match with the amount of released peptides from the hIgG1A, resulting in an underestimation of ADC1 concentration. In contrast, the second ADC (sulfo-SPDB-DM4 construct) demonstrated a tendency towards overestimation in cynomolgus monkey serum when measured against a hIgG1 in rat serum using the GPS (19.4 to 97.1%) and VVS peptides (13.6 to 24.2%). The best results in terms of accuracy and precision were obtained with the FNW and TTP peptides. Both peptides are located in H chain regions (FNW at position 276-289 and TTP at position 394-410) and were predicted during peptide mapping studies to be less prone for payload/linker conjugation compared to other regions such as at position 134-214 or 223-249 (Figure 2.6). Due to less peptide miscleavage, the amount of FNW and TTP peptides released from ADC2 was similar to the one released from the hIgG1, resulting in accurate and precise data.
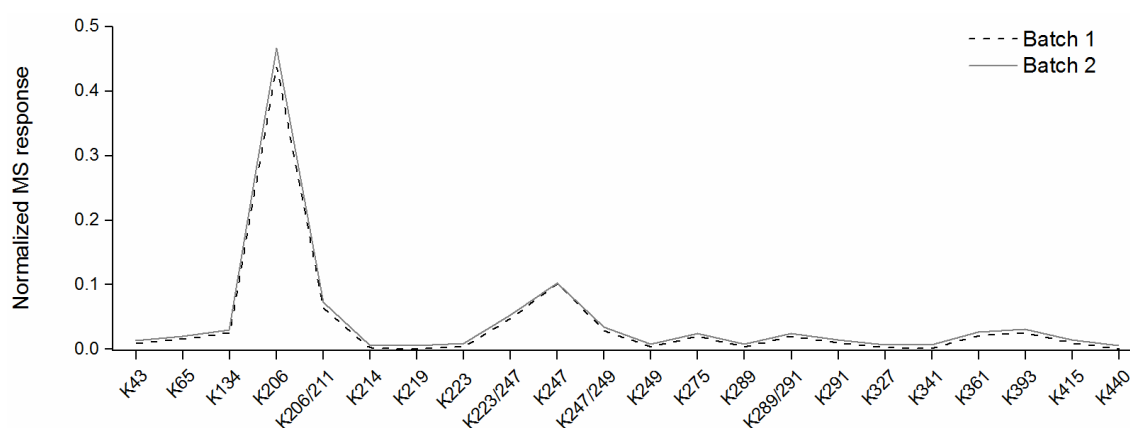
Figure 2.6 Peptide mapping results showing the position of H chain lysine residues, which are more prone for payload/linker conjugation in two different ADC2 production batches. The normalized MS response was calculated using the Genedata software by dividing the peak area of observed miscleaved peptides by the peak area of correctly released peptides multiplied with the reciprocal DAR value. Courtesy of Novartis Technical Research & Development.

2.1.3.6 Application to pre-clinical study samples

After successful quantification of both ADCs spiked in cynomolgus monkey serum samples against a calibration curve constructed with hIgG1A in rat serum using the FNW and TTP peptides, the interchangeability of this approach was further examined using specimen from pre-clinical studies. For this assessment, the mean ADC2 concentration-time profiles of three cynomolgus monkeys were compared, when the ADC2 concentration was determined with a calibration curve prepared either with the ADC2 in cynomolgus monkey serum (conventional approach) or the hIgG1A in rat serum (generic approach). As depicted in Figure 2.7a, both approaches resulted in identical mean concentration-time profiles using the TTP peptide.
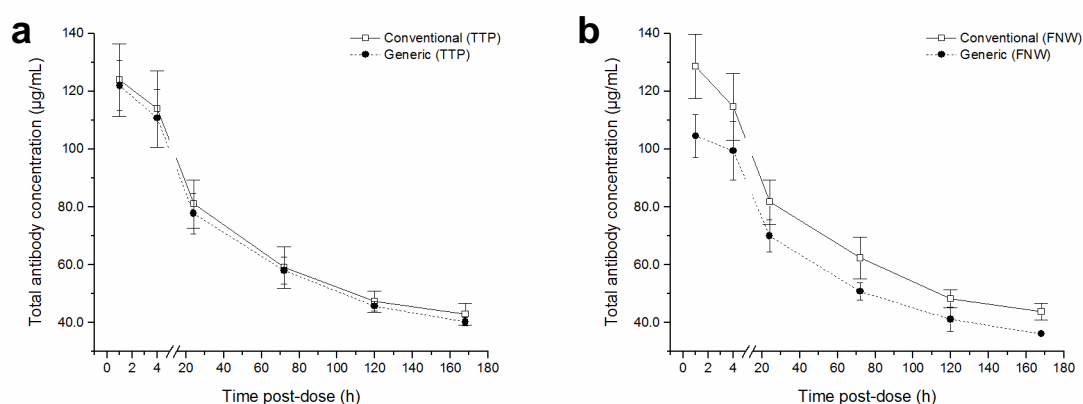
Figure 2.7 Mean ADC2 concentration-time profiles in three individual cynomolgus monkeys after intravenous ADC2 administration (5.00 mg/kg) obtained with the (**a**) TTP and (**b**) FNW peptides. The ADC2 concentration-time profiles were determined using a calibration curve constructed either with ADC2 in cynomolgus monkey serum (conventional approach) or hIgG1A in rat serum (generic approach).

Consequently, the concept of analyte and serum interchangeability was successfully demonstrated using *in vivo* samples from pre-clinical trial. In addition, the TTP peptide reflected the true ADC2 concentration with a high degree of certainty as the FNW peptide displayed a similar concentration-time profile using the conventional approach (Figure 2.7b). On the other hand, the ADC2 concentration was systematically underestimated by -16.2±2.3% with the FNW peptide following the generic approach, which was not observed with spiked samples. Differences in FNW peptide generation upon tryptic digestion might explain the deviation between both approaches. In order to avoid distortion of the quantitative data by lysine-containing tryptic peptides, a comparison of both approaches using an additional arginine-containing tryptic peptide (*e.g.* EPQVYTLPPSR) is reasonable. Moreover, the results additionally demonstrated the importance of incorporating at least two different tryptic peptides within such an interchangeable quantitative approach.

2.1.4 Conclusions

A single generic pellet digestion-based LC-MS/MS assay enabled the quantification of hIgG1-related therapeutic proteins in rat serum (1.00-1000 µg/mL) with potential method extension to hIgG4-related therapeutic proteins using the VVS peptide. Overall, a high degree of versatility was associated with the generic method, offering the following advantages:

- Serum interchangeability of rat and cynomolgus monkey serum due to the incorporation of a [^{13}C]-hIgG1 used as ISTD. By using spiked serum samples, it was successfully demonstrated that cynomolgus monkey serum samples containing a hIgG1 were accurately and precisely quantified based on a calibration curve prepared with the same analyte in rat serum. Since the trading of primates samples is regulated and requires international import and export permits, this interchangeable approach will facilitate Cs/QCs preparation if the availability of cynomolgus monkey serum is limited.[372]

- No exact analyte matching was required due to the incorporation of generic surrogate peptides, which are conserved in various hIgG isotype subclasses and constant region-containing mAb-related therapeutic proteins. However, the use of several generic surrogate peptides from different regions is recommended for such an interchangeable approach and extensive validation using spiked samples prior to the analysis of study samples is required.

Despite the promising benefits, certain limitations could also be assigned to the developed generic bottom-up methodology:

- Knowledge about introduced mAb modifications or payload/linker conjugation sites was mandatory.

- The quantification is limited to the total antibody concentration as the digestion of the protein-precipitated pellet does not allow distinction between active and inactive mAb species.

2.1.5 Scientific communication

The work described in this chapter was published.

Peer-reviewed scientific article:

Lanshoeft C *et al*. The flexibility of a generic LC-MS/MS method for the quantitative analysis of therapeutic proteins based on human immunoglobulin G and related constructs in animal studies. *J Pharm Biomed Anal*, 2016, 131, 214-222. Copyright 2016, reprinted with permission from Elsevier.

The flexibility of a generic LC–MS/MS method for the quantitative analysis of therapeutic proteins based on human immunoglobulin G and related constructs in animal studies

Christian Lanshoeft [a,b], Thierry Wolf [a], Markus Walles [a], Samuel Barteau [a], Franck Picard [a], Olivier Kretz [a], Sarah Cianférani [b], Olivier Heudi [a,*]

[a] Novartis Institutes for Biomedical Research, Drug Metabolism and Pharmacokinetics, Fabrikstrasse 14 – Novartis Campus, 4056, Basel, Switzerland
[b] Laboratoire de Spectrométrie de Masse BioOrganique, Institut Pluridisciplinaire Hubert Curien, CNRS-Université de Strasbourg, UMR 7178, 25 rue Becquerel, 67087, Strasbourg, France

ARTICLE INFO

ABSTRACT

An increasing demand of new analytical methods is associated with the growing number of biotherapeutic programs being prosecuted in the pharmaceutical industry. Whilst immunoassay has been the standard method for decades, a great interest in assays based on liquid chromatography tandem mass spectrometry (LC–MS/MS) is evolving. In this present work, the development of a generic method for the quantitative analysis of therapeutic proteins based on human immunoglobulin G (hIgG) in rat serum is reported. The method is based on four generic peptides GPSVFPLAPSSK (GPS), TTPPVLDSDGSFFLYSK (TTP), VVSVLTVLHQDWLNGK (VVS) and FNWYVDGVEVHNAK (FNW) originating from different parts of the fraction crystallizable (Fc) region of a reference hIgG1 (hIgG1A). A tryptic pellet digestion of rat serum spiked with hIgG1A and a stable isotope labeled protein (hIgG1B) used as internal standard (ISTD) was applied prior LC–MS/MS analysis. The upper limit of quantification was at 1000 µg/mL. The lower limit of quantitation was for GPS, TTP and VVS at 1.00 µg/mL whereas for FNW at 5.00 µg/mL. Accuracy and precision data met acceptance over three days. The presented method was further successfully applied to the quantitative analysis of other hIgG1s (hIgG1C and hIgG1D) and hIgG4-based therapeutic proteins on spiked quality control (QC) samples in monkey and rat serum using calibration standards (Cs) prepared with hIgG1A in rat serum. In order to extend the applicability of our generic approach, a bispecific-bivalent hIgG1 (bb-hIgG1) and two lysine conjugated antibody-drug conjugates (ADC1 and ADC2) were incorporated as well. The observed values on spiked QC samples in monkey serum were satisfactory with GPS for the determination of bb-hIgG1 whereas the FNW and TTP peptides were suitable for the ADCs. Moreover, comparable mean concentration-time profiles were obtained from monkeys previously dosed intravenously with ADC2 measured against Cs samples prepared either with hIgG1A in rat serum (presented approach) or with the actual ADC2 in monkey serum (conventional approach). The results of this study highlight the great flexibility of our newly developed generic approach and that the choice of the surrogate peptide still remains critical when dealing with different matrix types or modalities.

© 2016 Elsevier B.V. All rights reserved.

1. Introduction

The strategies of pharmaceutical companies in the development of therapeutic proteins for the treatment of various diseases such as cancer, immune disorders or inflammatory diseases have improved within the last 2–3 decades [1,2]. Only in 2015,

nine novel antibody therapeutics were granted first marketing approval in the US or Europe: Cosentyx® (secukinumab, Novartis), Nucala® (mepolizumab, GlaxoSmithKline), Unituxin® (dinutuximab, United Therapeutics), Repatha® (evolocumab, Amgen), Praxbind® (idarucizumab, Boehringer-Ingelheim), Darzalex™ (daratumumab, Janssen), Empliciti® (elotuzumab, Bristol-Myers Squibb), Portrazza® (necitumumab, Eli Lilly) and Praluent® (alirocumab, Sanofi/Regeneron Pharmaceuticals). Moreover, seven therapeutic antibodies are currently in review and more than 50 therapeutic proteins are in phase III clinical trial [3]. Besides monoclonal antibodies (mAbs), a second generation of mAb based

biotherapeutics with different mode of actions and physical characteristics were developed including antibody-drug conjugates (ADCs) or bispecific antibodies [4,5]. The majority of these antibody-derived therapeutic proteins are based on the framework of human immunoglobulin G1 (hIgG1), whereas a minority is either based on the hIgG isotype subclass 2 or 4. Latest state-of-the-art mass spectrometry (MS) methods are used along the whole drug development process, for instance, to characterize therapeutic proteins with their various glycan forms [6,7] or ADCs in-depth [8–10]. Some other applications are intended to gain better structural insights of proteins where conformational changes were studied [11]. In a later development phase, quantitative analysis of mAbs [12,13], ADCs [14,15] or chimeric antibodies [16,17] in biological fluids is conducted with liquid chromatography tandem mass spectrometry (LC–MS/MS) besides ligand binding assays (LBAs) as complementary analytical method to support data collection during pharmacokinetic (PK), pharmacodynamic (PD) or toxicokinetic (TK) studies [18]. Due to the limited mass range of triple quadrupole mass analyzers, highly specific surrogate peptides after tryptic digestion are required for the analysis of high molecular weight proteins. Unique peptides for each antibody are located in the complementary determining regions (CDR) of an antibody intended for therapeutic use [19,20]. However, an entire new assay has to be developed for another therapeutic protein in development when using CDR peptides. In order to avoid tedious method development, Li et al. published a general LC–MS/MS method using four different peptides which are located in the fraction crystallizable (Fc) region for the quantitative analysis of hIgG1 and hIgG2-based therapeutic proteins in pre-clinical species [21]. A few months later, Furlong et al. published an universal LC–MS/MS method using an unique generic peptide for hIgG1 and hIgG4 analysis [22]. All these Fc region peptides are conserved throughout all hIgGs whereas they are absent in other pre-clinical species such as rat, dog or monkey. Additional generic peptides were identified and the applicability of such generic LC–MS/MS methods for the quantitative analysis of therapeutic proteins based on different hIgG isotypes was demonstrated [23,24]. The first aim of this work was to develop a generic quantitative assay for a hIgG1 (hIgG1A) in rat serum using four different generic surrogate peptides and a fully isotopically labeled hIgG1 (hIgG1B) as internal standard (ISTD). Afterwards, the developed method was extended to different species and various modalities based on hIgGs. The flexibility of such a generic approach was assessed in the following manner:

(1) Accuracy and precision determination on quality control (QC) samples spiked with hIgG1A in monkey serum measured against calibration standards (Cs) prepared with the hIgG1A in rat serum.
(2) Different therapeutic proteins from the same isotype subclass (hIgG1C, hIgG1D) and another subclass (hIgG4) were prepared

in different matrices (monkey and rat) and quantified against Cs samples prepared with hIgG1A in rat serum.
(3) QC samples were prepared in monkey serum with other hIgG1 related biotherapeutics such as a bispecific-bivalent hIgG1 (bb-hIgG1) or two lysine conjugated ADCs (ADC1 and ADC2) which were measured against Cs samples prepared with hIgG1A in rat serum.
(4) Application to pre-clinical samples where the TK profile of individual monkeys previously dosed with the ADC2 was compared after analysis against Cs samples prepared either with hIgG1A in rat serum (presented approach) or with ADC2 in monkey serum (standard approach).

2. Material and methods

2.1. Chemicals and reagents

All therapeutic proteins used during this study (Table 1) were produced at Novartis Pharma AG (Basel, Switzerland) including three different proteins from the hIgG1 isotype (hIgG1A, hIgG1C, hIgG1D) and one from the hIgG4 subclass. A fully stable isotope labeled protein (hIgG1B) being labeled with [^{13}C]-lysine/arginine moieties was used as ISTD. Three different modalities based on hIgG1 were also incorporated into the investigations: A bb-hIgG1 and two lysine conjugated ADCs (ADC1 and ADC2). The first ADC consisted of a non-cleavable linker (4-[N-maleimidomethyl]-cyclohexane-1-carbonyl, MCC) and N$^{2'}$-Deacetyl-N$^{2'}$-(3-mercapto-1-oxopropyl)maytansine (DM1) as payload whereas the second was constructed with a cleavable charged sulfonate-bearing linker (N-succinimidyl-4-(2-pyridyldithio)butanoate, sulfo-SPDB) and N$^{2'}$-Deacetyl-N$^{2'}$-(4-mercapto-4-methyl-1-oxopentyl) maytansine (DM4) as cytotoxic drug. The synthetically generated reference peptides GPSVFPLAPSSK (GPS), VVSVLTVLHQDWLNGK (VVS) and TTPPVLDSDGSFFLYSK (TTP) used for MS tuning were provided by Thermo Fisher Scientific (Ulm, Germany), whereas blank human serum was used for MS tuning of FNWYVDGVEVH-NAK (FNW) after tryptic digestion. DL-Dithiothreitol (DTT), iodoacetamide (IAA), ammonium bicarbonate, bovine pancreas trypsin, acetic acid, trifluoroacetic acid (TFA), ammonium hydroxide (28–30%), methanol (MeOH), acetonitrile (ACN), isopropanol and MS grade water were obtained from Sigma-Aldrich (Buchs, Switzerland). Formic acid (FA) and acetone were purchased from Merck (Darmstadt, Germany) whereas phosphate buffered saline (PBS; 12 mM phosphate, 137 mM sodium chloride, 2.7 mM potassium chloride, pH 7.4) was provided by Amresco (Solon, OH, USA). All solvents (LC–MS grade) as well as reagents were of high analytical grade (≥99%) and were used without further purification. Blank batches of rat, cynomolgus and marmoset monkey as well as human serum were delivered from Fisher Clinical Services (Allschwil, Switzerland).

Table 1
Summary of investigated therapeutic proteins throughout this study.

Therapeutic protein	hIgG isotype	Modification/intention during study
hIgG1A	1	none, simple mAb, Cs/QCs in rat serum, QCs in cynomolgus monkey serum
hIgG1B	1	fully stable isotope labeled protein ([^{13}C]-lysine/arginine) used as ISTD
hIgG1C	1	none, simple mAb, QCs in cynomolgus monkey serum
hIgG1D	1	none, simple mAb, QCs in cynomolgus monkey serum
hIgG4	4	none, simple mAb, QCs in rat and cynomolgus monkey serum
bb-hIgG1	1	bispecific-bivalent hIgG1, knob (T366W), hole (Y407V) and additional disulfide bridges in C$_H$3 domain, QCs in marmoset monkey serum
ADC1	1	Lysine conjugated ADC, 4-[N-maleimidomethyl]-cyclohexane-1-carbonyl (MCC) as non-cleavable linker; N$^{2'}$-Deacetyl-N$^{2'}$-(3-mercapto-1-oxopropyl)maytansine (DM1) as payload, QCs in cynomolgus monkey serum
ADC2	1	Lysine conjugated ADC, sulfo-N-succinimidyl-4-(2-pyridyldithio)butanoate (sulfo-SPDB) as cleavable linker, N$^{2'}$-Deacetyl-N$^{2'}$-(4-mercapto-4-methyl-1-oxopentyl)maytansine (DM4) as payload, Cs/QCs in cynomolgus monkey serum

2.2. Preparation of Cs and QC samples

The stock solution of hIgG1A at 20.0 mg/mL was serially diluted into PBS. The resultant working solutions were spiked into blank rat serum with a ratio of 1:20 (v/v) yielding in nine Cs concentrations at 1.00, 5.00, 10.0, 20.0, 50.0, 200, 500, 800 and 1000 μg/mL as well as four QC levels at 3.00, 15.0, 450 and 750 μg/mL. In addition, several QC sets with the different modalities of therapeutic proteins were prepared in the same fashion in rat, cynomolgus or marmoset monkey serum resulting in the same QC concentration levels.

2.3. TK study samples from cynomolgus monkey

A single dose of ADC2 (5.00 mg/kg) was administrated intravenously (i.v.) to three individual cynomolgus monkeys. At designated time points (pre-dose, 1, 4, 24, 72, 120 and 168 h post-dose) blood samples (approximately 2.0 mL) were drawn into tubes containing no anticoagulant. The blood was allowed to clot at room temperature for at least 30 min. Subsequently, the samples were centrifuged at $1500 \times g$ and 4 °C for 10 min. The resulting serum was aliquoted (200 μL each) and stored ≤ -70 °C pending analysis. The pre-clinical study was conducted in compliance with the Animal Welfare Act, the Guide for the Care and Use of Laboratory Animals, the Office of Laboratory Animal Welfare and in accordance with the Novartis Animal Care and Use Committee (NACUC).

2.4. Sample preparation

A pellet digestion was used for sample preparation including reduction of the protein's intra- and inter-disulfide bounds with DTT with subsequent alkylation of the free thiol groups with IAA. The enzymatic digestion with trypsin was quenched with TFA after 1 h at 60 °C. An off-line solid phase extraction (SPE) was applied as a last step during sample preparation prior to LC–MS/MS analysis. A detailed description of the pellet digestion protocol was published elsewhere [25].

2.5. Digestion kinetics

The performance of the digestion process was monitored with hIgG1A, ADC1 and the ISTD spiked in serum samples. For this, 7.5, 15.0 or 11.0 μL from each stock solution at 20.0 (hIgG1A), 10.0 (ADC1) and 13.7 mg/mL (ISTD) was mixed with PBS (total volume of 130 μL each). Subsequently, 50 μL of this solution was spiked into 950 μL serum. The sample preparation was identical as described previously [25]. The only differences were that the added volumes were up-scaled by a factor of 20 and that only a volume of 4.0 mL of MeOH was used for the generation of the pellet. Aliquots (200 μL) were collected prior as well as after 0.5, 1, 2, 3, 4, 5 and 19 h (overnight) of digestion at 60 °C. For the subsequent SPE procedure, 150 μL were loaded on the cartridge. The obtained peak areas for each peptide after LC–MS/MS analysis were normalized against the highest peak area in each set for visualization purposes.

2.6. LC–MS/MS

A volume of 10 μL (pickup zero loss injection mode) was introduced into a Symbiosis Pro LC (Spark Holland B.V, Emmen, The Netherlands) equipped with a Reliance unit (conditioned stack and auto-sampler with 100 μL loop) and a Mistral column oven maintained at 60 °C. Tryptic peptides were separated on an ACE C_{18}, 150 × 4.6 mm, 3 μm column from Hichrom (Berkshire, U.K.) with a flow rate of 800 μL/min. The mobile phases consisted of 0.1% FA in water (A) and 0.1% FA in ACN (B). The binary elution gradient program with a double wash step was set as follows

[T(min:s), %(B)]: (0:00, 20); (2:30, 30); (4:30, 90); (5:18, 90); (5:24, 10); (5:36, 10); (5:42, 90); (6:24, 90); (6:30, 20); (8:00, 20). The auto-sampler syringe and the injection valve were successively washed with MeOH/water (1:1, v/v) containing 0.05% FA, MeOH/acetone/water/isopropanol/TFA (50:50:50:50:1, v/v/v/v/v) and ACN/water (1:1, v/v) containing 0.05% FA to reduce carryover. After chromatographic separation, the eluent was introduced with a Turbo V™ electrospray ionization (ESI) probe into an API 6500 linear quadrupole ion trap (QTRAP) mass spectrometer (AB Sciex, Framingham, MA, USA). The MS operated in positive mode using the selected reaction monitoring (SRM) acquisition mode with unit resolution under following parameters: ion spray voltage +5500 V, heater temperature 550 °C, curtain gas 40 psig, nebulizer gas (GS1) 45 psig, turbo ion spray gas (GS2) 50 psig and entrance potential (EP) 10 V. A detailed description of MS/MS parameters for each monitored generic surrogate peptide with a dwell time of 25 ms for each SRM transition including optimized declustering potential (DP), collision energy (CE) and cell exit potential (CXP) is listed in Table S1 (Supplementary data).

2.7. Data acquisition and processing

The LC–MS/MS system was controlled by Analyst 1.6 (AB Sciex). Peak integration, construction of the calibration curve and the back-calculation of the concentrations were performed with the quantification tab in Analyst 1.6. Graphical illustration was conducted with OriginPro (v9.1.0, OriginLab Coorperation, Northampton, MA, USA).

2.8. Construction and acceptance criteria for calibration curve

One set of calibration standards was injected at the beginning and at the end of each analytical run. For FNW, GPS and VVS, a linear ($y = ax + b$) regression model was used whereas for the TTP peptide, a quadratic function ($y = ax^2 + bx + c$) was more appropriate due to the saturation of the detector at higher concentrations. y was the peak area ratio of the surrogate peptide to the $[^{13}C_6]$-lysine labeled version whereas x represented the nominal concentration of the protein in the Cs samples. A weighting factor of $1/x^2$ was used regardless of the regression model. The acceptance criteria were set ±20.0% (±25.0% at the lower limit of quantification [LLOQ] and upper limit of quantification [ULOQ]) from nominal values for at least 75.0% of Cs samples in one analytical run. Additionally, at least one replicate per each Cs concentration should meet the above mentioned acceptance criteria.

2.9. QC acceptance criteria

The accuracy of the analytical assay was evaluated by the deviation (% bias) from the nominal concentration whereas the percentage of the coefficient of variation (CV) determined the precision for each QC level. The accuracy and precision were evaluated in triplicate on each day (intra-day) whereas the inter-day accuracy and precision was determined over several days. A mean bias within ±20.0% of the nominal values and a precision of ≤20.0% were set as acceptance criteria.

3. Results and discussion

3.1. Selection of surrogate peptides and their digestion kinetics

Four different surrogate peptides originating from different parts of the constant region of the hIgG1 heavy chain (C_H) were selected in order to perform the quantitation. The GPS and the TTP peptides are located in the C_H1 and C_H3 domain respectively
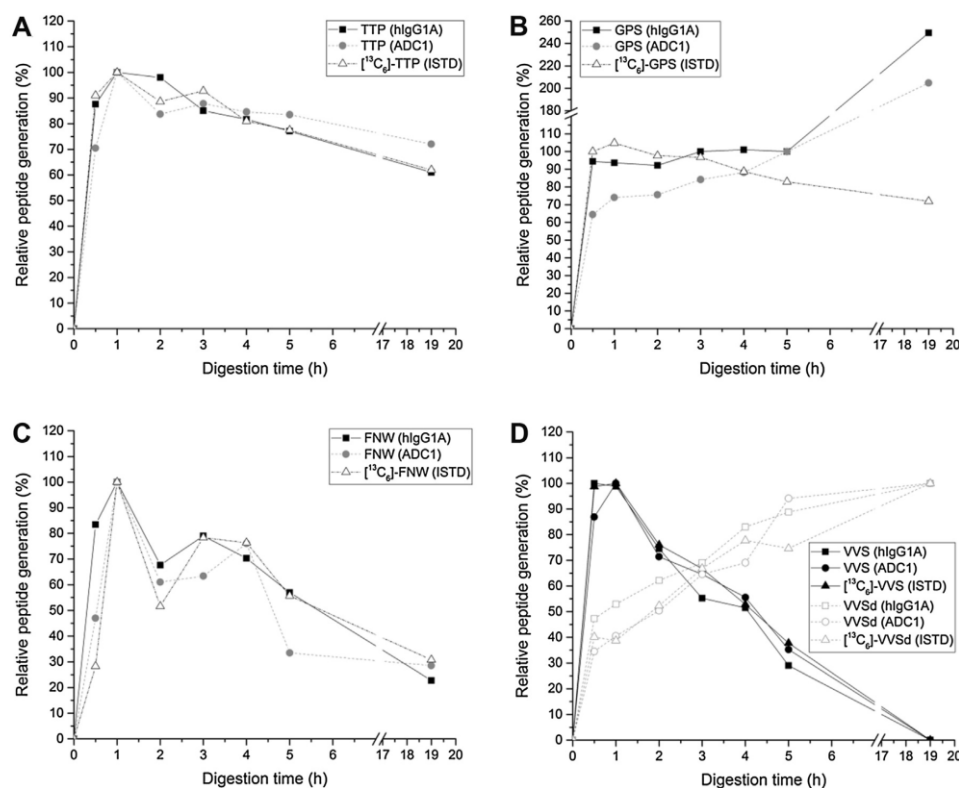
Fig. 1. Digestion kinetics for (A) TTP, (B) GPS, (C) FNW and (D) VVS in its non-deamidated as well as deamidated form (VVSd) obtained either from hIgG1A, ADC1 or its [$^{13}C_6$]-labeled versions from the internal standard (ISTD).

whereas the C_H2 region contained the FNW and VVS peptide. Furthermore, the VVS peptide was also present in the hIgG4 isotype. A reproducible digestion across different therapeutic proteins was one key prerequisite to further extend the applicability of such a LC–MS/MS method based on four generic surrogate peptides. The kinetics of the overnight tryptic digestion of hIgG1A, ADC1 and the fully labeled protein used as ISTD spiked in serum are depicted for each surrogate peptide in Fig. 1. The digestion pattern with the TTP peptide displayed similar profiles irrespective of the therapeutic proteins used (Fig. 1A) indicating that the ISTD would compensate for differences in digestion efficiencies. However, a significant increase in signal intensity (up to 250%) was observed with the GPS peptide originating either from hIgG1A or ADC1 whereas the heavy labeled version originating from the ISTD demonstrated a similar profile to the ones obtained with the TTP peptide (Fig. 1B). Further investigations with high-resolution mass spectrometry indicated a mass shift of 0.02 Da on each a/x-ion of this peptide from hIgG1A and ADC1 after overnight digestion (data not shown). This caused interferences with the monitored SRM transitions of the GPS surrogate peptide being responsible for the significant signal increase. As a result, differences in digestion efficiencies can no longer be corrected accordingly after overnight digestion despite the use of a fully isotopically labeled hIgG1 as ISTD. Hence for GPS a short digestion time (2–3 h) should be favored. An increased deamidation at elevated temperatures over time was the reason for the decrease in signal intensity for the FNW peptides regardless of their origin (Fig. 1C). However, the ISTD compensated for the loss in signal as [$^{13}C_6$]-FNW behaved accordingly. Nevertheless, the decrease in sig-

nal intensity would result in a higher LLOQ of the analytical method when an overnight digestion was favored. The same phenomenon was observed for the second C_H2 peptide (Fig. 1D): the signal of the non-deamidated form decreased over time whereas the deamidated VVS signal (VVSd) increased. Overall, a digestion period of 1 h was sufficient as the maximum signal intensity for each generic surrogate peptide or its [$^{13}C_6$]-labeled version was obtained after this time whereas the deamidation process was not that advanced (e.g. 35–50% for VVSd). In the end, the SRM transitions for the non-deamidated C_H2 peptides were used for quantitation.

3.2. hIgG1A and hIgG4 in rat serum

The linearity of Cs samples prepared with hIgG1A in rat serum was achieved with a coefficient of determination (R^2) value ≥0.99 for all four generic surrogate peptides and a ULOQ of 1000 μg/mL (Supplementary data Table S2). The LLOQ was set to 1.00 μg/mL for the GPS, TTP and VVS peptides whereas the FNW resulted in a slightly higher LLOQ at 5.00 μg/mL (Supplementary data Table S2). The developed generic LC–MS/MS method for the quantitative analysis of hIgG1A met acceptance regarding accuracy and precision on all four QC levels (3.00, 15.0, 450 and 750 μg/mL) on five different days in triplicate (n = 15). For the investigated peptides, the inter-day accuracy ranged from −5.0 to 8.5% whereas the inter-day precision was between 4.1 and 14.8% for hIgG1A (Table 2). As the variation of the mean inter-peptide concentration on each spiked QC level was ≤3.2% (Table 2), similar digestion efficiencies were obtained with each generic peptide confirming the results in

218   C. Lanshoeft et al. / Journal of Pharmaceutical and Biomedical Analysis 131 (2016) 214–222

Table 2
Inter-day accuracy and precision of quality control (QC) samples using four generic peptides from a human immunoglobulin G1 (hIgG1A) on five different days (n = 15) and a hIgG4 (n = 3) spiked in rat serum.

Subclass	Peptide		QC nominal concentration (µg/mL) in rat serum			
			750	450	15.0	3.00
			Inter-day accuracy and precision (n = 15)			
hIgG1	FNW	Mean concentration (µg/mL)	742	430	16.3	–
		Inter-day accuracy (% bias)	−1.0	−4.5	8.4	–
		Inter-day precision (% CV)	5.8	5.9	12.1	–
	GPS	Mean concentration (µg/mL)	797	428	15.8	2.95
		Inter-day accuracy (% bias)	6.2	−5.0	5.2	−1.7
		Inter-day precision (% CV)	7.2	9.4	9.1	8.3
	TTP	Mean concentration (µg/mL)	753	438	15.7	3.02
		Inter-day accuracy (% bias)	0.4	−2.6	4.7	0.6
		Inter-day precision (% CV)	4.1	5.0	13.6	9.7
	VVS	Mean concentration (µg/mL)	751	436	16.3	3.12
		Inter-day accuracy (% bias)	0.2	−3.1	8.5	3.9
		Inter-day precision (% CV)	6.7	7.6	14.8	9.7
	Inter-peptide	Mean concentration (µg/mL)	761	433	16.0	3.03
		Standard deviation (µg/mL)	25	5	0.3	0.09
		CV (%)	3.2	1.1	2.0	2.8
			Accuracy and precision[a] (n = 3)			
hIgG4	VVS	Mean concentration (µg/mL)	662	369	13.3	2.24
		Accuracy (% bias)	−11.7	−17.9	−11.1	−25.2[b]
		Precision (% CV)	2.5	0.4	1.6	3.6

[a] Measured against Cs prepared with hIgG1A in rat serum.
[b] Acceptance criterion of ±20.0% not met.

Fig. 1 and indicated that the hIgG1A concentration was determined in an accurate and precise manner in rat serum regardless of the surrogate peptide selected. In addition, the developed LC–MS/MS method was not only limited to hIgG1-based therapeutic proteins as the VVS peptide was also conserved in the hIgG4 isotype subclass. Consequently, this peptide was used to further extend the applicability of the method. The accuracy of the low QC sample at 3.00 µg/mL did not fulfill the acceptance criterion with −25.2% bias (Table 2). However, the remaining QC levels met acceptance with maximum values of −17.9 and 2.5% regarding accuracy and precision, respectively.

3.3. hIgG1A and hIgG4 in cynomolgus monkey measured against Cs prepared in rat serum

It has been demonstrated previously that endogenous compounds in complex matrices could significantly affect the analyte's MS response which further impacts the accuracy and precision of the quantitative data [26,27]. Matching the matrix of the real samples (pre-clinical and clinical samples) to the one used for the preparation of Cs and QC samples is the most common approach in order to avoid any issues during the sample analysis. However, the impracticability of exact matching of the matrix of Cs and QCs with all samples leads to some remaining uncertainties. In order to correct for the matrix effect (ion suppression or enhancement) at the expected retention time of the surrogate peptides, a stable isotope labeled hIgG1 was used as ISTD. Each generic surrogate peptide and its corresponding ISTD experienced the same sort of ionization effect in the ESI source as already demonstrated with the digestion kinetics (Fig. 1). Similar MS responses were observed for the ISTD in QC samples (n = 12) with the [$^{13}C_6$]-FNW peptide when switching from rat to cynomolgus monkey serum (Fig. 2). In contrast, different MS responses of the [$^{13}C_6$]-GPS, [$^{13}C_6$]-TTP and [$^{13}C_6$]-VVS peptides were observed in both seras with a tendency towards ion suppression in cynomolgus monkey serum (Fig. 2). However, the back-calculated concentration of hIgG1A remained unaffected as the analyte to ISTD ratio were similar to the expected ratio of the nominal QC concentration with each generic surrogate peptide regardless of the matrix selected (Supplementary data Table

S3). Consequently, the calibration curve prepared in rat serum can be used to determine the QC concentrations in cynomolgus monkey serum. The resultant accuracy and precision data obtained on spiked QC samples in cynomolgus monkey serum measured against Cs samples prepared in rat serum are summarized in Table 3. The whole calibration range was accurately and precisely covered with the TTP peptide. Nevertheless, the lower QC level (3.00 µg/mL) exceeded the inter-day accuracy acceptance criterion of ±20.0% by 8.4 and 13.7% for the GPS and VVS peptide, respectively. For the GPS peptide, the y_4^+ product ion at m/z 418.5 was selected for quantitative analysis which displayed less interferences as opposed to other fragments such as the singly charged y_7^+ product ion at m/z 699.4 or the y_8^+ fragment (m/z 846.4) being previously used for quantitative purposes [23,24]. Nevertheless, an endogenous compound found in blank monkey serum interfered with the GPS SRM transitions resulting in an overestimation of the lower concentrations as described earlier [24]. The overestimation of the hIgG4 concentration by 48.2% at the low spiked QC in cynomolgus monkey serum with the VVS peptide could also be attributed to some endogenous interferences found in monkey serum under the selected experimental conditions. This would be in contradiction with the previously reported selectivity data of the VVS peptide in monkey serum [22]. In order to avoid an overestimation of hIgG4, the LLOQ could further be increased from 1.00 to 5.00 µg/mL. Overall, the results on the other remaining QC levels indicated that no significant changes in terms of accuracy and precision were observed on three different days with three different batches of blank serum when switching from rat to cynomolgus monkey serum (Table 3).

3.4. Other hIgG1-based therapeutic proteins spiked in cynomolgus monkey serum and measured against Cs prepared in rat serum with hIgG1A

As the matrix had no significant impact on the accuracy and precision of the quantitative data, further investigations were conducted with additional mAbs based on the hIgG1 isotype (hIgG1C and hIgG1D) which were spiked in cynomolgus monkey serum and measured against Cs prepared with hIgG1A in rat serum in order to demonstrate the flexibility of the method. The corresponding
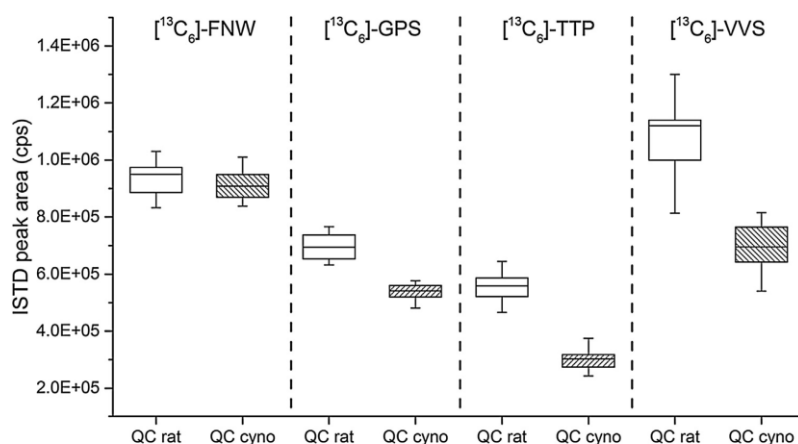
Fig. 2. Boxplot showing the peak area of the internal standard (ISTD) in QC samples (n = 12) observed in rat or cynomolgus monkey serum for all four investigated generic surrogate peptides.

Table 3
Inter-day accuracy and precision of quality control (QC) samples prepared either with a human immunoglobulin G1 (hIgG1A) on three different days (n = 9) or hIgG4 on one day (n = 3) spiked in cynomolgus monkey serum measured against calibration standards (Cs) prepared with hIgG1A in rat serum.

			QC nominal concentration (µg/mL) in cynomolgus monkey serum			
			750	450	15.0	3.00
Subclass	Peptide		Inter-day accuracy and precision[a] (n = 9)			
hIgG1	FNW	Mean concentration (µg/mL)	748	451	15.4	–
		Inter-day accuracy (% bias)	−0.2	0.2	2.8	–
		Inter-day precision (% CV)	9.3	6.8	2.1	–
	GPS	Mean concentration (µg/mL)	824	493	15.6	3.85
		Inter-day accuracy (% bias)	9.9	9.5	3.8	28.4[b]
		Inter-day precision (% CV)	7.5	8.7	8.3	11.6
	TTP	Mean concentration (µg/mL)	812	493	15.4	3.21
		Inter-day accuracy (% bias)	8.3	9.7	3.0	6.9
		Inter-day precision (% CV)	9.4	7.6	5.7	7.6
	VVS	Mean concentration (µg/mL)	777	477	14.3	1.99
		Inter-day accuracy (% bias)	3.7	6.0	−4.9	−33.7[b]
		Inter-day precision (% CV)	10.6	13.1	10.1	17.2
			Accuracy and precision[a] (n = 3)			
hIgG4	VVS	Mean concentration (µg/mL)	680	425	16.1	4.45
		Accuracy (% bias)	−9.3	−5.6	7.3	48.2[b]
		Precision (% CV)	5.9	1.2	13.2	19.1

[a] Measured against Cs prepared with hIgG1A in rat serum.
[b] Acceptance criterion of ±20.0% not met.

accuracy and precision data are summarized in Table 4. The accuracy acceptance criterion of ±20.0% was again not met for the low QC level at 3.00 µg/mL using the VVS peptide. The ratio between the deamidated and non-deamidated version of the VVS peptide increased with decreasing QC concentrations. Consequently, the deamidation process affected the lower QC concentrations causing an underestimation of hIgG1C and hIgG1D at this concentration level similar to the results of hIgG1A (Table 3). In contrast, the protein concentration at the low QC level was overestimated with the GPS peptide by 18.3 and 24.4% for hIgG1C and hIgG1D respectively due to the inference in monkey serum (already discussed). The FNW and TTP accuracy data met acceptance for both hIgG1-based therapeutic proteins ranging from −10.3 to 7.6% and −5.0 to 13.8% respectively with corresponding maximum CV values ≤5.4 and ≤15.9%, respectively. In general, the TTP peptide was the best out of the four investigated surrogate peptides and was suitable for the quantitative of analysis of hIgG1-based therapeutic proteins in

both monkey and rat serum with a LLOQ of 1.00 µg/mL without any significant deviation from the set acceptance criteria. Overall, the quantitation can be performed with the three other peptides as well but an increased LLOQ of 5.00 µg/mL is suggested.

3.5. Bispecific antibody and lysine conjugated ADCs spiked in monkey serum and measured against Cs prepared in rat serum with hIgG1A

The developed method was also applied to different modalities including a bb-hIgG1 and two lysine conjugated ADCs. In order to avoid heterodimerization of the bb-hIgG1, a so called knob-into-hole approach was used to merge two different hIgG1s together [28,29]. A "knob" was artificially created in the C_H3 domain of one heavy chain by replacing one amino acid (threonine, T) with a larger one (tryptophan, W) at position 366 (T366W) whereas on the partner heavy chain a "hole" was created by inserting a

Table 4
Accuracy and precision of quality control (QC) samples prepared with different human immunoglobulin G1 antibodies (hIgG1C, hIgG1D) spiked in cynomolgus monkey serum measured against calibration standards (Cs) prepared with another hIgG1A in rat serum (n = 3).

Peptide		QC nominal concentration (µg/mL) in cynomolgus monkey serum							
		750	450	15.0	3.00	750	450	15.0	3.00
		Accuracy and precision[a] (n = 3)							
		hIgG1C				hIgG1D			
FNW	Mean concentration (µg/mL)	762	450	16.1	–	752	404	14.5	–
	Accuracy (% bias)	1.6	0.1	7.6	–	0.3	–10.3	–3.6	–
	Precision (% CV)	0.6	1.8	5.0	–	5.4	4.3	0.4	–
GPS	Mean concentration (µg/mL)	638	360	12.2	3.55	724	416	13.9	3.73
	Accuracy (% bias)	–14.9	–20.1[b]	–18.7	18.3	–3.4	–7.6	–7.3	24.4[b]
	Precision (% CV)	1.1	3.4	3.8	7.2	9.8	5.0	3.3	15.4
TTP	Mean concentration (µg/mL)	802	479	15.1	3.41	815	463	15.2	2.85
	Accuracy (% bias)	6.9	6.4	0.7	13.8	8.6	2.8	1.3	–5.0
	Precision (% CV)	2.1	4.1	1.8	10.3	5.0	1.1	3.7	15.9
VVS	Mean concentration (µg/mL)	738	453	14.3	2.19	689	384	11.9	1.52
	Accuracy (% bias)	–1.6	0.6	–4.4	–26.9[b]	–8.1	–14.7	–20.4[b]	–49.3[b]
	Precision (% CV)	3.1	2.8	3.1	7.0	4.5	0.5	3.8	4.6

[a] Measured against Cs prepared with hIgG1A in rat serum.
[b] Acceptance criterion of ±20.0% not met.

Table 5
Accuracy and precision of quality control (QC) samples prepared with different modalities based on human immunoglobulin G1 (hIgG1) including two lysine conjugated antibody-drug conjugates (ADC1, ADC2) and one bispecific-bivalent hIgG1 (bb-hIgG1) spiked in monkey serum measured against calibration standards (Cs) prepared with hIgG1A in rat serum (n = 3).

Peptide		QC nominal concentration (µg/mL) in monkey serum											
		750	450	15.0	3.00	750	450	15.0	3.00	750	450	15.0	3.00
		Accuracy and precision[a] (n = 3)											
		ADC1[b]				ADC2[b]				bb-hIgG1[c]			
FNW	Mean concentration (µg/mL)	602	347	14.0	–	712	444	16.6	–	617	332	10.7	–
	Accuracy (% bias)	–19.8	–23.0[d]	–6.9	–	–5.1	–1.3	10.9	–	–17.7	–26.1[d]	–28.4[d]	–
	Precision (% CV)	3.9	3.8	4.2	–	7.3	4.4	3.0	–	2.0	4.9	4.7	–
GPS	Mean concentration (µg/mL)	562	352	11.7	4.81	897	537	20.5	5.91	869	478	14.7	3.09
	Accuracy (% bias)	–25.1[d]	–21.7[d]	–22.2[d]	60.2[d]	19.6	19.4	36.9[d]	97.1[d]	15.8	6.2	–2.2	3.0
	Precision (% CV)	6.8	3.4	9.2	11.5	4.3	3.3	4.5	13.0	2.4	2.5	2.8	6.3
TTP	Mean concentration (µg/mL)	662	395	13.2	3.08	746	480	17.5	3.77	248	134	3.51	BLOQ
	Accuracy (% bias)	–11.7	–12.1	–12.0	2.8	–0.5	6.6	16.9	25.6[d]	–67.0[d]	–70.3[d]	–76.6[d]	–
	Precision (% CV)	2.1	3.0	1.3	9.6	4.8	2.7	7.6	8.1	4.3	1.1	8.0	–
VVS	Mean concentration (µg/mL)	610	357	12.2	5.59	852	530	18.6	3.60	451	244	6.25	BLOQ
	Accuracy (% bias)	–18.7	–20.7[d]	–18.9	86.3[d]	13.6	17.9	24.2[d]	20.1[d]	–39.9[d]	–45.7[d]	–58.4[d]	–
	Precision (% CV)	7.1	5.7	5.5	57.7[e]	5.5	4.0	2.2	5.9	2.0	6.9	5.9	–

BLOQ: Below lower limit of quantification of 1.00 µg/mL.
[a] Measured against Cs prepared with hIgG1A in rat serum.
[b] Spiked in cynomolgus monkey serum.
[c] Spiked in marmoset monkey serum.
[d] Acceptance criterion of ±20.0% not met.
[e] Acceptance criterion of ≤20.0% not met.

smaller amino acid (valine, V) instead of a larger one (tyrosine, Y) at position 407 (Y407V). Besides, the knob-into-hole technology, additional stabilizing disulfide bridges were introduced into the bb-hIgG1. Accurate and precise data was only obtained on spiked QC samples with the GPS surrogate peptide whereas the FNW, TTP and VVS peptide resulted in inaccurate data for the quantitative analysis of bb-hIgG1 in monkey serum (Table 5). This phenomenon was most likely due to the fact that the GPS peptide was located in the C_H1 region of the bb-hIgG1 which was not affected by the above mentioned modifications. However, another hypothesis leading to an underestimation of bb-hIgG1 using the FNW, VVS or TTP peptide could be that there was a difference in the digestion efficiency between the hIgG1A (being used for Cs preparation) and the bb-hIgG1 due to the introduced modifications which could interfere with the enzyme during tryptic

digestion. The lysine conjugated ADCs used in the present study were based on two different constructs: ADC1 carried DM1 as payload which was conjugated through a non-cleaveable linker (MCC) to the mAb whereas DM4 was linked via a cleavable linker (sulfo-SPDB) to the mAb in the case of ADC2. In case of ADC1, the GPS and VVS peptide displayed a lower concentration when measured against hIgG1A (Table 5). A potential miscleavages of the lysine residue due to steric hindrance of the payload with the GPS peptide resulting in an underestimation of the ADC concentration was recently observed which could be one possible explanation of the obtained underestimation [30]. However, this was not the case for ADC2 as the ADC concentration was overestimated using the GPS and VVS surrogate peptide. Nevertheless, the other two peptides (TTP and FNW) were found satisfactory for both ADCs regarding accuracy and precision data. Thus, both peptides could be used for
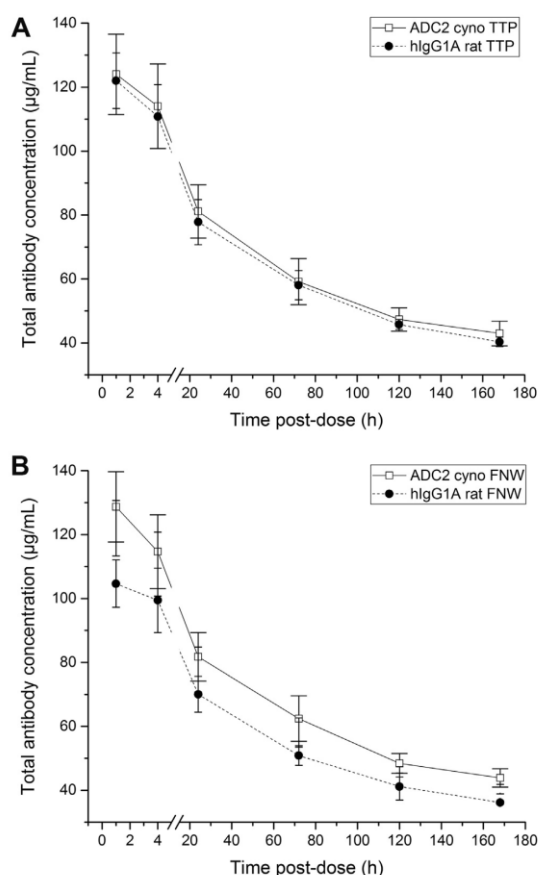
Fig. 3. Mean concentration-time profile of pre-clinical cynomolgus monkey serum samples from a toxicokinetic study measured against calibration standards (Cs) prepared either with the ADC2 spiked in cynomolgus monkey serum or a simple unmodified hIgG1A in rat serum using the (A) TTP or (B) FNW peptide.

the quantitation of ADC1 and ADC2 using the generic LC–MS/MS approach.

3.6. Application to a pre-clinical TK study

In order to demonstrate the generic approach not only based on spiked QC samples, pre-clinical samples from three individual cynomolgus monkeys after i.v. administration of ADC2 (5.00 mg/kg) were analysed. The serum concentration-time profile was acquired either with Cs and QC samples prepared with the same analyte (ADC2) in cynomolgus monkey serum or with a simple hIgG1 (hIgG1A) in rat serum not carrying any linker or payload. Since the TTP and FNW peptide demonstrated the best performance in QC samples, they were used to determine the total antibody concentration in monkey serum. The profile obtained with ADC2 in cynomolgus monkey serum was similar to the one measured against Cs/QC samples prepared with hIgG1A in rat serum when using the TTP peptide (Fig. 3A). The highest serum concentrations were obtained directly with the first post-dose sampling time point at 1 h with corresponding mean concentrations (n = 3) of 124 ± 13 and 122 ± 9 µg/mL when an ADC2 or a hIgG1A was used for the preparation of Cs/QC samples in different matrices, respectively. The mean bias between the mean concentrations using both

approaches at each time point was $3.3 \pm 1.6\%$ with the TTP peptide. A similar trend was also observed with the FNW peptide (Fig. 3B). The mean concentration-time profile obtained with the FNW peptide using Cs samples prepared with the ADC2 in monkey serum was in agreement with the ones obtained with the TTP peptide regardless of the approach selected. This confirmed the quantitative data obtained with the TTP peptide. A systematic bias in the total antibody concentration was observed when measured against Cs prepared with the hIgG1A in rat serum or ADC2 in cynomolgus monkey serum using the FNW peptide. Nevertheless, the acceptance criterion of $\pm 20.0\%$ during cross-check was still met as the mean bias was $-16.2 \pm 2.3\%$. One hypothesis explaining the systematic bias with the FNW compared to the TTP peptide would be that conjugation of the linker/payload to the FNW peptide was more frequent compared to the TTP peptide. In general, each lysine containing peptide could be the origin of an underestimation of lysine conjugated ADCs due to steric hindrance of the linker and cytotoxic payload upon tryptic digestion resulting in a potential miscleavage of the lysine residue and consequently lower concentrations when measured against Cs samples prepared with a simple unmodified hIgG1 [30]. Thus, further experiments have to be conducted to clarify if arginine containing peptides work better for the quantitative analysis of lysine conjugated ADCs compared to lysine containing peptides in order to avoid any underestimation in the total antibody concentration.

4. Conclusions

In the present study, we have developed a generic LC–MS/MS method for the quantitative analysis of hIgG1 and hIgG4-based therapeutic proteins using four generic surrogate peptides in rat or cynomolgus monkey serum. In addition, we have demonstrated that our method using a fully labeled protein as ISTD is flexible enough to allow matrix switching from rat to cynomolgus monkey serum. However, adequate experiments with QC samples are suggested prior to matrix exchange as there might be cases where such an exchange of matrices will not be successful even though an appropriate ISTD is used. We also observed that one single generic LC–MS/MS approach cannot always be applied to each type of therapeutic protein due to the complexity of biotherapeutics (especially with ADCs). Besides this, a certain knowledge about introduced modifications are one key prerequisite when using such a generic approach in order to avoid under- or overestimation of the total antibody concentration. Furthermore, when using the same peptide, we found that the in-vivo data differed from the in-vitro ones in terms of quantitation. Thus, the selection of an appropriate surrogate peptide appears critical and choosing several (generic) surrogate peptides for quantitative purposes would be worthwhile. With our present method that uses four generic peptides, we believe that the early development of biotherapeutics could be accelerated particularly by enabling PK analysis across animal species and candidate molecules with minimal effort in method development.

Conflict of interest

Acknowledgements

Appendix A. Supplementary data

Supplementary data associated with this article can be found, in the online version, at http://dx.doi.org/10.1016/j.jpba.2016.08.039.

References

[1] A. Beck, T. Wurch, C. Bailly, N. Corvaia, Strategies and challenges for the next generation of therapeutic antibodies, Nat. Rev. Immunol. 10 (2010) 345–352.

[2] D.S. Dimitrov, Therapeutic proteins, in: V. Voynov, A.J. Caravella (Eds.), Therapeutic Proteins: Methods and Protocols, Humana Press, Totowa, NJ, 2012, pp. 1–26.

[3] J.M. Reichert, Antibodies to watch in 2016, mAbs (2015) 1–8.

[4] A. Beck, J.F. Haeuw, T. Wurch, L. Goetsch, C. Bailly, N. Corvaia, The next generation of antibody-drug conjugates comes of age, Discov. Med. 10 (2010) 329–339.

[5] H. Byrne, P.J. Conroy, J.C. Whisstock, R.J. O'Kennedy, A tale of two specificities: bispecific antibodies for therapeutic and diagnostic applications, Trends Biotechnol. 31 (2013) 621–632.

[6] U. Aich, J. Lakbub, A. Liu, State-of-the-art technologies for rapid and high-throughput sample preparation and analysis of N-glycans from antibodies, Electrophoresis 37 (2016) 1468–1488.

[7] B.Q. Tran, C. Barton, J. Feng, A. Sandjong, S.H. Yoon, S. Awasthi, T. Liang, M.M. Khan, D.P. Kilgour, D.R. Goodlett, Y.A. Goo, Glycosylation characterization of therapeutic mAbs by top- and middle-down mass spectrometry, Data Brief 6 (2016) 68–76.

[8] A. Beck, G. Terral, F. Debaene, E. Wagner-Rousset, J. Marcoux, M.-C. Janin-Bussat, O. Colas, A.V. Dorsselaer, S. Cianférani, Cutting-edge mass spectrometry methods for the multi-level structural characterization of antibody-drug conjugates, Expert Rev. Proteomics 13 (2016) 157–183.

[9] V. Gautier, A.J. Boumeester, P. Lössl, A.J.R. Heck, Lysine conjugation properties in human IgGs studied by integrating high-resolution native mass spectrometry and bottom-up proteomics, Proteomics 15 (2015) 2756–2765.

[10] M.-C. Janin-Bussat, M. Dillenbourg, N. Corvaia, A. Beck, C. Klinguer-Hamour, Characterization of antibody drug conjugate positional isomers at cysteine residues by peptide mapping LC–MS analysis, J. Chromatogr. B 981–982 (2015) 9–13.

[11] J. Stojko, S. Fieulaine, S. Petiot-Becard, A. Van Dorsselaer, T. Meinnel, C. Giglione, S. Cianferani, Ion mobility coupled to native mass spectrometry as a relevant tool to investigate extremely small ligand-induced conformational changes, Analyst 140 (2015) 7234–7245.

[12] O. Heudi, S. Barteau, D. Zimmer, J. Schmidt, K. Bill, N. Lehmann, C. Bauer, O. Kretz, Towards absolute quantification of therapeutic monoclonal antibody in serum by LC–MS/MS using isotope-labeled antibody standard and protein cleavage isotope dilution mass spectrometry, Anal. Chem. 80 (2008) 4200–4207.

[13] C. Lanshoeft, O. Heudi, S. Cianférani, A.P. Warren, F. Picard, O. Kretz, Quantitative analysis of hIgG1 in monkey serum by LC–MS/MS using mass spectrometric immunoassay, Bioanalysis 8 (2016) 1035–1049.

[14] S. Kaur, K. Xu, O.M. Saad, R.C. Dere, M. Carrasco-Triguero, Bioanalytical assay strategies for the development of antibody-drug conjugate biotherapeutics, Bioanalysis 5 (2013) 201–226.

[15] R.J. Sanderson, N.D. Nicholas, C. Baker Lee, S.M. Hengel, R.P. Lyon, D.R. Benjamin, S.C. Alley, Antibody-conjugated drug assay for protease-cleavable antibody-drug conjugates, Bioanalysis 8 (2016) 55–63.

[16] M. Dubois, F. Fenaille, G. Clement, M. Lechmann, J.C. Tabet, E. Ezan, F. Becher, Immunopurification and mass spectrometric quantification of the active form of a chimeric therapeutic antibody in human serum, Anal. Chem. 80 (2008) 1737–1745.

[17] M.A.V. Willrich, D.L. Murray, D.R. Barnidge, P.M. Ladwig, M.R. Snyder, Quantitation of infliximab using clonotypic peptides and selective reaction monitoring by LC–MS/MS, Int. Immunopharmacol. 28 (2015) 513–520.

[18] P. Bults, N.C. van de Merbel, R. Bischoff, Quantification of biopharmaceuticals and biomarkers in complex biological matrices: a comparison of liquid chromatography coupled to tandem mass spectrometry and ligand binding assays, Expert Rev. Proteomics 12 (2015) 355–374.

[19] H. Li, R. Ortiz, L.T. Tran, H. Salimi-Moosavi, J. Malella, C.A. James, J.W. Lee, Simultaneous analysis of multiple monoclonal antibody biotherapeutics by LC–MS/MS method in rat plasma following cassette-dosing, AAPS J. 15 (2013) 337–346.

[20] K. Xu, L. Liu, M. Maia, J. Li, J. Lowe, A. Song, S. Kaur, A multiplexed hybrid LC-MS/MS pharmacokinetic assay to measure two co-administered monoclonal antibodies in a clinical study, Bioanalysis 6 (2014) 1781–1794.

[21] H. Li, R. Ortiz, L. Tran, M. Hall, C. Spahr, K. Walker, J. Laudemann, S. Miller, H. Salimi-Moosavi, J.W. Lee, General LC–MS/MS method approach to quantify therapeutic monoclonal antibodies using a common whole antibody internal standard with application to preclinical studies, Anal. Chem. 84 (2012) 1267–1273.

[22] M.T. Furlong, Z. Ouyang, S. Wu, J. Tamura, T. Olah, A. Tymiak, M. Jemal, A universal surrogate peptide to enable LC–MS/MS bioanalysis of a diversity of human monoclonal antibody and human Fc-fusion protein drug candidates in pre-clinical animal studies, Biomed. Chromatogr. 26 (2012) 1024–1032.

[23] J.W. Lee, Generic method approaches for monoclonal antibody therapeutics analysis using both ligand binding and LC–MS/MS techniques, Bioanalysis 8 (2016) 19–27.

[24] Q. Zhang, D.S. Spellman, Y. Song, B. Choi, N.G. Hatcher, D. Tomazela, M. Beaumont, M. Tabrizifard, D. Prabhavalkar, W. Seghezzi, J. Harrelson, K.P. Bateman, Generic automated method for liquid chromatography–multiple reaction monitoring mass spectrometry based monoclonal antibody quantitation for preclinical pharmacokinetic studies, Anal. Chem. 86 (2014) 8776–8784.

[25] C. Lanshoeft, T. Wolf, O. Heudi, S. Cianférani, S. Barteau, M. Walles, F. Picard, O. Kretz, The use of generic surrogate peptides for the quantitative analysis of human immunoglobulin G1 in pre-clinical species with high-resolution mass spectrometry, Anal. Bioanal. Chem. 408 (2016) 1687–1699.

[26] A. Cappiello, G. Famiglini, P. Palma, E. Pierini, V. Termopoli, H. Trufelli, Overcoming matrix effects in liquid chromatography–mass spectrometry, Anal. Chem. 80 (2008) 9343–9348.

[27] P.J. Taylor, Matrix effects: the Achilles heel of quantitative high-performance liquid chromatography–electrospray–tandem mass spectrometry, Clin. Biochem. 38 (2005) 328–334.

[28] W. Schaefer, H.R. Volger, S. Lorenz, S. Imhof-Jung, J.T. Regula, C. Klein, M. Molhoj, Heavy and light chain pairing of bivalent quadroma and knobs-into-holes antibodies analyzed by UHR-ESI-QTOF mass spectrometry, mAbs 8 (2016) 49–55.

[29] Y. Xu, J. Lee, C. Tran, T.H. Heibeck, W.D. Wang, J. Yang, R.L. Stafford, A.R. Steiner, A.K. Sato, T.J. Hallam, G. Yin, Production of bispecific antibodies in knobs-into-holes using a cell-free expression system, mAbs 7 (2015) 231–242.

[30] H. Yang, M. Lame, S. Naughton, E. Chambers, Quantification of the antibody drug conjugate, trastuzumab emtansine, and the monocolonal antibody, Trastuzumab Plasma Using Generic Kit-Based Approach (2016), Application Note 720005619EN www.waters.com.

2.2 Evaluation of commercial digestion kits as standardized sample preparation for hIgG1 quantification in rat serum

2.2.1 Analytical context

The proteolytic digestion represents the most critical step of the protracted sample preparation procedure for LC-MS/MS-based bottom-up mAb quantification.[262] In order to assure an efficient, complete, and reproducible peptide generation, as prerequisite for accurate and precise mAb quantification, intensive assessment of the digestion is necessary.[218,373] This evaluation involves the selection of the most appropriate proteolytic enzyme, its source and quality as well as the suitable enzyme-to-protein ratio.[374-376] Furthermore, the digestion time, temperature, composition and pH of the digestion buffer must be optimized.[375-377] As a consequence, numerous digestion protocols are available in which overnight digestion is still frequently employed, although accelerated approaches based on immobilized trypsin,[378-382] ultrasound,[383] infrared radiation,[384] elevated digestion temperatures,[385-387] and the addition of organic solvents during digestion[388-390] enable fast peptide generation in less than one hour or even within minutes.[201,249,374] Moreover, analytical bias can be readily introduced during complex multistep protocols or method transfer, impacting the overall data quality. Hence, various commercially available digestion kits have been recently developed by MS vendors in order to circumvent tedious digestion optimization and provide an accelerated as well as standardized protocol for mAb quantification, while minimizing sample processing steps and required reagents.

2.2.2 Objectives

This project aimed to assess the applicability of two commercial digestion kits, namely the SMART Digest Kit (Thermo Fisher Scientific) and ProteinWorks eXpress Digest Kit (Waters), and to compare both kits with the developed pellet digestion protocol for hIgG1 quantification in spiked rat serum samples.

2.2.3 Results

2.2.3.1 Overview of sample preparation protocols

Both digestion kits are suitable for in-solution digestion of (immuno-purified) proteins or direct digestion of complex matrices containing the targeted protein. However, only direct serum digestion was evaluated with both provided test kits. For each direct digestion protocol, the same starting volume of rat serum was required, which was spiked with [^{13}C]-hIgG1 (ISTD) prior to sample preparation (Figure 2.8). In comparison to the pellet digestion, both kits omit the reduction
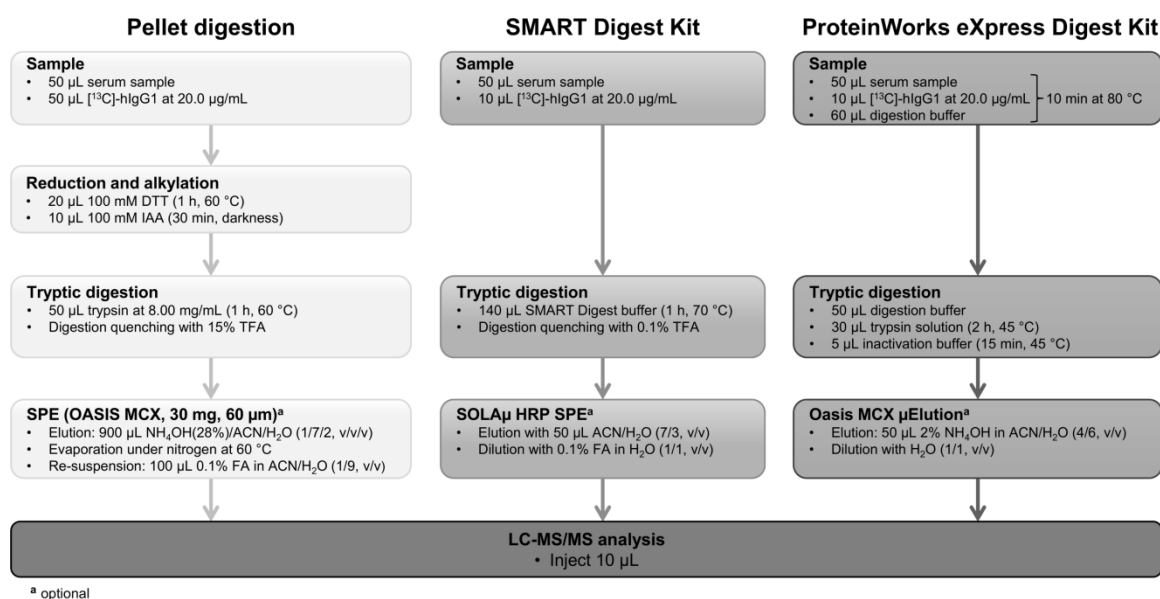
Figure 2.8 Overview of the investigated direct serum digestion protocols for bottom-up hIgG1 quantification in rat serum either based on the developed pellet digestion or commercially available digestion kits. NH_4OH: ammonium hydroxide, HRP: hydrophobic reverse phase, MCX: mixed-mode cation exchange

and alkylation steps to accelerate sample processing. In order to evaluate the relevance of both time-intensive steps during pellet digestion, the peak area of each generic surrogate peptide was compared following either the complete protocol (*i.e.* denaturation at 60 °C with in parallel-conducted reduction, alkylation, and tryptic digestion), the procedure without denaturation, or tryptic digestion only. For three out of four generic surrogate peptides, the highest signal intensities were obtained with the reduction and alkylation steps incorporated, demonstrating their importance during pellet digestion of the studied hIgG1 (Figure 2.9). On the other hand, an increase of temperature for protein denaturation during reduction did not significantly improve peptide formation. Following short-term tryptic digestion, the samples were subjected to an optional SPE clean-up prior to LC-MS/MS analysis (Figure 2.8). Time-consuming evaporation and reconstitution in a LC mobile phase-compatible solvent was necessary for the conventional SPE incorporated into the pellet digestion workflow. In contrast, both digestion kits utilized a micro-elution SPE, which allows efficient sample pre-concentration in a small volume without the requirement of evaporation and reconstitution steps, reducing re-solubility issues and non-specific binding of tryptic peptides. Although, micro-elution SPE formats are suitable for in-solution digestion of (immuno-purified) proteins, this SPE format is not ideal for direct serum digestion approaches. Both micro-elution formats have 2 mg of sorbent embedded, resulting in a maximum mass loading capacity of 400 µg. However, the amount of peptides generated from the recommended starting sample volume (50 µL) was almost nine-fold higher with 3.5 mg (section 2.1.3.2), resulting in a significant peptide loss during the SPE step due to limited loading capacity of the cartridges. However, increasing the cartridge sorbent amount will reintroduce the time-intensive evaporation and reconstitution steps, which were aimed to be eliminated by the vendors.
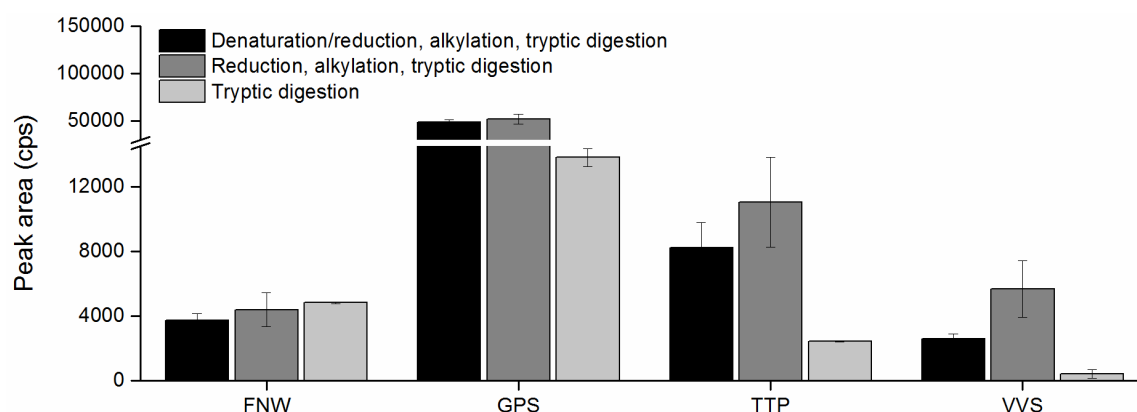
Figure 2.9 Peak area comparison (n=3) of the selected surrogate peptides upon pellet digestion using either the complete protocol (denaturation at 60 °C with in parallel-conducted reduction, alkylation, and tryptic digestion), the procedure without denaturation, or tryptic digestion only.

2.2.3.2 Sensitivity and linearity

By applying the digestion kits according to the manufacturers' instructions, the hIgG1 could be quantified in the same concentration range as with the pellet digestion protocol using the GPS, TTP, and VVS peptides (Table 2.4). However, the LLOQs of the FNW peptide were slightly increased for both kits (5.00 µg/mL) compared to the pellet digestion approach. In addition, each protocol provided comparable mean S/N ratios for the GPS and TTP peptides at the LLOQ. On the other hand, the S/N ratios of both asparagine-containing peptides varied tremendously between the three protocols, ranging from 4.8±0.8 to 13.0±0.6 and from 5.9±0.2 to 35.3±9.3 for the FNW and VVS peptides, respectively, which was related to the temperature-dependent deamidation process. As illustrated in Figure 2.10 for a rat serum sample spiked with the hIgG1 at 10.0 µg/mL, the lowest signal of deamidated peptides was observed with the ProteinWorks eXpress Digest Kit (45 °C), followed by the pellet digestion (60 °C), and the SMART Digest Kit (70 °C). Since the S/N ratio of the VVS peptide at 1.00 µg/mL was 35.3±9.3 using the ProteinWorks eXpress Digest Kit (Table 2.4), it is suspected that even a lower LLOQ can be obtained with this peptide and kit. In terms of linearity, each peptide exhibited an excellent correlation of determination over three non-consecutive days with mean r^2-values ≥0.9898, independent of the applied protocol (Table 2.4).

Table 2.4 Sensitivity and linearity of four selected generic surrogate peptides obtained either with the developed pellet digestion protocol, SMART Digest Kit, or ProteinWorks eXpress Digest Kit.

Peptide	Pellet digestion			SMART Digest Kit			ProteinWorks eXpress Digest Kit		
	Range (µg/mL)	r^2-value (n=3)	S/N ratio (n=3)	Range (µg/mL)	r^2-value (n=3)	S/N ratio (n=3)	Range (µg/mL)	r^2-value (n=3)	S/N ratio (n=3)
FNW	1.00-1000	0.9929	8.3±1.1	5.00-1000	0.9898	4.8±0.8	5.00-1000	0.9941	13.0±0.6
GPS	1.00-1000	0.9940	3.5±0.2	1.00-1000	0.9970	3.3±0.1	1.00-1000	0.9921	3.8±0.6
TTP	1.00-1000	0.9945	11.3±3.0	1.00-1000	0.9935	9.7±0.8	1.00-1000	0.9960	10.1±7.9
VVS	1.00-1000	0.9917	16.8±4.0	1.00-1000	0.9955	5.9±0.2	1.00-1000	0.9929	35.3±9.3
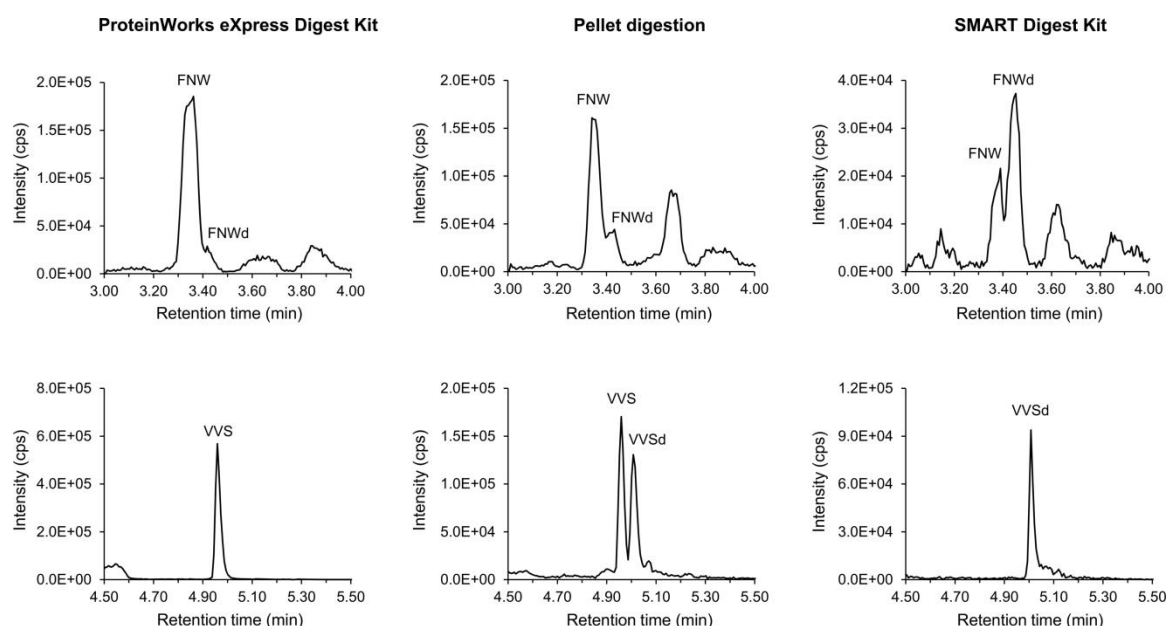
Figure 2.10 Chromatograms obtained from the analysis of a hIgG1-spiked rat serum sample (10.0 µg/mL) following digestion with the ProteinWorks eXpress Digest Kit (45 °C), pellet digestion (60 °C), or the SMART Digest Kit (70 °C) using the FNW (top panel) or VVS peptide (bottom panel). FNWd: deamidated FNW

2.2.3.3 Accuracy and precision

Regardless of the applied direct serum digestion protocol, the majority of intra and inter-day accuracy and precision values obtained with four QC concentrations (3.00, 15.0, 450, and 750 µg/mL) was lower than ±10.0% bias and <10.0% CV, respectively, meeting the acceptance criteria of ±20.0% bias and <20.0% CV from US FDA and EMA guidances (Table 2.5).

Table 2.5 Intra and inter-day accuracy and precision data of QCs in rat serum (3.00, 15.0, 450, and 750 µg/mL) for each generic surrogate peptide obtained either with the developed pellet digestion protocol, SMART Digest Kit, or ProteinWorks eXpress Digest Kit.

Peptide		Pellet digestion		SMART Digest Kit		ProteinWorks eXpress Digest Kit	
		Intra-day (n=3)	Inter-day (n=9)	Intra-day (n=3)	Inter-day (n=9)	Intra-day (n=3)	Inter-day (n=9)
FNW	Accuracy (% bias)	-11.5 to 15.3	-2.4 to 4.3	-11.8 to 7.8	-3.4 to 0.6	-7.3 to 2.7	-5.9 to -2.5
	Precision (% CV)	2.9 to 7.9	6.6 to 9.9	2.8 to 10.1	4.6 to 11.3	2.2 to 8.9	3.5 to 6.6
GPS	Accuracy (% bias)	-9.9 to 8.7	-8.3 to 4.6	-13.6 to 5.4	-6.6 to 2.0	-15.1 to 2.8	-9.9 to -2.2
	Precision (% CV)	1.0 to 7.5	4.7 to 5.4	0.9 to 12.6	6.1 to 7.7	2.1 to 10.3	5.4 to 8.8
TTP	Accuracy (% bias)	-6.9 to 8.3	-2.2 to 0.3	-12.0 to 4.5	-7.6 to 1.3	-9.9 to -0.2	-8.1 to -1.4
	Precision (% CV)	1.5 to 9.3	5.7 to 7.2	0.8 to 7.8	3.9 to 6.5	1.4 to 10.4	4.0 to 6.3
VVS	Accuracy (% bias)	-12.9 to 12.8	-6.1 to 3.8	-13.8 to 14.9	-7.3 to 0.7	-13.6 to 3.1	-11.6 to 1.8
	Precision (% CV)	1.7 to 11.3	8.0 to 14.5	2.9 to 18.1	4.3 to 18.7	2.4 to 11.5	3.0 to 8.4

2.2.4 Conclusions

In comparison to the pellet digestion, the standardized direct serum digestion approaches of both kits were suitable for hIgG1 quantification in rat serum as demonstrated with spiked samples. Moreover, similar sensitivity, linearity, accuracy, and precision data were obtained, regardless of the investigated generic surrogate peptide. Nevertheless, it is questionable if the micro-elution SPE, provided with both kits, is the most appropriate format for direct serum digestion approaches due to limited loading capacity. In case more sensitive assays (≤1.00 µg/mL) are required, each kit is implementable into IC-based workflows (not evaluated). Table 2.6 summarizes the remaining findings of both kits in comparison to the pellet digestion, which are outlined in more detail as follows. A simple handling was associated with both digestion kits, which do not require labor-intense optimization of the tryptic digestion or further method development compared to the pellet digestion. Moreover, less sample preparation steps and potentially interfering reagents were required for the digestion kits, which significantly decreased the sample processing time to maximum 3 h, while the tedious multistep pellet digestion lasts 6 h. On the other hand, the elevated digestion temperature of the SMART Digest Kit resulted in an increased likelihood to generate deamidated peptides, which might compromise assay sensitivity and robustness. In addition, considering the number of samples obtained from pre-clinical trial and the associated analytical costs, the pellet digestion still represents the most economic approach (5.40 € per sample) followed by the SMART Digest Kit (7.70 € per sample), and the ProteinWorks eXpress Digest Kit (10.10 € per sample).

Table 2.6 Advantages and disadvantages of investigated direct serum digestion protocols in ranked manner.

	Pellet digestion	SMART Digest Kit	ProteinWorks eXpress Digest Kit
Method development time	-	+	+
Reagents required	-	++	+
Handling	-	++	+
Sample processing time	-	++	+
Deamidated peptides generated	+	-	++
Costs per sample	++	+	-

2.2.5 Scientific communication

The work described in this chapter was partially published.

Peer-reviewed Note & Tips article:

Lanshoeft C, Heudi O, Cianférani S. SMART Digest™ compared with pellet digestion for analysis of human immunoglobulin G1 in rat serum by liquid chromatography tandem mass spectrometry. *Anal Biochem*, 2016, 501, 23-25. Copyright 2016, reprinted with permission from Elsevier.

Notes & Tips

SMART Digest™ compared with pellet digestion for analysis of human immunoglobulin G1 in rat serum by liquid chromatography tandem mass spectrometry

Christian Lanshoeft [a, b], Olivier Heudi [a, *], Sarah Cianférani [b]

[a] Drug Metabolism and Pharmacokinetics, Novartis Institutes for Biomedical Research, 4056 Basel, Switzerland
[b] Laboratoire de Spectrométrie de Masse BioOrganique, Institut Pluridisciplinaire Hubert Curien, CNRS–Université de Strasbourg, UMR 7178, 67087 Strasbourg, France

A R T I C L E   I N F O

A B S T R A C T

The newly developed SMART Digest™ kit was applied for the sample preparation of human immunoglobulin G1 (hIgG1) in rat serum prior to qualitative and quantitative analyses by liquid chromatography tandem mass spectrometry (LC–MS/MS). The sequence coverages obtained for the light and heavy chains of hIgG1A were 50 and 76%, respectively. The calibration curve was linear from 1.00 to 1000 µg/ml for three of four generic peptides. Overall, the SMART Digest™ kit resulted in similar quantitative data (linearity, sensitivity, accuracy, and precision) compared with the pellet digestion protocol. However, the SMART Digest™ required only 2 h of sample preparation with fewer reagents.

© 2016 Elsevier Inc. All rights reserved.

The quantitative analysis of high molecular weight macromolecules such as monoclonal antibodies [1–3] and antibody–drug conjugates [4,5] by liquid chromatography tandem mass spectrometry (LC–MS/MS) requires an enzymatic digestion of the protein into more workable peptide units due to the limited mass range of triple quadrupole mass analyzers operating in selected reaction monitoring acquisition mode [6–8]. The sample preparation for the analysis of therapeutic proteins is very time-consuming because additional steps are required, including (i) denaturation with heat, chaotropic agents (urea or guanidine), or organic solvents; (ii) reduction of the disulfide bridges with dithiothreitol or tris(2-carboxyethyl)phosphine; and (iii) alkylation of the free thiol groups with iodoacetamide or N-ethylmaleimide. Moreover, tryptic digestion with low enzyme-to-protein ratios is often performed overnight,

resulting in a sample preparation over 2 working days [9,10]. Even though recent accelerated approaches using immobilized trypsin [11–13] or pellet digestion [14–16] have been published, certain steps and chemical reagents are still required. Thus, several kits are currently in development or are already marketed to ease sample preparation, enabling fast analysis of protein therapeutics in complex biological matrices. In this respect, the purpose of the current work was to apply the newly developed SMART Digest™ kit (Thermo Fisher Scientific) to the sample preparation of a human immunoglobulin G1 (hIgG1) based therapeutic protein prior to its qualitative and quantitative analyses by mass spectrometry. Sequence coverage of tryptic peptides was determined by high-resolution mass spectrometry (HRMS) and compared with the results from a pellet digestion (reference) that served as a control. Furthermore, quantitative data (linearity, sensitivity, accuracy, and precision) were generated in rat serum using two generic surrogate peptides from the C_H2 domain of the fragment crystallizable (Fc) region of hIgG1, FNWYVDGVEVHNAK (FNW) and VVSVLTVLHQDWLNGK (VVS), whereas GPSVFPLAPSSK (GPS) and TTPPVLDSDGSFFLYSK (TTP) originated from the C_H1 and C_H3 domains, respectively.

The recombinant hIgG1A (analyte) and hIgG1B (internal standard) were both produced at Novartis Pharma AG (Basel, Switzerland). The latter was labeled with [13C]lysine/arginine

moieties. Nine calibration standard (Cs) concentrations at 1.00, 5.00, 10.0, 20.0, 50.0, 200, 500, 800, and 1000 µg/ml, as well as four quality control (QC) levels at 3.00, 15.0, 450, and 750 µg/ml, were prepared by serial dilution of the hIgG1A stock solution (20.0 mg/ml) with blank rat serum (Fisher Clinical Services, Allschwil, Switzerland) prior to digestion. Calibration curves for the FNW, GPS, and VVS surrogate peptides were constructed with a linear ($y = ax + b$) regression model, whereas a quadratic mathematical model ($y = ax^2 + bx + c$) was used for the TTP peptide due to saturation of the detector at higher concentrations. A weighting factor of $1/x^2$ was used in both cases. The acceptance criteria were ±20.0% (±25.0% at the lower limit of quantification, LLOQ) for 75.0% of the Cs from nominal values. The lowest concentration meeting the acceptance criteria of ±25.0% and ≤25.0% regarding accuracy and precision, respectively, was set as the LLOQ. The accuracy was evaluated by the deviation (% bias) from the nominal values of the QC concentration levels, whereas the percentage of the coefficient of variation (CV) determined the precision. Each QC level was analyzed in triplicate on each day to evaluate the intra-day accuracy and precision, whereas in total nine replicates over 3 days (a different batch of blank matrix was used for each day) were used to generate the inter-day data. A mean bias ±20.0% and a precision ≤20.0% were set as acceptance criteria.

For peptide mapping, a fixed amount of 500 µg of hIgG1A was digested. A volume of 50 µl from a working solution (10.0 mg/ml) was incubated with 150 µl of SMART Digest™ buffer (composition not disclosed from vendor) on a Thermomixer (Eppendorf, Hamburg, Germany) for 60 min at 70 °C and 1400 rpm. The digestion was quenched by adding 10 µl of 10% trifluoroacetic acid. The classical peptide mapping protocol used 170 µl of an hIgG1A solution at 3.00 mg/ml and included reduction with dithiothreitol, alkylation with iodoacetamide, and tryptic digestion for 1 h at 60 °C. Experimental details are described in the online supplementary material. The samples were vortexed shortly and centrifuged prior to LC–MS/MS analysis with an ACQUITY UPLC H-Class system coupled to a Xevo G2-S high-resolution time-of-flight mass spectrometer from Waters (Milford, MA, USA). The obtained MS and MS/MS data were compared against the sequences of the light and heavy chain of hIgG1A using Unifi 1.7 (Waters) with a mass tolerance of 5 ppm for the precursors and their fragment ions. A minimum of five b/y-ions were used for peptide confirmation. The following variable modifications were included: carbamidomethylation of cysteine, oxidation of methionine and tryptophan, deamidation of asparagine and glutamine, and N-terminal pyro-glutamylation of glutamic acid and glutamine. Detailed LC–HRMS settings can be extracted from the supplementary material.

The sample preparation for quantitative analysis using the SMART Digest™ was performed according to the manufacturer's protocol including a SOLAµ HRP solid phase extraction (Thermo Fisher Scientific) [17]. The pellet digestion protocol used as a reference protocol was described elsewhere [18]. A volume of 10 µl from each sample preparation protocol was injected into the LC–MS/MS system. The quantitative analysis of hIgG1A was conducted with a Symbiosis Pro LC system from Spark Holland (Emmen, The Netherlands) coupled to an API 6500 linear quadrupole ion trap (QTRAP) mass spectrometer from AB Sciex (Framingham, MA, USA). Complete LC–MS/MS system settings for quantitative analysis of hIgG1A are provided in Table S1 of the supplementary material.

The coverage of the amino acid sequence of hIgG1A after 1 h digestion time was 50% for the light chain regardless of the sample preparation used, whereas the heavy chain was covered with 84 and 76% after classical digestion (reference) and SMART Digest™, respectively. The four generic peptides used for quantitative analysis of hIgG1A were generated with both protocols after this time period along with other generic peptides from the Fc region. Thus, further investigations for the quantitative analysis with the SMART Digest™ kit were conducted. The linearity over the anticipated

calibration range (1.00–1000 µg/ml) was similar over 3 days for three surrogate peptides (GPS, TTP, and VVS) given that the coefficient of determination (R^2) was ≥0.99 ($n = 3$) regardless of the sample preparation approach used (see Tables S2 and S3 in supplementary material). Only the FNW peptide resulted in a lower mean R^2 value of 0.9898 ± 0.0062 with the SMART Digest™. An example for individual calibration curves for each peptide and sample preparation approach is provided in the supplementary material (Figs.S1 and S2). In general, similar signal-to-noise (S/N) ratios for the GPS and TTP peptides were obtained at the LLOQ with both sample preparation approaches (Table S4). Only the S/N ratios for the FNW and VVS peptides were significantly higher with the pellet digestion. The reason for an increased LLOQ for the FNW peptide was that the deamidated version of this peptide was significantly increased with the SMART Digest™ (Fig.1A) compared with the pellet digestion (Fig.1B).

The deamidation process was most likely caused by an increased digestion temperature (70 vs. 60 °C). Nevertheless, an LLOQ of 1.00 µg/ml (Table S2) was reached with each of the other three surrogate peptides similar to the pellet digestion (Table S3), indicating that the same overall sensitivity (low µg/ml range) was achieved in rat serum. Since the predefined acceptance criteria were fulfilled (Tables S2 and S3), the constructed calibration curve could serve for routine analysis of hIgG1A in rat serum. This was also reflected by the inter-day accuracy and precision data obtained with four QC levels (Table 1).

For three of four investigated surrogate peptides, the absolute values regarding the inter-day accuracy were better with the SMART Digest™, ranging from −3.4 to 0.6%, from −6.6 to 2.0%, and from −7.3 to 0.7% for the FNW, GPS, and VVS peptides, respectively. Only the accuracies for each QC level obtained with the TTP peptide were lower with the pellet digestion compared with the SMART Digest™, ranging from −2.2 to 0.3%. The maximum %CV values with the SMART Digest™ were 11.3, 7.7, 6.5, and 18.7% for FNW, GPS, TTP, and VVS, respectively, whereas with the pellet digestion the %CV was highest with 9.9, 5.4, 7.2, and 14.5% for FNW, GPS, TTP, and VVS, respectively. Since the intra-day accuracy and precision data (Tables S5 and S6) fulfilled the acceptance criteria on each of the 3 days, no concentration dependency was observed in the presence of different blank matrix batches. Thus, the matrix did not impact the quantification, for instance, causing overestimation due to matrix effects. Moreover, each surrogate peptide determined the hIgG1 concentration in rat serum consistently over the anticipated concentration range.
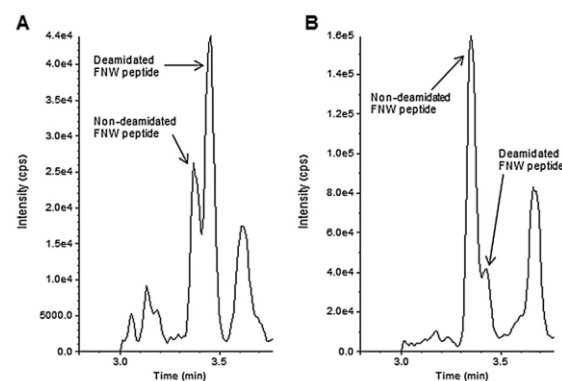

Fig.1. Chromatograms of the FNW peptide showing the non-deamidated peptide at 3.35 min and the deamidated version at 3.44 min after SMART Digest™ (A) and the pellet digestion (B).

Table 1
Inter-day accuracy and precision of quality control samples using SMART Digest™ and pellet digestion of four different generic peptides in rat serum.

Peptide		QC nominal concentration (µg/ml) in rat serum			
		750	450	15.0	3.00
		Inter-day accuracy and precision ($n = 9$)			
FNW	Mean concentration (µg/ml)	755 (732)	446 (440)	14.5 (15.6)	− (3.03[a])
	Inter-day accuracy (% bias)	0.6 (−2.4)	−0.9 (−2.1)	−3.4 (4.3)	− (0.9[a])
	Inter-day precision (% CV)	4.6 (8.5)	5.1 (6.6)	11.3 (9.9)	− (7.3[a])
GPS	Mean concentration (µg/ml)	757 (785)	441 (463)	14.0 (13.8)	3.06 (2.75)
	Inter-day accuracy (% bias)	0.9 (4.6)	−2.0 (2.9)	−6.6 (−7.7)	2.0 (−8.3)
	Inter-day precision (% CV)	7.7 (5.2)	6.4 (5.1)	6.9 (5.4)	6.1 (4.7)
TTP	Mean concentration (µg/ml)	736 (752)	456 (451)	13.9 (14.7)	2.77 (2.95)
	Inter-day accuracy (% bias)	−1.9 (0.3)	1.3 (0.2)	−7.1 (−2.2)	−7.6 (−1.6)
	Inter-day precision (% CV)	4.5 (7.2)	4.0 (6.4)	6.5 (5.7)	3.9 (6.7)
VVS	Mean concentration (µg/ml)	744 (768)	453 (467)	14.7 (14.1)	2.78 (3.00)
	Inter-day accuracy (% bias)	−0.8 (2.4)	0.7 (3.8)	−2.0 (−6.1)	−7.3 (−0.1)
	Inter-day precision (% CV)	4.3 (9.0)	6.7 (8.0)	18.7 (9.4)	13.0 (14.5)

Note. Pellet digestion values are reported in parentheses.
[a] $n = 6$; QC replicates on day 1 were below limit of quantification (1.00 µg/ml) and were excluded from calculations (see also Table S6 of supplementary material).

In conclusion, the same quality of data was obtained with both sample preparation approaches regardless of the surrogate peptide selected. More important, because no denaturation, reduction, or alkylation step was incorporated into the SMART Digest™, a significantly decreased sample preparation time was obtained (2 vs. 6 h), increasing sample throughput further with equivalent MS detection efficiency. Thus, the SMART Digest™ kit can be incorporated as an alternative sample preparation approach compared with pellet digestion, for instance, during dose–range finding studies or pharmacokinetic profiling where a concentration–time profile is acquired.

Acknowledgments

Appendix A. Supplementary data

Supplementary data related to this article can be found at http://dx.doi.org/10.1016/j.ab.2016.02.006.

References

[1] C. Hagman, D. Ricke, S. Ewert, S. Bek, R. Falchetto, F. Bitsch, Absolute quantification of monoclonal antibodies in biofluids by liquid chromatography–tandem mass spectrometry, Anal. Chem. 80 (2008) 1290–1296.
[2] O. Heudi, S. Barteau, D. Zimmer, J. Schmidt, K. Bill, N. Lehmann, C. Bauer, O. Krantz, Towards absolute quantification of therapeutic monoclonal antibody in serum by LC–MS/MS using isotope-labeled antibody standard and protein cleavage isotope dilution mass spectrometry, Anal. Chem. 80 (2008) 4200–4207.
[3] W.S. Law, J.-C. Genin, C. Miess, G. Treton, A.P. Warren, P. Lloyd, S. Dudal, C. Krantz, Use of generic LC–MS/MS assays to characterize atypical PK profile of a biotherapeutic monoclonal antibody, Bioanalysis 6 (2014) 3225–3235.
[4] H. Myler, V.S. Rangan, J. Wang, A. Kozhich, J.A. Cummings, R. Neely, D. Dail, A. Liu, B. Wang, H.E. Vezina, W. Freebern, M.C. Sung, D. Passmore, S. Deshpande, T. Kempe, H. Gu, M. Saewert, A. Manney, J. Lute, F. Zambito,

R.L. Wong, S.P. Piccoli, A.F. Aubry, R. Pillutla, M. Arnold, B. DeSilva, An integrated multiplatform bioanalytical strategy for antibody–drug conjugates: A novel case study, Bioanalysis 7 (2015) 1569–1582.
[5] R.J. Sanderson, N.D. Nicholas, C. Baker Lee, S.M. Hengel, R.P. Lyon, D.R. Benjamin, S.C. Alley, Antibody-conjugated drug assay for protease-cleavable antibody–drug conjugates, Bioanalysis 8 (2016) 55–63.
[6] P. Bults, N.C. van de Merbel, R. Bischoff, Quantification of biopharmaceuticals and biomarkers in complex biological matrices: A comparison of liquid chromatography coupled to tandem mass spectrometry and ligand binding assays, Expert Rev. Proteomics 12 (2015) 355–374.
[7] J.W. Lee, Generic method approaches for monoclonal antibody therapeutics analysis using both ligand binding and LC–MS/MS techniques, Bioanalysis 8 (2016) 19–27.
[8] J. Zheng, J. Mehl, Y. Zhu, B. Xin, T. Olah, Application and challenges in using LC–MS assays for absolute quantitative analysis of therapeutic proteins in drug discovery, Bioanalysis 6 (2014) 859–879.
[9] Y. Shen, G. Zhang, J. Yang, Y. Qiu, T. McCauley, L. Pan, J. Wu, Online 2D–LC–MS/MS assay to quantify therapeutic protein in human serum in the presence of pre-existing antidrug antibodies, Anal. Chem. 87 (2015) 8555–8563.
[10] K. Xu, L. Liu, M. Maia, J. Li, J. Lowe, A. Song, S. Kaur, A multiplexed hybrid LC–MS/MS pharmacokinetic assay to measure two co-administered monoclonal antibodies in a clinical study, Bioanalysis 6 (2014) 1781–1794.
[11] S. Jiang, Z. Zhang, L. Li, A one-step preparation method of monolithic enzyme reactor for highly efficient sample preparation coupled to mass spectrometry-based proteomics studies, J. Chromatogr. A 1412 (2015) 75–81.
[12] W. Ning, M.L. Bruening, Rapid protein digestion and purification with membranes attached to pipet tips, Anal. Chem. 87 (2015) 11984–11989.
[13] F.E. Regnier, J. Kim, Accelerating trypsin digestion: The immobilized enzyme reactor, Bioanalysis 6 (2014) 2685–2698.
[14] M.T. Furlong, Z. Ouyang, S. Wu, J. Tamura, T. Olah, A. Tymiak, M. Jemal, A universal surrogate peptide to enable LC–MS/MS bioanalysis of a diversity of human monoclonal antibody and human Fc-fusion protein drug candidates in pre-clinical animal studies, Biomed. Chromatogr. 26 (2012) 1024–1032.
[15] Z. Ouyang, M.T. Furlong, S. Wu, B. Sleczka, J. Tamura, H. Wang, S. Suchard, A. Suri, T. Olah, A. Tymiak, M. Jemal, Pellet digestion: A simple and efficient sample preparation technique for LC–MS/MS quantification of large therapeutic proteins in plasma, Bioanalysis 4 (2011) 17–28.
[16] Q. Zhang, D.S. Spellman, Y. Song, B. Choi, N.G. Hatcher, D. Tomazela, M. Beaumont, M. Tabrizifard, D. Prabhavalkar, W. Seghezzi, J. Harrelson, K.P. Bateman, Generic automated method for liquid chromatography–multiple reaction monitoring mass spectrometry based monoclonal antibody quantitation for preclinical pharmacokinetic studies, Anal. Chem. 86 (2014) 8776–8784.
[17] Thermo Fisher Scientific, SMART Digest Kit User Guide XX21147-EN 0415S Revision A, 2015. http://www.thermoscientific.com.
[18] C. Lanshoeft, T. Wolf, O. Heudi, S. Cianférani, S. Barteau, M. Walles, F. Picard, O. Kretz, The use of generic surrogate peptides for the quantitative analysis of human immunoglobulin G1 in pre-clinical species with high-resolution mass spectrometry, Anal. Bioanal. Chem. 408 (2016) 1687–1699.

2.3 Generic tip-based IC-LC-MS/MS method for sensitive bottom-up hIgG1 quantification in cynomolgus monkey serum

2.3.1 Analytical context

The majority of direct serum digestion approaches, regardless of the involvement of digestion kits, offer sufficient sensitivity (*i.e.* high ng/mL to low µg/mL range) for most pre-clinical PK studies. Yet, assays with enhanced sensitivity (*i.e.* low ng/mL range) are demanded for the quantification of (i) highly potent mAb-related therapeutic proteins requiring low dosing regimen,[200,391] (ii) mAbs administrated by alternative routes (*i.e.* pulmonary, intravitreal, or subcutaneous),[392-397] or (iii) biotherapeutics in tissue samples exhibiting lower concentrations compared to the corresponding one in the systemic circulation.[265,398] In such cases, the demanded sensitivity cannot be achieved regularly using direct serum digestion approaches. On the one hand, this is attributed to the low proportion of mAb-related therapeutic protein (≈0.01%) compared to the total endogenous serum protein content whose concentration range spans over 10 orders of magnitude.[399-401] On the other hand, proteolytic peptides of endogenous origin create a tremendous background noise, causing ion suppression and interferences with the selected SRM transition(s) of the mAb-related therapeutic protein's surrogate peptide(s). Moreover, the proteolytic digestion of the whole serum is further constrained due to the presence of highly abundant endogenous protease inhibitors.[248]

Several analytical platforms including two or three-dimensional chromatography,[402-409] QTRAPs operating in MS-cubed (MS^3) acquisition mode,[410-413] ion mobility,[414-417] or HRMS (Part 3) have the potential to improve the assay selectivity and hence sensitivity (S/N ratio) in highly complex samples. Additionally, nano and micro-flow applications extend the amount of ions detected as a result of an enhanced peak concentration and improved efficiency of analyte ionization in the MS source.[418-420] Although low-flow applications exhibit beneficial features such as decreased sample volume consumption and increased sensitivity, their broad application in regulated bioanalysis is still hampered due to frequent system maintenance caused by clogging, extended analytical run times, poor analytical reproducibility/robustness (particularly with nano-flow applications), and limited loading capacity.[200,201,265,421] In order to address the latter issue, approaches based on trapping columns with wider internal diameter compared to the analytical column have been frequently applied.[422-425] However, direct serum digestion approaches are incompatible with most low-flow applications and require additional sample clean-up.[426-428]

Depletion of highly abundant endogenous proteins (*e.g.* albumin) or (partial) protein precipitation using salts, organic solvents, acids, or reducing agents represent a simple option for sample clean-up in order to increase the relative concentration of the mAb-related therapeutic protein prior its proteolytic digestion.[248,429-431] In contrast, high sample costs, tedious handling, limitations for automation, or significant losses of the target mAb due to co-precipitation represent disadvantages of such approaches. Alternatively, double pellet digestion[358] or 2D-SPE approaches[303,432] (*e.g.* 1st dimension reversed-phase, 2nd dimension ion exchange) serve as cost-effective sample

clean-up procedures although the latter is mainly limited to therapeutic proteins with low molecular weight. Another antibody-free enrichment, suitable for histidine-rich or phosphorylated therapeutic protein quantification, is based on metal-ion affinity.[208,433,434] In addition to the clean-up strategies mentioned before, peptide-level (SISCAPA) or protein-level IC using either generic (*e.g.* protein A/G, anti-kappa or lambda L chain, anti-hIgG Fc) or specific capture antibodies (*e.g.* anti-idiotype or pharmacological target) have evolved as frequently applied enrichment methodologies for MS-based mAb-related therapeutic protein quantification. Besides a single enrichment step at the protein or peptide-level, sequential protein and peptide-level-based IC protocols were reported, achieving sensitivities in the pg/mL range.[435,436] Several IC-based protocols have been established due to the versatility of available capture antibodies and platforms. Such protocols include magnetic beads varying in size and surface material,[437-439] ELISA plate-based formats,[440] or tip-based IC platforms such as the PhyNexus,[441-443] Agilent's Bravo,[444-446] and Thermo Fisher Scientific's mass spectrometric immunoassay disposable automated research tips (MSIA D.A.R.T.'S), allowing a fully automated high-throughput sample preparation.[447-451]

2.3.2 Objectives

This project aimed to decrease the LLOQ of the generic LC-MS/MS method for bottom-up hIgG1 quantification in pre-clinical species by implementing a tip-based IC format for sample preparation. Moreover, critical parameters of the tip-based IC format for hIgG1 extraction from cynomolgus monkey serum were identified and optimized. Prior to its application to pre-clinical study samples, the developed tip-based IC-LC-MS/MS assay was validated in accordance to US FDA and EMA guidances.

2.3.3 Results

2.3.3.1 Sample preparation workflow

For the present investigation, a fully automated Versette liquid handler (MSIA D.A.R.T.'S technology) was used as tip-based IC format, allowing parallel processing of 96 samples. A detailed scheme of the developed generic tip-based IC-LC-MS/MS method is illustrated in Figure 2.11. Each tip contains tiny micro-channels, which are coated either with protein A, protein G, protein A/G, streptavidin, insulin, or a customized capture antibody. For the intended purpose, streptavidin-coated tips were selected, providing the possibility to load a broad variety of specific biotinylated capture antibodies onto the tips. A generic biotinylated mouse anti-hIgG Fc capture antibody (b-mAb$_{capture}$) was employed due to its universal capability to extract any kind of mAb-related therapeutic protein bearing the Fc region from pre-clinical serum samples regardless of its hIgG isotype subclass. Additionally, dilution of the serum sample with phosphate buffered saline (PBS) prior to hIgG1 extraction was important to reduce the sample viscosity and prevent micro-
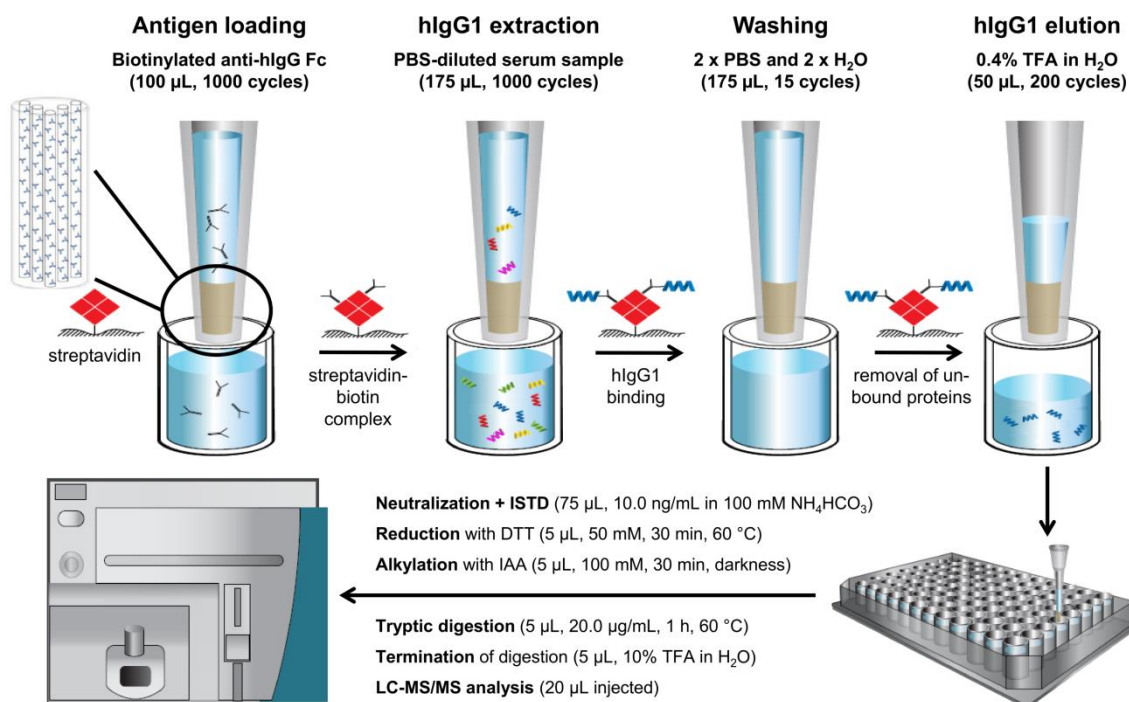
Figure 2.11 Detailed workflow of developed generic tip-based IC-LC-MS/MS method for bottom-up hIgG1 quantification in cynomolgus monkey serum. Adapted from Thermo Fisher Scientific Application Note.[452]

column clogging. Unbound serum proteins were removed from the tips by four washing steps prior to hIgG1 elution by acid dissociation. In order to allow the proceeding with a conventional in-solution digestion protocol including reduction, alkylation, and tryptic digestion, the sample was neutralized and the ISTD was introduced. Unlike previous protocols described in this thesis, a structural analog peptide was used instead of the [^{13}C]-hIgG1 to maximize hIgG1 extraction from cynomolgus monkey serum and avoid binding competition. Of note, later-stage projects revealed that the initially expected binding competition was not a major concern and that [^{13}C]-hIgG1 introduction prior to hIgG1 extraction is the best option (section 3.2.3.1). The *single conservative amino acid replacement* (SCAR) approach was utilized for the analog peptide (TTPPVLDSDGSFFL_VSK), differing by one single amino acid compared to the selected surrogate peptide (TTPPVLDSDGSFFLYSK). However, only variations induced during LC-MS/MS analysis or peptide stability could be corrected with such analog peptide-based ISTD whereas protein losses during IC or variability introduced upon hIgG1 digestion could not be compensated.

2.3.3.2 Monitoring of biotin incorporation by middle-up HRMS analysis

In contrast to colorimetric assays provided with certain biotinylation kits (*e.g.* 4'-hydroxyazobenzene-2-carboxylic acid assay), top-down or middle-up HRMS analyses represent more straightforward and accurate analytical approaches to validate biotin incorporation with an expected mass shift of 244 Da per biotin. In the present analysis up to three or six biotin residues were conjugated to the L and H chain, respectively, as indicated by a mass shift of 226 Da (after the loss of water) in Figure 2.12. Similar to the average DAR calculation using middle-up

approaches,[453] the average biotin-to-antibody ratio was determined (n=3). The L and H chain was conjugated with 0.87±0.05 and 3.58±0.24 biotin residues, respectively, suggesting a total number of 8-9 biotin molecules attached to each anti-hIgG Fc capture antibody.
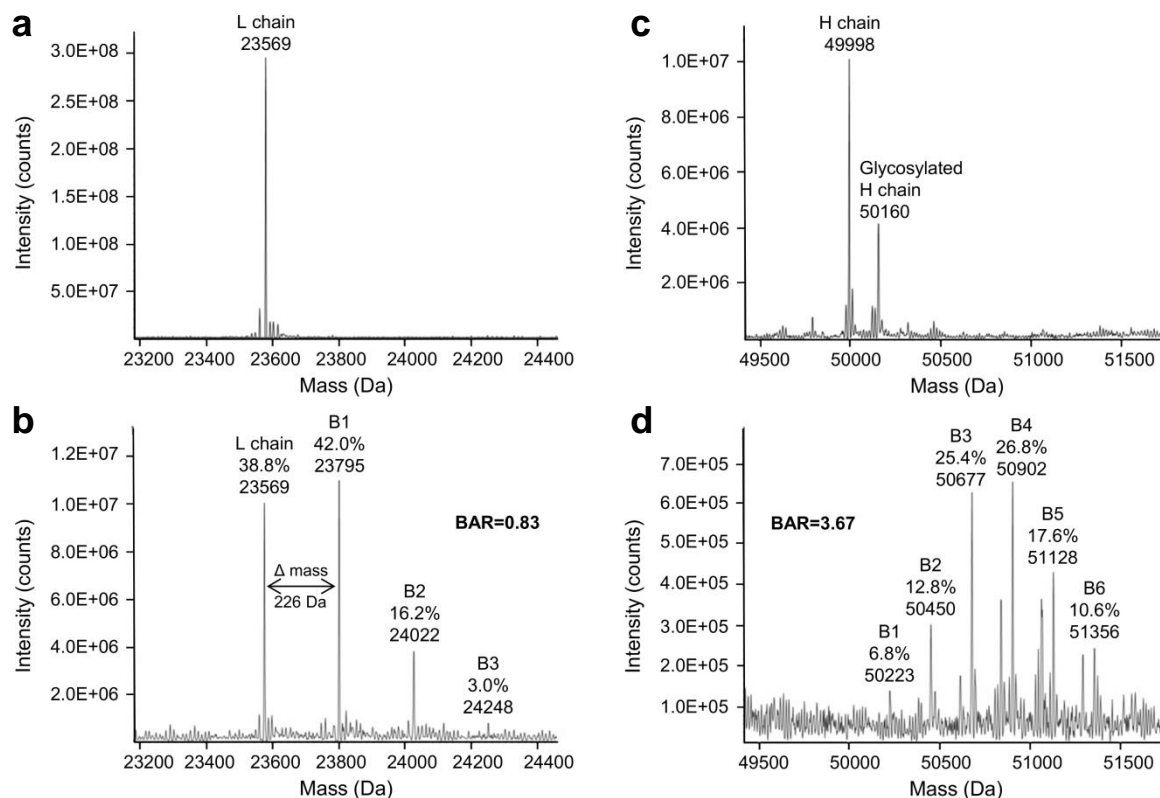
Figure 2.12 Determination of biotin incorporation. Deconvoluted MS spectrum of (**a**) L chain of non-biotinylated mouse anti-hIgG Fc capture antibody (mAb$_{capture}$), (**b**) L chain of biotinylated mAb$_{capture}$ (b-mAb$_{capture}$), (**c**) H chain of mAb$_{capture}$, and (**d**) H chain of b-mAb$_{capture}$. The average biotin-to-antibody ratio (BAR) indicated in total 8-9 biotin residues attached per b-mAb$_{capture}$.

2.3.3.3 Identification and optimization of critical parameters for tip-based IC

Amount of biotinylated capture antibody loaded onto tips

The loading of the b-mAb$_{capture}$ (antigen) onto the streptavidin-coated tips, which was governed by the size of the antigen and potential steric hindrance, was identified as first critical parameter for tip-based IC formats (Figure 2.13, left panel). The amount of immobilized streptavidin was fixed with 4.00 µg per tip. Since streptavidin has four potential binding sites for biotin, a maximum of 16.0 µg biotinylated antigen can be theoretically loaded onto the tips, assuming an equivalent size of the antigen compared to streptavidin.[454,455] However, the molecular weight of the b-mAb$_{capture}$ (149 kDa) was more than two-fold higher compared to streptavidin (66 kDa), indicating a lower loading capacity than theoretically expected. The maximum loading capacity for the b-mAb$_{capture}$ was determined to be 5.20 µg (52.0%), whereby a saturation of the tips was indicated by the
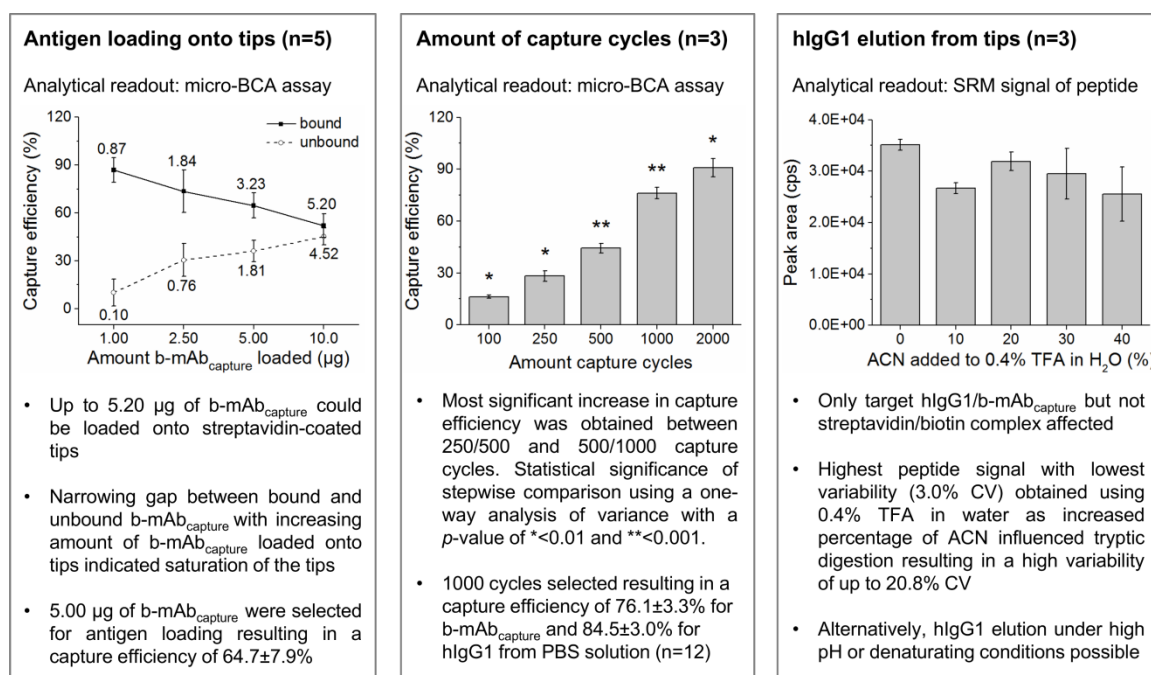
Figure 2.13 Identification and optimization of critical tip-based IC parameters including antigen loading, amount of aspiration/dispensing (capture) cycles, and hIgG1 elution. BCA: bicinchoninic acid assay

narrowing gap between bound and unbound b-mAb$_{capture}$ with increasing amount of b-mAb$_{capture}$ loaded onto the tips (1.00-10.0 µg). Due to limited quantity of b-mAb$_{capture}$, 5.00 µg of b-mAb$_{capture}$ was selected for antigen loading per tip, which resulted in a capture efficiency of 64.7±7.9% (3.23 µg, n=5) and was in agreement with the recommendation from the vendor for biotinylated mAb-related antigens.

Number of aspiration/dispensing cycles

The number of aspiration/dispensing (capture) cycles was identified as second critical parameter. The number of capture cycles did not only influence the antigen loading onto the tips and hIgG1 extraction from serum samples, but also governed the time required for sample preparation and subsequently the method throughput. Increasing the number of capture cycles (*i.e.* 100, 250, 500, 1000, and 2000 cycles) significantly improved the capture efficiency as indicated by the one-way analysis of variance using a *p*-value <0.01 (Figure 2.13, middle panel). However, the most significant impact on the capture efficiency (*p*-value <0.001) was obtained when the number of cycles was increased from 250 to 500 or from 500 to 1000. Although the capture efficiency could be further increased to 90.8±5.3% by applying 2000 capture cycles compared to 76.1±3.3% using only 1000 cycles, the time required for sample processing exceeded the desired sample preparation time including in-solution digestion of one working day (8 h). By applying 1000 capture cycles for hIgG1 extraction from PBS solution (25.0 µg/mL), on average 84.5±3.0% of the hIgG1 were enriched.

Elution process

The elution process of the immuno-captured hIgG1 from the tips was identified as the last and most critical parameter. Similar to other published applications,[456-458] the elution was conducted at low pH (acid dissociation) to disrupt non-covalent interactions between the b-mAb$_{capture}$ and the immuno-captured hIgG1, while the streptavidin-biotin complex remained unaffected due to its affinity constant in the femtomolar range.[454,455] For the elution solvent, TFA and ACN were selected due to their lower acidity (pk$_a$ value) and higher elution strength compared to FA and methanol, respectively. Five different aqueous solutions containing 0.4% TFA with varying percentages of ACN (0-40%) were investigated (Figure 2.13, right panel). An increase of ACN in the elution solvent correlated with the higher variability in the MS signal of the surrogate peptide (3.0-20.8% CV), potentially resulting from an influence of organic solvent on the tryptic digestion.[262,264] Consequently, 0.4% TFA in water was selected as elution solvent, which resulted in the highest MS signal. Alternatively to low pH elution conditions, dissociation of the b-mAb$_{capture}$/hIgG1 complex can be conducted under high pH (*e.g.* 200 mM sodium hydroxide) or denaturing conditions (*e.g.* 8M urea in 50 mM ammonium bicarbonate), which was not considered for this project due to successful hIgG1 elution under acidic conditions.[259,459]

2.3.3.4 Method validation

The developed tip-based IC-LC-MS/MS method was validated in terms of selectivity, signal contribution, linearity, carry-over, accuracy, precision, and dilution integrity. With regard to stability investigations, only the auto-sampler stability of the generated tryptic surrogate peptide was assessed as any other hIgG1-related stability such as its stability in serum or during freeze and thaw cycles were not directly governed by the tip-based IC-LC-MS/MS method and were assessed previously. The validation outcome, meeting the acceptance criteria from US FDA and EMA guidances, is summarized in Table 2.7.[352,353]

Table 2.7 Method validation of generic tip-based IC-LC-MS/MS method for bottom-up hIgG1 quantification in cynomolgus monkey serum.

Parameter	Outcome
Selectivity: three blank batches (n=3)	TTP: ≤7.4%, ISTD: ≤0.1%
Contribution of signal	TTP to ISTD: 0.1% , ISTD to TTP: 19.0%
Linearity (n=3), $y=ax^2+bx+c$, 1/x weighting	10.0-1000 ng/mL, r^2=0.9938±0.0014
Carry-over (blank after ULOQ sample)	TTP: 60.2% below LLOQ signal, ISTD: 0.1% of zero sample response
Accuracy (% bias) and precision (% CV) QCs at 10.0, 25.0, 400, and 800 ng/mL	Intra-day (n=3): -6.9 to 19.9% bias, 1.2 to 14.3% CV Inter-day (n=9): -3.1 to 8.9% bias, 7.4 to 10.3% CV
Dilution integrity (50.0 µg/mL, 500-fold, n=5)	Mean bias of 12.8% with precision of 7.3% CV
Auto-sampler stability at 10 °C (n=3)[a] QCs at 25.0 and 800 ng/mL	24 h: 2.1% bias (800 ng/mL), ≤14.4% CV (25.0 ng/mL) 72 h: -15.2% bias (25.0 ng/mL), ≤24.7% CV[b] (25.0 ng/mL)

[a] Only maximum values are reported, [b] out of acceptance criterion of ≤20.0%

2.3.3.5 Application of tip-based IC-LC-MS/MS method to pre-clinical study samples

As a result of insufficient sample volume, a 50-fold sample dilution was mandatory prior to PK sample analysis, which decreased the hIgG1 concentration in the sample. Thus, especially early and late sampling time points or samples from the low dosing regimen could no longer be analyzed by ELISA with a validated LLOQ of 200 ng/mL. Consequently, the highly sensitive tip-based IC-LC-MS/MS-method was applied to analyze the samples from two individual cynomolgus monkeys, dosed intravitreally with a hIgG1 at 1.00 and 3.00 mg per eye, respectively. The administrated hIgG1 slowly distributed from the eye into the systemic circulation, representing a typical serum concentration-time profile for extravascular administration (Figure 2.14).
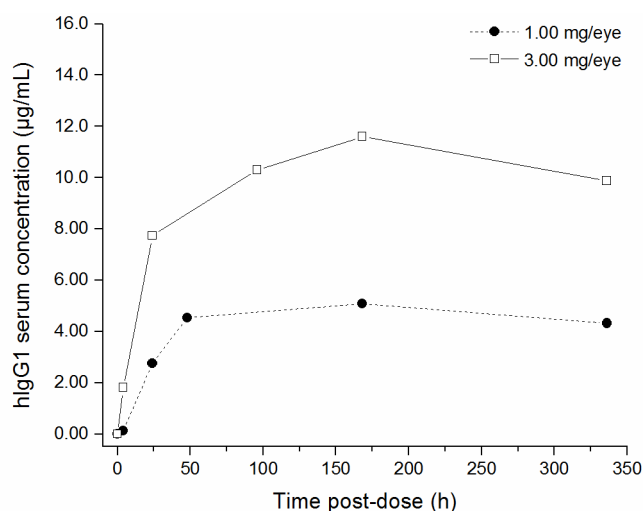
Figure 2.14 Serum concentration-time profiles of a hIgG1 after intravitreal administration at 1.00 and 3.00 mg per eye in two individual cynomolgus monkeys. Analysis was conducted using the developed generic tip-based IC-LC-MS/MS method after 50-fold sample dilution.

2.3.4 Conclusions

The implementation of a generic tip-based IC sample preparation strategy into MS-based workflows exhibited the following features and benefits:

- Significant extension of the application range of generic LC-MS/MS-based workflows for bottom-up hIgG1 quantification in cynomolgus monkey serum samples due to 100-fold increased sensitivity (validated LLOQ of 10.0 ng/mL) compared to pellet digestion approaches.

- Valuable alternative to the generic magnetic bead-based IC-LC-MS/MS assay (KingFisher™ platform), which demonstrates similar throughput (96-well format) and performance in terms of selectivity, accuracy, and precision, but exhibits a higher LLOQ of 25.0 ng/mL.[242]

- Suitable sample preparation strategy for quantitative HRMS analysis of Fc region-containing mAb-related therapeutic proteins at a higher protein level (chapter 3.2 and 3.3).

2.3.5 Scientific communications

The work described in this chapter was published and presented on several occasions.

Peer-reviewed scientific article:

Lanshoeft C, Heudi O, Cianférani S, Warren AP, Picard F, Kretz O. Quantitative analysis of hIgG1 in monkey serum by LC-MS/MS using mass spectrometric immunoassay. *Bioanalysis*, 2016, 8(10), 1035-1049. Copyright 2016, reprinted with permission from Future Science Ltd.

Poster presentation:

Lanshoeft C, Heudi O, Cianférani S, Niederkofler EE, Chaudhari R, Warren AP, Picard F, Kretz O. *Generic quantitative LC-MS/MS assay for analysis of hIgG1-based therapeutic proteins in cynomolgus monkey serum using immuno-capture with MSIA D.A.R.T.'S™*. 64th Annual Conference on Mass Spectrometry and Allied Topics of the American Society for Mass Spectrometry (ASMS), Jun 5-9th 2016, San Antonio (TX, USA).

Oral presentation:

Quantitative LC-MS/MS analysis of hIgG1-based therapeutic proteins in cynomolgus monkey serum using immuno-capture with MSIA D.A.R.T.'S™. Thermo Fisher Scientific Biopharmaceutical Characterization Seminar, Mar 2nd 2016, Basel (Switzerland).

Research Article

Bioanalysis

Quantitative analysis of hIgG1 in monkey serum by LC–MS/MS using mass spectrometric immunoassay

Aim: A sensitive generic LC–MS/MS method for hIgG1 quantification in cynomolgus monkey serum using mass spectrometric immunoassay disposable automation research tips (MSIA-D.A.R.T.'S™) is reported. **Results:** The hIgG1 was captured with a biotinylated mouse anti-hIgG antibody (50.0 μg/ml) targeting the fragment crystallizable (Fc) region. Elution from the streptavidin-coated MSIA-D.A.R.T.'S was conducted with 0.4% trifluoroacetic acid in water. The method was selective and linear from 10.0 to 1000 ng/ml using 100 μl of serum. The method was evaluated regarding accuracy, precision, carry-over, dilution, auto-sampler stability and applied for the determination of hIgG1 concentration in monkey serum after intravitreal administration. **Conclusion**: The present assay is suitable for quantitative analysis of hIgG1-based therapeutic proteins in monkey serum at low levels.

Christian Lanshoeft[1,2],
Olivier Heudi*[,1],
Sarah Cianférani[2],
Andrew P Warren[1],
Franck Picard[1] & Olivier Kretz[1]
[1]Novartis Institutes for Biomedical Research, Drug Metabolism & Pharmacokinetics, Novartis Campus, Fabrikstrasse 14, 4056 Basel, Switzerland
[2]Laboratoire de Spectrométrie de Masse BioOrganique, Institut Pluridisciplinaire Hubert Curien, CNRS-Université de Strasbourg, UMR 7178, 25 rue Becquerel, 67087 Strasbourg, France
*Author for correspondence:
Tel.: +41 79 53 59 611
Fax: +41 61 696 85 84
olivier.heudi@novartis.com

Therapeutic proteins including monoclonal antibodies (mAbs) are nowadays included in the portfolio of almost all pharmaceutical companies. Bioanalytical assays have generally been based on ligand-binding assays (LBAs) such as the ELISA performed either in a 96-well plate format or in an automated fashion using the Gyrolab™ platform [1,2]. Even though LBAs offer high sensitivity and throughput at low investment costs, the limitations associated with LBAs are restricted dynamic range, occasional nonspecific binding and most significantly limitations on assay specificity imposed by the lack of suitable capture antibodies. As a consequence, MS based analytical assays have emerged during recent years as a complementary technology to LBAs due to the high degree of specificity, dynamic range, ease in operation and relatively short method development times [3–5]. The majority of MS assays used for quantitative analysis of proteins are based

on LC–MS/MS. This technology has been applied to a variety of therapeutic proteins such as smaller peptides/proteins [6,7] as well as on macromolecules such as mAbs [8–11] or antibody–drug conjugates (ADCs) [12,13]. Due to the size of therapeutic proteins and the limited mass range of triple quadrupole (QqQ) mass analyzers operating in selected reaction monitoring (SRM) mode, a proteolytic enzyme (typically trypsin) has to be incorporated in the sample preparation in order to reduce the target protein to more workable peptide fragments. One potential disadvantage of the proteolytic approach is that the digestion generates a complex matrix with a large number of potential endogenous compounds that can impact the assay selectivity and sensitivity [14]. Recent improvements in high resolution MS (HRMS) [15–17], hybrid MS-instruments such as quadrupole ion traps (QTRAP) operating in cubic SRM (MS³) acquisition mode [18,19] or multi-

FUTURE SCIENCE part of **fsg**

Research Article   Lanshoeft, Heudi, Cianférani, Warren, Picard & Kretz

dimensional chromatography [20,21] have allowed the achievement of enhanced selectivity for the quantification of proteins in biological fluids. Despite the method selectivity improvement especially with the use of accurate mass, the sensitivity still remains in the low microgram per milliliter level [22,23]. Consequently, an appropriate sample cleanup is highly desirable to reduce the sample complexity in order to improve the sensitivity of developed LC–MS/MS methods. Immunocapture in combination with LC–MS/MS analysis has been commonly used to increase the method sensitivity to low nanogram per milliliter levels for some given proteins [24,25]. Immunocapture can either be performed on protein level with appropriate capture antibodies (e.g., Protein A or G) or on peptide level using stable isotope standards and capture by antipeptide antibodies (SISCAPA) [26,27]. However, only a minority of assays is described in recent literature combining immunocapture on both levels [28,29]. Moreover, analytical methods based on immunocapture can be performed with different materials or platforms, for example, several authors have used magnetic beads to extract low-abundant target proteins from plasma or serum [30–32]. The magnetic particles exist in various sizes and are suitable for automation enabling high-throughput [33]. In another study, ELISA plates coated with streptavidin were used to enrich samples with the protein of interest in order to achieve a low nanogram per milliliter limits of quantification [34]. More recently the mass spectrometric immunoassay with disposable automation research tips (MSIA-D.A.R.T.'S™) platform was applied for the quantitative analysis of bovine somatropin in serum at low nanogram per milliliter levels [35]. The MSIA-D.A.R.T.'S technology was further applied to the analysis of cytokines [36] or hormones such as insulin variants in human serum [37]. Additionally, this technology was used for the screening of clinical relevant proteins [38] and for the determination of the proteomic signature of serum albumin bound proteins from stroke patients [39]. Multiplexing capabilities [40] and the interlaboratory reproducibility of this technology during quantitative analysis of a prostate-specific antigen was also reported [41]. To date, published work using the MSIA-D.A.R.T.'S technology has been limited to low- and medium-sized molecular weight proteins to the best of our knowledge. In this respect, the present work assesses the suitability of MSIA-D.A.R.T.'S on a Versette™ automated liquid handler in order to decrease the LLOQ for the quantitative analysis of a hIgG1-based therapeutic protein currently under development by a generic LC–MS/MS assay to support preclinical studies. The immunocapture was performed on intact protein level with an anti-hIgG capture antibody recognizing the frag-

ment crystallizable (Fc) region of hIgG whereas quantification was achieved on peptide level after tryptic digestion using a generic surrogate peptide from the Fc part of the hIgG1-based therapeutic protein. Once the method was developed, the assay performance was evaluated regarding linearity, accuracy, precision, dilution, carry-over and auto-sampler stability. Finally the MSIA-D.A.R.T.'S platform was applied to pharmacokinetic (PK) samples from two individual cynomolgus monkeys previously dosed with the hIgG1 intravitreally (i.v.t).

Materials & methods
Chemicals & reagents
The recombinant hIgG1-based therapeutic protein and the mouse monoclonal anti-hIgG antibody ($mAb_{capture}$) were both synthesized at Novartis Pharma AG (Basel, Switzerland). The generic surrogate peptide TTP-PVLDSDGSFFLYSK and the analog peptide TTP-PVLDSDGSFFL$\underline{V}$SK differing by one single amino acid (underlined) used as internal standard (ISTD) were produced by Thermo Fisher Scientific (Ulm, Germany) and Bachem AG (Budendorf, Switzerland), respectively. Phosphate-buffered saline (PBS; 10×; 100 mM phosphate, 154 mM sodium chloride, pH 7.4), ammonium bicarbonate (ABC), DL-Dithiothreitol (DTT), iodoacetamide (IAA), acetic acid, trifluoroacetic acid (TFA), water and acetonitrile (ACN) were purchased from Sigma-Aldrich (Buchs, Switzerland). Formic acid (FA) and sequencing grade modified trypsin were provided by Merck (Darmstadt, Germany) and Promega (Madison, WI, USA), respectively. All reagents (high analytical grade, ≥99% purity) and MS grade solvents were used without any further purification. The micro-BCA™ protein assay kit, EZ-Link™ Sulfo-NHS-Biotinylation kit and the streptavidin-coated MSIA-D.A.R.T.'S were obtained from Thermo Fisher Scientific (Waltham, MA, USA). Leucine enkephalin and sodium iodide solutions were delivered from Waters (Milford, MA, USA). Blank batches of cynomolgus monkey serum intended for the preparation of calibration standards (Cs) and quality control (QC) samples were obtained from Fisher Clinical Services (Allschwil, Switzerland).

Cs & QC samples
Eight Cs concentrations at 10.0 (LLOQ), 50.0, 75.0, 100, 250, 500, 750 and 1000 ng/ml (upper limit of quantification, ULOQ) were prepared by spiking working solutions after serial dilution of hIgG1 stock solution (20.0 mg/ml) in 1× PBS into blank cynomolgus monkey serum (working solution/matrix, 3/97, v/v). Four QC levels at 10.0, 25.0, 400 and 800 ng/ml were prepared similar to the Cs samples.

PK study samples from cynomolgus monkey

Two individual male cynomolgus monkeys were administrated 1.00 and 3.00 mg/eye of hIgG1 solution (50 μl) on the first day of the study by intravitreal injection into both eyes. Approximately 3.0 ml of blood was collected from the animals at predose, 4, 24, 48, 96, 168 and 336 h postdose. After centrifugation, serum aliquots (500 μl) were stored ≤-70°C prior to analysis. The preclinical study was conducted in compliance with the Guide for the Care and Use of Laboratory Animals, the Office of Laboratory Animal Welfare, the Animal Welfare Act and in accordance with the Novartis Animal Care and Use Committee.

Biotinylation of mAb$_{capture}$ & monitoring of biotin incorporation by LC-HRMS

The biotinylation of the mAb$_{capture}$ was performed with the EZ-Link™ Sulfo-NHS-Biotinylation kit according to the manufacturer's protocol (20-fold molar excess of biotin). For the determination of biotin incorporation, a volume of 10 μl of nonbiotinylated or biotinylated antigen was mixed with 10 μl of 100 mM DTT in water and incubated at 60°C for 1 h. The reduced nonbiotinylated mAb$_{capture}$ and resultant biotinylated mAb$_{capture}$ (b-mAb$_{capture}$) was analyzed with an ACQUITY UPLC H-Class system coupled to a Xevo G2-S high-resolution mass spectrometer from Waters to monitor the biotin incorporation (resolution ≥10,000 at full-width at half maximum for leucine enkephalin at *m/z* 556.2766 and mass accuracy ≤1 ppm with sodium iodide). A complete description of the LC-HRMS parameters can be extracted from the Supplementary Information.

Enrichment of b-mAb$_{capture}$ on streptavidin MSIA-D.A.R.T.'S

Initially, the MSIA-D.A.R.T.'S were prewashed with 175 μl of 1× PBS solution (15 cycles). A volume of 100 μl of b-mAb$_{capture}$ solution at 50.0 μg/ml was drawn through the streptavidin-coated tips for enrichment (1000 cycles). Afterward, a wash step using 1× PBS (175 μl) was incorporated to remove unbound b-mAb$_{capture}$ (15 cycles). The degree of b-mAb$_{capture}$ enrichment was determined with the micro-BCA™ protein assay prior to and after enrichment following the manufacturer's instructions. The colorimetric readout was performed with a SpectraMax 340 UV spectrophotometer controlled by SoftMax® Pro (version 5.4.1) from Molecular Devices (Sunnyvale, CA, USA).

Affinity purification of hIgG1 from cynomolgus serum

A volume of 100 μl from serum samples was loaded into a 500 μl Protein LoBind 96-well plate from Eppendorf (Hamburg, Germany) and was diluted with the same volume of 1× PBS buffer prior to immunocapture. Then, the MSIA-D.A.R.T.'S were pre-rinsed with a volume of 175 μl 1× PBS (15 cycles). The hIgG1 enrichment was performed by repeatedly aspirating and dispensing 175 μl of diluted serum sample through the microcolumn previously immobilized with b-mAb$_{capture}$ (1000 cycles). Subsequently, the tips were sequentially rinsed twice with 175 μl 1× PBS from another microplates followed by two-times with 175 μl of water from two additional 96-well plates in order to remove unbound hIgG1 (15 cycles each). The immuno-enriched protein was then eluted into a clean 500 μl Protein LoBind 96-well plate by drawing and expelling 50 μl 0.4% TFA in water through the MSIA-D.A.R.T.'S (200 cycles).

Neutralization, reduction, alkylation & tryptic digestion

After elution, the samples were neutralized with 75 μl of 100 mM ABC in water containing the ISTD at a concentration of 10.0 ng/ml and the samples were shortly mixed on a Thermomixer. For blank samples, 75 μl of 100 mM ABC in water was used instead. Reduction of the protein's disulfide bonds was achieved by adding 5 μl of 50.0 mM DTT dissolved in 100 mM ABC in water. The plate was shaken for 30 min at 60°C. Afterward, 5 μl of 100 mM IAA prepared in 100 mM ABC in water was pipetted to the samples and the plate was agitated gently for 30 min at room temperature protected from light. Tryptic digestion was initiated by adding 5 μl of trypsin solution (20.0 μg/ml in 50 mM acetic acid) to each well. After incubation for 1 h at 60°C, the digestion was quenched with 5 μl of 10% TFA in water. The samples were vortexed shortly and centrifuged for 5 min at 10°C and 900 × *g* prior to LC–MS/MS analysis.

Quantification of hIgG1 by LC–MS/MS

The quantitative analysis of hIgG1 was conducted with a Symbiosis Pro LC system (Spark Holland B.V, Emmen, The Netherlands) equipped with a Reliance unit and a Mistral column oven maintained at 50°C. Tryptic peptides were separated on an Ascentis Express C$_{18}$, 50 × 2.1 mm, 2.7 μm column from Supelco (Bellefonte, PA, USA) at a flow rate of 500 μl/min. Acidified water and ACN (0.1% FA each) were used as mobile phase A and B respectively with an optimized binary elution gradient. After chromatographic separation, the peptides were analyzed with an API 6500 linear QTRAP mass spectrometer from AB Sciex (Framingham, MA, USA) using positive electrospray ionization (ESI+) and the SRM acquisition mode. Complete LC–MS/MS system settings for quantitative analysis

of hIgG1 are provided in the Supplementary Table 1. The LC–MS/MS system was controlled by Analyst 1.6 (AB Sciex).

Evaluation of analytical assay performance

The performance of the developed assay was evaluated in accordance to internal Novartis standard operation procedures which are based on the guidelines either from the EMA [42], the US FDA [43] or the white paper currently published for protein analysis by LC–MS/MS [44].

Selectivity

The mean peak area (n = 3) of the SRM transition in three different batches of blank cynomolgus monkey serum at the retention time of the surrogate peptide and the ISTD relative to the signal at the LLOQ was used to assess the selectivity of the analytical method. Any potential contribution of the ISTD to the surrogate peptide was determined by comparing the analytical response of the surrogate peptide in a blank sample spiked only with the ISTD (zero sample) relative to its response at the LLOQ. In order to investigate a potential contribution of the surrogate peptide to the ISTD, the mean peak area for the ISTD in a sample spiked only with hIgG1 at the ULOQ concentration without any ISTD was compared with the mean ISTD response obtained in the zero samples. The analytical response for the surrogate peptide should be five-times lower than the LLOQ signal and ≤5% for the ISTD signal at the working concentration to meet acceptance.

Linearity & sensitivity

The hIgG1 serum concentrations were back-calculated with an eight point calibration curve (duplicate on each day) using a weighted (1/x) quadratic regression model in the form of $y = ax^2 + bx + c$ where y was the peak area ratio between the response of the surrogate peptide over the ISTD and x represented the nominal hIgG1 concentration in the Cs samples. At least 75% of the Cs samples with one replicate per concentration level should be within ±20% (±25% at the LLOQ and ULOQ) of the nominal hIgG1 concentration in order to meet acceptance. The lowest concentration fulfilling the acceptance criteria of ±25% and ≤25% regarding accuracy and precision was set as the LLOQ.

Carry-over

Directly after the ULOQ sample at 1000 ng/ml, a series of blank samples was injected in one run to assess the carry-over. The extent of carry-over should be ≤20% of the response of the tryptic surrogate peptide relative to the LLOQ response and ≤5% for the ISTD signal relative to the working concentration.

Accuracy & precision

The error in percentage (% bias) from the nominal QC concentration on four levels (LLOQ, 2–3 × LLOQ, mid and high) was used to evaluate the accuracy of the analytical method whereas the precision of the assay was determined by the percentage of the coefficient of variation (CV). The intraday accuracy and precision were determined on each day for each QC level in triplicate whereas the interday data were generated over three different days with in total nine replicates. A mean bias within ±20% (±25% at the LLOQ) of the nominal values and a precision of ≤20% (≤25% at the LLOQ) were set as acceptance criteria.

Dilution

One additional QC sample at 50.0 μg/ml was prepared and diluted with blank cynomolgus monkey serum. Two dilution factors (100- and 500-fold) were evaluated in replicates of five. The accuracy of the mean back-calculated concentration with the dilution factor incorporated should be within ±20% and the precision ≤20%. In addition, at least 60% of the replicates should meet the acceptance on individual level.

Auto-sampler stability

Two QC levels at 25.0 and 800 ng/ml were used to assess the stability of tryptic peptides on the auto-sampler (10°C) for 24 and 72 h. The stability was deemed acceptable if the deviation from the nominal concentration was ±20% with a precision ≤20%. As the stability of the hIgG1 lyophilizate, its stock solution after reconstitution and the protein's stability at room temperature after spiking in serum were evaluated previously, these investigations were not included in this work.

Results & discussion
Biotin incorporation

The determination of the biotin incorporation into the mAb$_{capture}$ was the first step to be monitored during targeted-MS immunoassay development. The nonbiotinylated version of the mAb$_{capture}$ light chain exhibited a molecular weight of 23,569 Da (Figure 1A). After biotinylation, additional peaks with a mass shift of 226 Da appeared on the light chain of the mAb$_{capture}$ after MS spectra deconvolution (Figure 1B). This mass shift was an indication for the incorporation of biotin (244 Da) on amino acids with primary amines such as lysine after the loss of water. Based on the peak height, 38.8% of the light chain was nonbiotinylated, whereas 42.0, 16.2 and 3.0% carried either one, two or three biotin moieties, respectively. On the other hand, the heavy chain with a molecular weight of 49,998 Da and its glycoform at 50,160 Da (Figure 1C) carried after biotinylation between one and six biotin molecules (Figure 1D). As

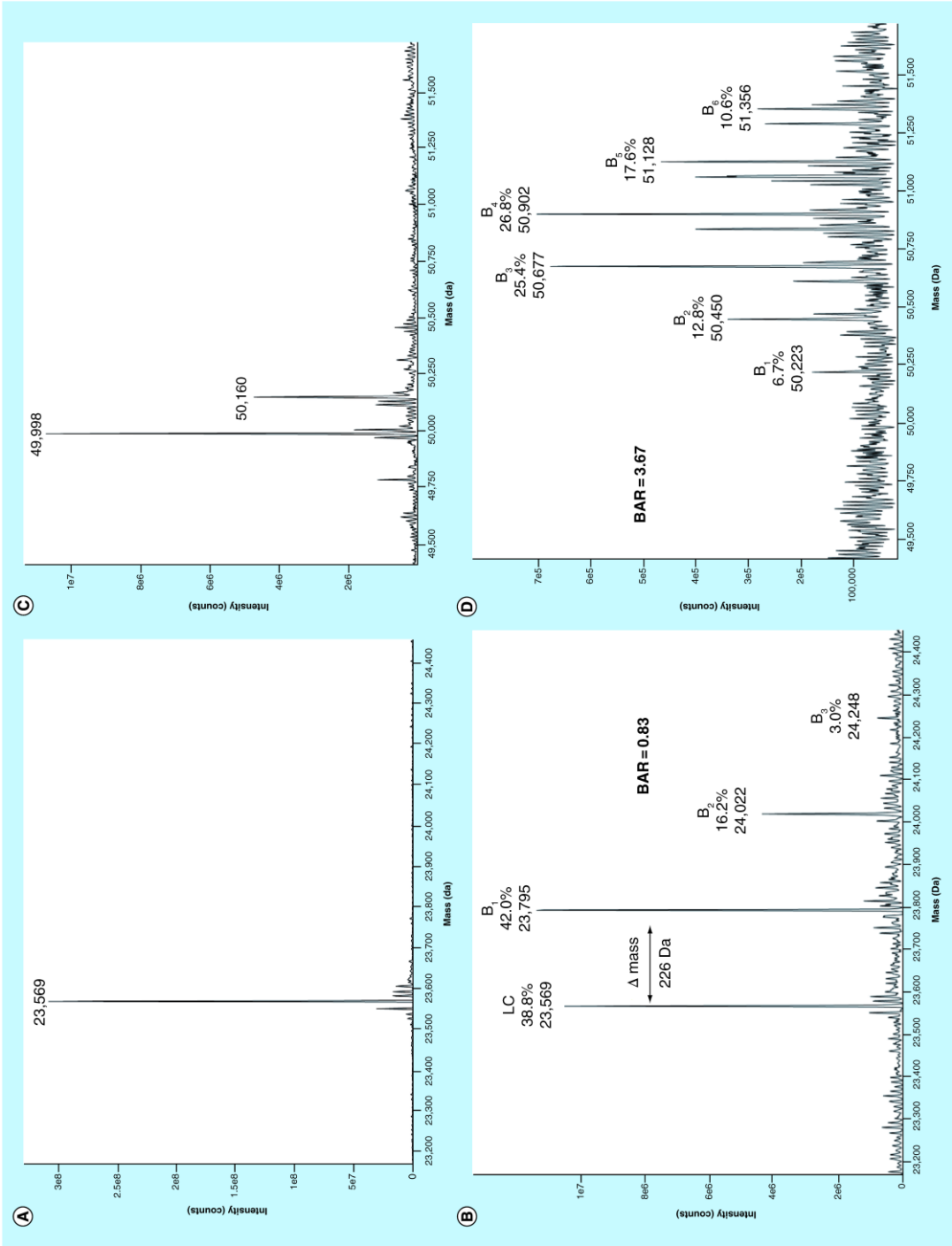**Figure 1. Determination of biotin incorporation.** Deconvoluted MS spectrum of **(A)** light chain of nonbiotinylated capture antibody (mAb$_{capture}$), **(B)** light chain of biotinylated mAb$_{capture}$ (b-mAb$_{capture}$), **(C)** heavy chain of mAb$_{capture}$, and **(D)** heavy chain of b-mAb$_{capture}$. The biotin–antibody ratio (BAR) calculated in total 8–9 biotin per mAb$_{capture}$.

the sample was not deglycosylated with PNGaseF prior to LC-HRMS analysis, additional peaks between the individual biotin species appeared in the deconvoluted MS spectrum of the HC corresponding to the glyco-form of each individual biotin specie. Similar to the drug–antibody ratio (DAR) [45,46], the biotin–antibody ratio (BAR) was calculated. The mean BAR (n = 3) on the light and heavy chain was 0.87 ± 0.05 and 3.58 ± 0.24 respectively indicating that in total 8–9 biotin entities were incorporated in the mAb$_{capture}$.

Optimization of b-mAb$_{capture}$ loaded on streptavidin MSIA-D.A.R.T.'S

The MSIA-D.A.R.T.'S contained approximately 4.00 µg of streptavidin per tip. As streptavidin has four potential biotin-binding sites, in theory, the maximum loading capacity was 16.0 µg of biotinylated capture antibody. However, this assumption is only true when the molecular weight of streptavidin and the biotinyl-ated capture antibody is similar. Consequently, the size of capture antibody plays an important role dur-ing the loading process due to steric hindrance. Thus, four different amounts of b-mAb$_{capture}$ ranging from 1.00 to 10.0 µg were investigated in replicates of five to optimize the loading of b-mAb$_{capture}$ on the streptav-idin-coated tips. As depicted in Figure 2A, the percent-age of unbound b-mAb$_{capture}$ was increasing with larger amounts of b-mAb$_{capture}$ loaded on the tip. However, the capture efficiency expressed in percent was decreas-ing with increasing amount of loaded b-mAb$_{capture}$. Nonetheless, the absolute amount of capture antibody was important: even though 0.87 µg of bound protein resulted in a high capture efficiency of approximately 90% when 1.00 µg was loaded, the maximum level of loading capacity of the MSIA-D.A.R.T.'S was not reached since up to 5.20 µg of biotinylated protein could be captured being equal to 52.0% of capture effi-ciency when in total 10.0 µg b-mAb$_{capture}$ were loaded. It was assumed that a saturation on the streptavidin MSIA-D.A.R.T.'S was reached beyond this level as the gap between bound and unbound protein narrowed with increasing amount of loaded b-mAb$_{capture}$. For our assay, an amount of 5.00 µg of b-mAb$_{capture}$ was selected exhibiting a capture efficiency of 64.6%. The resultant amount of capture antibody loaded on the tip was in agreement with the recommendations from the vendor for IgG1-based capture antibodies. In a second step, the amount of capture cycles using 5.00 µg of b-mAb$_{capture}$ was assessed (n = 3). For each level of capture cycles, a significant increase with a p-value <0.01 (*) was deter-mined by the stepwise comparison using a one-way analysis of variance (Figure 2B). The most significant impact of the amount of capture cycles on the cap-ture efficiency with a p-value <0.001 (**) was obtained

between 250 and 500 as well as 500 and 1000 cycles. Although the efficiency could further be increased from 76.1 to 90.8% when the capture cycles were increased from 1000 to 2000, the time required for capture of the antibody was also taken into account when a sample preparation within one working day was targeted. Thus, 1000 capture cycles were selected which took approxi-mately 75 min for b-mAb$_{capture}$ enrichment on the tips including all rinse/wash steps.

Immuno-enrichment & elution optimization of hIgG1

In average, 84.5% (n = 12) of hIgG1 at 25.0 µg/ml were extracted out of 1× PBS solution with the b-mAb$_{capture}$ under the selected conditions. Investigations directly in serum were not conducted due to the high protein con-tent in serum exceeding the quantification range of the BCA assay. Nevertheless, we felt confident to extract the hIgG1 out of cynomolgus monkey serum. As last and most critical parameter of the MSIA-D.A.R.T.'S-based assay, the elution of protein had to be assessed. Acid dis-sociation of the antibody–antigen complex was selected and five different aqueous solutions were monitored containing 0.4% TFA with varying ratios of organic sol-vent (0–40%) to stabilize the hIgG1. TFA was selected over FA due to its lower acidity (pk$_a$) value and ACN was selected as organic solvent due to the higher elu-tion strength compared with MeOH. The higher the ratio of organic solvent, the higher the variability (up to 20.8% CV) in the MS signal of the surrogate peptide after tryptic digestion of the eluted hIgG1 (Figure 3). The highest signal with the lowest variation of 3.0% was obtained with 0.4% TFA in water being selected as elution solvent. The enrichment and elution proce-dure of hIgG1 took additional 2.5 h. In total, the whole immuno-enrichment took 3.75 h when the previous b-mAb$_{capture}$ capture step was also taken into account.

Evaluation of analytical assay performance
Selectivity

The MS responses of the SRM transition of the sur-rogate peptide and the ISTD did not reveal any endog-enous interference in blank cynomolgus monkey serum (Figure 4A). The interferences in three different batches of blank monkey serum found for the surrogate peptide and its ISTD ranged from 0.4 to 7.4% and from 0.0 to 0.1%, respectively meeting the acceptance criterion of ≤20% and ≤5% (Supplementary Table 2). In addi-tion, no significant interference between the surrogate peptide and the ISTD was observed (Figure 4B), as the mean contribution of the surrogate peptide to the ISTD was only 0.1% (Supplementary Table 3). However, the contribution of the ISTD to the peptide was on the upper limit with 19.0% relative to the LLOQ signal
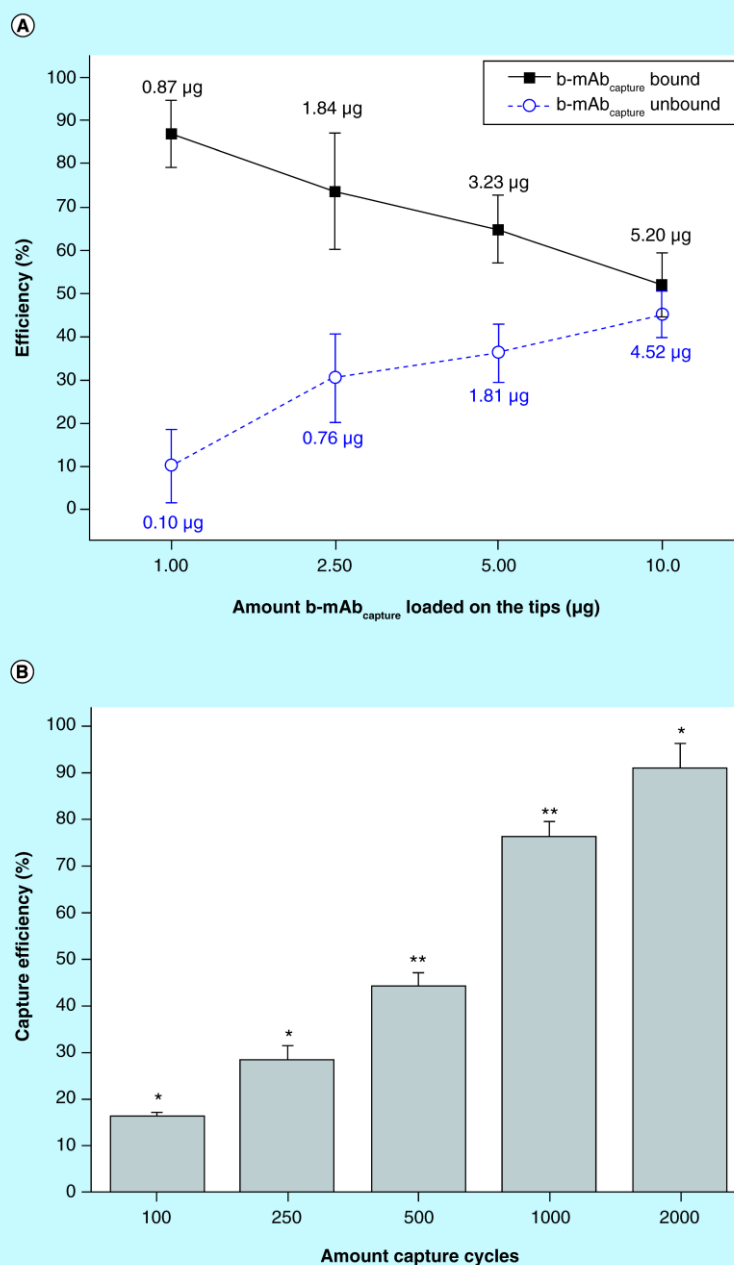
Figure 2. Enrichment of biotinylated capture antibody (b-mAb$_{capture}$) on streptavidin tips. Optimization of **(A)** amount of b-mAb$_{capture}$ loaded on the tips (n = 5) and **(B)** amount of aspirating and dispensing cycles using 5.00 μg of b-mAb$_{capture}$ (n = 3).
*p < 0.01; **p < 0.001.
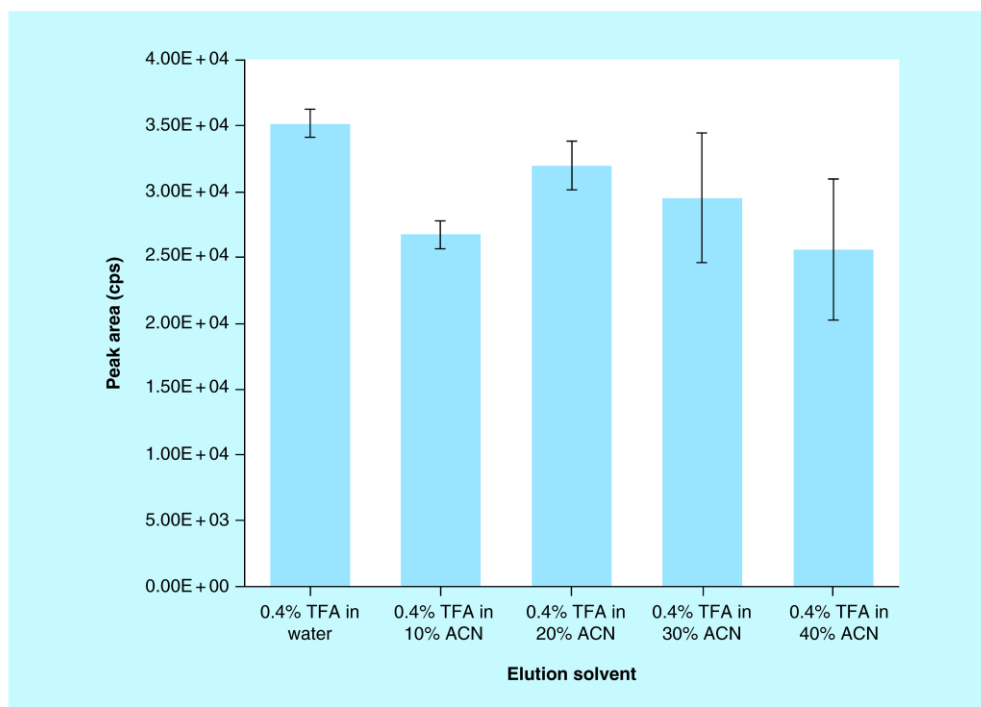
Figure 3. Optimization of elution process from the tips. Several ACN ratios (0–40%) were screened for the elution of enriched hIgG1 from the tips using acid dissociation with 0.4% TFA. The elution optimization of the protein was performed by comparing the mass spectrometric response of the surrogate peptide after tryptic digestion. ACN: Acetonitrile; TFA: Trifluoroacetic acid.

(Figure 4C) to meet acceptance (Supplementary Table 3). Nevertheless, no impact on the LLOQ signal due to this contribution was caused as the signal of the contribution was still 81% lower compared with the LLOQ signal. This contribution could further be reduced when the concentration of the ISTD would be decreased to 5.00 ng/ml. Nevertheless, the above-stated results indicated that the selected SRM transitions of the surrogate peptide and the ISTD were selective for the quantitative analysis of the recombinant hIgG1 in cynomolgus monkey serum.

Linearity & sensitivity

Although a linear regression model in the form of $y = ax + b$ could have also been used to construct the calibration curve on each day, a slightly better coefficient of determination (R^2) over a calibration range from 10.0 to 1000 ng/ml was obtained with a quadratic regression model (Supplementary Figure 1). Previous experiments with an extended calibration range confirmed this observation with this surrogate peptide [10,22]. The resultant mean R^2 value on three different days was 0.9938 (ranging from 0.9924 to 0.9952). The inter-

day accuracy of Cs samples ranged from -8.9 to 7.0% with a precision ranging from 5.1 to 11.8% (Table 1). As the predefined acceptance criteria were fulfilled, the constructed calibration curve could be used for routine analysis of hIgG1 in cynomolgus monkey serum.

Carry-over

No carry-over was found for the ISTD as the response directly after the injection of the ULOQ sample was 0.1% compared with the response at the ISTD working concentration (Supplementary Table 4). Even though, the carry-over of the surrogate peptide (39.8%) exceeded the acceptance criterion by 19.8% (Supplementary Table 4), the response was still 60.2% below the response of the signal at the LLOQ. Consequently, no overestimation was observed with Cs and QC samples since accurate and precise results were obtained (Tables 1 & 2). However, caution should be taken with unknown samples to avoid overestimation.

Accuracy & precision

On each day, a different batch of cynomolgus monkey serum was used for the preparation of QC samples.
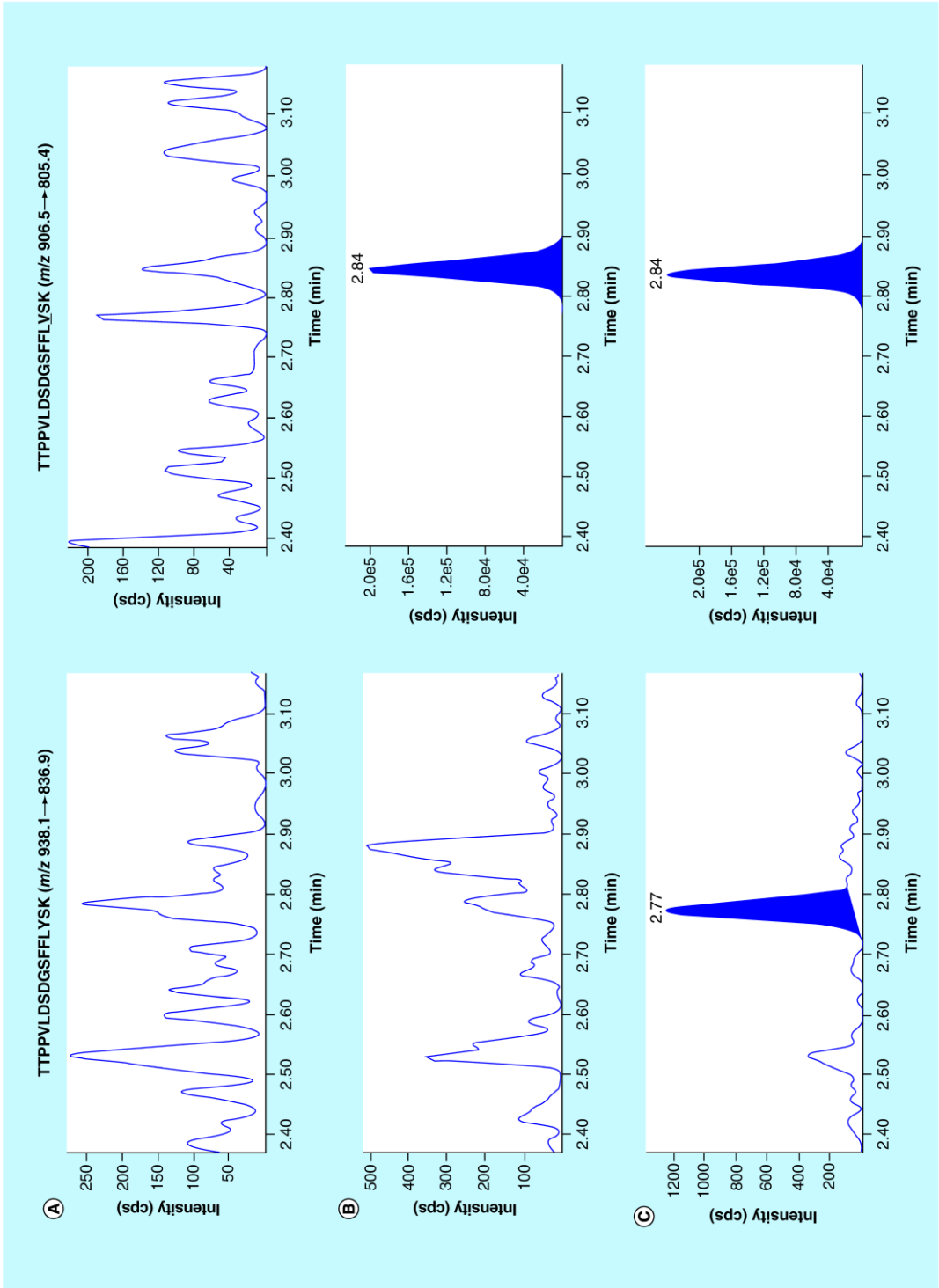
Figure 4. Chromatograms for the selected reaction monitoring mass transitions of the surrogate peptide TTPPVLDSDGSFFLYSK (*m/z* 938.1→836.9, left panel) and the analog peptide TTPPVLDSDGSFFLVSK (*m/z* 906.5→805.4, right panel). (A) Blank cynomolgus monkey serum sample, **(B)** zero sample (blank spiked only with the internal standard) and **(C)** sample at the LLOQ (10.0 ng/ml).

Research Article   Lanshoeft, Heudi, Cianférani, Warren, Picard & Kretz

Table 1. Interday accuracy and precision for calibration standards.

| | Cs nominal concentration (ng/ml) in cynomolgus monkey serum | | | | | | | |
	1000	750	500	250	100	75.0	50.0	10.0
Interday accuracy and precision								
Mean concentration (ng/ml)	1003	735	506	261	94.4	68.3	51.9	10.7
Interday accuracy (% bias)	0.3	-2.0	1.1	4.3	-5.6	-8.9	3.7	7.0
Interday precision (% CV)	5.6	7.9	9.1	5.1	8.3	9.9	11.8	8.7
n	6	5	6	6	4	6	4	5
CV: Coefficient of variation.								

The selectivity in these batches was previously demonstrated (Supplementary Table 2). The intraday bias and precision of four QC levels at 10.0 ng/ml (LLOQ), 25.0, 400 and 800 ng/ml across the first two days ranged from -6.9 to 11.0% and 1.2 to 14.3%, respectively (Table 2). However, the accuracy on the third day using batch 3 for the preparation of QC samples was slightly higher with a maximum of 19.9% with a precision below 14.3%. The highest interference during selectivity investigation (Supplementary Table 2) was observed with this batch of blank cynomolgus monkey serum which could be an explanation for the higher accuracy and precision values. The interday accuracy ranged from -3.1 to 8.9% whereas the precision was ≤10.3% (Table 2). Since the accuracy and precision fulfilled the acceptance criteria on three different days, no concentration dependency was observed in presence of the matrix. Thus, the matrix did not impact the quantification and the surrogate peptide determined the protein concentration in cynomolgus monkey serum consistently and reliably over the entire concentration range.

Dilution factor

Both dilution factors (100- and 500-fold) were within the set acceptance criteria (Supplementary Table 5). Since a mean back calculated concentration of 56.4 μg/ml with an accuracy of 12.8% bias and a precision of 7.3% CV was obtained with the 500-fold dilution factor incorporated, study samples exhibiting a higher concentration than the qualified calibration range can be readily diluted with blank cynomolgus serum prior to analysis without the introduction of any significant bias.

Table 2. Intra- and inter-day accuracy and precision of quality control samples in cynomolgus monkey serum on three different days.

| | | QC nominal concentration (ng/ml) in cynomolgus monkey serum | | | |
		800	400	25.0	10.0
Intraday accuracy and precision (n = 3)					
Day 1	Mean concentration (ng/ml)	888	406	24.5	10.1
	Intraday accuracy (% bias)	11.0	1.4	-2.0	0.8
	Intraday precision (% CV)	1.2	4.3	14.3	14.0
Day 2	Mean concentration (ng/ml)	799	399	23.3	10.1
	Intraday accuracy (% bias)	-0.1	-0.2	-6.9	1.0
	Intraday precision (% CV)	6.6	4.0	12.1	3.6
Day 3	Mean concentration (ng/ml)	926	480	24.9	9.69
	Intraday accuracy (% bias)	15.8	19.9	-0.4	-3.1
	Intraday precision (% CV)	3.1	4.4	6.1	14.3
Interday accuracy and precision (n = 9)					
Overall	Mean concentration (ng/ml)	871	428	24.2	9.95
	Interday accuracy (% bias)	8.9	7.1	-3.1	-0.5
	Interday precision (% CV)	7.4	9.8	10.3	10.3
CV: Coefficient of variation; QC: Quality control.					

Table 3. Stability data of surrogate peptide on the auto-sampler at 10°C determined with two quality control concentrations (25.0 and 800 ng/ml).							
	Storage period on auto-sampler						
	24 h				72 h		
	Measured concentration (ng/ml) and individual bias (%)						
Replicate 1	822	2.8	29.6	18.4	884	10.5	27.2	8.8
Replicate 2	756	-5.5	23.7	-5.2	946	18.3	18.9	-24.4[†]
Replicate 3	873	9.1	22.9	-8.4	838	4.8	17.5	-30.0[†]
Mean concentration (ng/ml)	817		25.4		889		21.2	
Accuracy (% bias)	2.1		1.6		11.2		-15.2	
Precision (% CV)	7.2		14.4		6.1		24.7[‡]	

[†]Out of acceptance criterion of ± 20%;
[‡]Out of acceptance criterion of ≤20%;
CV: Coefficient of variation.

Auto-sampler stability

The surrogate peptide was stable on the auto-sampler at 10°C for at least 24 h as the mean percent bias (n = 3) relative to the nominal concentration on two QC levels at 25.0 and 800 ng/ml was below 2.1% (Table 3). The highest precision value with 14.4% CV was obtained at the lower QC concentration for the 24 h storage period. For a time period of 72 h, the both QC levels met acceptance regarding the mean accuracy with 11.2 and -15.2% for the QC at 800 and 25.0 ng/ml, respectively. However, the precision of the low QC exceeded the acceptance criterion by 4.7% as two individual accuracy values did not meet acceptance with -24.4 and -30.0%. As a consequence, auto-sampler stability was not guaranteed for 72 h.

Application to preclinical PK study

In some cases, only a limited amount of sample volume is left for analysis during PK, PD and immunogenicity (IG) assessment. As a consequence, the study samples have to be further diluted with blank matrix. This could decrease the sample concentration, especially at later time-points or at low doses below the LLOQ of a specific method, for instance, an ELISA with a LLOQ of 200 ng/ml. Thus, a more sensitive analytical assay is required. The developed sensitive LC–MS/MS assay was applied to serum samples previously diluted by 50-fold from two cynomolgus monkeys that had been administrated a single i.v.t dose of hIgG1 at 1.00 and 3.00 mg/eye into both eyes. The obtained hIgG1 serum concentration-time profiles were typical for extravascular administration of a mAb as the dosed hIgG1 was distributed slowly out of the eye into the systemic circulation (Figure 5). The highest hIgG1 serum concentration (C_{max}) was observed at 168 h postdose with corresponding C_{max} values of 5.08 and 11.6 µg/ml

for the 1.00 and 3.00 mg/eye dose, respectively. This demonstrated the applicability of the developed sensitive LC–MS/MS assay based on MSIA-D.A.R.T.'S for PK profiling of low abundant hIgG1-based therapeutic proteins in cynomolgus monkey serum.

Conclusion

A sensitive LC–MS/MS assay incorporating the MSIA-D.A.R.T.'S technology over the range from 10.0 to 1000 ng/ml was developed to quantify hIgG1-based therapeutic proteins at low levels (ng/ml) in cynomolgus monkey serum. Since a generic surrogate peptide from the hIgG1 Fc region was used, the method could be applied to support the quantitative analysis of any kind of hIgG1-based therapeutic proteins in various types of preclinical species, for example, mouse, rat or monkey. In general, the sample preparation is achieved within one working day using this developed bottom-up approach on a Versette automated robotic platform (96-well plate format) with subsequent LC–MS/MS analysis overnight. Thus, a reasonable throughput is also achievable with our methodology. Additionally, the MSIA-D.A.R.T.'S platform and can be used as an alternative to an already in-house existing LC–MS/MS assay based on magnetic beads using the KingFisher™ platform [47]. Both MS-based assays are complementary approaches to conventional LBAs. As any kind of biotinylated antigen can be captured on the streptavidin tips, low abundant proteins can be enriched and quantified in case the biotinylated antigen exhibits the required specificity and affinity to the target protein. However for clinical samples, the developed method cannot be applied as endogenous hIgG1 would highly interfere with the assay. Subsequently, hIgG1-specific peptides from the complementary determining region have to be selected as surrogate peptide. Moreover,
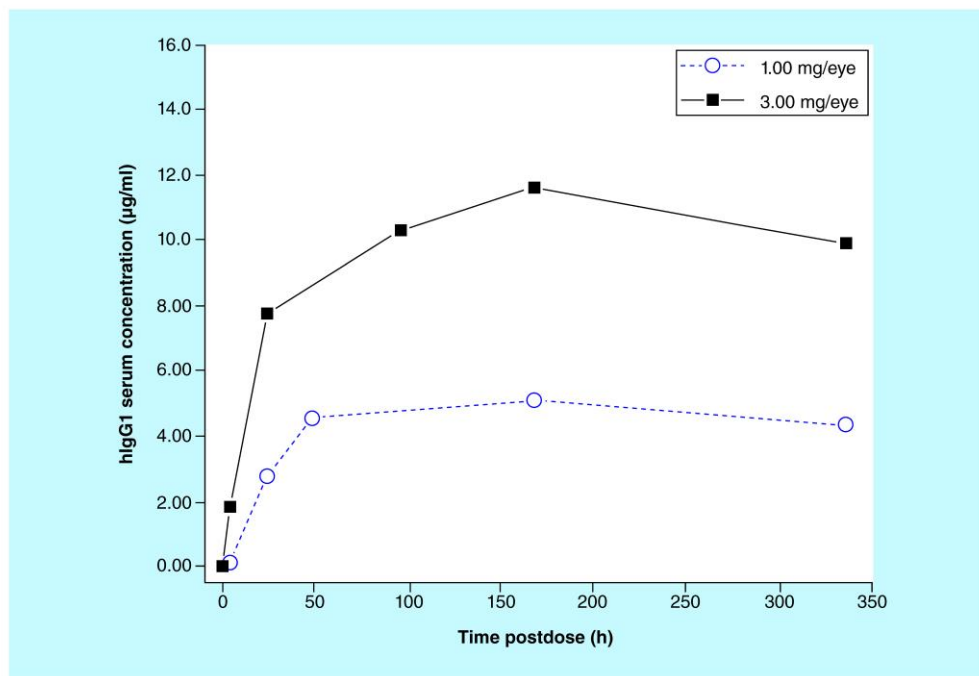
Figure 5. Concentration-time profile of the hIgG1 after intravitreal administration. Two individual cynomolgus monkeys were dosed intravitreally with hIgG1 into both eyes at 1.00 and 3.00 mg/eye and serum samples were analyzed by LC–MS/MS using immunocapture with MSIA-D.A.R.T.'S.

another capture antibody highly specific to the targeted hIgG1-based therapeutic protein has to be utilized for immunocapture in order to achieve a low LLOQ in human serum similar to the one obtained in cynomolgus monkey.

Future perspective

Quantitative analysis of therapeutic proteins using MSIA-D.A.R.T.'S is not only limited to the bottom-up approach using an enzymatic digestion since the quantification of targeted proteins can also be performed on intact protein level using the MSIA-D.A.R.T.'S technology in combination with HRMS instead of QqQ instruments. Besides the quantitative aspect, the characterization of therapeutic proteins plays an important role during in the drug development and production process. As the eluted proteins are fairly clean after immunocapture, the MSIA-D.A.R.T.'S technology could be used for glycan analysis of a specific mAb or to provide valuable information regarding the DAR measurement of ADCs. When it would be possible to disrupt the antigen–antibody complex under nondenaturing conditions, even intact analysis of proteins under native conditions could be performed to study, for instance, protein–protein interactions of complexes. In conclusion, this technology can serve

as promising tool for the quantitative and qualitative analysis of therapeutic proteins during the drug development process of biotherapeutics.

No writing assistance was utilized in the production of this manuscript.

Ethical conduct of research

The authors state that they have obtained appropriate institutional review board approval or have followed the principles outlined in the Declaration of Helsinki for all human or animal experimental investigations. In addition, for investigations involving human subjects, informed consent has been obtained from the participants involved.

Executive summary

Background

- A highly sensitive mass spectrometric immunoassay with disposable automation research tips (MSIA-D.A.R.T.'S) in combination with LC–MS/MS has been developed in order to extract low level hIgG1-based therapeutic proteins out of cynomolgus monkey serum.

Results

- A mouse anti-hIgG antibody containing eight to nine biotins was utilized to extract the hIgG1.
- The developed LC–MS/MS assay with MSIA-D.A.R.T.'S was evaluated in regards to selectivity, linearity, carry-over, accuracy, precision and auto-sampler stability.
- A typical concentration-time profile for extravascular administration was obtained from two cynomolgus monkeys previously dosed intravitreally with hIgG1.

Conclusion

- MSIA-D.A.R.T.'S represents a promising alternative to other immunocapture protocols based on magnetic beads in combination with LC–MS/MS analysis or ligand-binding assays for protein quantification.
- The present method can be applied to any preclinical species in order to quantify hIgG1-based therapeutic proteins using the bottom-up approach.
- MSIA-D.A.R.T.'S can also be used to quantify proteins on intact level or characterize antibody–drug conjugates.

References

Papers of special note have been highlighted as:
• of interest; •• of considerable interest

1   Lee JW, Kelley M. Quality assessment of bioanalytical quantification of monoclonal antibody drugs. *Ther. Deliv.* 2(3), 383–396 (2011).

2   Mora JR, Obenauer-Kutner L, Vimal Patel V. Application of the Gyrolab™ platform to ligand-binding assays: a user's perspective. *Bioanalysis* 2(10), 1711–1715 (2010).

3   An B, Zhang M, Qu J. Toward sensitive and accurate analysis of antibody biotherapeutics by liquid chromatography coupled with mass spectrometry. *Drug. Metab. Dispos.* 42(11), 1858–1866 (2014).

4   Hopfgartner G, Lesur A, Varesio E. Analysis of biopharmaceutical proteins in biological matrices by LC–MS/MS II. LC–MS/MS analysis. *Trends. Analyt. Chem.* 48, 52–61 (2013).

5   Van Den Broek I, Niessen WM, Van Dongen WD. Bioanalytical LC–MS/MS of protein-based biopharmaceuticals. *J. Chromatogr. B* 929, 161–179 (2013).

6   Ocana MF, Neubert H. An immunoaffinity liquid chromatography-tandem mass spectrometry assay for the quantitation of matrix metalloproteinase 9 in mouse serum. *Anal. Biochem.* 399(2), 202–210 (2010).

7   Van Dorsselaer A, Carapito C, Delalande F *et al.* Detection of prion protein in urine-derived injectable fertility products by a targeted proteomic approach. *PLoS ONE* 6(3), e17815 (2011).

8   Heudi O, Barteau S, Zimmer D *et al.* Towards absolute quantification of therapeutic monoclonal antibody in serum by LC–MS/MS using isotope-labeled antibody standard and protein cleavage isotope dilution mass spectrometry. *Anal. Chem.* 80(11), 4200–4207 (2008).

9   Ladwig PM, Barnidge DR, Snyder MR, Katzmann JA, Murray DL. Quantification of serum IgG subclasses by use of subclass-specific tryptic peptides and liquid chromatography–tandem mass spectrometry. *Clin. Chem.* 60(8), 1080–1088 (2014).

10   Lanshoeft C, Heudi O, Cianférani S. SMART Digest™ compared with pellet digestion for analysis of human immunoglobulin G1 in rat serum by liquid chromatography tandem mass spectrometry. *Anal. Biochem.* 501, 23-25 (2016).

11   Willrich MaV, Murray DL, Barnidge DR, Ladwig PM, Snyder MR. Quantitation of infliximab using clonotypic peptides and selective reaction monitoring by LC–MS/MS. *Int. Immunopharmacol.* 28(1), 513–520 (2015).

12   Beck A, Debaene F, Diemer H *et al.* Cutting-edge mass spectrometry characterization of originator, biosimilar and biobetter antibodies. *J. Mass. Spectrom.* 50(2), 285–297 (2015).

13   Myler H, Rangan VS, Wang J *et al.* An integrated multiplatform bioanalytical strategy for antibody–drug conjugates: a novel case study. *Bioanalysis* 7(13), 1569–1582 (2015).

14   Hortin GL, Sviridov D. The dynamic range problem in the analysis of the plasma proteome. *J. Proteomics* 73(3), 629–636 (2010).

15   Gallien S, Domon B. Detection and quantification of proteins in clinical samples using high resolution mass spectrometry. *Methods* 81, 15–23 (2015).

16   Morin LP, Mess JN, Garofolo F. Large-molecule quantification: sensitivity and selectivity head-to-head comparison of triple quadrupole with Q-TOF. *Bioanalysis* 5(10), 1181–1193 (2013).

17   Plumb RS, Fujimoto G, Mather J *et al.* Comparison of the quantification of a therapeutic protein using nominal and accurate mass MS/MS. *Bioanalysis* 4(5), 605–615 (2012).

••   **The quantification of therapeutic proteins by HRMS is described.**

18   Jeudy J, Salvador A, Simon R *et al.* Overcoming biofluid protein complexity during targeted mass spectrometry detection and quantification of protein biomarkers by MRM cubed (MRM3). *Anal. Bioanal. Chem.* 406(4), 1193–1200 (2014).

19   Sidibé J, Varesio E, Hopfgartner G. Quantification of ghrelin and des-acyl ghrelin in human plasma by using cubic-selected reaction-monitoring LCMS. *Bioanalysis* 6(10), 1373–1383 (2014).

20   Stoll DR, Harmes DC, Danforth J *et al.* Direct identification of rituximab main isoforms and subunit analysis by online selective comprehensive two-dimensional liquid chromatography-mass spectrometry. *Anal. Chem.* 87(16), 8307–8315 (2015).

21   Vonk RJ, Gargano AF, Davydova E *et al.* Comprehensive two-dimensional liquid chromatography with stationary-phase-assisted modulation coupled to high-resolution mass spectrometry applied to proteome analysis of saccharomyces cerevisiae. *Anal. Chem.* 87(10), 5387–5394 (2015).

22   Lanshoeft C, Wolf T, Heudi O *et al.* The use of generic surrogate peptides for the quantitative analysis of human immunoglobulin G1 in pre-clinical species with high-resolution mass spectrometry. *Anal. Bioanal. Chem.* 408(6), 1687–1699 (2016).

23   Mekhssian K, Mess JN, Garofolo F. Application of high-resolution MS in the quantification of a therapeutic monoclonal antibody in human plasma. *Bioanalysis* 6(13), 1767–1779 (2014).

24   Jiang H, Xu W, Titsch CA *et al.* Innovative use of LC–MS/MS for simultaneous quantitation of neutralizing antibody, residual drug, and human immunoglobulin G in immunogenicity assay development. *Anal. Chem.* 86(5), 2673–2680 (2014).

25   Sleczka BG, Mehl JT, Shuster DJ *et al.* Quantification of human mAbs in mouse tissues using generic affinity enrichment procedures and LC–MS detection. *Bioanalysis* 6(13), 1795–1811 (2014).

26   Becker JO, Hoofnagle AN. Replacing immunoassays with tryptic digestion-peptide immunoaffinity enrichment and LC–MS/MS. *Bioanalysis* 4(3), 281–290 (2012).

27   Whiteaker JR, Zhao L, Abbatiello SE *et al.* Evaluation of large scale quantitative proteomic assay development using peptide affinity-based mass spectrometry. *Mol. Cell. Proteomics* 10(4), M110.005645 (2011).

28   Kushnir MM, Rockwood AL, Roberts WL, Abraham D, Hoofnagle AN, Meikle AW. Measurement of thyroglobulin by liquid chromatography-tandem mass spectrometry in serum and plasma in the presence of antithyroglobulin autoantibodies. *Clin. Chem.* 59(6), 982–990 (2013).

29   Neubert H, Muirhead D, Kabir M, Grace C, Cleton A, Arends R. Sequential protein and peptide immunoaffinity capture for mass spectrometry-based quantification of total human β-nerve growth factor. *Anal. Chem.* 85(3), 1719–1726 (2012).

30   Chappell DL, Lee AY, Castro-Perez J *et al.* An ultrasensitive method for the quantitation of active and inactive GLP-1 in human plasma via immunoaffinity LC–MS/MS. *Bioanalysis* 6(1), 33–42 (2014).

31   Fernandez Ocana M, James IT, Kabir M *et al.* Clinical pharmacokinetic assessment of an anti-MAdCAM monoclonal antibody therapeutic by LC–MS/MS. *Anal. Chem.* 84(14), 5959–5967 (2012).

32   Li H, Ortiz R, Tran L *et al.* General LC–MS/MS method approach to quantify therapeutic monoclonal antibodies using a common whole antibody internal standard with application to preclinical studies. *Anal. Chem.* 84(3), 1267–1273 (2012).

33   Schneck NA, Lowenthal M, Phinney K, Lee SB. Current trends in magnetic particle enrichment for mass spectrometry-based analysis of cardiovascular protein biomarkers. *Nanomedicine* 10(3), 433–446 (2015).

34   Yang W, Kernstock R, Simmons N, Alak A. ELISA microplate: a viable immunocapture platform over magnetic beads for immunoaffinity-LC–MS/MS quantitation of protein therapeutics? *Bioanalysis* 7(3), 307–318 (2015).

••   **Interesting article describing the use of ELISA plates for quantitative MS-based assays for therapeutic proteins.**

35   Smits NE, Blokland M, Wubs K, Nessen M, Van Ginkel L, Nielen MF. Monolith immuno-affinity enrichment liquid chromatography tandem mass spectrometry for quantitative protein analysis of recombinant bovine somatotropin in serum. *Anal. Bioanal. Chem.* 407(20), 6041–6050 (2015).

36   Sherma ND, Borges CR, Trenchevska O *et al.* Mass spectrometric immunoassay for the qualitative and quantitative analysis of the cytokine macrophage migration inhibitory factor (MIF). *Proteome Sci.* 12(1), 52 (2014).

37   Peterman S, Niederkofler EE, Phillips DA *et al.* An automated, high-throughput method for targeted quantification of intact insulin and its therapeutic analogs in human serum or plasma coupling mass spectrometric immunoassay with high resolution and accurate mass detection (MSIA-HR/AM). *Proteomics* 14(12), 1445–1456 (2014).

•   **A highly sensitive MSIA-D.A.R.T.'S based assay for insulin analogs is described.**

38   Krastins B, Prakash A, Sarracino DA *et al.* Rapid development of sensitive, high-throughput, quantitative and highly selective mass spectrometric targeted immunoassays for clinically important proteins in human plasma and serum. *Clin. Biochem.* 46(6), 399–410 (2013).

•   **The screening of clinical relevant proteins in human plasma/serum by MSIA-D.A.R.T.'S is described in this article.**

39   Lopez MF, Krastins B, Sarracino DA *et al.* Proteomic signatures of serum albumin-bound proteins from stroke patients with and without endovascular closure of PFO are

significantly different and suggest a novel mechanism for cholesterol efflux. *Clin. Proteomics* 12(1), 2 (2015).

40 Lopez MF, Rezai T, Sarracino DA *et al.* Selected reaction monitoring-mass spectrometric immunoassay responsive to parathyroid hormone and related variants. *Clin. Chem.* 56(2), 281–290 (2010).

41 Prakash A, Rezai T, Krastins B *et al.* Interlaboratory reproducibility of selective reaction monitoring assays using multiple upfront analyte enrichment strategies. *J. Proteome. Res.* 11(8), 3986–3995 (2012).

• **The interlaboratory reproducibility of the MSIA-D.A.R.T.'S is reported.**

42 Guideline on Bioanalytical Method Validation. European Medicines Agency, London, UK. (2011). www.ema.europa.eu

43 Guidance for Industry: Bioanalytical Method Validation. US FDA, Rockville, MD, USA. (2001). www.fda.gov/downloads/Drugs/Guidances/ucm070107.pdf

44 Jenkins R, Duggan JX, Aubry AF *et al.* Recommendations for validation of LC–MS/MS bioanalytical methods for protein biotherapeutics. *AAPS J.* 17(1), 1–16 (2015).

45 Chen J, Yin S, Wu Y, Ouyang J. Development of a native nanoelectrospray mass spectrometry method for determination of the drug-to-antibody ratio of antibody–drug conjugates. *Anal. Chem.* 85(3), 1699–1704 (2013).

46 Debaene F, Bœuf A, Wagner-Rousset E *et al.* Innovative native MS methodologies for antibody drug conjugate characterization: high resolution native MS and IM-MS for average DAR and DAR distribution assessment. *Anal. Chem.* 86(21), 10674–10683 (2014).

47 Law WS, Genin J-C, Miess C *et al.* Use of generic LC–MS/MS assays to characterize atypical PK profile of a biotherapeutic monoclonal antibody. *Bioanalysis* 6(23), 3225–3235 (2014).

•• **The LC–MS/MS assay based on magnetic beads is described as an alternative to the recent MSIA-D.A.R.T.'S protocol.**

Part 3 - Quantitative HRMS-based approaches

Following the development of generic LC-MS/MS methods for bottom-up mAb-related therapeutic protein quantification in pre-clinical serum samples, the third part discusses the benefit of HRMS instruments as an alternative to conventional QqQ mass analyzers. In the upcoming three chapters, the potential of QTOF and quadrupole orbitrap instruments is illustrated for targeted bottom-up hIgG quantification and novel MS-based approaches for mAb-related therapeutic protein quantification at the intact level are presented.

Chapters

3.1   Generic quantitative bottom-up LC-HRMS method

3.2   Approach for intact hIgG1 quantification by IC-LC-HRMS

3.3   Combined qualitative and quantitative analysis of intact ADCs

3.1 Generic quantitative bottom-up LC-HRMS method

3.1.1 Analytical context

While HRMS has become a well-established technology for mAb-related therapeutic protein characterization or drug metabolite identification, most bioanalysts still hesitate to introduce quantitative HRMS (qHRMS) in regulated late-stage drug development.[460-466] MS-based quantification of mAb-related therapeutic proteins is still dominated by QqQ instruments (Part 2) due to their specificity, sensitivity, wide linear dynamic range, robustness, high-throughput, multiplexing capability, ease in operation, and relatively small data acquisition files.[319,467,468] Routine application of qHRMS in pharmaceutical industry is also hampered due to lacking guidance for qHRMS method validation from regulatory agencies (*i.e.* post-acquisition data processing) as authorities had previously mainly to deal with LC-MS/MS data.[468] However, deficits of QqQ instruments for mAb-related therapeutic protein quantification include a limited mass range (up to *m/z* 2000), labor-intense SRM optimization, suboptimal fragmentation of certain surrogate peptides, and more relevant inferior specificity due to low resolution and mass accuracy.[469-471]

In contrast, narrow mass spectral peak width can be obtained with HRMS instruments operating at high resolution (<1 000 000 depending on the type of HRMS instrument) and mass accuracy (≤5.0 ppm).[472-474] Subsequently, unresolved interferences from co-eluting matrix-related background ions can potentially be reduced, leading to an improved selectivity and hence sensitivity (increased S/N ratio).[475,476] Due to recent advancements in HRMS instrumentation, previous limitations such as high purchase and maintenance costs, low scan speed, inferior sensitivity, limited linear dynamic ranges, or complicated operation have nowadays been overcome, allowing reliable quantification.[467,469,471,476,477] Thus, a paradigm shift from conventional QqQ towards qHRMS is currently on-going.[478-481] From all commercially available HRMS instruments, QTOF[482-484] and orbitrap[485-487] mass analyzers have received the most interest in quantitative bioanalysis as expensive operation costs, large laboratory footprints, long optimization, and scan times are associated with Fourier transform ion cyclotron resonance instruments.[488] Quantitative HRMS was extensively explored in the bioanalytical field of small molecule quantification in serum or plasma,[489,490] cerebrospinal fluid,[491] dried blood spots,[492-495] or urine samples.[496-498] However, only a few research groups have explored this technology with respect to peptide,[469,487,499] low to mid-molecular weighted therapeutic protein (<70 kDa),[471,475,476] PEGylated protein,[500] or mAb-related therapeutic protein quantification in biological fluids.[467,470]

3.1.2 Objectives

The project aimed to implement a generic qHRMS approach for targeted bottom-up hIgG quantification in pre-clinical species. In addition, the validated LC-HRMS method was compared to

the developed pellet digestion-based generic LC-MS/MS assay using spiked serum samples and specimen from pre-clinical trial.

3.1.3 Results

3.1.3.1 Selection of the QTOF acquisition mode for qHRMS analysis

The previously reported pellet digestion protocol served as sample preparation whereby the LC gradient from the generic LC-MS/MS method (chapter 2.1) was extended to improve the separation of the TTP and VVS peptides with the ACE C_{18} column (150 x 4.6 mm, 3 µm), while maintaining the mobile phase conditions (0.1% FA in water and ACN). HRMS analysis was conducted using a Synapt G2-Si QTOF, which operated in sensitivity mode with a resolution of 20 000. Instead of the tuned nominal *m/z* values, the calculated exact (theoretical) monoisotopic values of the most intense precursor and product ions of each surrogate peptide were utilized after collision energy optimization (Table 3.1). The sensitivity as a function of an increased selectivity (improved S/N ratio) was not only governed by data processing parameters such as the width of the MXW or the amount of ions/isotopes selected for the generation of XICs, but also by the acquisition mode.[471] Hence, three acquisition modes namely TOF-MS, TOF-MS/MS, and TOF-MRM were evaluated. In TOF-MS, the quantification is based on the extraction of the exact monoisotopic *m/z* value of the peptide precursor ion from the full-scan MS spectrum. This acquisition mode resulted in high signal intensities for each peptide, but low S/N ratios (Figure 3.1). However by using TOF-MS/MS, the background noise was significantly reduced after extraction of the exact monoisotopic *m/z* value(s) of the product ion(s), leading to increased

Table 3.1 Monoisotopic *m/z* values of the precursor and product ion(s) for each surrogate peptide and its corresponding internal standard utilized for hIgG quantification in pre-clinical species by LC-HRMS.

Peptide	Mass-to-charge ratio				CE
	Precursor ion[a] (charge state)	Product ions[b] (ion type/charge state)			(eV)
FNW	559.9388 (+3)	697.3628 (y_6^+)	968.4796* (y_9^+)	708.8490 (y_{12}^{2+})	18
[$^{13}C_6$]-FNW[c]	561.9456 (+3)	703.3829 (y_6^+)	974.4997* (y_9^+)	711.8590 (y_{12}^{2+})	18
GPS	593.8270 (+2)	418.2296 (y_4^+)	699.4036* (y_7^+)	846.4720 (y_8^+)	18
[$^{13}C_6$]-GPS[c]	596.8370 (+2)	424.2498 (y_4^+)	705.4237* (y_7^+)	852.4921 (y_8^+)	18
TTP	937.4645 (+2)	836.4169* (y_{15}^{2+})	-	-	27
[$^{13}C_6$]-TTP[c]	940.4746 (+2)	839.4269* (y_{15}^{2+})	-	-	27
VVS	603.3403 (+3)	655.8462 (y_{11}^{2+})	712.3883 (y_{12}^{2+})	805.4385*,d (y_{14}^{2+})	16
[$^{13}C_6$]-VVS[c]	605.3471 (+3)	658.8563 (y_{11}^{2+})	715.3983 (y_{12}^{2+})	808.4485* (y_{14}^{2+})	16
VVSd	603.6684 (+3)	656.3382 (y_{11}^{2+})	712.8803 (y_{12}^{2+})	805.9305* (y_{14}^{2+})	16
[$^{13}C_6$]-VVSd[c]	605.6751 (+3)	659.3483 (y_{11}^{2+})	715.8903 (y_{12}^{2+})	808.9405* (y_{14}^{2+})	16

[a] Quadrupole mass isolation window of 1 Da for precursor ion selection, [b] product ion extraction window of 50 mDa, [c] labeled with [$^{13}C_6$]-lysine, [d] interference in rat serum, * product ion selected for enhancement, CE: collision energy

S/N ratios and hence improved sensitivities. Although, the signal intensities for each peptide were further increased due to duty cycle enhancement using TOF-MRM compared to TOF-MS/MS, the resulting S/N ratios were equivalent, indicating no further sensitivity improvement. Since the signal intensities of the TOF-MRM acquisition mode were increased, while maintaining the S/N ratios of the TOF-MS/MS acquisition mode, TOF-MRM was selected for the generic LC-HRMS method.
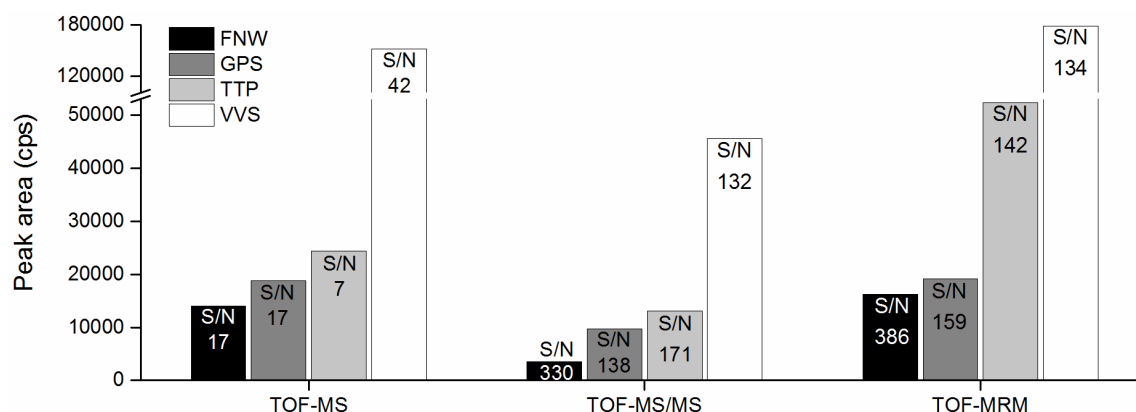
Figure 3.1 Selection of the QTOF acquisition mode for hIgG quantification based on four generic tryptic surrogate peptides. Numbers correspond to the obtained S/N ratio using the peak-to-peak model.

3.1.3.2 Elucidation of peptide deamidation by HRMS

In contrast to QqQ mass analyzers, HRMS provides an accelerated trouble shooting capability during method development as complete sample information is provided.[501] As outlined in section 2.1.3.5, a time-dependent decrease of signal intensities for both C_H2 peptides (FNW and VVS) was observed in the kinetic studies of the pellet digestion, as a result of asparagine deamidation *via* succinimide as cyclic intermediate to isoaspartic and aspartic acid under certain temperature and pH conditions.[502-507] *In vitro* or *in vivo* deamidation may alter the protein structure and potentially cause a decrease in its biological activity, especially if CDR peptides are affected.[508-512] This results in faster mAb clearance, increased toxicity, and enhanced IG.[513,514] Several amino acid motifs were identified to be predicted or prone to deamidation.[515] Since the VVS peptide contained only one of these sites, deamidation occurred within the "*LNG*" motif as confirmed by MS/MS (data not shown), which was in agreement with recently published data.[516] In contrast, the FNW peptide exhibited two potential deamidation motifs, namely "*FNW*" and "*HNA*", within its tryptic amino acid sequence. In order to examine if the FNW peptide underwent a single or double deamidation and which of the potential motifs was affected, the RADAR acquisition mode of the Synapt G2-Si QTOF was utilized by collecting alternately full-scan MS and MS/MS data in each acquisition cycle. In contrast to the MS[e] acquisition mode (switching between low and high collision energy), only MS/MS spectra from previously specified precursor ions were generated with the RADAR mode, resulting in markedly cleaner MS/MS spectra. Only one peak was obtained by extracting the exact *m/z* value of the monoisotopic $[M+3H]^{3+}$ precursor ion at *m/z* 559.9388 with

a MXW of 50 mDa (Figure 3.2a), corresponding to the non-deamidated FNW isoform as confirmed by MS/MS data (Figure 3.2b). In contrast, two additional peaks appeared using the exact m/z value of the deamidated (FNWd) $[M+3H]^{3+}$ precursor ion at m/z 560.2669 (Figure 3.2c), which was confirmed by the corresponding MS/MS spectra (Figure 3.2d+e). Since the signal intensity ratio between both FNWd isoforms was approximately 1:3, the smaller peak was identified as isoaspartic acid based on published data.[183] The peak for the FNW $[M+3H]^{3+}$ precursor ion was still present (Figure 3.2c) as the FNW $[(M+1)+3H]^{3+}$ isotope at m/z 560.2715 was extracted by the FNWd $[M+3H]^{3+}$ precursor ion due to a mass difference of 4.6 mDa. The MS/MS data indicated a single deamidation localized in the C-terminal "*HNA*" and not in the N-terminal "*FNW*" motif of the FNW peptide. This conclusion was derived from the obtained mass shift (0.9710-0.9920 Da), for all present singly charged y-fragments of the isoaspartic and aspartic acid isoforms (Figure 3.2d+e) compared to the non-deamidated y-fragments (Figure 3.2b). Moreover, no peak was observed by extracting the doubly-deamidated FNW $[M+3H]^{3+}$ precursor ion at m/z 560.5949 (data not shown). Due to inadequate peak integration, the FNW peptide was excluded from the peptide list for hIgG quantification.
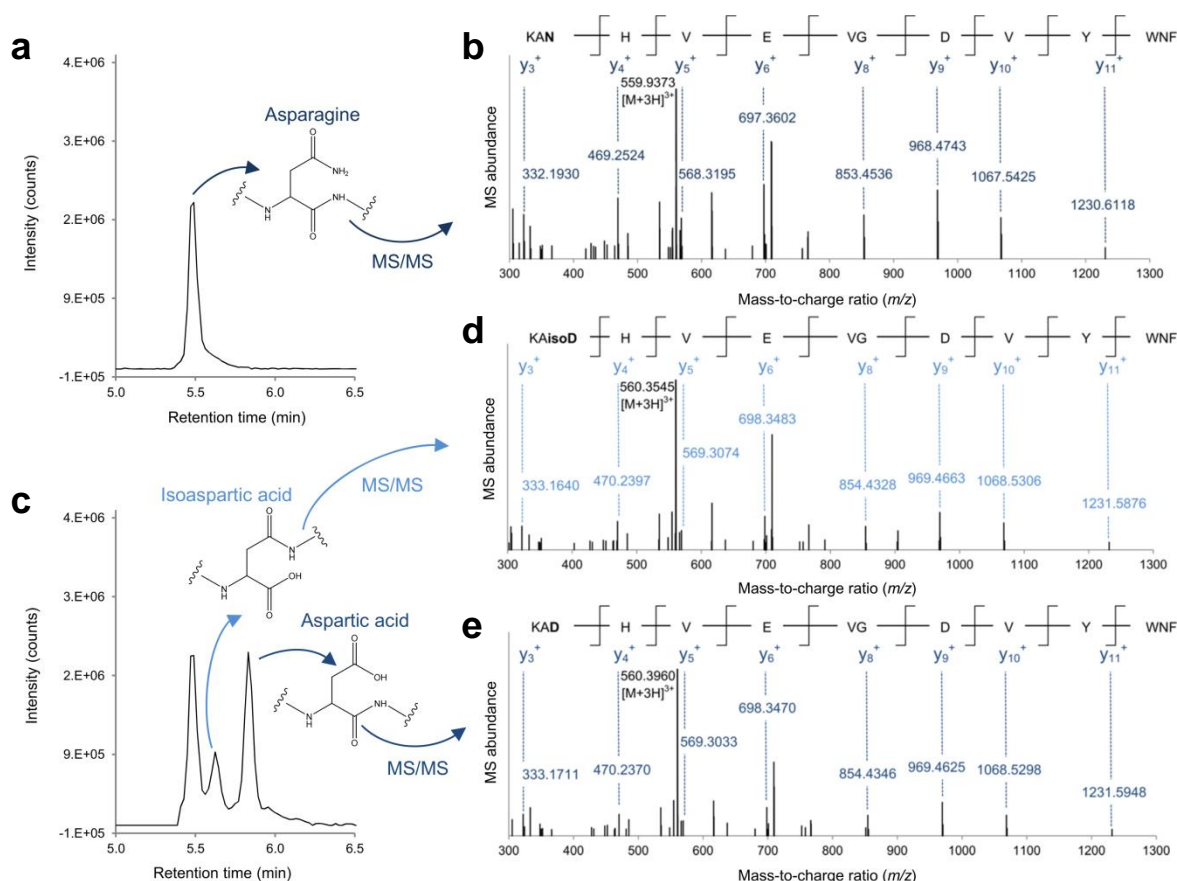
Figure 3.2 Elucidation of the FNW deamidation. (**a**) XIC and (**b**) MS/MS spectrum of the non-deamidated monoisotopic $[M+3H]^{3+}$ precursor ion at m/z 559.9388, (**c**) XIC of the deamidated monoisotopic $[M+3H]^{3+}$ precursor ion at m/z 560.2669 including MS/MS spectra for the (**d**) isoaspartic and (**e**) aspartic acid isoform.

3.1.3.3 Selectivity improvement for the VVS peptide in rat serum

As an additional benefit, an improved selectivity for the VVS peptide was obtained with qHRMS, due to the replacement of the last in unit resolution-operating quadrupole (QqQ instruments) by a high-resolution TOF mass analyzer. Following extraction of the exact *m/z* values of in total six VVS product ions (three from the non-deamidated and deamidated isoform), an interfering peak was found in blank rat serum (Figure 3.3a). The interference was caused by the $[(M+2)+2H]^{2+}$ ion at *m/z* 805.4466 of an unknown endogenous compound (Figure 3.3b). This product ion interfered due to its extraction together with the VVS y_{14}^{2+} $[M+2H]^{2+}$ product ion at *m/z* 805.4385 by applying a MXW of 50 mDa. A much narrower MXW of 16 mDa was required to distinguish between both
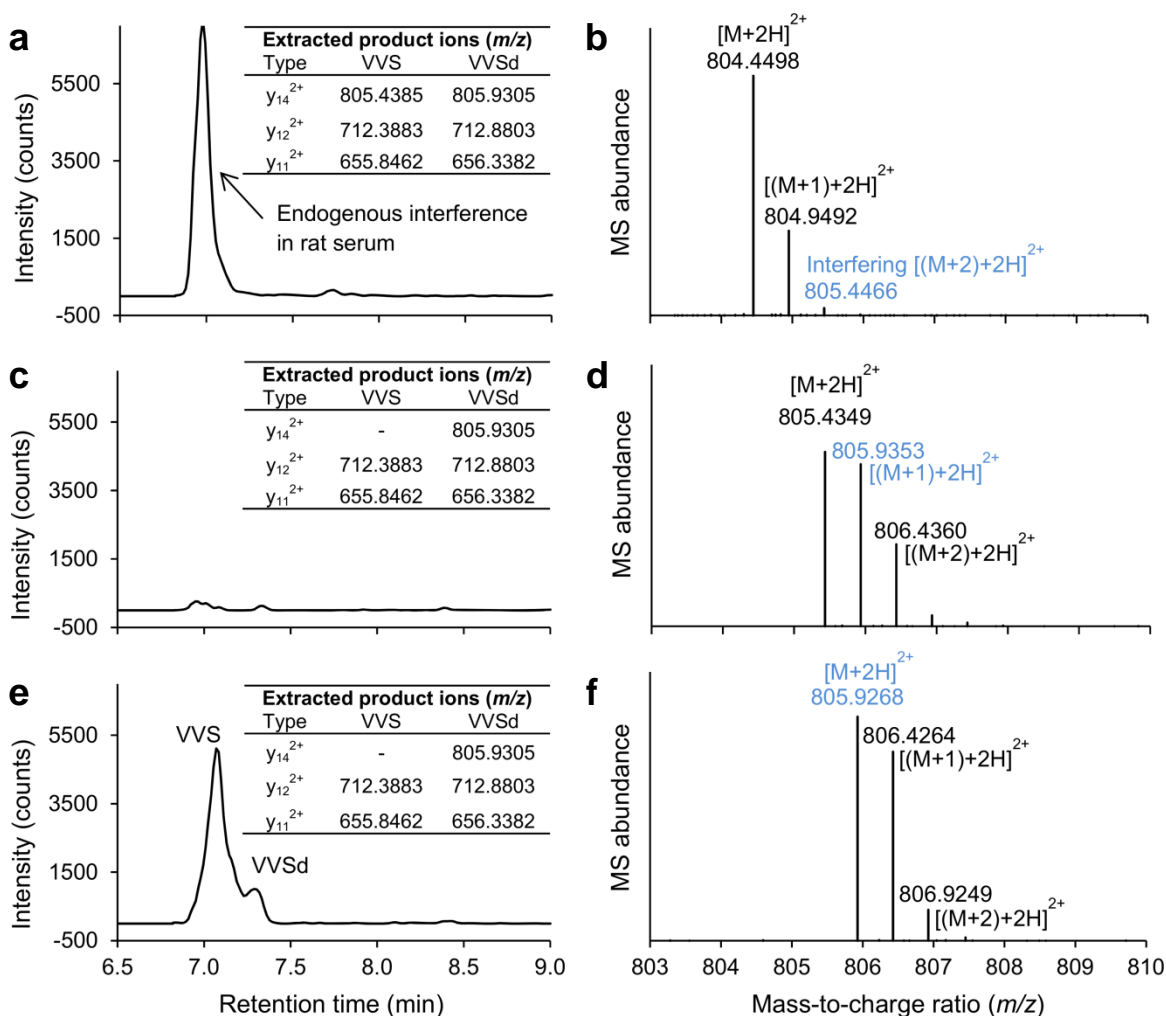
Figure 3.3 Selectivity improvement for the VVS peptide in rat serum using the VVSd instead of the VVS y_{14}^{2+} $[M+2H]^{2+}$ product ion. (**a**) XIC of blank rat serum using three product ions from each isoform, (**b**) MS/MS spectrum (zoom into *m/z* 803-810) of the interfering peak in rat serum, (**c**) XIC of blank rat serum after exclusion of the monoisotopic VVS y_{14}^{2+} product ion, (**d**) MS/MS spectrum (zoom into *m/z* 803-810) of the VVS $[M+3H]^{3+}$ precursor ion at *m/z* 603.3403, (**e**) extracted chromatogram of both VVS isoforms (in total five product ions) generated from a hIgG1-spiked rat serum sample at 10.0 µg/mL, (**f**) MS/MS spectrum (zoom into *m/z* 803-810) of the VVSd $[M+3H]^{3+}$ precursor ion at *m/z* 603.6684.

ions, which, however, would cause a significant loss in signal intensity as only a fraction of the ion peak would be extracted.[469,471] The highly resolved isotopic pattern offers the possibility to eliminate potential interferences by selecting the most appropriate *m/z* value for ion chromatogram extraction and hence quantification. The interference in blank rat serum almost completely disappeared after exclusion of the VVS y_{14}^{2+} $[M+2H]^{2+}$ product ion for XIC generation (Figure 3.3c). The sensitivity was not affected by this exclusion as the signal intensity of the VVS y_{14}^{2+} $[(M+1)+2H]^{2+}$ product ion at *m/z* 805.9353 was almost identical (91.6%) to the one of its $[M+2H]^{2+}$ product ion at *m/z* 805.4349 (Figure 3.3d). Moreover, the VVS isoform covered by its y_{14}^{2+} $[(M+1)+2H]^{2+}$ product ion was still extracted through the monoisotopic VVSd y_{14}^{2+} $[M+2H]^{2+}$ product ion as their *m/z* values differed by 8.5 mDa, considering the measured *m/z* value at 805.9268 (Figure 3.3f). Since both isoforms were extracted, a shoulder peak was observed with retention times of 7.1 and 7.4 min for VVS and VVSd, respectively (Figure 3.3e). In contrast to qHRMS analysis (Figure 3.4a), the interference was still present in blank rat serum using a QqQ instrument (Figure 3.4b). Consequently, the official selectivity acceptance criterion of ≤20.0% compared to the LLOQ response demanded by the US FDA and EMA,[352,353] is only fulfilled with the QTOF (Figure 3.4a+c), but not with the QqQ instrument (Figure 3.4b+d), demonstrating the superior selectivity of qHRMS compared to QqQ for LC-MS/MS analysis of large molecules.[517]
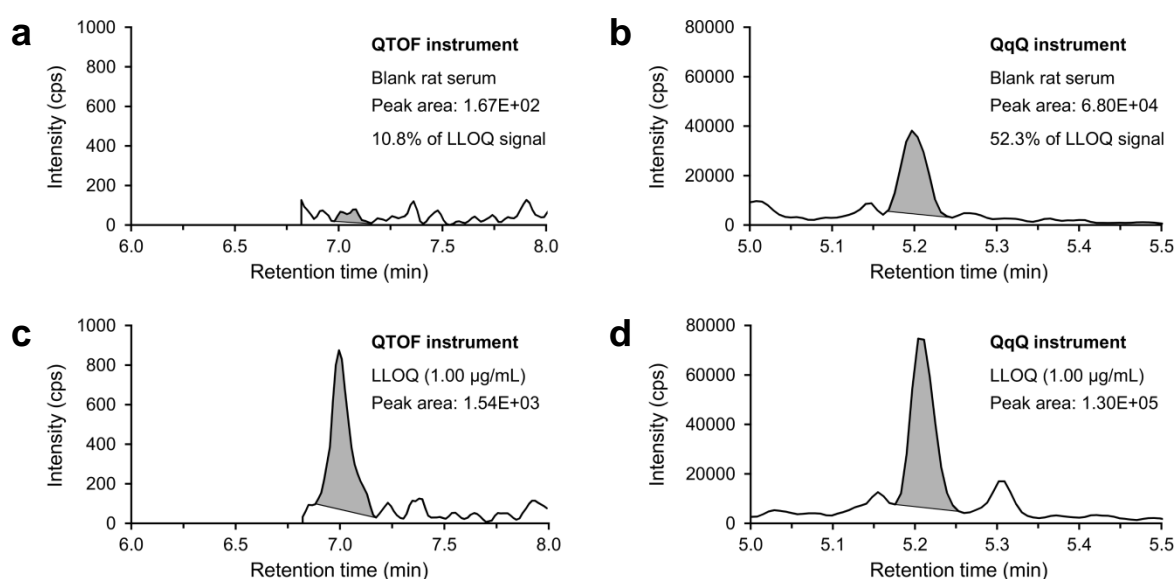
Figure 3.4 Selectivity comparison between QTOF and QqQ analysis using the VVS peptide. XIC obtained in blank rat serum using (**a**) a Waters Synapt G2-Si QTOF and (**b**) AB Sciex API 6500 QTRAP (QqQ) in comparison to the XIC at the LLOQ of 1.00 µg/mL for the (**c**) QTOF and (**d**) QqQ instrument.

3.1.3.4 Method validation in rat serum

The developed qHRMS approach was validated with regard to selectivity, linearity, carry-over, accuracy, precision, dilution integrity, auto-sampler stability of generated peptides, and short-term

stability of the hIgG1 in rat serum. The validation outcome is summarized in Table 3.2, meeting the acceptance criteria from US FDA and EMA guidances.[352,353]

Table 3.2 Method validation of generic TOF-MRM-based approach for hIgG1 quantification in rat serum.

Parameter	Validation outcome		
	GPS	TTP	VVS
Selectivity (n=3): three blank batches	GPS: <0.1% $[^{13}C_6]$-GPS: ≤1.8%	TTP: ≤5.0% $[^{13}C_6]$-TTP: ≤0.2%	VVS: ≤7.3% $[^{13}C_6]$-VVS: ≤0.4%
Linearity (n=3) $y(x)=ax^2+bx+c$, $1/x^2$ weighting	1.00-1000 µg/mL r^2=0.9868±0.0065	1.00-1000 µg/mL r^2=0.9911±0.0008	1.00-1000 µg/mL r^2=0.9906±0.0031
Carry-over (signal in blank after ULOQ)	<LLOQ signal	<LLOQ signal	<LLOQ signal
Intra-day (n=3) accuracy (% bias) and precision (% CV), QCs at 3.00, 15.0, 450, and 750 µg/mL	-11.9 to 9.4% bias 1.3 to 14.5% CV	-10.1 to 16.4% bias 1.9 to 13.3% CV	-13.3 to 16.8% bias 1.5 to 9.2% CV
Inter-day (n=9) accuracy (% bias) and precision (% CV), QCs at 3.00, 15.0, 450, and 750 µg/mL	-3.7 to 5.1% bias 4.6 to 8.4% CV	-3.6 to 11.4% bias 4.4 to 10.5% CV	-5.4 to 9.1% bias 7.8 to 9.8% CV
Dilution integrity (5.00 mg/mL, 100-fold, n=5)	3.2% bias 2.8% CV	3.1% bias 6.0% CV	14.0% bias 1.9% CV
Auto-sampler stability[a] (6 °C, 30 h, n=3) QCs at 15.0 and 750 µg/mL	7.0 to 9.7% bias	1.2 to 4.8% bias	0.2 to 1.7% bias
Short-term stability[a] (RT, 48 h, n=3) QCs at 15.0 and 750 µg/mL	-4.5 to -2.2% bias	-8.6 to 4.8% bias	3.5 to 3.7% bias

[a] % bias relative to expected concentration at t_0, RT: room temperature

3.1.3.5 Method transfer to cynomolgus monkey serum

As already mentioned in section 2.1.3.4, cynomolgus monkey serum samples spiked with a hIgG1 could be measured against Cs/QCs prepared with the same hIgG1 in rat serum due to the incorporation of $[^{13}C]$-hIgG1 as ISTD. The resultant accuracy values (n=3) obtained with qHRMS for GPS, TTP, and VVS ranged from -6.9 to 13.0% bias, fulfilling the acceptance criterion of ±20.0%. In contrast to QqQ instruments,[243] the hIgG1 concentration was not overestimated at the low QC level (3.00 µg/mL) as a result of the increased selectivity of qHRMS. However, the precision acceptance criterion of ≤20.0% CV was exceeded at this concentration by 7.1%, which was the reason why the GPS was further excluded for the analysis of pre-clinical study samples. The precision for the other two remaining peptides (TTP and VVS) ranged from 1.0 to 13.3% CV.

3.1.3.6 Comparison of LC-HRMS with LC-MS/MS

In comparison to SRM-based analysis, TOF-MRM resulted in similar linearity and sensitivity data using spiked rat serum samples, regardless of the selected surrogate peptide (Table 3.3). The reason for the selection of a quadratic compared to a linear regression model using the TOF-MRM acquisition mode was a better r^2-value. The obtained results were in agreement with other studies and further supported the withdrawal of previous qHRMS limitations (*i.e.* sensitivity and dynamic range) as a result of instrumental improvements.[470,501,518]

Table 3.3 Linearity comparison between a QTOF and QqQ mass analyzer over three non-consecutive days using hIgG1-spiked rat serum samples in a concentration range from 1.00 to 1000 µg/mL.

Peptide	Acquisition mode	Type of regression	Weighting factor	r^2-value (n=3)	LLOQ (µg/mL)	ULOQ (µg/mL)
GPS	TOF-MRM[a]	Quadratic	$1/x^2$	0.9868±0.0065	1.00	1000
	QqQ SRM[b]	Linear	$1/x^2$	0.9884±0.0060	1.00	1000
TTP	TOF-MRM[a]	Quadratic	$1/x^2$	0.9911±0.0008	1.00	1000
	QqQ SRM[b]	Quadratic	$1/x^2$	0.9958±0.0008	1.00	1000
VVS	TOF-MRM[a]	Quadratic	$1/x^2$	0.9906±0.0031	1.00	1000
	QqQ SRM[b]	Linear	$1/x^2$	0.9963±0.0014	1.00	1000

[a] Waters Synapt G2-Si QTOF, [b] AB Sciex API 6500 QTRAP

The analysis of serum samples from five cynomolgus monkeys, dosed with a hIgG1-related therapeutic protein at 5.00 mg/kg, using LC-HRMS (Waters Synapt G2-Si QTOF) and LC-MS/MS (AB Sciex API 6500 QTRAP) resulted in identical mean concentration-time profiles (mean concentration of TTP and VVS peptide) as depicted in Figure 3.5a. The mean variation between the obtained TTP and VVS concentrations over the mean PK profile was 2.7±1.7% CV for LC-HRMS analysis. In contrast, the variation between both surrogate peptides was slightly increased for LC-MS/MS analysis ranging from 3.7 to 8.5% CV. Considering individual concentrations for each cynomolgus monkey instead of the mean concentration, no significant deviation was revealed by the Bland-Altman plot, indicating equivalent data generation by both platforms (Figure 3.5b). The mean bias between both MS-based assays was 6.5±6.7% and -0.1±6.6% for the TTP and VVS peptide, respectively.
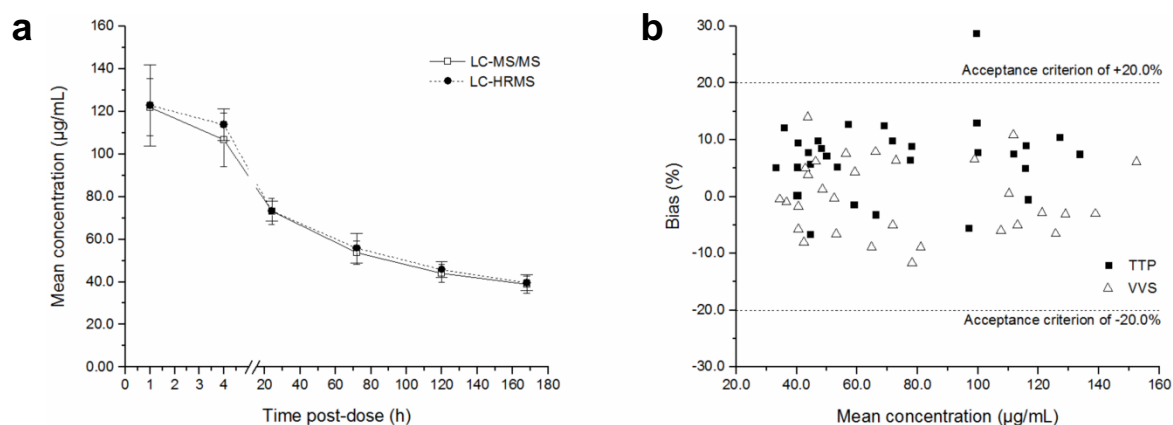
Figure 3.5 Comparison of LC-HRMS and LC-MS/MS analysis using serum samples from five cynomolgus monkeys, dosed intravenously with a hIgG1-related therapeutic protein at 5.00 mg/kg. (**a**) Mean concentration-time profile of serum samples (n=30) using the mean concentration of the TTP and VVS peptides and (**b**) Bland-Altman plot displaying the bias *versus* mean concentration from both assays for each generic peptide.

3.1.4 Conclusions

A generic targeted LC-HRMS approach based on TOF-MRM was developed for bottom-up hIgG quantification in pre-clinical species. This approach provided consistent quantitative data for spiked serum and pre-clinical study samples with regard to linearity, accuracy, and precision. Furthermore, the obtained TOF-MRM-based results were comparable with corresponding data from SRM-based analysis using a QqQ mass analyzer over the same calibration range (1.00-1000 µg/mL). In one case (VVS peptide), however, superior selectivity and hence sensitivity (S/N ratio) was obtained due to the high-resolution of the QTOF, enabling the selection of the most appropriate isotope for quantification. Additionally, LC-HRMS was demonstrated to be a valuable and supportive tool for bottom-up method development as exemplified with the elucidation of the peptide deamidation site. Lastly, the extended mass range of HRMS instruments allow mAb-related therapeutic protein quantification at subunit or intact level as outlined in the next chapter.

3.1.5 Scientific communications

The work described in this chapter was published and presented on several occasions.

Peer-reviewed scientific article:

Lanshoeft C *et al*. The use of generic surrogate peptides for the quantitative analysis of human immunoglobulin G1 in pre-clinical species with high-resolution mass spectrometry. *Anal Bioanal Chem*, 2016, 408(6), 1687-1699. Copyright 2016, reprinted with permission from Springer.

Poster presentation:

Lanshoeft C, Wolf T, Heudi O, Cianférani S, Barteau S, Walles M, Doering KB, Béchade G, Picard F, Kretz O. *The use of generic surrogate peptides for the quantitative analysis of hIgG1 in pre-clinical species with high-resolution mass spectrometry*. 64th Annual ASMS Conference on Mass Spectrometry and Allied Topics, Jun 5-9th 2016, San Antonio (TX, USA).

Oral presentation:

Quantitative analysis of biotherapeutics in pre-clinical species by LC-HRMS either at the peptide or directly at the intact protein level. 1st Quantitative HRMS Workshop, May 16th 2017, Muttenz (Switzerland).

The use of generic surrogate peptides for the quantitative analysis of hIgG in pre-clinical species with high-resolution mass spectrometry. Waters ASMS Users' Meeting, Jun 4th 2016, San Antonio (TX, USA).

Quantitative analysis of hIgG1-based therapeutic proteins in pre-clinical species with LC-HRMS using generic surrogate peptides. Waters MS Technology Day, Oct 21st 2015, Lausanne (Switzerland).

RESEARCH PAPER

The use of generic surrogate peptides for the quantitative analysis of human immunoglobulin G1 in pre-clinical species with high-resolution mass spectrometry

Christian Lanshoeft[1,2] · Thierry Wolf[1] · Olivier Heudi[1] · Sarah Cianférani[2] · Samuel Barteau[1] · Markus Walles[1] · Franck Picard[1] · Olivier Kretz[1]

Abstract In the present study, the application of a liquid chromatography high-resolution mass spectrometry (LC-HRMS) analytical assay for the quantitative analysis of a recombinant human immunoglobulin G1 (hIgG1) in rat serum is reported using three generic peptides GPSVFPLAPSSK (GPS), TTPPVLDSDGSFFLYSK (TTP), and VVSVLTVLHQDWLNGK (VVS). Moreover, the deamidation site of a fourth peptide FNWYVDGVEVHNAK (FNW) was identified and further excluded from the assay evaluation due to the inaccuracy of the quantitative results. The rat serum samples were spiked with a fully labeled hIgG1 as internal standard (ISTD). The digestion with trypsin was performed onto the pellet prior to peptide analysis by LC-HRMS using a quadrupole time of flight (QTOF) mass analyzer operating in selected reaction monitoring (SRM) mode with enhanced duty cycles (EDC). The assay linearity for the three investigated peptides was established for a hIgG1 (hIgG1A) from 1.00 to 1000 µg mL^{-1} with a mean coefficient of determination (R^2) higher than 0.9868. The inter-day accuracy and precision

obtained in rat serum over 3 days were ≤11.4 and ≤10.5 %, respectively. Short-term stability on the auto-sampler at 6 °C for 30 h, at RT for 48 h, and a 100-fold dilution factor were demonstrated. In addition, QC samples prepared in cynomolgus monkey serum and measured with the present method met the acceptance criteria of ±20.0 and ≤20.0 % for all three peptides regarding accuracy and precision, respectively. The LC-HRMS method was applied to the analysis of samples from five individual cynomolgus monkeys dosed with a second hIgG1 (hIgG1B) and consistent data were obtained compared to the LC-MS/MS method (conventional triple quadrupole (QqQ) mass analyzer operating in SRM). The present data demonstrate that LC-HRMS can be used for the quantitative analysis of hIgG1 in both species and that quantification is not only limited to classical QqQ instruments.

Introduction

The analysis of therapeutic proteins in complex biological matrices by liquid chromatography coupled to tandem mass spectrometry (LC-MS/MS) has emerged during the last years in the field of bioanalysis as an alternative to conventional ligand binding assays [1–5]. In this respect, several bioanalytical groups have reported the use of mass spectrometry-based methods for the quantitative analysis of different type of proteins including high molecular weight proteins such as monoclonal antibodies (mAb) [6–8], chimeric mAbs [9], antibody-drug conjugates [10], or PEGylated proteins [11–13] as well as smaller proteins/peptides such as the parathyroid hormone, insulin analogues or prion proteins

[14–16]. More recently, universal analytical assays for the quantification of mAbs in pre-clinical species using generic peptides originating from the human fragment crystallizable (Fc) region were extensively developed [17–19]. Nowadays, the majority of quantitative assays for protein analysis are still routinely performed (similar to small molecules) with LC systems hyphenated to triple quadrupole (QqQ) mass analyzers operating in selected reaction monitoring (SRM) acquisition mode due to their high specificity, dynamic range and ease of operation [20–22]. The selection of one or more surrogate peptides after trypsin digestion is the most common approach in proteomics for quantification of a whole protein in various matrices. Although LC-MS/MS provides great selectivity and sensitivity, interferences from other generated tryptic peptides in complex matrices (serum or plasma) at the retention time of the surrogate peptide(s) of interest cannot be excluded, even though appropriate sample cleanup strategies such as solid phase extraction (SPE) can reduce the sample complexity [23]. As a result, an increased lower limit of quantification (LLOQ) is generally observed due to high background noise during the quantitative analysis of a specific protein.

The use of high resolution mass spectrometry (HRMS) performed on quadrupole time of flight (QTOF), orbitrap or Fourier transform ion cyclotron resonance (FTICR) mass analyzers is a promising way to improve the method selectivity for the quantitative analysis [24–26]. The high mass accuracy between 0.1 and 5.0 ppm as well as the highly resolved isotopic pattern with a resolution ranging from 25,000 to 1,000,000 (depending on the type of HRMS instrument) are the major advantages compared to conventional LC-MS/MS.

General limitations associated in the past with HRMS instruments can nowadays be overcome to comply with a reliable quantitation since the new generation of HRMS instruments exhibit enhanced acquisition speed, increased sensitivity, and linear dynamic range [27].

Recently, the use of HRMS for the quantification of small molecules and larger peptides in human plasma was successfully demonstrated [28, 29]. Moreover, the selectivity of HRMS methods has been improved by decreasing the background in complex human plasma resulting in a better signal to noise (S/N) ratio [30]. Mekhssian et al. [31] analyzed a mAb quantitatively in human plasma over a calibration range from 1.00 to 200 µg mL^{-1} using a LC system coupled to a TripleTOF™ 5600 mass spectrometer.

The present study aims at exploring the capabilities of HRMS for the quantitative analysis of human immunoglobulin G1 (hIgG1) in pre-clinical species. The development of a generic LC-HRMS method for the quantification of a hIgG1 in rat serum is described using pellet digestion as sample preparation combined with HRMS detection of generic peptides. In the quantitative data obtained on three different days, the dynamic ranges and LLOQs for the selected peptides were determined. Furthermore, the method developed in rat serum was applied to the quantitative analysis of another hIgG1 in cynomolgus monkey serum.

Material and methods

Chemicals and reagents

The recombinant hIgG1A used for the preparation of calibration standards (Cs) and quality control (QC) samples, hIgG1B (pre-clinical study samples), and the stable isotope-labeled protein internal standard (ISTD, hIgG1C) were produced at Novartis Pharma AG (Basel, Switzerland). The latter was labeled with [^{13}C]-lysine/arginine moieties using the stable isotope labeling with amino acids in cell culture (SILAC) approach. The reference peptides GPSVFPLAPSSK (GPS), TTPPVLDSDGSFFLYSK (TTP), and VVSVLTVLHQDWLNGK (VVS) used for MS tuning and SPE optimization were synthesized by Thermo Fisher Scientific (Ulm, Germany). Phosphate buffered saline (PBS; 12.0 mM phosphate, 137 mM sodium chloride, 2.70 mM potassium chloride, pH 7.4) and formic acid (FA) were purchased from Amresco (Solon, OH, USA) and Merck (Darmstadt, Germany), respectively. Sodium iodide and leucine enkephalin solutions were obtained from Waters (Milford, MA, USA). DL-Dithiothreitol (DTT), iodoacetamide (IAA), ammonium bicarbonate (ABC), bovine pancreas trypsin, trifluoroacetic acid (TFA), acetic acid, ammonium hydroxide (NH$_4$OH, 28–30 %), acetonitrile (ACN), methanol (MeOH), and MS grade water were provided by Sigma-Aldrich (Buchs, Switzerland). All solvents (LC-MS grade) as well as reagents were of high analytical grade (≥99 %) and were used without further purification. The drug-free batches of rat and cynomolgus monkey sera used for the preparation of Cs and QC samples were delivered from Fisher Clinical Services (Allschwil, Switzerland).

Preparation of Cs and QC samples with hIgG1A

Working solutions were prepared by serial dilution of hIgG1A stock solution (20.0 mg mL^{-1} in PBS, storage at 2–8 °C) into PBS. Subsequently, the resultant solutions were spiked into blank rat serum (1:20, v/v) yielding in nine Cs concentrations of 1.00, 5.00, 10.0, 20.0, 50.0, 200, 500, 800, and 1,000 µg mL^{-1} as well as four QC levels at 3.00, 15.0, 450, and 750 µg mL^{-1}. Additionally, one set of hIgG1A QC samples was prepared with the same concentration levels for the method cross-check in cynomolgus monkey serum.

Pre-clinical study samples from cynomolgus monkey with hIgG1B

A single dose of hIgG1B (5.00 mg kg^{-1}) was administrated intravenously (i.v.) to five different female cynomolgus monkeys. Blood samples were taken at designated time points (pre-dose, 1, 4, 24, 72, 120, and 168 h post-dose). At each sampling time point, approximately 2.0 mL of blood was drawn into tubes containing no anticoagulant and was allowed to clot at room temperature for at least 30 min. Subsequently, the samples were centrifuged for 10 min at 1,500×g and 4 °C. The resulting serum was aliquoted (200 μL) and stored ≤−70 °C pending analysis. The pre-clinical study was conducted in compliance with the Animal Welfare Act, the Guide for the Care and Use of Laboratory Animals, the Office of Laboratory Animal Welfare, and in accordance with the Novartis Animal Care and Use Committee (NACUC).

Sample preparation

The sample preparation protocol was slightly modified from the one published by Ouyang et al. [32]. Briefly, 50 μL of serum either from study samples, Cs, QC, or blank samples was pipetted in a 2.0-mL Protein LoBind 96-well plate from Eppendorf (Hamburg, Germany). Then, 50 μL of ISTD solution at 20.0 μg mL^{-1} in 100 mM ABC in water was added, whereas for blank samples, 50 μL of 100 mM ABC in water was added instead. Zero samples referred to a later stage in this paper are blank samples spiked with ISTD. Afterwards, 20 μL of 100 mM DTT prepared in water was added to each well in order to reduce intra- and inter-disulfide bonds by incubating the samples on a ThermoMixer for 60 min at 60 °C. Subsequently, resulting free thiol groups were alkylated by pipetting 10 μL of 100 mM IAA in water into the plate being incubated at room temperature for 30 min in darkness. For the generation of the pellet, 400 μL of MeOH was added to the samples. The resulting samples were mixed using a ThermoMixer and centrifuged at 4 °C for 5 min at 900×g. The supernatant was removed by inverting the plate on a blotter, and the pellet was re-suspended in 200 μL of 200 mM ABC buffer in 10 % MeOH. A volume of 50 μL of trypsin at 8.00 mg mL^{-1} in 100 mM ABC in water was added to each sample, and the digestion was performed for 1 h at 60 °C. The digestion process was terminated by the addition of 50 μL 15 % TFA. The samples were centrifuged at 900×g for 5 min at 4 °C. An off-line SPE was performed by passing 250 μL of the digested sample through an Oasis MCX 96-well plate (30 mg, 60 μm) from Waters (Milford, MA, USA) being pre-washed two times with 1.0 mL of ACN followed by 2×1.0 mL of 1 % acetic acid. After loading, the cartridges were washed once with 1.0 mL ACN/1 % acetic acid (50:50, v/v). Finally, the peptides were eluted with 900 μL NH$_4$OH/ACN/water (10:70:20, $v/v/v$) into a clean 1.0 mL Protein

LoBind 96-well plate. The eluent was evaporated to dryness under a stream of nitrogen at 60 °C. The samples were reconstituted in 100 μL of 0.1 % FA in ACN/water (10:90, v/v) followed by centrifugation for 5 min at 4 °C and 900×g prior to LC-MS analysis.

LC-HRMS

Chromatographic separation of the tryptic peptides was achieved with an ACQUITY UPLC I-Class system from Waters (Milford, MA, USA). Twenty microliters of sample was loaded on an ACE C$_{18}$, 150 × 4.6 mm, 3 μm column from Hichrom (Berkshire, UK) which was maintained at 60 °C. The flow rate was set to 1.0 mL min^{-1}. The mobile phases consisted of 0.1 % FA in water (A) and 0.1 % FA in ACN (B) with an optimized elution gradient program set as follows: 0.0–1.0 min, 5 % B; 1.0–1.5 min, 5–20 % B; 1.5–7.0 min; 20–35 % B; 7.0–8.0 min, 35–90 % B; 8.0–10.0 min, 90 % B; 10.0–10.5 min, 90–5 % B; 10.5–13.0 min, 5 % B.

The UPLC system was hyphenated to a SYNAPT G2-Si HD high-resolution mass spectrometer from Waters (Milford, MA, USA) whereas the effluent was split (MS/Waste, 1:8, v/v) prior to MS detection. The peptides were ionized with a Zspray™ ion source using electrospray ionization (ESI) in positive mode. The MS was operating in TOF-SRM (sensitivity mode) with enhanced duty cycles (EDC) resulting in a resolution of 20,000 at full width at half maximum (FWHM). The parameters were as follows: mass range m/z 400–1500, capillary voltage 2.2 kV, source temperature 120 °C, sampling cone voltage 50 V, cone gas flow 25 L h^{-1}, desolvation temperature 300 °C, the flow rate of desolvation gas (N$_2$) 1000 L h^{-1}. The optimized TOF-SRM parameters for each peptide including the m/z values for the selected precursor and the most abundant fragment ions as well as their identification and charge states are summarized in Table 1. The asterisk indicates the enhanced fragment for each peptide. The quadrupole mass isolation window for the precursor selection was 1 Da (low and high mass resolution set to 15 arbitrary units). An ion current extraction window (XIC) of 50 mDa was used for the fragment ions to reconstruct the chromatograms. The difference between exact (theoretical) and accurate (experimental) m/z values for the selected product ions was usually on the third decimal even though the m/z ratios were reported with four decimals. This was in agreement with the observed mass accuracy of the QTOF mass analyzer since the mass accuracy achieved upon calibration with sodium iodide was below 5 ppm. Leucine enkephalin was used as lock mass during data acquisition.

Data acquisition and processing

The LC-HRMS system was controlled by MassLynx 4.1 whereas peak area integration, construction of the calibration

C. Lanshoeft et al.

Table 1 Summary of optimized TOF-SRM parameters for generic surrogate peptides and their internal standards

Peptide		Mass to charge ratio (m/z)				CE
Amino acid sequence	Abbrev.	Precursor[a] (charge state)	Fragment ions[b] (ion type/charge state)			(eV)
GPSVFPLAPSSK	GPS	593.8 (+2)	418.2296 (y_4^+)	699.4036[e] (y_7^+)	846.4720 (y_8^+)	18
GPSVFPLAPSSK[c]	[$^{13}C_6$]-GPS	596.8 (+2)	424.2498 (y_4^+)	705.4237[e] (y_7^+)	852.4921 (y_8^+)	18
TTPPVLDSDGSFFLYSK	TTP	937.5 (+2)	836.4169[e] (y_{15}^{2+})	-	-	27
TTPPVLDSDGSFFLYSK[c]	[$^{13}C_6$]-TTP	940.5 (+2)	839.4269[e] (y_{15}^{2+})	-	-	27
VVSVLTVLHQDWLNGK	VVS	603.3 (+3)	805.4385[e,d] (y_{14}^{2+})	712.3883 (y_{12}^{2+})	655.8462 (y_{11}^{2+})	16
VVSVLTVLHQDWLNGK[c]	[$^{13}C_6$]-VVS	605.3 (+3)	808.4485* (y_{14}^{2+})	715.3983 (y_{12}^{2+})	658.8563 (y_{11}^{2+})	16
VVSVLTVLHQDWLDGK	VVSd	603.7 (+3)	805.9305[e] (y_{14}^{2+})	712.8803 (y_{12}^{2+})	656.3382 (y_{11}^{2+})	16
VVSVLTVLHQDWLDGK[c]	[$^{13}C_6$]-VVSd	605.7 (+3)	808.9405[e] (y_{14}^{2+})	715.8903 (y_{12}^{2+})	659.3483 (y_{11}^{2+})	16

CE Collision energy

[a] Quadrupole mass isolation window of 1 Da for precursor selection

[b] fragment ion current extraction window of 50 mDa

[c] labeled with [$^{13}C_6$]-lysine

[d] interference in rat serum

[e] fragment selected for enhancement

curve, and the back-calculation of the concentrations were performed with TargetLynx XS from Waters (Milford, MA, USA). Graphical illustration was conducted with OriginPro (version 9.1.0) from OriginLab Coorperation (Northhampton, MA, USA).

Evaluation of analytical assay performance

Selectivity

The selectivity of the method was determined by comparing the mean apparent analytical response for each peptide at the expected retention time and measured SRM transition(s) in blank samples (three different batches per species) relative to the peptide signal at the LLOQ. The comparison between the mean peak area at the SRM transition(s) of the surrogate peptide in a zero sample relative to the mean analytical response obtained for the surrogate peptide at the LLOQ was used to assess potential contribution of [$^{13}C_6$]-labeled peptide to the light version of the peptide. The contribution of surrogate peptide to heavy labeled version of the peptide was assessed by comparing the mean analytical response for [$^{13}C_6$] peptide in a blank sample spiked with the protein at the upper limit of quantification (ULOQ) to the mean analytical response obtained for zero samples. The acceptance criterion for each

peptide was set to ≤20.0 % of the analytical response at the LLOQ and for the heavy labeled peptides ≤5.0 % of the analytical response at the working concentration of the ISTD.

Linearity and sensitivity

Calibration curves (in duplicate on each day) were constructed using a quadratic mathematical model ($y = ax^2 + bx + c$) with a weighting factor of $1/x^2$ to calculate the concentrations where y represented the peak area ratio of the response for the peptide to the response of [$^{13}C_6$]-lysine labeled peptide version and x was the nominal concentration of the protein in the Cs samples. The acceptance criteria were ±20.0 % (±25.0 % at the LLOQ and ULOQ) for 75.0 % of the Cs from nominal values (with a minimum of six different levels). Additionally, at least 50.0 % of the Cs tested at each concentration level should meet the abovementioned acceptance criteria and the derived coefficient of determination (R^2) should be at least 0.95. The lowest concentration meeting the acceptance criteria of ±25.0 and ≤25.0 % regarding accuracy and precision was set as the LLOQ.

Carry-over

A series of three blank samples were injected in one run directly after the ULOQ sample at 1000 μg mL^{-1} to evaluate

any carry-over. The extent of carry-over should be ≤20.0 % of the response of the tryptic peptide observed at the LLOQ and ≤5.0 % of the response observed for the corresponding isotopically labeled peptide at the working concentration of the ISTD.

Accuracy and precision

The accuracy of the analytical assay was evaluated by the deviation (% bias) from the nominal value of at least three QC concentration levels (3× LLOQ, mid and high) whereas the percentage of the coefficient of variation (CV) determined the precision of the method. Each QC level was analyzed in triplicate on each day to evaluate the intra-day accuracy and precision whereas in total nine replicates from three different days were utilized to calculate the inter-day accuracy and precision. A mean bias within ±20.0 % of the nominal values and a precision of ≤20.0 % were set as acceptance criteria.

Dilution

In case pre-clinical samples exhibit a higher concentration than the ULOQ, an appropriate dilution factor has to be assessed. Thus, an additional QC sample at five times the ULOQ was prepared and diluted 100-fold with blank rat serum in replicates of five resulting in a nominal concentration of 50.0 μg mL^{-1}. The back-calculated mean concentration (with the dilution factor incorporated) should be ±20.0 % of the initial concentration with a precision ≤20.0 %. Additionally, three out of five individual concentrations should meet the acceptance criteria.

Stability

The protein stability during this method evaluation was assessed with two QC levels (15.0 and 750 μg mL^{-1}) at room temperature for a period of 48 h. Stability on the auto-sampler of the generated peptides was investigated at 6 °C for two storage periods (16 and 30 h). After storage, the samples were measured against a freshly prepared calibration curve including an independent set of QC samples. The stability was deemed acceptable if the deviation from the initial concentration was ±20.0 %. Stability data of the mAb bulk material and stock solution were evaluated previously and were not part of this investigation.

Method comparison with LC-MS/MS

Analytical method comparison between LC-HRMS and an existing LC-MS/MS assay was performed on in vivo samples from a toxicokinetic study. The LC-MS/MS system consisted of a Symbiosis Pro from Spark Holland B.V (Emmen, Netherlands) equipped with a Reliance unit (conditioned

stack and auto-sampler) and a Mistral column oven coupled to an API 6500 QTRAP mass spectrometer controlled by Analyst 1.6 from Applied Biosystems (Foster City, CA, USA). The sample preparation was similar to the one described in section Sample preparation. A detailed description of the LC-MS/MS parameters is summarized in the Electronic Supplementary Material (ESM, Table S1).

Results and discussion

Surrogate peptide selection

Besides the light and the heavy chain, the structure of antibodies can be further subdivided into variable and constant regions. The latter is only suitable for a universal MS-based assay in pre-clinical species as the majority of the amino acid sequence is conserved over all human antibodies exhibiting common peptides after tryptic digestion, whereas the former contains antibody specific peptides located in the complementarity determining region (CDR) being responsible for specific target binding. For the identification of conserved peptides, the amino acid sequences of the Fc region from several mAbs were aligned with each other and an in-silico digestion was performed. Fifteen common peptides were identified and were further selected by the following criteria: (1) oxidation sites such as methionine (M), cysteine (C), or tryptophan (W) should be avoided if possible; (2) peptides with glycosylation sites on nitrogen (NxS and NxT, whereas x can be any amino acid except proline (P), serines (S), or threonines (T)) [33], on oxygen (S and T rich domains) [34], or carbon-linked motifs (WxxW, WS/TC) [35, 36] were excluded; (3) if P was located downstream from lysine (K) or arginine (R) as well as two basic amino acids were located next to each other (RR, KK, or RK), the peptides were not taken into account to prevent miscleavage of peptides; and (4) the peptide should have at least 8 amino acids and its isoelectric point should not be too high or too low to guarantee adequate retention under reversed-phase chromatographic conditions. Out of the initial 15 peptides GPS (from the C$_H$1 region), TTP (from the C$_H$3 region) and two peptides from the C$_H$2 region (FNW and VVS) were identified as candidates for the generic assay development.

Deamidation site in both C$_H$2 peptides

During kinetic studies of the digestion, a decrease in signal intensity for both C$_H$2 peptides was observed, whereas two additional peaks were generated during overnight digestion at 37 °C. Chelius et al. [37] identified several amino acid motifs causing deamidation on asparagine (N) via a cyclic intermediate state (succinimide) to isoaspartic (isoD) and aspartic acid (D) under certain temperature and pH conditions. As a result,

two additional peaks with a ratio of approximately 1:3 appear over time [38]. It has been shown that the LNG motif in the VVS peptide is subjected for deamidation [39]. Concerning the FNW peptide, the motif FNW and HNA are likely to be deamidated, but occurrence is less prone. In order to confirm the potential deamidation of the FNW peptide, the ion chromatogram of the single deamidated form was extracted from the full scan resulting in the appearance of two additional peaks with a retention time shift of 0.15 and 0.35 min from the unmodified FNW.

In addition, the MS/MS data obtained on the precursor ion of the FNW peptide (*m/z* 559.9373) showed that all y-fragment ions (beyond the y_{11}^+ ion) from the isoaspartic acid (Fig. 1a) and aspartic acid forms (Fig. 1b) differ by approximately 1 Da in mass in comparison with the non-deamidated

form (Fig. 1c). The same experiments were performed on the doubly deamidated versions, but no additional peaks were identified. Thus, the FNW peptide underwent a single deamidation on the C-terminal asparagine in the HNA motif. The three individual chromatographic peaks of the FNW peptide that originated from the deamidation could not be combined in a single peak under the selected conditions. As a result of inadequate peak integration, inaccurate quantitative data with the FNW peptide was observed. Consequently, this peptide was not included in the final method.

Selection of QTOF quantification mode

Three different acquisition modes were assessed for quantitative purposes with the SYNAPT G2-Si HD HRMS

Fig. 1 MS/MS spectra of **a** isoaspartic acid, **b** aspartic acid, and **c** non-deamidated isoform of the FNWYVDGVEVHNAK precursor at *m/z* 559.9373 to determine deamidation site
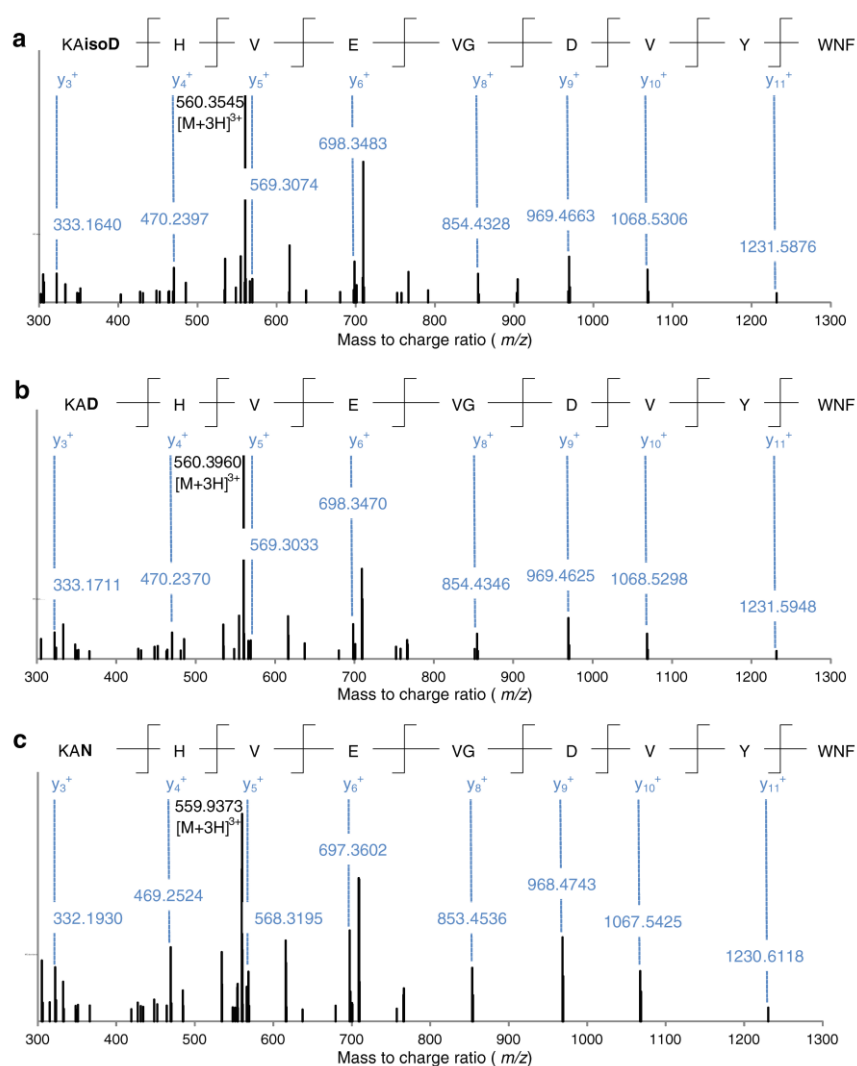
QTOF instrument (i) TOF-MS, (ii) TOF-MS/MS, and (iii) TOF-SRM. The general advantages and working principles for each mode were previously reported by Morin et al. [29], whereas the modes used with their TripleTOF™ 5600 instrument were entitled TOF-MS, $SRM^{HR/HS}$, and SRM^{HS} enhance. In the first acquisition mode, quantification was performed by extracting the accurate mass of the analyte of interest from the full scan. This resulted in high signal intensities for each surrogate peptide as no signal was lost due to fragmentation (Table 2). However, sensitivity was affected as well since high additional background noise was obtained in full scan mode resulting in low S/N ratios (peak to peak model) ranging from 7–42. In TOF-MS/MS, a precursor was selected by the quadrupole and fragmented in the collision cell. Subsequently, a single or multiple product ion(s) was/were used for quantitative purposes. Although the signal intensities in TOF-MS/MS were not as high as in TOF-MS due to possible distribution of the signal over several product ions, the resultant S/N ratios were significantly improved (up to 24-fold increase with the TTP peptide) as the chemical noise decreased. The working principle of TOF-SRM is in general based on TOF-MS/MS. However, the pusher region of a TOF analyzer was synchronized with the release of one specific product ion for each analyte from the TWave™ collision cell allowing maximum transmission. As a result, TOF-SRM with maximized duty cycles for a specific m/z range gave similar signal intensities compared to TOF-MS, whereas the S/N ratios were comparable to the TOF-MS/MS mode. This trend was consistent for each surrogate peptide and was also in agreement with the results for other peptides reported by Morin et al. [29]. This demonstrated that TOF-SRM increased not only selectivity but also sensitivity of the analytical method.

Selectivity improvement using the monoisotopic $[M+2H]^{2+}$ ion of the VVSd y_{14}^{2+} fragment ion

Since the deamidation of the VVS peptide was expected during the tryptic digestion process, six fragment ions covering the non-deamidated (VVS) and deamidated isoform (VVSd) were included for the quantitative analysis (Table 1). As the mass difference of the triply charged precursor for both isoforms was approximately 0.3 Da, the quadrupole could also not distinguish between the corresponding precursor for each isoform due to the mass isolation window of 1 Da. During selectivity investigations, an interfering peak was found in the extracted ion chromatogram using the exact (theoretical) m/z ratio of six fragments (three from each isoform) in blank rat serum (Fig. 2a). The MS/MS spectrum of the interfering peak revealed a doubly charged fragment originating from an unknown endogenous compound with a monoisotopic $[M+2H]^{2+}$ ion at m/z 804.4498, a $[(M+1)+2H]^{2+}$ ion at m/z 804.9492 and a $[(M+2)+2H]^{2+}$ ion at m/z 805.4466 (Fig. 2b). The interference was caused by the $[(M+2)+2H]^{2+}$ ion being close to the exact monoisotopic mass of the VVS y_{14}^{2+} fragment at m/z 805.4385. The advantage of HRMS in the SRM acquisition mode compared to classical QqQ instruments is that the isotopic pattern of a given compound is highly resolved offering the possibility to select the most appropriate m/z value for quantification. Hence, the interference could significantly be reduced by excluding the y_{14}^{2+} fragment of the VVS peptide at m/z 805.4385 during chromatogram extraction (Fig. 2c). As the $[(M+1)+2H]^{2+}$ ion of the VVS fragment at m/z 805.9353 represented 91.6 % of the signal intensity of its monoisotopic y_{14}^{2+} product ion at m/z 805.4349 (Fig. 2d), no significant loss of sensitivity was observed by excluding the $[M+2H]^{2+}$ ion of the VVS peptide. The reason was that both isoforms were still extracted with a XIC window of 50 mDa as the accurate mass of the $[(M+1)+2H]^{2+}$ ion of the VVS y_{14}^{2+} fragment at m/z 805.9353 (Fig. 2d) differed by approximately 9 mDa compared to the accurate mass of the selected $[M+2H]^{2+}$ ion of the VVSd y_{14}^{2+} product ion at m/z 805.9268 (Fig. 2f). Both isoforms were not fully baseline separated using in total five fragments and the retention time of VVS and VVSd was at 7.1 and 7.4 min, respectively (Fig 2e). This example demonstrated how HRMS can be used to solve selectivity issues in complex matrices.

Peptide	TOF-MS		TOF-MS/MS		TOF-SRM	
	Peak area (counts)	S/N ratio[a]	Peak area (counts)	S/N ratio[a]	Peak area (counts)	S/N ratio[a]
GPS	18774	17	9576	138	19102	159
TTP	24403	7	13109	171	52329	142
VVS	151583	42	45552	132	178803	134

Table 2 Peak areas and corresponding signal to noise (S/N) ratios of three generic peptides using different acquisition modes

[a] S/N ratio was determined with the MassLynx software (version 4.1) using the peak to peak model

Fig. 2 Selectivity improvement for VVS peptide in rat serum by using the $[M+2H]^{2+}$ ion of the deamidated VVS y_{14}^{2+} fragment instead of the $[M+2H]^{2+}$ ion of the non-deamidated VVS y_{14}^{2+} fragment. **a** extracted chromatogram of blank rat serum using three fragments from each isoform, **b** MS/MS spectrum from interfering peak showing interference from the $[(M+2)+2H]^{2+}$ ion at m/z 805.4466 of an unknown endogenous compound in rat serum, **c** extracted chromatogram of blank rat serum after exclusion of VVS y_{14}^{2+} fragment , **d** MS/MS spectrum (zoom into m/z 803–810) of the triply charged non-deamidated VVS precursor ion at m/z 603.3, **e** extracted chromatogram of both VVS isoforms (in total five fragments) generated from hIgG1A spiked in rat serum at 10.0 μg mL^{-1}, and **f** MS/MS spectrum (zoom into m/z 803–810) of the triply charged deamidated VVS precursor ion at m/z 603.7
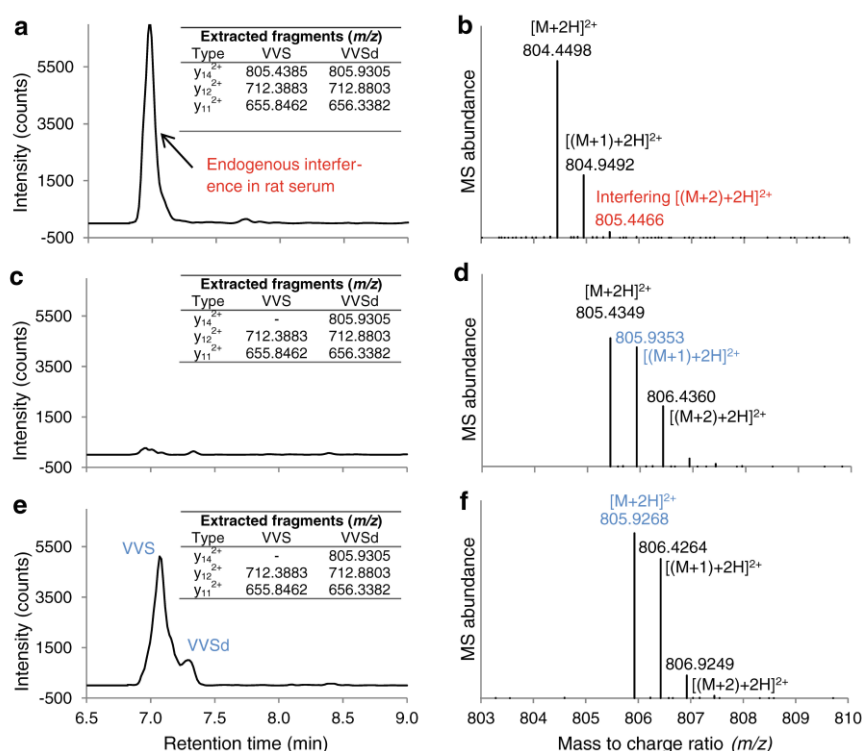
Evaluation of analytical assay performance

Selectivity

The mean percentage of the endogenous interference for TTP was 3.4 ± 1.4 %, VVS resulted in an interference below 7.3 % by using the $[M+2H]^{2+}$ ion of the VVSd y_{14}^{2+} fragment as described in the previous section, whereas no endogenous interference was detected for GPS for rat serum using three different batches (ESM, Table S2). Moreover, the interferences detected on the SRM transitions for the isotopically labeled peptides were for TTP and VVS below 0.2 and 0.4 %, respectively. Only for $[^{13}C_6]$-GPS, the interference was slightly higher with maximum 1.8 %. The working concentration of the stable isotope-labeled protein internal standard was set to 20.0 μg mL^{-1} to fulfill the acceptance criterion regarding the ISTD contribution to the surrogate peptide signal. No significant contribution of the analyte to the signal of the heavy peptides was observed. As the acceptance criteria were fulfilled, it was demonstrated that the analytical method was not only highly selective for the generic tryptic peptides but also for their $[^{13}C_6]$-lysine labeled versions in rat serum. The only interferences at the LLOQ of 1.00 μg mL^{-1} in cynomolgus monkey serum was caused by the SRM transitions of the GPS peptide confirming the results by Zhang et al. [23].

Consequently, the GPS peptide is not suitable for the quantitative analysis in cynomolgus monkey serum with a LLOQ of 1.00 μg mL^{-1}.

Linearity and sensitivity

The slope of the calibration curve reached a plateau with higher concentrations (>800 μg mL^{-1}) especially with the TTP surrogate peptide. The calibration curves were described more adequately by a quadratic instead of a linear regression model with a weighting factor of $1/x^2$ resulting in a better curve fit [better coefficient of determination (R^2) values for each surrogate peptide with good accuracy and precision data over the anticipated calibration range]. The resultant R^2 values obtained over 3 days ranged from 0.9868 to 0.9911 for the three surrogate peptides (Table 3). For two out of three generic peptides, the highest inter-day precision with a maximum of 14.8 % was observed at 1.00 μg mL^{-1} whereas the accuracy at this concentration ranged from 0.8 to 1.7 %. As this concentration level met the set acceptance criteria of ± 25.0 % and ≤ 25.0 % regarding accuracy and precision, it was set as the LLOQ. The accuracy of the eight remaining concentration levels ranged from -8.2 to 5.2 % for GPS, for TTP from -7.3 to 5.9 % and for VVS from -9.8 to 3.4 %. The precision was below 14.2, 9.5, and 12.4 % for GPS, TTP, and VVS,

The use of generic surrogate peptides   1695

Table 3 Inter-day accuracy and precision for calibration standards (Cs) on three validation days using a quadratic regression in the form of $y = ax^2 + bx + c$ with a weighting factor of $1/x^2$. Coefficient of determination (R^2) was used to assess linearity

Peptide R^2 ($n = 3$)		Cs nominal concentration ($\mu g\ mL^{-1}$) in rat serum								
		1,000	800	500	200	50.0	20.0	10.0	5.00	1.00
		Inter-day accuracy and precision ($n = 6$)								
GPS 0.9868 ± 0.0065	Mean ($\mu g\ mL^{-1}$)	1,022	783	483	206	52.6	19.7	10.1	4.59	1.01
	Inter-day accuracy (% bias)	2.2	−2.2	−3.4	3.2	5.2	−1.3	1.3	−8.2	1.4
	Inter-day precision (% CV)	11.5	13.2	14.2	9.0	7.2	4.5	9.8	7.8	6.3
TTP 0.9911 ± 0.0008	Mean ($\mu g\ mL^{-1}$)	1,002	805	492	203	52.6	19.8	10.6	4.64	1.01
	Inter-day accuracy (% bias)	0.2	0.7	−1.7	1.5	5.2	−1.1	5.9	−7.3	0.8
	Inter-day precision (% CV)	9.3	6.0	8.4	7.5	7.1	7.4	9.5	5.8	14.8
VVS 0.9906 ± 0.0031	Mean ($\mu g\ mL^{-1}$)	1,010	801	486	206	51.7	20.6	10.2	4.51	1.02
	Inter-day accuracy (% bias)	1.0	0.1	−2.8	2.8	3.4	2.8	2.2	−9.8	1.7
	Inter-day precision (% CV)	12.4	8.9	6.5	6.7	5.4	6.0	6.6	4.6	14.1

respectively. Thus, the constructed calibration curves of the surrogate peptides could be used to reliably determine the protein concentration in rat serum in a consistent fashion over the anticipated concentration range suitable for the routine analysis.

Carry-over

No carry-over for all three peptides was found in the second and third blank rat serum sample directly after the injection of a sample at the ULOQ (ESM, Table S3). However, the extent of carry-over for TTP and VVS exceeded in the first blank the acceptance criterion of ≤20.0 % compared to the signal at the LLOQ with 64.8 and 71.2 %, respectively. This result demonstrated that an injection of at least one rinse or blank sample after highly concentrated samples is required prior to low concentration samples to avoid overestimation caused by carry-over.

Accuracy and precision in rat serum

The accuracy and precision for the four QC levels at 3.00, 15.0, 450, and 750 $\mu g\ mL^{-1}$ in three different rat serum batches fulfilled the acceptance criteria. For the investigated peptides, the inter-day accuracy ranged from -5.4 to 11.4 % whereas the precision was between 4.4 and 10.5 % (Table 4). The intra-run bias and precision across three different batches ranged from −13.3 to 16.8 % and 1.3

to 14.5 %, respectively (ESM, Table S4). The results indicated that the developed LC-HRMS method was accurate and precise not only between different serum batches but also within individual batches. As the same inter-peptide concentration values with a variation ≤3.0 % at each QC level (Table 4) were obtained, it was demonstrated that the peptides were generated in a similar fashion during tryptic digestion and that the same concentration values were observed regardless of the tryptic surrogate peptide selected.

Dilution factor

The QC sample at 5.00 mg mL^{-1} was diluted by a factor of 100-fold using blank rat serum resulting in a nominal concentration of 50.0 $\mu g\ mL^{-1}$. The mean back calculated concentration was 5.34 ± 0.31 mg mL^{-1} with a bias and precision ranging from 3.1 to 14.0 % and 1.9 to 6.0 %, respectively (ESM, Table S5). These results indicated that pre-clinical samples exhibiting a higher concentration than the qualified calibration range can be diluted with blank matrix prior to analysis.

Stability

The short-term stability data determined with two QC levels at 750 and 15.0 $\mu g\ mL^{-1}$ (ESM, Table S6) revealed that the recombinant hIgG1A, was stable at room

⌂ Springer

Table 4 Inter-day accuracy and precision of the three generic peptides in spiked rat serum on three different days ($n = 9$)

Peptide		QC nominal concentration ($\mu g\ mL^{-1}$) in rat serum			
		750	450	15.0	3.00
		Inter-day accuracy and precision ($n = 9$)			
GPS	Mean ($\mu g\ mL^{-1}$)	722	435	15.8[a]	2.91
	Inter-day accuracy (% bias)	−3.7	−3.3	5.1	−2.9
	Inter-day precision (% CV)	6.8	4.6	6.0	8.4
TTP	Mean ($\mu g\ mL^{-1}$)	744	434	16.7[a]	3.03[a]
	Inter-day accuracy (% bias)	−0.8	−3.6	11.4	0.9
	Inter-day precision (% CV)	9.2	8.6	4.4	10.5
VVS	Mean ($\mu g\ mL^{-1}$)	722	426	16.4[a]	2.93
	Inter-day accuracy (% bias)	−3.7	−5.4	9.1	−2.5
	Inter-day precision (% CV)	8.7	8.1	7.8	9.8
	Inter-peptide mean ($\mu g\ mL^{-1}$)	730	432	16.3	2.95
	Inter-peptide SD ($\mu g\ mL^{-1}$)	13	5	0.5	0.06
	Inter-peptide precision (% CV)	1.8	1.2	3.0	2.1

[a] $n = 8$, one QC replicate on day 1 was excluded from calculations due to an issue during sample preparation

temperature up to 48 h, since the % bias compared to the expected concentration at t_0 was between −8.6 and 4.8 % depending which peptide was considered. It was further demonstrated that the generated peptides were stable on the auto-sampler after tryptic digestion for at least 30 h, as the calculated mean bias was within ±20.0 % acceptance criterion (GPS ≤9.7 %, TTP ≤4.8 %, and VVS ≤1.7 %).

Accuracy and precision in cynomolgus monkey serum

The question if mAbs can be quantified in a consistent manner when spiked in a different matrix than rat serum was also addressed in our investigations to further expand the method. In this respect, hIgG1A was spiked at four QC concentration levels in cynomolgus monkey serum. Subsequently, the QC concentrations were back-calculated against a calibration curve and an additional set of QC samples prepared in rat serum (Table 5). The resultant accuracies for GPS, TTP, and VVS ranged from −6.9 to 13.0 % fulfilling the acceptance criterion of ±20.0 %. High matrix interference on the SRM transitions of GPS caused inaccurate results at low concentrations in cynomolgus monkey serum with the QqQ instruments reported by Zhang et al. [23]. In contrast, a low bias with −6.9 % was observed with TOF-SRM for the GPS peptide at the low QC level (3× LLOQ) demonstrating its advantage over QqQ instruments. Moreover, the precision with the HRMS method was also within the acceptance criterion of ≤20.0 % ranging from 1.0 to 13.3 %. Only the precision in the GPS sample for the low QC level at 3.00 $\mu g\ mL^{-1}$ exceeded the criterion by 7.1 % and was therefore excluded for the analysis of hIgG1B in cynomolgus monkey samples.

Application to pre-clinical study

The present method was applied to one pre-clinical study including five female cynomolgus monkeys which were dosed i.v. once with the hIgG1B at 5.00 mg kg^{-1}. In total, 35 serum samples were either analyzed by LC-HRMS or with the conventional LC-MS/MS approach. The mean concentration-time profile of five individual monkeys taking the results from both peptides (TTP and VVS) into account was typical for i.v. administration of a therapeutic protein (Fig. 3a). The data found with the GPS peptide were not included in the present comparison due to the high variability in the cynomolgus monkey QC samples. The reason for this high variability remained unknown. No hIgG1B was detected in the pre-dose samples for each individual cynomolgus monkey. The obtained hIgG1B serum concentration-time profiles were identical at each time point regardless the analytical assay. The variation in the mean concentrations of five individual cynomolgus monkeys obtained either with the TTP or the VVS peptide was 2.7 ± 1.7 % CV for the LC-HRMS analysis. In contrast, the variation between both surrogate peptides was slightly increased for the LC-MS/MS assay ranging from 3.7 to 8.5 % CV.

When the individual concentrations for each cynomolgus monkey instead of the mean concentration were considered, no significant deviation was revealed by plotting the mean concentration for each surrogate peptide from the LC-HRMS and LC-MS/MS assay against the bias between both analytical assays (Fig. 3b). The mean bias between both analytical instruments observed with TTP and VVS was 6.5 ± 6.7 and −0.1 ± 6.6 %, respectively. All samples with exception of one sample for TTP were within the acceptance criterion of ±20.0 % (dashed lines). These results indicated that equivalent

Table 5 Accuracy and precision of the three generic peptides in spiked cynomolgus monkey serum ($n = 3$)

Peptide		QC nominal concentration ($\mu g\ mL^{-1}$) in cynomolgus monkey serum			
		750	450	15.0	3.00
		Accuracy and precision[a] ($n = 3$)			
GPS	Mean ($\mu g\ mL^{-1}$)	778	497	14.8	2.79
	Accuracy (% bias)	3.7	10.4	−1.5	−6.9
	Precision (% CV)	2.5	13.0	4.4	27.1[b]
TTP	Mean ($\mu g\ mL^{-1}$)	745	452	16.9	3.20
	Accuracy (% bias)	−0.6	0.4	13.0	6.6
	Precision (% CV)	11.5	13.3	4.2	4.4
VVS	Mean ($\mu g\ mL^{-1}$)	745	466	16.7	2.89
	Accuracy (% bias)	−0.7	3.6	11.3	−3.7
	Precision (% CV)	7.7	9.2	1.0	5.8

[a] Measured against Cs prepared in rat serum, [b] acceptance criterion of ≤20.0 % CV not met
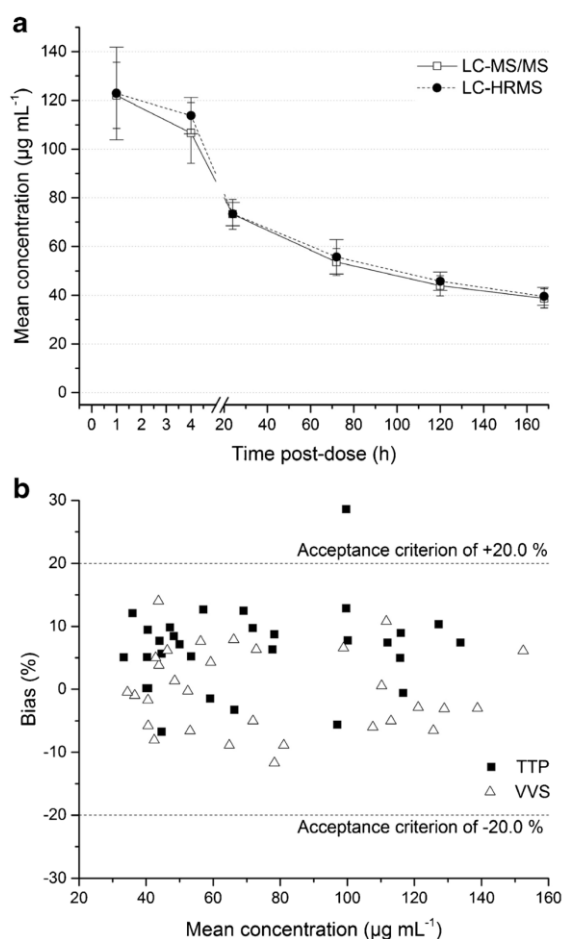
Fig. 3 a Mean concentration-time profile of pre-clinical cynomolgus monkey serum samples analyzed with LC-HRMS and LC-MS/MS ($n = 30$) and **b** bias versus mean concentration of both assays for individual peptides (TTP and VVS) including ±20.0 % acceptance criterion (*dashed lines*)

data was generated on both platforms regardless of the peptide selected. Thus, the developed LC-HRMS method was quantifying the hIgG1B in a reliable fashion as already demonstrated with QC samples in cynomolgus monkey serum and could be used as an alternative to conventional analytical assays using QqQ mass analyzers.

Conclusion

The application of HRMS instruments in the field of qualitative proteomics provides valuable information regarding drug-antibody ratios or the determination of various glycan forms of a mAb. However, therapeutic proteins can also be quantified in a reliable fashion with HRMS instruments using the bottom-up approach as demonstrated. Consequently, the combination of qualitative/quantitative approaches in targeted and non-targeted analysis by one single instrument has a significant impact and opens new opportunities to the pharmaceutical industry to support pre-clinical and clinical studies during their drug development process of biotherapeutics in a regulated environment. The major advantage associated with HRMS instruments is the highly resolved isotopic pattern which can increase the method selectivity, whereas the same linear range, accuracy, and precision were obtained compared to classical low resolution QqQ mass analyzers widely used for quantification. Thus, more quantitative HRMS methods will be established in the future as quantitative bioanalytical LC-MS based assays are generally no longer limited to QqQ instruments only due to the evolution of recent HRMS instruments. As four different peptides were incorporated in the described method, the approach can easily be adapted to other modalities such as hIgG4, antibody-drug conjugates, or even chimeric/bispecific antibodies based on human immunoglobulin G. Since the samples can be prepared within one working day and the analysis can run overnight by LC-HRMS, a

certain throughput is also associated being an important aspect for pharmaceutical industry.

Compliance with ethical standards The pre-clinical study was conducted in compliance with the Animal Welfare Act, the Guide for the Care and Use of Laboratory Animals, the Office of Laboratory Animal Welfare and in accordance with the Novartis Animal Care and Use Committee (NACUC).

Conflict of interest In case of Christian Lanshoeft, the work was mainly conducted in fulfillment for the degree of Ph.D. from the University of Strasbourg under the academic supervision of Dr. Sarah Cianférani. Novartis Pharma AG completely funded this project financially. The work was performed at the facilities of Novartis only for research purposes and was not related to any Novartis project currently in development.

No relevant affiliations, financial involvement with any organization, entity with a financial interest in or financial conflict with the subject matter was associated with the remaining authors. This includes employment, consultancies, honoraria, stock ownership, expert testimony, grants, patents or royalties.

References

1. An B, Zhang M, Qu J. Toward sensitive and accurate analysis of antibody biotherapeutics by liquid chromatography coupled with mass spectrometry. Drug Metab Dispos. 2014;42(11):1858–66. doi:10.1124/dmd.114.058917.

2. Bults P, van de Merbel NC, Bischoff R. Quantification of biopharmaceuticals and biomarkers in complex biological matrices: a comparison of liquid chromatography coupled to tandem mass spectrometry and ligand binding assays. Expert Rev Proteomics. 2015;12(4):355–74. doi:10.1586/14789450.2015.1050384.

3. Hopfgartner G, Lesur A, Varesio E. Analysis of biopharmaceutical proteins in biological matrices by LC-MS/MS II. LC-MS/MS analysis. Trends Anal Chem. 2013;48:52–61.

4. van den Broek I, Niessen WM, van Dongen WD. Bioanalytical LC-MS/MS of protein-based biopharmaceuticals. J Chromatogr B. 2013;929:161–79. doi:10.1016/j.jchromb.2013.04.030.

5. Zheng J, Mehl J, Zhu Y, Xin B, Olah T. Application and challenges in using LC–MS assays for absolute quantitative analysis of therapeutic proteins in drug discovery. Bioanalysis. 2014;6(6):859–79. doi:10.4155/bio.14.36.

6. Hagman C, Ricke D, Ewert S, Bek S, Falchetto R, Bitsch F. Absolute quantification of monoclonal antibodies in biofluids by liquid chromatography – tandem mass spectrometry. Anal Chem. 2008;80(4):1290–6. doi:10.1021/ac702115b.

7. Heudi O, Barteau S, Zimmer D, Schmidt J, Bill K, Lehmann N, et al. Towards absolute quantification of therapeutic monoclonal antibody in serum by LC-MS/MS using isotope-labeled antibody standard and protein cleavage isotope dilution mass spectrometry. Anal Chem. 2008;80(11):4200–7. doi:10.1021/ac800205s.

8. Ladwig PM, Barnidge DR, Snyder MR, Katzmann JA, Murray DL. Quantification of serum IgG subclasses by use of subclass-specific tryptic peptides and liquid chromatography–tandem mass spectrometry. Clin Chem. 2014;60(8):1080–8. doi:10.1373/clinchem.2014.222208.

9. Willrich MAV, Murray DL, Barnidge DR, Ladwig PM, Snyder MR. Quantitation of infliximab using clonotypic peptides and selective reaction monitoring by LC–MS/MS. Int Immunopharmacol. 2015;28(1):513–20. doi:10.1016/j.intimp.2015.07.007.

10. Myler H, Rangan VS, Wang J, Kozhich A, Cummings JA, Neely R, et al. An integrated multiplatform bioanalytical strategy for antibody-drug conjugates: a novel case study. Bioanalysis. 2015;7(13):1569–82. doi:10.4155/bio.15.80.

11. Dawes ML, Gu H, Wang J, Schuster AE, Haulenbeek J. Development of a validated liquid chromatography tandem mass spectrometry assay for a PEGylated adnectin in cynomolgus monkey plasma using protein precipitation and trypsin digestion. J Chromatogr B. 2013;934:1–7. doi:10.1016/j.jchromb.2013.06.027.

12. Gong J, Gu X, Achanzar WE, Chadwick KD, Gan J, Brock BJ, et al. Quantitative analysis of polyethylene glycol (PEG) and PEGylated proteins in animal tissues by LC-MS/MS coupled with in-source CID. Anal Chem. 2014;86(15):7642–9. doi:10.1021/ac501507g.

13. Liu Q, De Felippis MR, Huang L. Method for characterization of PEGylated bioproducts in biological matrixes. Anal Chem. 2013;85(20):9630–7. doi:10.1021/ac401921z.

14. Kumar V, Barnidge DR, Chen LS, Twentyman JM, Cradic KW, Grebe SK, et al. Quantification of serum 1–84 parathyroid hormone in patients with hyperparathyroidism by immunocapture in situ digestion liquid chromatography-tandem mass spectrometry. Clin Chem. 2010;56(2):306–13. doi:10.1373/clinchem.2009.134643.

15. Peterman S, Niederkofler EE, Phillips DA, Krastins B, Kiernan UA, Tubbs KA, et al. An automated, high-throughput method for targeted quantification of intact insulin and its therapeutic analogs in human serum or plasma coupling mass spectrometric immunoassay with high resolution and accurate mass detection (MSIA-HR/AM). Proteomics. 2014;14(12):1445–56. doi:10.1002/pmic.201300300.

16. Van Dorsselaer A, Carapito C, Delalande F, Schaeffer-Reiss C, Thierse D, Diemer H, et al. Detection of prion protein in urine-derived injectable fertility products by a targeted proteomic approach. PLoS One. 2011;6(3):e17815. doi:10.1371/journal.pone.0017815.

17. Furlong MT, Ouyang Z, Wu S, Tamura J, Olah T, Tymiak A, et al. A universal surrogate peptide to enable LC-MS/MS bioanalysis of a diversity of human monoclonal antibody and human Fc-fusion protein drug candidates in pre-clinical animal studies. Biomed Chromatogr. 2012;26(8):1024–32. doi:10.1002/bmc.2759.

18. Law WS, Genin J-C, Miess C, Treton G, Warren AP, Lloyd P, et al. Use of generic LC–MS/MS assays to characterize atypical PK profile of a biotherapeutic monoclonal antibody. Bioanalysis. 2014;6(23):3225–35. doi:10.4155/bio.14.167.

19. Li H, Ortiz R, Tran L, Hall M, Spahr C, Walker K, et al. General LC-MS/MS method approach to quantify therapeutic monoclonal antibodies using a common whole antibody internal standard with application to preclinical studies. Anal Chem. 2012;84(3):1267–73. doi:10.1021/ac202792n.

20. Gallien S, Duriez E, Domon B. Selected reaction monitoring applied to proteomics. J Mass Spectrom. 2011;46(3):298–312. doi:10.1002/jms.1895.

21. Lebert D, Picard G, Beau-Larvor C, Troncy L, Lacheny C, Maynadier B, et al. Absolute and multiplex quantification of antibodies in serum using PSAQ™ standards and LC-MS/MS. Bioanalysis. 2015;7(10):1237–51. doi:10.4155/bio.15.56.

22. Yost RA, Enke CG. Triple quadrupole mass spectrometry for direct mixture analysis and structure elucidation. Anal Chem. 1979;51(12):1251–64. doi:10.1021/ac50048a002.

23. Zhang Q, Spellman DS, Song Y, Choi B, Hatcher NG, Tomazela D, et al. Generic automated method for liquid chromatography–multiple reaction monitoring mass spectrometry based monoclonal antibody quantitation for preclinical pharmacokinetic studies. Anal Chem. 2014;86(17):8776–84. doi:10.1021/ac5019827.

24. Gallien S, Domon B (2015) Advances in high-resolution quantitative proteomics: implications for clinical applications. Expert Rev Proteomics; 1–10. doi:10.1586/14789450.2015.1069188

25. Gallien S, Domon B. Detection and quantification of proteins in clinical samples using high resolution mass spectrometry. Methods. 2015;81:15–23. doi:10.1016/j.ymeth.2015.03.015.

26. Gallien S, Duriez E, Demeure K, Domon B. Selectivity of LC-MS/MS analysis: implication for proteomics experiments. J Proteomics. 2013;81:148–58. doi:10.1016/j.jprot.2012.11.005.

27. Huang MQ, Lin ZJ, Weng N. Applications of high-resolution MS in bioanalysis. Bioanalysis. 2013;5(10):1269–76. doi:10.4155/bio.13.100.

28. Dillen L, Cools W, Vereyken L, Lorreyne W, Huybrechts T, de Vries R, et al. Comparison of triple quadrupole and high-resolution TOF-MS for quantification of peptides. Bioanalysis. 2012;4(5):565–79. doi:10.4155/bio.12.3.

29. Morin LP, Mess JN, Garofolo F. Large-molecule quantification: sensitivity and selectivity head-to-head comparison of triple quadrupole with Q-TOF. Bioanalysis. 2013;5(10):1181–93. doi:10.4155/bio.13.87.

30. Ramagiri S, Garofolo F. Large molecule bioanalysis using Q-TOF without predigestion and its data processing challenges. Bioanalysis. 2012;4(5):529–40. doi:10.4155/bio.12.10.

31. Mekhssian K, Mess JN, Garofolo F. Application of high-resolution MS in the quantification of a therapeutic monoclonal antibody in human plasma. Bioanalysis. 2014;6(13):1767–79. doi:10.4155/bio.14.111.

32. Ouyang Z, Furlong MT, Wu S, Sleczka B, Tamura J, Wang H, et al. Pellet digestion: a simple and efficient sample preparation technique for LC–MS/MS quantification of large therapeutic proteins in plasma. Bioanalysis. 2011;4(1):17–28. doi:10.4155/bio.11.286.

33. Mellquist JL, Kasturi L, Spitalnik SL, Shakin-Eshleman SH. The amino acid following an Asn-X-Ser/Thr sequon is an important determinant of N-linked core glycosylation efficiency. Biochemistry. 1998;37(19):6833–7. doi:10.1021/bi972217k.

34. Van den Steen P, Rudd PM, Dwek RA, Opdenakker G. Concepts and principles of O-linked glycosylation. Crit Rev Biochem Mol Biol. 1998;33(3):151–208. doi:10.1080/10409239891204198.

35. Krieg J, Hartmann S, Vicentini A, Glasner W, Hess D, Hofsteenge J. Recognition signal for C-mannosylation of Trp-7 in RNase 2 consists of sequence Trp-x-x-Trp. Mol Biol Cell. 1998;9(2):301–9.

36. Pan Y, Karagiannis K, Zhang H, Dingerdissen H, Shamsaddini A, Wan Q, et al. Human germline and pan-cancer variomes and their distinct functional profiles. Nucleic Acids Res. 2014;42(18):11570–88. doi:10.1093/nar/gku772.

37. Chelius D, Rehder DS, Bondarenko PV. Identification and characterization of deamidation sites in the conserved regions of human immunoglobulin gamma antibodies. Anal Chem. 2005;77(18):6004–11. doi:10.1021/ac050672d.

38. Zhang YT, Hu J, Pace AL, Wong R, Wang YJ, Kao YH. Characterization of asparagine 330 deamidation in an Fc-fragment of IgG1 using cation exchange chromatography and peptide mapping. J Chromatogr B. 2014;965:65–71. doi:10.1016/j.jchromb.2014.06.018.

39. Ren D, Pipes GD, Liu D, Shih LY, Nichols AC, Treuheit MJ, et al. An improved trypsin digestion method minimizes digestion-induced modifications on proteins. Anal Biochem. 2009;392(1):12–21. doi:10.1016/j.ab.2009.05.018.

3.2 Approach for intact hIgG1 quantification by IC-LC-HRMS

3.2.1 Analytical context

Bottom-up approaches, either based on low or high-resolution mass spectrometers, feature a series of bottlenecks for mAb-related therapeutic protein quantification in complex matrices. First, the identification of the most appropriate surrogate peptide(s) with subsequent SRM transition optimization can be challenging and time-consuming.[315,519] In addition, depending on the location within the quaternary structure of the protein, certain surrogate peptide(s) of interest cannot readily be generated during proteolytic digestion.[520] Second, complex multistep sample preparation procedures, which govern the method throughput, introduce variations and artefactual modifications at the peptide level.[521,522] Third, surrogate peptides, even the incorporation of several peptides from different regions, cannot entirely reflect the heterogeneity of mAbs, resulting in a loss of essential information about the proteoform, biological activity, and post-translational modifications of the intact mAb.[521,523-525] Lastly, the biotransformation and elimination pathways of mAbs are more complex compared to small molecules including mAb truncations, lysosomal degradation, and clearance processes mediated by ADAs, the antibody Fc, or carbohydrates.[526] However, bottom-up approaches cannot distinguish between *in vitro* or *in vivo* generated metabolites and catabolites carrying the unchanged peptide segment, which subsequently may result in a misrepresentation of the true concentration.[527,528] Hence, quantitative approaches at a higher protein level would be beneficial, omitting the proteolytic digestion step.[521,525] Although intact protein quantification was successfully implemented for several small therapeutic proteins including insulin,[529,530] serum amyloid A,[531] myoglobin,[532-534] leptin,[535] or somatropin[536] using QqQ[537-541] or HRMS,[528,542-545] intact mAb quantification is still in its infancy. Limiting factors for intact mAb quantification are mostly related to specificity and sensitivity issues as the spectral spacing is impacted by the dense isotopic peak distribution and the S/N ratio decreases with increasing molecular weight and charge state.[223] In order to overcome the specificity issue, novel analytical concepts such as protein decharging,[546] the use of mobile phase additives,[547] and native MS[166,548,549] were explored to shift the charge state distribution of intact mAb-related therapeutic proteins. On the other hand, appropriate affinity-based sample preparation techniques, advancements in HRMS instrumentation, or targeted ion parking[373,550] are promising strategies to increase the sensitivity. In combination with advanced computational tools for data processing and the ability to produce full-length SIL-mAbs as appropriate ISTDs,[238,305,307,309] higher level mAb quantification is nowadays feasible. Notwithstanding, the majority of sparsely reported protocols still utilize middle-up approaches,[311,427,525] whereas only a minority of researchers performed targeted intact mAb quantification.[527,551-553]

3.2.2 Objectives

This work aimed to establish a generic method for targeted intact hIgG1 quantification in pre-clinical species by hybridizing existing IC technologies with LC-HRMS detection. Furthermore, two method comparisons between intact hIgG1 and conventional peptide level quantification were conducted using spiked rat serum samples and specimen from a rat PK study. Lastly, multiplexing capabilities at the intact hIgG1 level were explored.

3.2.3 Results

3.2.3.1 Intact hIgG1 quantification workflow

The existing generic quantitative tip-based IC-LC-MS/MS-based workflow (chapter 2.3) was slightly modified, resulting in the generic IC-LC-HRMS method for targeted intact hIgG1 quantification (Figure 3.6). The availability of [^{13}C]-hIgG1 as ideal ISTD, was one key feature, enabling intact hIgG1 quantification. Nevertheless, the introduction of the [^{13}C]-hIgG1 within the workflow represented a crucial step. At first, the addition of the [^{13}C]-hIgG1 following hIgG1 extraction from rat serum samples using a biotinylated mouse anti-hIgG Fc capture antibody was expected to be the most appropriate approach in order to avoid binding competition between both hIgG1s due to a limited binding capacity of the IC-tips. However, this approach, displaying a constant [^{13}C]-hIgG1 peak area across the calibration range (Figure 3.7a), was unable to
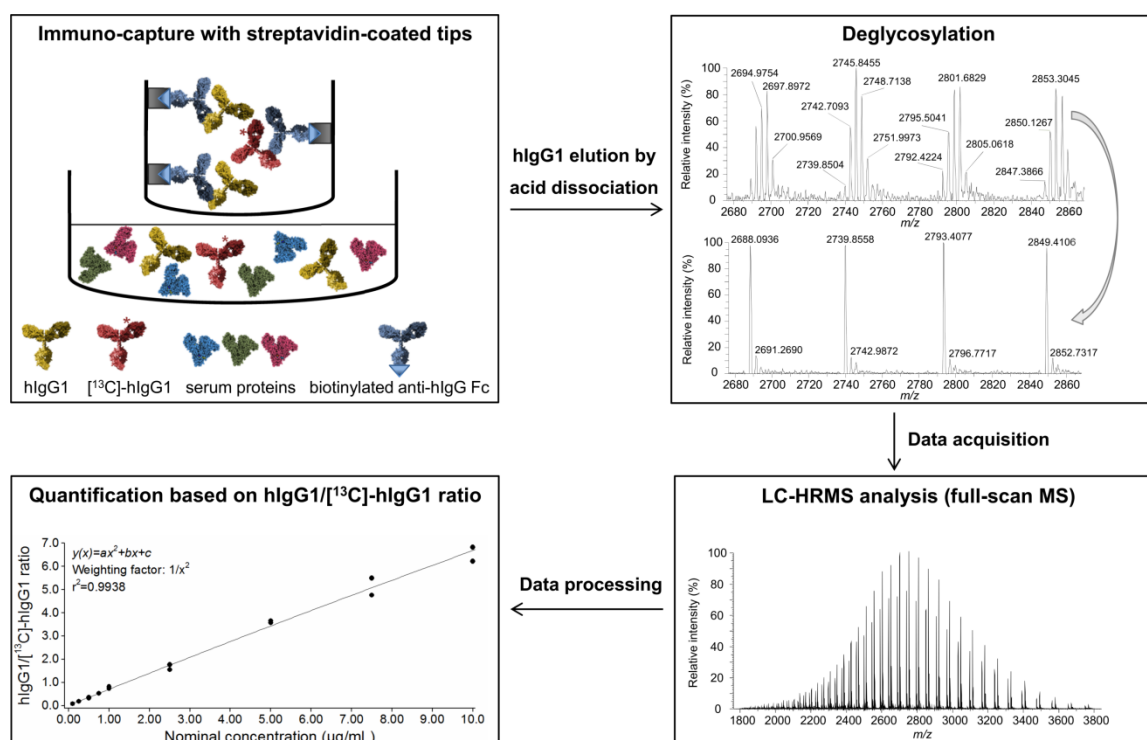
Figure 3.6 Overview of the IC-LC-HRMS-method for intact hIgG1 quantification in pre-clinical species.
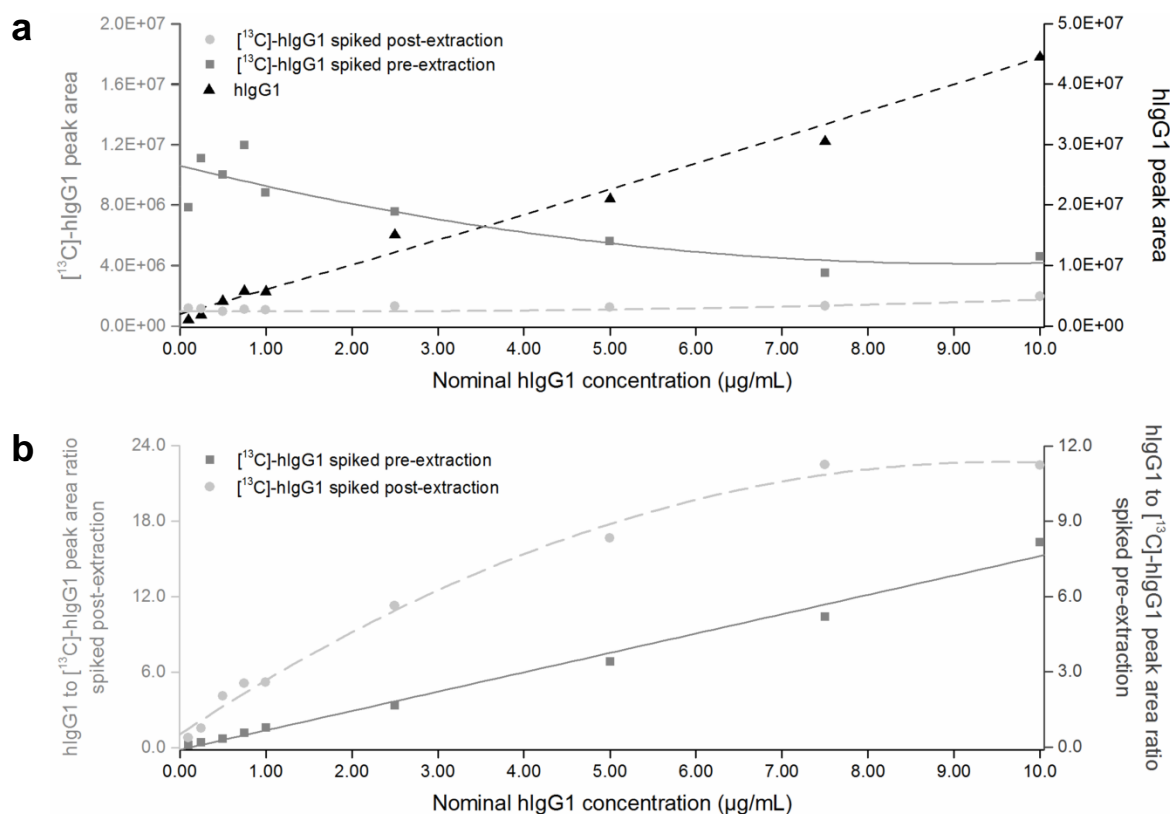
Figure 3.7 Investigation of [^{13}C]-hIgG1 addition during sample preparation. (**a**) Obtained peak areas for [^{13}C]-hIgG1 at 1.00 µg/mL either spiked pre or post-hIgG1 extraction from rat serum samples and (**b**) obtained calibration curves.

compensate for variations introduced during hIgG1 extraction such as differences in binding to the capture antibody. Moreover, the reciprocal correlation between the MS response factor (analyte to ISTD peak area ratio multiplied by the ISTD to analyte concentration ratio) and the hIgG1 concentration resulted in a non-linear bending of the calibration curve (Figure 3.7b). In contrast, saturation effects of the streptavidin-coated tips during hIgG1 extraction were compensated by the co-extracted [^{13}C]-hIgG1 as its response decreased with increasing hIgG1 concentration (Figure 3.7a), recovering the linear behavior of the calibration curve (Figure 3.7b). Hence, the [^{13}C]-hIgG1 was introduced directly at the beginning of the sample preparation in order to compensate for extraction losses or other variations introduced during sample treatment. Although non-deglycosylated hIgG quantification was reported,[527] additional glycan removal reduced the heterogeneity of the hIgG1 and complexity of the full-scan MS spectrum, resulting in an enhanced selectivity and signal intensity. The kinetic studies of the deglycosylation revealed a time-dependent increase in signal intensities of the deglycosylated *m/z* values for the most abundant charge states (51+ to 56+), which seemed to reach a plateau after 4 h of N-glycosidase F (PNGase F) treatment (Figure 3.8). However, overnight deglycosylation (18 h) was identified as the preferred protocol as a significant increase in signal intensity was obtained for the QC at 0.250 and 8.00 µg/mL (Figure 3.8a+b, respectively). Potential possibilities for a faster and more efficient hIgG1 deglycosylation include: (i) increased amount of enzyme added to the sample, which was
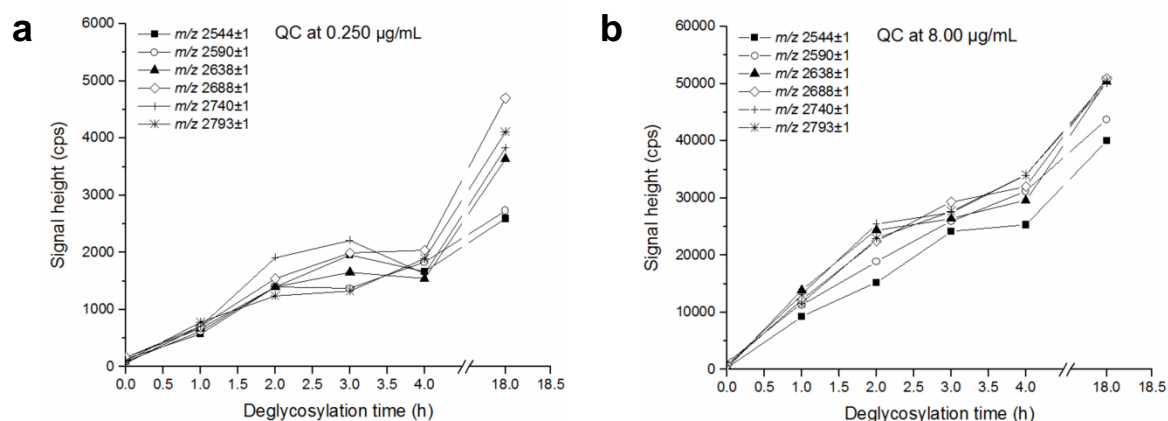
Figure 3.8 Kinetic profile of hIgG1 deglycosylation after hIgG1 extraction from rat serum and hIgG1 elution from the tips using a QC at (**a**) 0.250 or (**b**) 8.00 µg/mL. The deglycosylated *m/z* values of the six most abundant charge states of the hIgG1 (51+ to 56+) were monitored during PNGase F treatment.

not considered due to an increase in analytical costs per sample or (ii) the selection of another glycosidase such as Endo S (*i.e.* IgGZERO from Genovis, Lund, Sweden), which was not evaluated throughout this project, but for intact ADC quantification (section 3.3.4.2). Prior to establishing the final HRMS method, several Q-Exactive orbitrap parameters were optimized by injecting 1 µg of deglycosylated hIgG1 onto a ProSwift RP-4H (250 x 1mm) monolithic column. The Q-Exactive orbitrap operated in positive ionization mode (*m/z* 1800-4200), whereby the resolution was set to the lowest value of 17 500 at *m/z* 200 for maximum sensitivity. A two-fold signal increase was obtained by lowering the spray voltage from 4.00 to 3.20 kV (Figure 3.9a). In addition, a slight increase of the intact hIgG1 signal was gained by increasing the S-lens Rf level from 40 to 80 V, which enhanced the fragmentation of fragile ions and hence resulted in an
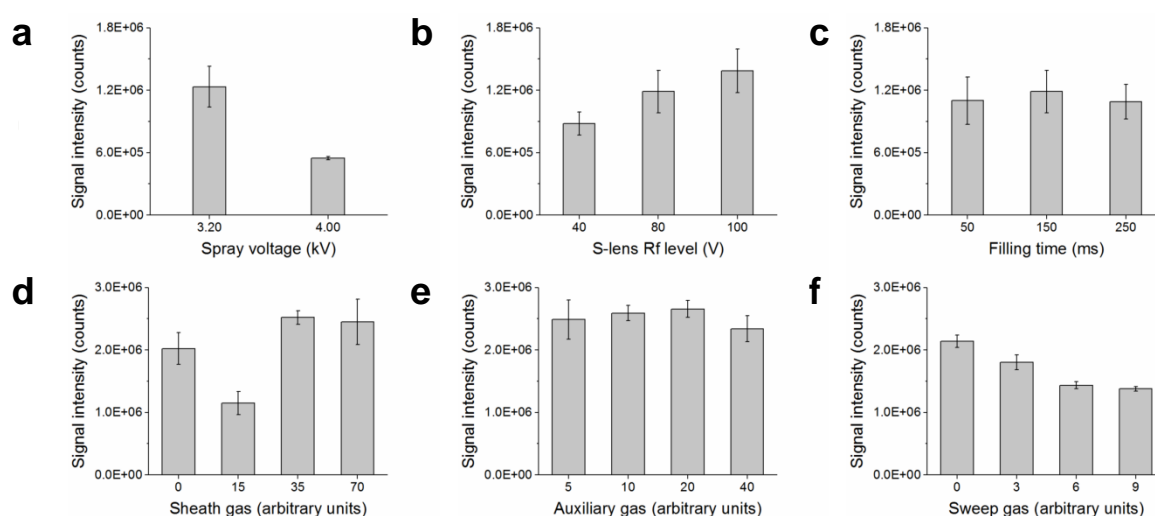
Figure 3.9 Optimization of the Q-Exactive orbitrap parameters for intact hIgG1 quantification including (**a**) spray voltage, (**b**) S-lens Rf level, (**c**) C-Trap filling time, (**d**) sheath, (**e**) auxiliary, and (**f**) sweep gas. Signal intensities are based on the summed XIC (51+ to 56+ charge states) of deglycosylated hIgG1 (1 µg).

increased transmission of high compared to low *m/z* ions through the S-lens (Figure 3.9b).On the other hand, the C-trap filling time had no significant impact on the intact hIgG1 signal intensity when an automatic gain control of 3.0E+06 was used (Figure 3.9c). In terms of the gas flows, a two-fold boost in hIgG1 signal intensity was generated by increasing the sheath gas from 15 to 35 arbitrary units (Figure 3.9d), whereas the auxiliary (Figure 3.9e) and sweep gas (Figure 3.9f) had no or a negative impact on the intact hIgG1 signal intensity, respectively.

3.2.3.2 Selection of the intact hIgG1 quantification mode

After hIgG1 elution, two distinct charge stage envelopes (38+ to 73+) were present in the full-scan MS spectrum, corresponding to the hIgG1 and [^{13}C]-hIgG1 whose charge states are labeled with an asterisk (Figure 3.10a). As a first option, intact hIgG1 quantification can be conducted after MS deconvolution of the most abundant charge states (in this case 42+ to 59+) by plotting the resulting peak height ratio of the generated deglycosylated zero charged species against the nominal hIgG1 concentration (Figure 3.10b). However, due to the low signal intensity of the charge state envelope at decreased hIgG1 concentrations and the tendency of outer charge states (*e.g.* 59+ to 57+ and 44+ to 42+) to disappear within the background noise, non-hIgG1 specific background ions interfered in each iteration cycle during data processing. Consequently, additional analytical bias was introduced resulting in an overestimation of the lower QC concentrations at 0.100 and 0.250 µg/mL by 58.2 and 33.4%, respectively, whereas the mid (5.00 µg/mL, 2.0% bias) and high QC (8.00 µg/mL, 0.7% bias) concentrations were accurately be
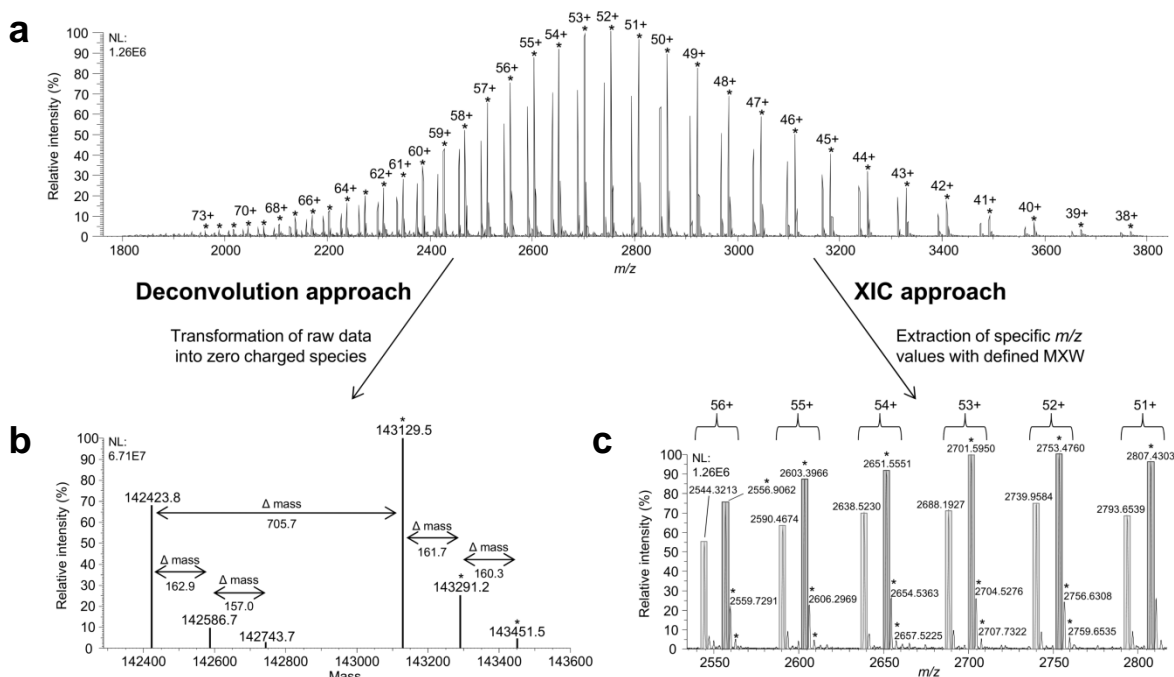
Figure 3.10 Options for intact hIgG1 quantification after (**a**) full-scan MS spectrum acquisition either based on (**b**) MS deconvolution using the peak height ratio of the deglycosylated zero charged species or (**c**) the XIC approach by extracting individual charge states from the full-scan MS spectrum with a defined MXW.

determined. One option to circumvent this issue might be to narrow the input range for MS deconvolution (*e.g.* 49+ to 56+), which was not evaluated in this project. According to general recommendations outlined in a recent review, the MS deconvolution approach may lead to errors in quantitative data and should generally be evaluated with great caution as it moves away from the raw data.[521] Alternatively, individual charge states can be extracted from the full-scan MS spectrum based on a defined width of the MXW (Figure 3.10c), summed up, and the resultant peak height or area can be used for intact hIgG1 quantification. In general, the peak area is preferred for quantitative purposes as it remains constant for the same amount of detected hIgG1, whereas the peak height is affected by peak dispersion effects causing variation in their values. This consideration was in agreement with the experimental data as accurate and precise data were only obtained with the XIC approach based on the peak area. In contrast, the peak height approach resulted in an overestimation of the lower hIgG1 QC concentrations with a maximum of 37.6% (Table 3.4). Further data processing experiments with the XIC approach based on the peak area demonstrated that the number of individual charge states (3, 6, 9, or 18) selected for ion chromatogram extraction had no significant impact on the quantitative data. The accuracy ranged from 1.1% bias (6 charge states) to 19.2% bias (18 charge states) with a precision of maximum 11.3% CV (3 charge states), meeting acceptance criteria from US FDA and EMA guidances. In contrast, the width of the MXW significantly impacted the quantitative data. The difference in *m/z* values between the deglycosylated and remaining glycated isoforms within one charge state was approximately 3 *m/z* units (Figure 3.10c). Consequently, a MXW width of maximum 6 *m/z* units was only adequate for accurate and precise intact hIgG1 quantification as both isoforms (deglycosylated and glycated one) was extracted with wider MXWs (*i.e.* 8 *m/z* units), resulting in an overestimation of the hIgG1 concentration by up to 50.6% (Table 3.5). For the final intact hIgG1 quantification method using IC-LC-HRMS, the six most abundant charge states (51+ to 56+) were extracted with a narrow MXW width of 2 *m/z* units.

Table 3.4 Accuracy and precision of QCs obtained with the XIC approach either based on the peak height or area (values reported in brackets) using different numbers of charge states and a MXW width of 2 *m/z* units.

Number of charge states		Nominal QC concentration in rat serum (µg/mL)			
Linearity of Cs		8.00	5.00	0.250	0.100
3 (from 51+ to 53+)	Intra-day accuracy (% bias)	13.3 (8.7)	4.7 (8.7)	23.7[a] (9.4)	22.1 (9.0)
r^2=0.9811 (0.9891)	Intra-day precision (% CV)	4.6 (3.2)	3.6 (11.3)	10.0 (8.4)	19.5 (1.9)
6 (from 51+ to 56+)	Intra-day accuracy (% bias)	1.6 (1.1)	6.5 (9.0)	20.3[a] (5.9)	37.6[b] (12.3)
r^2=0.9958 (0.9932)	Intra-day precision (% CV)	3.8 (3.6)	2.9 (3.5)	10.9 (4.1)	8.5 (6.7)
9 (from 48+ to 56+)	Intra-day accuracy (% bias)	1.4 (6.4)	8.2 (11.0)	21.4[a] (15.6)	21.9 (15.4)
r^2=0.9908 (0.9876)	Intra-day precision (% CV)	2.6 (6.1)	3.7 (3.9)	7.5 (3.4)	13.2 (7.7)
18 (from 42+ to 59+)	Intra-day accuracy (% bias)	-0.5 (4.0)	9.0 (10.6)	22.2[a] (16.6)	37.0[b] (19.2)
r^2=0.9925 (0.9928)	Intra-day precision (% CV)	3.9 (6.2)	1.3 (1.0)	7.2 (1.6)	8.8 (3.3)

[a] Out of acceptance criterion of ±20.0%, [b] out of acceptance criterion of ±25.0%

Table 3.5 Accuracy and precision of QCs obtained with the XIC approach based on the peak area of the six most abundant charge states (51+ to 56+) using different MXW widths.

Width of MXW		Nominal QC concentration in rat serum (µg/mL)			
Linearity of Cs		8.00	5.00	0.250	0.100
2 *m/z* units	Intra-day accuracy (% bias)	1.5	9.1	12.1	15.3
r^2=0.9925	Intra-day precision (% CV)	3.6	3.5	7.1	4.0
4 *m/z* units	Intra-day accuracy (% bias)	0.9	10.3	13.2	3.8
r^2=0.9914	Intra-day precision (% CV)	0.3	4.6	4.0	14.1
8 *m/z* units	Intra-day accuracy (% bias)	1.5	14.7	32.2[a]	50.6[b]
r^2=0.9921	Intra-day precision (% CV)	4.7	1.1	5.1	18.2

[a] Out of acceptance criterion of ±20.0%, [b] out of acceptance criterion of ±25.0%

3.2.3.3 Method validation

The generic IC-LC-HRMS assay was validated by transferring the defined acceptance criteria for peptide level to intact protein level analysis. The outcome of the method validation is summarized in Table 3.6, fulfilling the acceptance criteria from US FDA and EMA guidances.[352,353]

Table 3.6 Method validation of the generic IC-LC-HRMS workflow for intact hIgG1 quantification in rat serum.

Parameter	Outcome
Selectivity: three blank batches (n=3)	hIgG1: ≤3.0%, [^{13}C]-hIgG1: ≤0.3%
Contribution of signal	[^{13}C]-hIgG1 to hIgG1: 12.8%, hIgG1 to [^{13}C]-hIgG1: 13.0%
Linearity (n=3), $y=ax^2+bx+c$, $1/x^2$ weighting	0.100-10.0 µg/mL, r^2=0.9919±0.0027
Carry-over (blank after ULOQ sample)	hIgG1: <LLOQ signal, [^{13}C]-hIgG1: 0.0% of zero sample response
Accuracy (% bias) and precision (% CV) QCs at 0.100, 0.250, 5.00, and 8.00 µg/mL	Intra-day (n=3): -2.7 to 16.0% bias, 1.3 to 11.7% CV Inter-day (n=9): -0.1 to 9.3% bias, 6.1 to 8.7% CV
Dilution integrity (300 µg/mL, 50-fold, n=5)	Mean bias of 2.9% with precision of 8.6% CV
Reproducibility (sample analysis on two days)	Concentration bias within ±20.0% for 29 out of 30 incurred samples

3.2.3.4 Intact *versus* peptide level hIgG1 quantification

In total, 30 spiked rat serum samples and 24 pre-clinical study samples were employed for hIgG1 quantification either at the intact protein or conventional peptide level. A good linear correlation was observed for the spiked and pre-clinical study samples as indicated by Pearson's r-values of 0.9829 and 0.9546, respectively (Figure 3.11a+b). The corresponding Passing-Bablok regressions were almost ideal with slopes of 1.0452 and 0.9913 and intercepts of -0.0211 and 0.0430 for the spiked samples and real specimen, respectively. Since the confidence intervals for the slopes approximated the optimal value of 1 in both comparisons, no significant proportional difference existed statistically between both approaches. Furthermore, both methods did not differ from any constant amount of bias as the 95% confidence intervals for the intercepts from both linear regression analyses incorporated the zero value. The mean bias between the intact protein and

peptide level analysis was -4.2% for the spiked samples, whereas two samples were not located inside the 95% limits of agreement ranging from -23.2 to 14.8% bias (Figure 3.11c). An excellent method agreement was likewise obtained with the *in vivo* samples with only one rat PK sample located outside the 95% limits of agreements (-22.7 to 25.8% bias), whereas the mean bias between both methods was 1.6% (Figure 3.11d). Consequently, equivalent quantitative data were generated at the intact hIgG1 level compared to conventional bottom-up MS-based approaches.
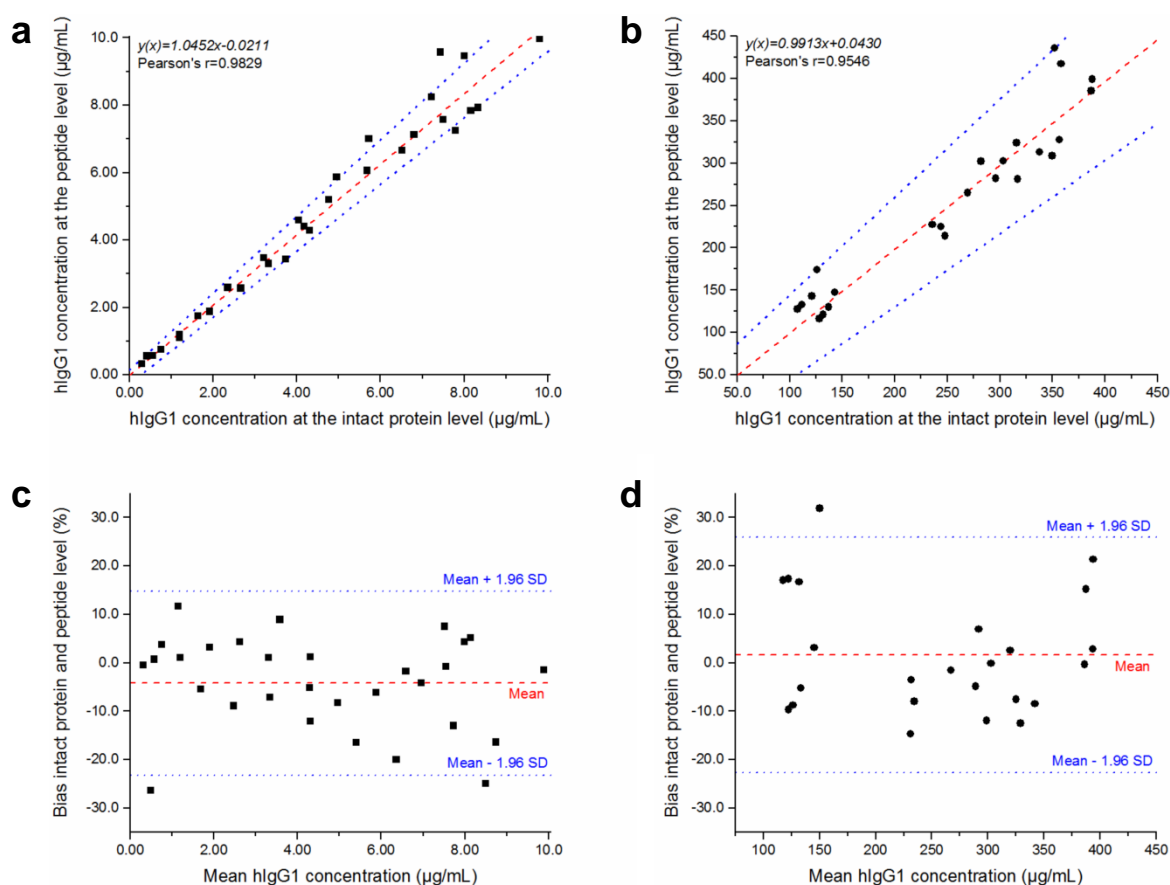
Figure 3.11 Comparison of hIgG1 concentration determined either at the intact protein or peptide level. Correlation plots with linear regression (dashed red line) and 95% confidence intervals from Passing-Bablok regression (dotted blue lines) for (**a**) spiked rat serum samples (n=30) and (**b**) *in vivo* samples from a rat PK study (n=24). Bland-Altman plots with 95% limits of agreement (dotted blue lines) for method agreement assessment between both approaches for (**c**) spiked rat serum and (**d**) *in vivo* samples. SD: standard deviation

3.2.3.5 Multiplexed hIgG1 quantification

The multiplexed quantification was conducted using two hIgG1s (hIgG1A and hIgG1B), which exhibit only minor differences in amino acid sequences (*e.g.* in the CDR region). Both hIgG1s were baseline separated under the selected chromatographic conditions and were simultaneously quantified directly at the intact protein level within the same rat serum sample using the

[^{13}C]-hIgG1 as common ISTD. Due to ion suppression effects caused by excessive PNGase F co-eluting with hIgG1B at 8.2 min, the LLOQ of the hIgG1B was slightly increased (0.250 µg/mL) compared to the one of the hIgG1A (0.100 µg/mL), eluting 30 s earlier. The corresponding intra and inter-day accuracy and precision data for both hIgG1s fulfilled the acceptance criteria on three non-consecutive days (Table 3.7).

Table 3.7 Linearity, accuracy, and precision data (QCs at 0.100, 0.250, 5.00, and 8.00 µg/mL) obtained during multiplexed intact hIgG1 quantification in rat serum using the generic IC-LC-HRMS method.

Analyte	Retention time	Linearity		Accuracy (% bias)		Precision (% CV)	
		Range (µg/mL)	r^2-value (n=3)	Intra-day (n=3)	Inter-day (n=9)	Intra-day (n=3)	Inter-day (n=9)
hIgG1A	7.7 min	0.100-10.0	0.9891±0.0009	-3.6 to 17.7	2.6 to 10.4	1.3 to 12.1	5.2 to 8.8
hIgG1B	8.2 min	0.250-10.0	0.9840±0.0063	-7.3 to 5.6	-1.0 to 1.6	3.8 to 14.6	8.1 to 9.8

3.2.4 Conclusions

The generic IC-LC-HRMS-based workflow has proven its potential for intact hIgG1 quantification by combining the advantages of existing IC technologies for selective enrichment with the extended mass range of HRMS instruments.

- A high sensitivity of 100 ng/mL was obtained suitable for most pre-clinical application, differing only one order of magnitude from the developed IC-LC-MS/MS approach (10.0 ng/mL).

- Less complex sample preparation was mandatory with only one post-elution step (deglycosylation) compared to multistep bottom-up approaches, eliminating the generation of artefactual peptide modifications upon reduction, alkylation, and proteolytic digestion.

- Equivalent quantitative data based on spiked rat serum and pre-clinical study samples were provided by the intact hIgG1 approach compared to orthogonal bottom-up workflows.

- In contrast to the presented generic bottom-up MS-based workflows, multiplexing of two hIgGs from the same isotype subclass (hIgG1) was feasible at the intact level. In addition, simultaneous targeted quantification of co-administered Fc region-bearing mAb-related therapeutic proteins would be possible without the requirement to select analyte-specific surrogate peptides.

- The provided information level exceeded the one of ELISA and bottom-up MS-based approaches. Closely related proteoforms, *in vivo* generated metabolites and catabolites could be identified and quantified with the presented approach, which might not be recognized by ELISA in case the modification occurs in the detection antibody-targeting binding site or which could not be revealed at the peptide level in case the modification occurs in regions that are not covered by the selected surrogate peptide(s). Consequently, an improved characterization of the fate of mAb-related therapeutic proteins is granted with the intact approach.

3.2.5 Scientific communications

The work described in this chapter was published and presented on several occasions.

Peer-reviewed scientific article:

Lanshoeft C, Cianférani S, Heudi O. Generic hybrid ligand binding assay liquid chromatography high-resolution mass spectrometry-based workflow for multiplexed human immunoglobulin G1 quantification at the intact protein level: application to preclinical pharmacokinetic studies. *Anal Chem*, 2017, 89(4), 2628-2635. Copyright 2017, reprinted with permission from American Chemical Society.

Oral presentation:

A generic hybrid LBA-LC-HRMS-based workflow for multiplexed hIgG1 quantification in pre-clinical species directly at the intact protein level. 45th International Symposium on High-Performance Liquid Phase Separations and Related Techniques (HPLC2017), Jun 19th 2017, Prague (Czech Republic).

Quantitative analysis of biotherapeutics in pre-clinical species by LC-HRMS either at the peptide or directly at the intact protein level. 1st Quantitative HRMS Workshop, May 16th 2017, Muttenz (Switzerland).

Generic Hybrid Ligand Binding Assay Liquid Chromatography High-Resolution Mass Spectrometry-Based Workflow for Multiplexed Human Immunoglobulin G1 Quantification at the Intact Protein Level: Application to Preclinical Pharmacokinetic Studies

Christian Lanshoeft,[†,‡] Sarah Cianférani,[‡] and Olivier Heudi*,[†]

[†]Novartis Institutes for Biomedical Research, Drug Metabolism and Pharmacokinetics, Novartis Campus, 4056 Basel, Switzerland

[‡]Laboratoire de Spectrométrie de Masse BioOrganique, Université de Strasbourg, CNRS, IPHC UMR 7178, 67000 Strasbourg, France

S *Supporting Information*

ABSTRACT: The quantitative analysis of human immunoglobulin G1 (hIgG1) by mass spectrometry is commonly performed using surrogate peptides after enzymatic digestion. Since some limitations are associated with this approach, a novel workflow is presented by hybridizing ligand binding assay (LBA) with liquid chromatography–high-resolution mass spectrometry (LC–HRMS) for hIgG1 quantification directly at the intact protein level. Different hIgG1s, including a $[^{13}C]$-labeled version used as internal standard, were immuno-enriched from rat serum with a fully automated platform based on streptavidin coated tips and a biotinylated mouse anti-hIgG capture antibody targeting the fragment crystallizable region followed by overnight deglycosylation prior to LC–HRMS analysis. The proposed quantitative workflow utilized extracted ion chromatograms (XICs) from the non-deconvoluted full-scan MS spectrum. The assay was validated in terms of selectivity, sensitivity, accuracy/precision, carry-over, dilution linearity, and reproducibility. Consistent data between the conventional approach based on surrogate peptide analysis and our proposed workflow were obtained *in vitro* and *in vivo* with the advantage of a less extensive sample pretreatment. Multiplexing capabilities for simultaneous quantification of different hIgG1s within the same spiked sample were also exemplified. Altogether our results pave the way not only for the thorough application of intact hIgG1 quantification by LBA-LC–HRMS but also as a generic quantitative analytical method for other hIgG isotypes or next generation biotherapeutics.
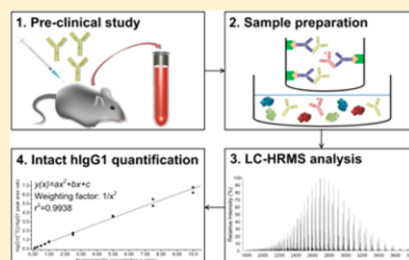
L iquid chromatography–tandem mass spectrometry (LC–MS/MS) based assays have rapidly evolved in recent years as a complementary analytical method to ligand binding assays (LBAs) for the quantification of monoclonal antibodies (mAbs).[1−4] The majority of these quantitative LC–MS/MS assays is based on the bottom-up approach using specific surrogate peptides either from the complementary determining regions[5−7] or the fragment crystallizable (Fc) region (generic approach) after enzymatic digestion.[8−11] Potential advantages of the latter mass spectrometry (MS) based approach are the faster method development time, the increase in the linear dynamic range, and the ease of multiplexing. However, the LC–MS/MS approach also presents a series of limitations among which the artifactual generation at the peptide level of various modifications after enzymatic digestion (e.g., deamidation of asparagine to iso-aspartic and aspartic acid).[12] Besides these possible modifications, glycosylation, oxidation, site-specific conjugation, or other biotransformations occurring *in vivo* can only be covered partially at the peptide level. Thus, the heterogeneity of the (modified) mAb is not entirely reflected which may result in discrepancies in the absolute concentration. Consequently, the development of novel analytical MS-based

approaches at the intact protein level for an absolute and unbiased quantification is highly required. The current improvements of new generation high-resolution mass spectrometry (HRMS) instruments such as hybrid quadrupole-time-of-flight or orbitrap mass analyzers have permitted the quantification of small molecules,[13−15] peptides,[16−18] low molecular weight therapeutic proteins (6.0 to 28.7 kDa in size),[19−21] or mAbs using the bottom-up approach.[12,22] More recently, LC–HRMS has also been successfully applied to the quantification of different human immunoglobulin G (hIgG) isotypes, namely, hIgG1 or eculizumab, a hIgG2/4 kappa mAb, using larger hIgG subunits after selective proteolysis with subsequent reduction (2 × Fc, Fab light chain, and Fab heavy chain) or simple reduction only (intact light chain in the case of eculizumab).[23−25] As outlined in a recent review, mAb quantification at the intact protein level is not straightforward as the protein signal is distributed over several charge states.[26] This increases the complexity of the full-scan MS spectrum

which can compromise the assay's selectivity and sensitivity. In order to simplify the data interpretation, the MS deconvolution was recently used for mAb quantification at the intact protein level.[27,28] However, it is questionable whether the deconvoluted data can always be used for the quantitative analysis as the data processing after acquisition could lead to any loss of original information which might impact the method's robustness especially in complex samples. Thus, the quantification of Infliximab was recently performed without any MS deconvolution in ultrafiltrated mouse serum representing a less complex matrix as opposed to neat sera or plasma.[29] Until now, to the best of our knowledge there is no published work dealing with hIgG1 quantification at the intact protein level based on the extracted ion chromatograms (XICs) in plasma or sera. Consequently, the purposes of this work were to (i) develop a hybrid LBA-LC−HRMS-based workflow for hIgG1 quantification at the intact protein level in rat serum using its stable isotope labeled version ($[^{13}C]$-hIgG1) as internal standard, (ii) further investigate its multiplexing capabilities for the simultaneous quantification of different hIgG1s, (iii) apply the developed workflow to rat pharmacokinetic (PK) studies, and (iv) compare the hybrid LBA-LC−HRMS data with those originating from classical bottom-up LC−MS/MS analysis.

■ EXPERIMENTAL SECTION

Chemicals and Reagents. The hIgG1A, its $[^{13}C]$-lysine/arginine labeled version ($[^{13}C]$-hIgG1A), the mouse anti-hIgG Fc capture antibody, and the second hIgG1 (entitled hIgG1B) used during multiplexing studies were produced at Novartis Pharma AG (Basel, Switzerland). Tween 20, DL-Dithiothreitol (DTT), iodoacetamide (IAA), ammonium bicarbonate (ABC), bovine pancreas trypsin, ammonium hydroxide (NH$_4$OH, 28−30%), trifluoroacetic acid (TFA), acetic acid, methanol (MeOH), acetonitrile (ACN), and MS grade water were delivered from Sigma-Aldrich (Buchs, Switzerland). Formic acid (FA) and PNGase F (10 u/μL) were purchased from Merck (Darmstadt, Germany) and Promega (Madison, WI), respectively. The EZ-Link Sulfo-NHS-Biotinylation kit, BupH modified Dulbecco's phosphate buffered saline packs (PBS, 0.1 M sodium phosphate, 0.15 M sodium chloride, pH 7.2), as well as the streptavidin coated mass spectrometric immunoassay disposable automation research tips (MSIA D.A.R.T.'S) and magnetic beads (Pierce, 10.0 mg/mL) were obtained from Thermo Fisher Scientific (Waltham, MA). Sodium iodide solution was provided by Waters (Milford, MA). All LC−MS grade solvents as well as reagents were of high analytical grade (≥99%) and were used without any purification. Blank rat serum used for the preparation of calibration standards (Cs) and quality control (QC) samples was obtained from Fisher Clinical Services (Allschwil, Switzerland).

Preparation of Cs and QC Samples. Stock solution of the hIgG1A (or cospiked with hIgG1B during multiplexing studies) was serially diluted in PBS. The resultant working solutions were spiked into blank rat serum (5:95, v/v) resulting in nine Cs levels (0.100, 0.250, 0.500, 0.750, 1.00, 2.50, 5.00, 7.50, and 10.0 μg/mL) and four QC concentrations (0.100, 0.250, 5.00, and 8.00 μg/mL).

Serum Samples from Rat PK Study. Eight different female Han Wistar rats were dosed intravenously with hIgG1A at 10.0 mg/kg. A volume of 250 μL of blood was drawn into serum collection tubes at predose as well as 1, 6, and 23.5 h postdose after puncturing of the sublingual vein. The collected blood was allowed to clot upright at room temperature for 1 h

prior to centrifugation at 2500g and 4 °C for 10 min. Afterward the resultant serum was shipped to the analytical lab and stored ≤−70 °C pending analysis. The preclinical study was conducted in compliance with the Novartis Animal Care and Use Committee, the Animal Welfare Act, the Office of Laboratory Animal Welfare and in accordance with the Guide for the Care and Use of Laboratory Animals.

Immuno-Enrichment from Rat Serum for Intact hIgG1 Quantification. The mouse anti-hIgG Fc capture antibody was biotinylated with a 20-fold molar excess of biotin using the EZ-Link Sulfo-NHS-Biotinylation kit. The streptavidin coated tips were prerinsed with 175 μL of PBS (15 cycles) using the Versette platform, a 96-well plate based automated liquid handler (Thermo Fisher Scientific) prior to loading of the biotinylated capture antibody (5.00 μg/tip, 1000 cycles) followed by a postrinse step with PBS (175 μL, 15 cycles). A volume of 50 μL of rat serum sample was loaded into a 500 μL Protein LoBind 96-well plate from Eppendorf (Hamburg, Germany), and 5 μL of $[^{13}C]$-hIgG1A were added to the samples (except for blank samples) resulting in a final $[^{13}C]$-hIgG1A concentration of 1.00 μg/mL. The hIgG1s were enriched on the tips by repeatedly aspirating and dispensing 250 μL of diluted serum sample (serum/PBS, 1:7, v/v, 1000 cycles). After enrichment, the tips were rinsed twice with PBS and two times with water (175 μL, 15 cycles each). The immuno-enriched hIgG1s were eluted into a clean 200 μL ABgene V-bottom 96-well plate (Thermo Fisher Scientific) by drawing and expelling 30 μL of 2% FA in water/MeOH (9:1, v/v, 200 cycles). The eluate was neutralized with 5 μL of NH$_4$OH/water (2:3, v/v) prior to overnight deglycosylation using 4 μL of PNGase F/50 mM ABC (1:3, v/v). The enzymatic activity was terminated the day after by adding elution solvent to the samples (total end volume of 120 μL) prior to LC−HRMS analysis.

LC−HRMS Method for Intact hIgG1 Quantification. A volume of 60 μL was injected into a Dionex UltiMate 3000 LC system coupled to a Q-Exactive hybrid quadrupole orbitrap mass spectrometer (Thermo Fisher Scientific). The monolithic ProSwift RP-4H (1 mm × 250 mm) column was maintained at 70 °C. The mobile phases consisted of 0.1% FA in water (A) and 0.1% FA in ACN (B) whereas the following gradient was used: 0.0−2.5 min, 10% B; 2.5−5.5 min, 10−28% B; 5.5−12.0 min, 28−32% B; 12.0−12.5 min, 32−90% B; 12.5−14.5 min, 90% B; 14.5−15.0 min, 90−10% B; 15−20 min, 10% B. For the multiplexing studies, a slightly modified gradient was used: 0.0−2.5 min, 20% B; 2.5−12.0 min, 20−60% B; 12.0−12.5 min, 60−90% B; 12.5−14.5 min, 90% B; 14.5−15.0 min, 90−20% B; 15−20 min, 20% B. For both gradients, the flow rate was set to 200 μL/min. For MS detection, a full-scan MS spectrum (m/z 1800−4200) including 10 microscans was acquired in positive ion-mode. The nominal MS resolution was set to 17 500 at full width at half-maximum at m/z 200. A target value of 3.00 × 10⁶ ions was selected for the automatic gain control setting with a maximum inject time of 150 ms. The other MS parameters were the following: spray voltage at 3.2 kV, capillary temperature at 275 °C, heater temperature at 350 °C, S-lens rf level at 80 V, sheath and auxiliary gas flow rate at 35 and 10 arbitrary units, respectively. The orbitrap's mass accuracy was ≤1 ppm with an effective average resolution ≥3600 over the calibrated mass range on each day of analysis using sodium iodide.

Data Processing. The LC−HRMS system was controlled by XCalibur v2.2 (Thermo Fisher Scientific). The six most
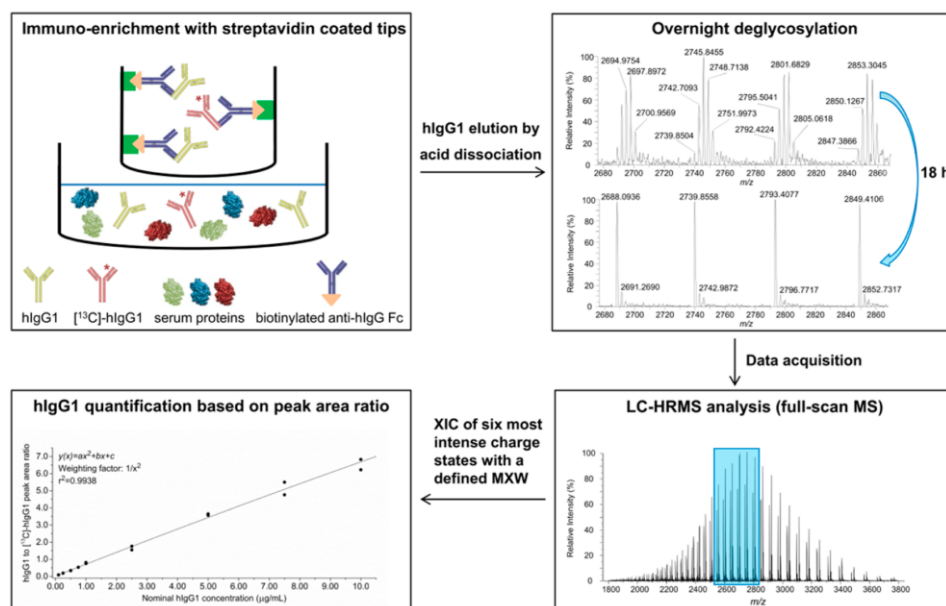
Figure 1. General scheme of the proposed hybrid LBA-LC−HRMS-based workflow using immuno-enrichment with streptavidin coated tips being loaded with a biotinylated anti-hIgG Fc capture antibody, hIgG1 and spiked [^{13}C]-hIgG1 extraction from rat serum, hIgG1s elution from the tips followed by full-scan MS acquisition and intact hIgG1 quantification using the XIC approach based on the peak area ratio.

intense charge states for each hIgG1 were extracted in LCquan v2.7 (Thermo Fisher Scientific) using a mass extraction window (MXW) of 2 m/z units with a mass tolerance of 5 ppm: hIgG1A [m/z 2543−2545 (56+), 2589−2591 (55+), 2637−2639 (54+), 2687−2689 (53+), 2739−2741 (52+), 2792−2794 (51+)]; [^{13}C]-hIgG1A [m/z 2556−2558 (56+), 2602−2604 (55+), 2651−2653 (54+), 2701−2703 (53+), 2752−2754 (52+), 2806−2808 (51+)]; and hIgG1B [m/z 2678−2680 (54+), 2729−2731 (53+), 2781−2783 (52+), 2836−2838 (51+), 2893−2895 (50+), 2952−2954 (49+)]. The resultant XICs were summed up and integrated in order to obtain an area under the curve. MS spectra were deconvoluted with the Protein Deconvolution software 4.0 (Thermo Fisher Scientific) using the ReSpect algorithm for isotopically unresolved spectra. The input mass range was set from m/z 2400−3400 covering in total 18 charge states whereas the output mass range was restricted to 142−146 kDa with a noise rejection confidence interval of 95%.

LC−MS/MS Method for hIgG1A Quantification at the Peptide Level. The hIgG1A was immuno-enriched from rat serum with streptavidin coated magnetic beads previously loaded with a biotinylated mouse anti-hIgG Fc capture antibody, reduced and alkylated prior to tryptic digestion. A solid phase extraction was conducted prior to LC−MS/MS analysis using an API 6500 linear quadrupole ion trap mass spectrometer from AB Sciex (Framingham, MA). A detailed protocol for the sample preparation and complete LC−MS/MS settings (Table S-1) are provided in the Supporting Information.

RESULTS AND DISCUSSION

General Workflow for Intact hIgG1 Quantification. In order to address the current need for accurate hIgG1 quantification at the intact protein level in biological fluids, a hybrid LBA-LC-HRMS-based workflow was developed (Figure 1). Hybridizing LBA to LC−HRMS combines the advantage of a selective target enrichment from complex biological matrixes resulting in a significant sensitivity gain by reducing the background noise whereas further specificity is introduced by high-resolution quantification as outlined previously.[30] In our workflow, the [^{13}C]-hIgG1A was added to the rat serum samples right at the beginning of the sample preparation in order to compensate for any possible losses during extraction or different ionization efficiencies during HRMS analysis. The fact that a biotinylated mouse anti-hIgG Fc capture antibody was used for hIgG1 enrichment, the sample preparation is applicable to all hIgG-based therapeutic proteins bearing the Fc region. The incorporation of an overnight deglycosylation step with PNGase F after hIgG1 elution from the tips resulted in a less complex full-scan MS spectrum (Figure 1, upper right panel) increasing the signal for each charge state significantly which further improved the selectivity and sensitivity of our assay. Of note, the postelution deglycosylation step can also be omitted, e.g., when active or inactive glycan forms are of analytical interest. However, this might compromise the assay's sensitivity. In the end, the intact hIgG1 quantification was performed on the peak area ratio of the target hIgG1 and the [^{13}C]-hIgG1A after ion chromatogram extraction using a defined mass extraction window (MXW).

MS Deconvolution versus XIC Approach. A typical hIgG1 charge state envelope (38+ to 73+) was obtained in the full-scan MS spectrum after injecting a reference solution containing an equimolar amount of hIgG1A and [^{13}C]-hIgG1A (Figure 2A). In the present work, two approaches were tested for intact hIgG1 quantification. In the first one based on MS deconvolution (18 charge states, 42+ to 59+), the most intense intact MS signals were attributed to the deglycosylated hIgG1A and [^{13}C]-hIgG1A forms whereas two other remaining minor
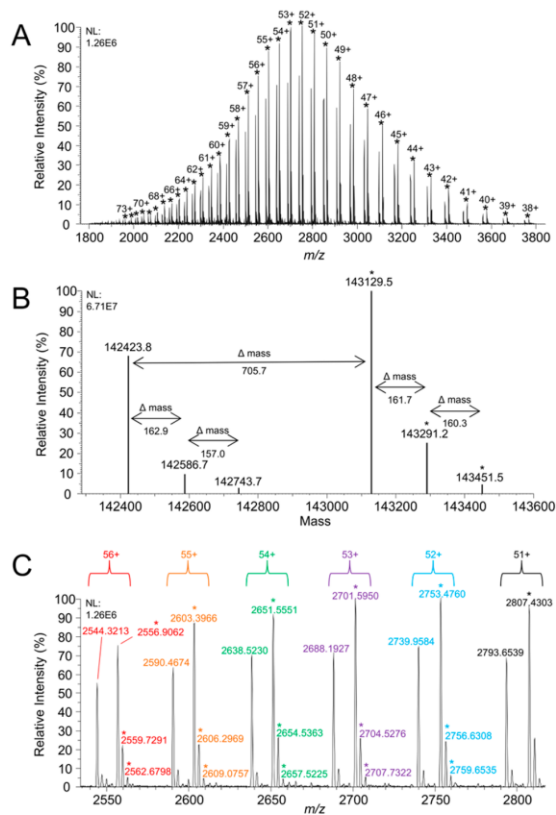
Figure 2. MS spectrum of hIgG1A and [13C]-hIgG1A reference solution at 0.500 mg/mL (2 μL injected). (A) Full-scan MS spectrum, (B) deconvoluted MS spectrum, and (C) zoom into 51+ to 56+ charge states used for XIC approach. Asterisks indicate charge states corresponding to [13C]-hIgG1A.

signals represented the residual glycoforms due to incomplete overnight deglycosylation (Figure 2B). A complete deglycosylation can be achieved (if required) either with a longer incubation time (>18 h) or larger amounts of enzyme added. However, this will increase the analysis cost and decrease the sample throughput. The experimental intact mass of the deglycosylated hIgG1A (142423.8 ± 6.0 Da) exhibited an accuracy of 42 ppm compared to its theoretical intact mass. The mass difference of the deglycosylated signals between the hIgG1A and its [13C]-labeled version was 706 Da indicating no overlapping intact masses (Figure 2B). An acceptable linearity with a coefficient of determination (r^2-value) of 0.9825 was observed over the calibration range from 0.100 to 10.0 μg/mL by plotting the peak height ratio of the deconvoluted MS signals of hIgG1A to [13C]-hIgG1A against the nominal hIgG1A concentration (Table S-2). However, the accuracy (% bias) obtained on the low QC concentrations did not meet the acceptance of ±20% [±25% at the lower limit of quantification (LLOQ)] with a maximum bias of 58.2%. Consequently, the method's LLOQ would have been increased even though the selectivity (analytical response 5-fold higher compared to blank serum sample) and precision [expressed by the coefficient of variation (CV), ≤20% CV and ≤25% CV at the LLOQ] met the acceptance criteria. The inaccuracy can be

explained by the fact that the deconvolution process was impacted by the weak MS signal at low concentrations. As a second option for intact hIgG1 quantification, ion chromatograms from several individual charge states were extracted from the full-scan MS with a defined MXW (XIC approach). The zoom into the most abundant charge states (51+ to 56+) revealed a mass shift of approximately 13 m/z units between the deglycosylated hIgG1A and [13C]-hIgG1A for each charge state (Figure 2C). Similar to the deconvolution approach, inaccurate data were obtained at the low QC concentrations using the peak height ratio of hIgG1A to [13C]-hIgG1A plotted against the hIgG1A concentration regardless of the number of charge states used for the XIC approach (Table S-2). However, accurate and precise data were obtained on QC samples when the ratio of the peak area instead of the peak height was used (Table 1). Consequently, the XIC approach based on the peak area ratio was selected for further investigations.

Table 1. Accuracy and Precision Data Obtained in QC Samples Spiked with hIgG1A Based on the Peak Area Ratio Using the XIC Approach with Different Numbers of Charge States and a MXW Width of 2 m/z Units[a]

		nominal QC concentration in rat serum (μg/mL)			
		8.00	5.00	0.250	0.100
no. of charge states		intraday accuracy and precision (n = 3)			
3 (51+ to 53+)	mean concentration (μg/mL)	8.70	5.44	0.273	0.109
r^2 = 0.9891	intraday accuracy (% bias)	8.7	8.7	9.4	9.0
	intraday precision (% CV)	3.2	11.3	8.4	1.9
6 (51+ to 56+)	mean concentration (μg/mL)	8.09	5.45	0.265	0.112
r^2 = 0.9932	intraday accuracy (% bias)	1.1	9.0	5.9	12.3
	intraday precision (% CV)	3.6	3.5	4.1	6.7
9 (48+ to 56+)	mean concentration (μg/mL)	8.51	5.55	0.289	0.115
r^2 = 0.9876	intraday accuracy (% bias)	6.4	11.0	15.6	15.4
	intraday precision (% CV)	6.1	3.9	3.4	7.7
18 (42+ to 59+)	mean concentration (μg/mL)	8.32	5.53	0.291	0.119
r^2 = 0.9928	intraday accuracy (% bias)	4.0	10.6	16.6	19.2
	intraday precision (% CV)	6.2	1.0	1.6	3.3

[a]Coefficient of determination (r^2-value) indicated linearity of calibration standards for each approach.

Effect of the Number of Charge States Selected for XIC Approach. Even though a high specificity was associated with a large number of charge states used for the XIC approach, the less intense charge states tend to disappear within the background noise with the decreasing concentrations of hIgG1 which could impact the assay's accuracy and precision. Thus, the linearity of Cs samples as well as the accuracy and precision for QC samples were compared when the hIgG1A was
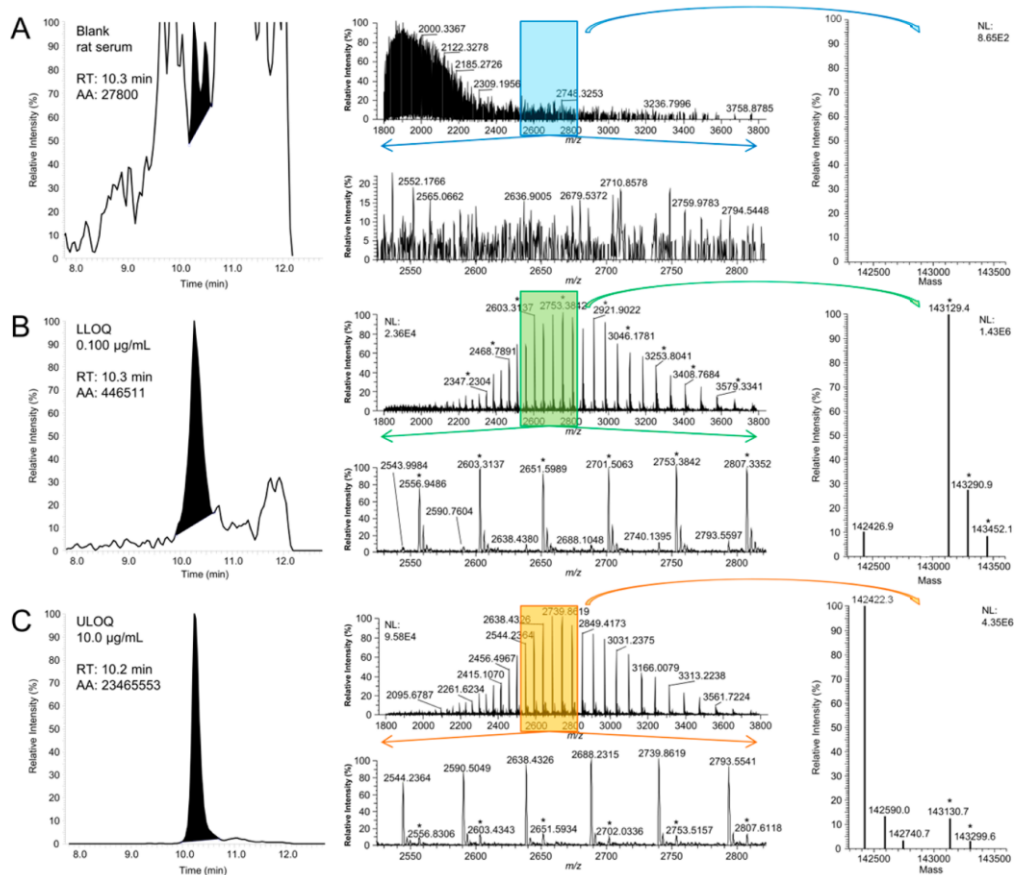
Figure 3. Sum of six individual XICs (51+ to 56+; left panel), full-scan MS spectrum (upper middle panel) and zoom into six most abundant charge states (51+ to 56+; lower middle panel) as well as the deconvoluted MS spectrum (42+ to 59+ used for deconvolution; right panel) for (A) blank rat serum sample, (B) LLOQ sample at 0.100 μg/mL, and (C) ULOQ sample at 10.0 μg/mL. Asterisks indicate charge states corresponding to [^{13}C]-hIgG1A.

quantified based on the peak area ratio using either 3, 6, 9, or 18 charge states for ion chromatogram extraction. The data from this investigation suggested that the number of charge states did not impact the assay's accuracy and precision as all QCs were within the defined acceptance criteria (Table 1). It should be noted that a trend toward more inaccurate data was observed at the LLOQ QC sample with a higher number of charge states used for the XIC approach. Another parameter being considered was the width of the MXW. In case of a complete deglycosylation, the theoretical maximum MXW width would be 26 m/z units as the difference in m/z values between the deglycosylated hIgG1A and [^{13}C]-hIgG1A signal for the same charge state (e.g., 51+) was approximately 13 m/z units (Figure 2C). However, as the overnight deglycosylation was incomplete, the m/z difference per charge state between the deglycosylated and the remaining glycoforms was approximately 3 m/z units allowing only a limited MXW width of maximum 6 m/z units (Figure 2C). Higher MXW widths (e.g., 8 m/z units) resulted in inaccurate data, as both deglycosylated isoform and glycan forms were extracted to a certain extend for each charge state (Table S-3). Hence a MXW width of 2 m/z units was selected for the XIC approach using

six charge states (51+ to 56+) exhibiting the best linearity (r^2-value) as well as accurate and precise results (Table 1). No significant interference was observed at the retention time of the hIgG1A in blank rat serum under these XIC conditions (Figure 3A) whereas a significant peak above the background noise was detected at the LLOQ of 0.100 μg/mL (Figure 3B). Two typical hIgG1 charge state envelopes were observed in the full-scan MS spectrum of the LLOQ with a higher signal for the [^{13}C]-hIgG1A (upper middle MS spectrum in Figure 3B) whereas the hIgG1A charge states were still detected to a minor extend (lower middle MS spectrum in Figure 3B). In order to check that the charge state envelopes corresponded to the actual hIgG1s, the MS spectrum was deconvoluted (right MS spectrum in Figure 3B). The observed intact masses for the deglycosylated hIgG1A (142426.9 ± 8.3 Da) at the LLOQ and the [^{13}C]-hIgG1A (143129.4 ± 4.8 Da) at the working concentration differed from its experimental reference masses (Figure 2B) by 22 ppm and >−1 ppm, respectively, confirming the clear distinction of the target hIgG1s from other endogenous rat serum proteins. The most intense signals in the full-scan MS spectrum of the sample at the upper limit of quantification (ULOQ) originated from the hIgG1A with

Table 2. Summary of Hybrid LBA-LC−HRMS Method Validation for Intact hIgG1A Quantification in Rat Serum

parameter	results
selectivity: three blank batches ($n = 3$)	hIgG1A: ≤3.0%, [^{13}C]-hIgG1A: ≤0.3%
contribution of signal	[^{13}C]-hIgG1A to hIgG1A: 12.8%, hIgG1A to [^{13}C]-hIgG1A: 13.0%
linearity ($n = 3$), $y = ax^2 + bx + c$, $1/x^2$ weighting	0.100−10.0 μg/mL, $r^2 = 0.9919 \pm 0.0027$
carry-over (blank after ULOQ sample)	hIgG1A: <LLOQ, [^{13}C]-hIgG1A: 0.0% of response in zero sample
accuracy (% bias) and precision (% CV)	intraday ($n = 3$): −2.7 to 16.0% bias, 1.3 to 11.7% CV
QC at 0.100, 0.250, 5.00, and 8.00 μg/mL	interday ($n = 9$): −0.1 to 9.3% bias, 6.1 to 8.7% CV
dilution linearity (300 μg/mL, 50-fold, $n = 5$)	mean bias of 2.9% with precision of 8.6% CV
reproducibility	97% of incurred samples ($n = 30$) met acceptance criterion of ±20%

minor signals for the [^{13}C]-hIgG1A (Figure 3C). The deconvoluted MS spectrum proved once more that the hIgG1A was measured with a mass accuracy of −11 ppm (mass of deglycosylated isoform, 142422.3 ± 5.1 Da) whereas the deglycosylated [^{13}C]-hIgG1A signal (143130.7 ± 5.9 Da) deviated by 8 ppm from its reference spectrum (Figure 2B).

Method Validation. The developed hybrid LBA-LC−HRMS-based workflow for intact hIgG1 quantification was successfully validated in terms of selectivity, sensitivity, accuracy/precision, carry-over, dilution linearity, and reproducibility. The method validation data are summarized in Table 2 meeting acceptance from international guidance.[31−33] A detailed description for each individual parameter including its acceptance criteria and the corresponding raw data can be extracted from the Supporting Information (Tables S-4−S-9).

Comparison of hIgG1A Quantification at the Intact Protein and Peptide Level. For the *in vivo* samples ($n = 24$), a good linear correlation with a Pearson's r-value of 0.9546 was observed when the hIgG1A concentration was determined either at the intact protein or the peptide level (Figure 4A). The corresponding Passing-Bablok regression was almost ideal with a slope of 0.9913 and an intercept of 0.0430 (dashed red line). As the confidence intervals for the slope enclosed the optimal value of 1, no significant proportional difference existed statistically between the concentrations obtained from intact hIgG1 quantification or from peptide level quantification. Both methods did not differ from any constant amount of bias, as the 95% confidence interval for the intercept of the linear regression included each time the zero value. An excellent method agreement was obtained with the *in vivo* samples, as only one of the preclinical study samples was located outside the 95% limits of agreements (from −22.7 to 25.8%) whereas the mean bias ($n = 24$) between both methods was only 1.6% (Figure 4B). A similar trend was also obtained with the *in vitro* rat serum samples (Figure S-1 and Table S-10). This demonstrated that the developed hybrid LBA-LC−HRMS-based workflow at the intact protein level leads to at least equivalent results for hIgG1 quantification compared to the conventional LC−MS/MS analysis at the peptide level with the additional advantage of reduced sample pretreatment.

Multiplexing Capabilities of Developed Hybrid LBA-LC−HRMS-Based Workflow. Simultaneous quantification of different hIgGs exhibiting minor changes in amino acid sequences can also be conducted directly at the intact protein level and is not only limited to peptide level analysis as described earlier.[34] In order to demonstrate the multiplexing capability of our method, two different hIgG1s (hIgG1A and hIgG1B) were spiked in the same rat serum sample. Both target hIgG1s were baseline separated from each other after a slight modification of the LC gradient (Figure 5A). The peak at 7.7 min contained the hIgG1A and [^{13}C]-hIgG1A whereas the
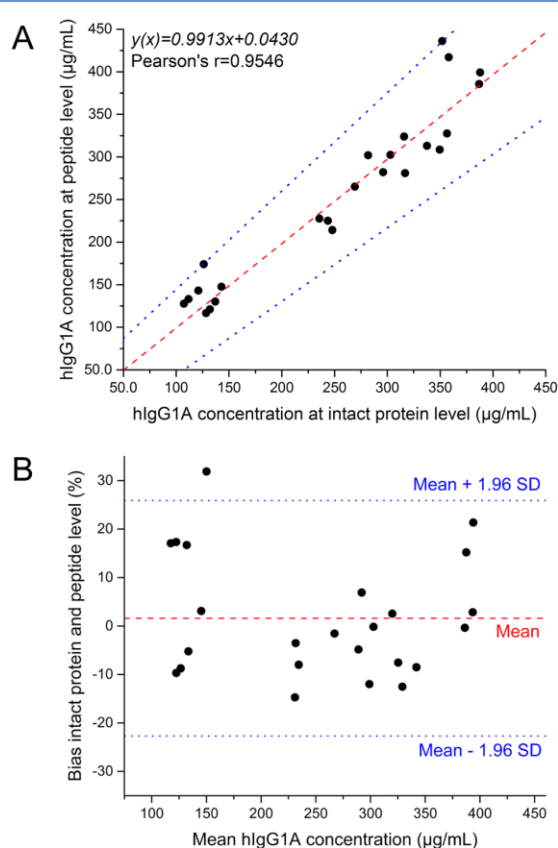
Figure 4. Comparison of measured hIgG1A concentration either at the intact protein or peptide level using rat PK study samples ($n = 24$). (A) Correlation plot with linear regression (dashed red line) and 95% confidence intervals from Passing-Bablok regression (dotted blue lines) and (B) Bland-Altman plot with 95% limits of agreement (dotted blue lines, mean bias ±1.96 standard deviation) for assessment of agreement between both analytical approaches. The concentration difference between the intact protein and peptide level divided by the mean concentration was used to calculate the bias.

hIgG1B eluted at 8.2 min. Both hIgG1s were quantified in parallel using our previously described optimized XIC approach with the [^{13}C]-hIgG1A as internal standard for both hIgG1s. As the PNGase F was coeluting with hIgG1B, ion suppression occurred in the HESI source resulting in a decreased signal in the full-scan MS spectrum and consequently a higher LLOQ (0.250 μg/mL) compared to the one for hIgG1A (0.100 μg/mL). The linearity obtained for Cs samples on three
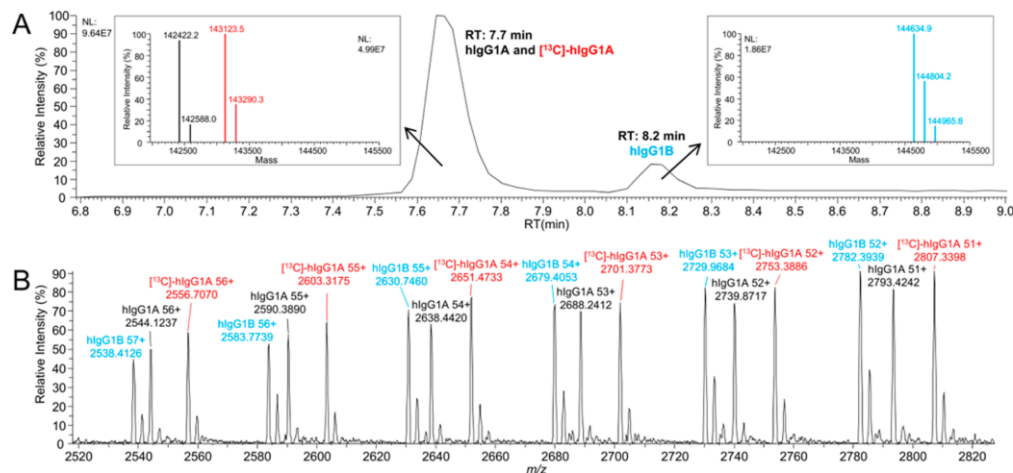
Figure 5. Multiplexing of different cospiked hIgG1s (hIgG1A and hIgG1B) in rat serum using [^{13}C]-hIgG1A as internal standard. (A) Total ion chromatogram using a ProSwift RP-4H monolithic column. Inlets showing deconvoluted MS spectrum for each peak. (B) Zoom into full-scan MS spectrum of coeluting hIgG1s in case no separation is achieved.

Table 3. Interday Accuracy and Precision of QC Samples in Rat Serum Spiked with hIgG1A, hIgG1B, and [^{13}C]-hIgG1A Used As Internal Standard for Both hIgG1s over Three Nonconsecutive Days during Multiplexing Studies[a]

		nominal QC concentration in rat serum (µg/mL)			
		8.00	5.00	0.250	0.100
therapeutic protein		interday accuracy and precision (n = 9)			
hIgG1A, RT 7.7 min	mean concentration (µg/mL)	8.21	5.38	0.276[c]	0.110
r^2 = 0.9891 ± 0.0009	interday accuracy (% bias)	2.6	7.6	10.4	10.2
	interday precision (% CV)	8.8	5.2	7.5	7.3
hIgG1B[b], RT 8.2 min	mean concentration (µg/mL)	7.92[c]	5.04	0.254	-
r^2 = 0.9840 ± 0.0063	interday accuracy (% bias)	−1.0	0.9	1.6	-
	interday precision (% CV)	9.8	8.1	9.6	-

[a]The coefficient of determination (r^2-value) indicates the linearity of calibration standards obtained over these days. [b]LLOQ was set to 0.250 µg/mL. [c]n = 8, one replicate did not meet accuracy acceptance criterion of ±20% and was excluded from calculations.

nonconsecutive days was acceptable with a r^2-value of 0.9891 and 0.9840 for hIgG1A and hIgG1B, respectively (Table 3). The interday accuracy (n = 9, three replicates per concentration on 3 days) of hIgG1B ranging from −1.0 to 1.6% bias was slightly better compared to the hIgG1A one with a maximum bias of 10.4% (Table 3). Nevertheless, the acceptance criterion of ±20% and ±25% at the LLOQ was met for both hIgG1s. The corresponding interday precision data met also acceptance not only for hIgG1A but also for the cospiked hIgG1B in rat serum on 3 days with a maximum of 8.8 and 9.8% CV, respectively. Thus, we clearly demonstrate here the multiplexing capabilities of our hybrid LBA-LC−HRMS-based workflow which affords a simultaneous quantification of multiple coadministrated or *in vivo* generated hIgG1s at an intact protein level. In addition, our method can be extended for the quantification of different hIgG1s that would not be chromatographically separated. Indeed for coeluting hIgG1s the specific identification for each hIgG1 is provided through accurate mass measurement by the power of HRMS (Figure 5B).

■ **CONCLUSIONS**

Here we report an innovative, generic, and sensitive fully automated hybrid LBA-LC−HRMS-based workflow for the simultaneous quantitative analysis of intact hIgG1s originating from rat serum in one single run. The six most intense charge states of each hIgG1 were extracted from the nondeconvoluted full-scan MS spectrum using a defined MXW. Consistent data were obtained between our hybrid LBA-LC−HRMS method at the intact hIgG1 level and the conventional quantitative LC−MS/MS analysis using surrogate peptides with additional advantages. The first major benefit associated with our workflow is a less tedious sample preparation, as only a postelution deglycosylation step was required prior to LC−HRMS analysis. Consequently, less artifactual modifications (e.g., deamidated peptides) are generated as neither a reduction/alkylation at elevated temperatures nor a tryptic digestion at suboptimal pH conditions is required. The second advantage of our methodology is that potential product variants of bispecific formats or antibody-drug conjugates (ADCs) bearing different amount of payloads can be distinguished from each other using either specific nonoverlapping *m/z* values or different intact masses for quantification which is currently impossible at the peptide level. Finally, besides the quantitative data, structural information can also be derived in parallel revealing any kind of modifications at the intact protein level in order to get some insights on the biotransformation of hIgGs, bispecific mAbs, ADCs or dual payload conjugated ADCs (e.g.,

changes in drug-to-antibody ratio over the PK profile). In summary, this innovative hybrid LBA-LC−HRMS-based workflow appears very attractive for the combined quantitative and qualitative analysis of new generation biotherapeutics and would greatly reduce the number of samples to be collected accelerating the development of such compounds further.

■ ASSOCIATED CONTENT

ⓈSupporting Information

The Supporting Information is available free of charge on the ACS Publications website at DOI: 10.1021/acs.analchem.6b04997.

LC−MS/MS method description for hIgG1A quantification, validation raw data for hIgG1A quantification at the intact protein level and *in vitro* comparison (PDF)

■ AUTHOR INFORMATION

Corresponding Author
*Phone: +41 79 53 59 611. Fax: +41 61 696 85 84. E-mail: olivier.heudi@novartis.com.

ORCID ⃝
Christian Lanshoeft: 0000-0002-2405-0227

Notes

■ ACKNOWLEDGMENTS

■ REFERENCES

(1) Jourdil, J. F.; Lebert, D.; Gautier-Veyret, E.; Lemaitre, F.; Bonaz, B.; Picard, G.; Tonini, J.; Stanke-Labesque, F. *Anal. Bioanal. Chem.* **2017**, *409*, 1195.

(2) Qu, M.; An, B.; Shen, S.; Zhang, M.; Shen, X.; Duan, X.; Balthasar, J. P.; Qu, J. *Mass Spectrom. Rev.* **2016**, DOI: 10.1002/mas.21500.

(3) van den Broek, I.; Niessen, W. M.; van Dongen, W. D. *J. Chromatogr. B: Anal. Technol. Biomed. Life Sci.* **2013**, *929*, 161−179.

(4) Zheng, J.; Mehl, J.; Zhu, Y.; Xin, B.; Olah, T. *Bioanalysis* **2014**, *6*, 859−879.

(5) Budhraja, R.; Shah, M.; Suthar, M.; Yadav, A.; Shah, S.; Kale, P.; Asvadi, P.; Valan Arasu, M.; Al-Dhabi, N.; Park, C.; Kim, Y.-O.; Kim, H.; Agrawal, Y.; Krovidi, R. *Molecules* **2016**, *21*, 1464.

(6) Heudi, O.; Barteau, S.; Zimmer, D.; Schmidt, J.; Bill, K.; Lehmann, N.; Bauer, C.; Kretz, O. *Anal. Chem.* **2008**, *80*, 4200−4207.

(7) Iwamoto, N.; Umino, Y.; Aoki, C.; Yamane, N.; Hamada, A.; Shimada, T. *Drug Metab. Pharmacokinet.* **2016**, *31*, 46−50.

(8) Furlong, M. T.; Ouyang, Z.; Wu, S.; Tamura, J.; Olah, T.; Tymiak, A.; Jemal, M. *Biomed. Chromatogr.* **2012**, *26*, 1024−1032.

(9) Lanshoeft, C.; Wolf, T.; Walles, M.; Barteau, S.; Picard, F.; Kretz, O.; Cianférani, S.; Heudi, O. *J. Pharm. Biomed. Anal.* **2016**, *131*, 214−222.

(10) Li, H.; Ortiz, R.; Tran, L.; Hall, M.; Spahr, C.; Walker, K.; Laudemann, J.; Miller, S.; Salimi-Moosavi, H.; Lee, J. W. *Anal. Chem.* **2012**, *84*, 1267−1273.

(11) Li, W.; Lin, H.; Fu, Y.; Flarakos, J. *J. Chromatogr. B: Anal. Technol. Biomed. Life Sci.* **2017**, *1044-1045*, 166−176.

(12) Lanshoeft, C.; Wolf, T.; Heudi, O.; Cianférani, S.; Barteau, S.; Walles, M.; Picard, F.; Kretz, O. *Anal. Bioanal. Chem.* **2016**, *408*, 1687−1699.

(13) Fung, E. N.; Xia, Y.-q.; Aubry, A.-F.; Zeng, J.; Olah, T.; Jemal, M. *J. Chromatogr. B: Anal. Technol. Biomed. Life Sci.* **2011**, *879*, 2919−2927.

(14) Huang, M. Q.; Lin, Z. J.; Weng, N. *Bioanalysis* **2013**, *5*, 1269−1276.

(15) Zhang, Z.; He, L.; Lu, L.; Liu, Y.; Dong, G.; Miao, J.; Luo, P. *J. Pharm. Biomed. Anal.* **2015**, *109*, 62−66.

(16) Dillen, L.; Cools, W.; Vereyken, L.; Lorreyne, W.; Huybrechts, T.; de Vries, R.; Ghobarah, H.; Cuyckens, F. *Bioanalysis* **2012**, *4*, 565−579.

(17) Morin, L. P.; Mess, J. N.; Garofolo, F. *Bioanalysis* **2013**, *5*, 1181−1193.

(18) Ramagiri, S.; Garofolo, F. *Bioanalysis* **2012**, *4*, 529−540.

(19) Gucinski, A. C.; Boyne, M. T., 2nd *Anal. Chem.* **2012**, *84*, 8045−8051.

(20) Kellie, J. F.; Kehler, J. R.; Szapacs, M. E. *Bioanalysis* **2016**, *8*, 169−177.

(21) Kim, Y. J.; Gallien, S.; El-Khoury, V.; Goswami, P.; Sertamo, K.; Schlesser, M.; Berchem, G.; Domon, B. *Proteomics* **2015**, *15*, 3116−3125.

(22) Mekhssian, K.; Mess, J. N.; Garofolo, F. *Bioanalysis* **2014**, *6*, 1767−1779.

(23) Kellie, J. F.; Kehler, J. R.; Mencken, T. J.; Snell, R. J.; Hottenstein, C. S. *Bioanalysis* **2016**, *8*, 2103−2114.

(24) Ladwig, P. M.; Barnidge, D. R.; Willrich, M. A. V. *J. Am. Soc. Mass Spectrom.* **2016**, 1−7.

(25) Liu, H.; Manuilov, A. V.; Chumsae, C.; Babineau, M. L.; Tarcsa, E. *Anal. Biochem.* **2011**, *414*, 147−153.

(26) van den Broek, I.; van Dongen, W. D. *Bioanalysis* **2015**, *7*, 1943−1958.

(27) Jian, W.; Kang, L.; Burton, L.; Weng, N. *Bioanalysis* **2016**, *8*, 1679−1691.

(28) Macchi, F. D.; Yang, F.; Li, C.; Wang, C.; Dang, A. N.; Marhoul, J. C.; Zhang, H. M.; Tully, T.; Liu, H.; Yu, X. C.; Michels, D. A. *Anal. Chem.* **2015**, *87*, 10475−10482.

(29) Buscher, B.; Toersche, J.; van Holthoon, F.; Kleinnijenhuis, A. *J. Res. Anal.* **2015**, *1*, 01−08.

(30) Ramagiri, S.; Moore, I. *Bioanalysis* **2016**, *8*, 483−486.

(31) U.S. Food and Drug Administration. *Guidance for Industry: Bioanalytical Method Validation*, May 2001; http://www.fda.gov/downloads/Drugs/Guidance/ucm070107.pdf (accessed December 14, 2016).

(32) European Medicines Agency. *Guideline on Bioanalytical Method Validation*, July 2011; http://www.ema.europa.eu/docs/en_GB/document_library/Scientific_guideline/2011/08/WC500109686.pdf (accessed December 14, 2016).

(33) Jenkins, R.; Duggan, J. X.; Aubry, A. F.; Zeng, J.; Lee, J. W.; Cojocaru, L.; Dufield, D.; Garofolo, F.; Kaur, S.; Schultz, G. A.; Xu, K.; Yang, Z.; Yu, J.; Zhang, Y. J.; Vazvaei, F. *AAPS J.* **2015**, *17*, 1−16.

(34) Lebert, D.; Picard, G.; Beau-Larvor, C.; Troncy, L.; Lacheny, C.; Maynadier, B.; Low, W.; Mouz, N.; Brun, V.; Klinguer-Hamour, C.; Jaquinod, M.; Beck, A. *Bioanalysis* **2015**, *7*, 1237−1251.

3.3 Combined qualitative and quantitative analysis of intact ADCs

3.3.1 Analytical context

While IC-LC-HRMS-based approaches at the subunit or intact level are applied for qualitative *in vivo* DLD/DAR profiling of site specific,[554-557] cysteine,[558,559] and lysine-conjugated ADCs,[560] the assessment of ADC PK properties is still routinely realized using bottom-up MS or LBA-based assays. However, both platforms require at least two specific capture antibodies in order to discriminate between the total mAb (*e.g.* anti-hIgG Fc) and total ADC concentration (*e.g.* anti-payload).[194,561] Moreover, neither quantitative bottom-up MS nor LBA-based approaches are capable to distinguish between individual ADC drug load species bearing different amounts of cytotoxic payloads. In contrast, intact ADC analysis by IC-LC-HRMS would theoretically allow the quantification of individual ADC drug load species in addition to the determination of the total mAb and total ADC concentration, using only one generic antibody-targeting capture antibody.

3.3.2 Objective

This project aimed to demonstrate the potential of IC-LC-HRMS for a combined qualitative and quantitative analysis of intact lysine-conjugated ADCs in rat serum samples.

3.3.3 Experimental

3.3.3.1 Chemicals and reagents

The ADC1 (MCC-DM1 construct), its tritiated version ([³H]-ADC1), ADC2 (sulfo-SPDB-DM4 construct), the mouse anti-hIgG Fc and anti-maytansinoid capture antibodies, and the hIgG1 used as ISTD were produced at Novartis Pharma AG (Basel, Switzerland). BupH modified Dulbecco's PBS (0.1 M sodium phosphate, 0.15 M sodium chloride, pH 7.2) and magnetic beads (Pierce) were obtained from Thermo Fisher Scientific (Waltham, MA, USA). Tween 20, 2N hydrochloric acid, TFA, bovine serum albumin (BSA), isopropanol, ammonium bicarbonate, methanol, ACN, and MS grade water were purchased from Sigma-Aldrich (Buchs, Switzerland). FA and sodium iodide were provided by Merck (Darmstadt, Germany) and Waters (Milford, MA, USA), respectively. PNGase F, IgGZERO, and Remove-It PNGase F were obtained from Promega (Madison, WI, USA), Genovis (Lund, Sweden), and New England Biolabs Inc. (Ipswich, MA, USA), respectively. Ultima Gold XR scintillation cocktail and Solvable solution were purchased from Perkin Elmer (Waltham, MA, USA). All LC-MS grade solvents as well as reagents were of high analytical grade (≥99%) and were used without any further purification. Blank rat serum for Cs/QCs preparation was received from Fisher Clinical Services (Allschwil, Switzerland).

3.3.3.2 Cs/QCs preparation

The ADC1 and ADC2 stock solutions (each at 10.0 mg/mL) were diluted in PBS to obtain a final working concentration of 1.00 mg/mL. Afterwards, the working solution was spiked into blank rat serum, resulting in eight different Cs concentrations at 150, 120, 100, 80.0, 60.0, 40.0, 25.0, and 10.0 µg/mL after serial dilution. The four corresponding QC concentrations at 125, 75.0, 25.0, and 10.0 µg/mL were prepared in the same manner.

3.3.3.3 ADC1 stability study in rat serum

The ADC1 was spiked into two different batches of blank rat serum and additionally in surrogate matrix (PBS+0.5% BSA). Another set of samples was prepared by spiking the hIgG1 as positive control in both batches of blank rat serum. Afterwards, aliquots (100 µL) were incubated at 37 °C, while shaking at 600 rpm on a ThermoMixer (Eppendorf, Hamburg, Germany). After defined time points (0, 1, 6, 24, 30, 48, 72, and 168 h) samples were removed and stored at ≤−20 °C pending analysis.

3.3.3.4 ADC2 *in vivo* PK study

Three individual female Han Wistar rats were dosed intravenously with the ADC2 at 5.00 mg/kg. Blood (250 µL) was drawn into serum collection tubes after puncturing of the sublingual vein at pre-dose as well as 1, 24, 72, and 168 h after the first dose. Additional samples (1 and 168 h) were collected following the second dose on day 8. The collected blood was allowed to clot upright at room temperature for 1 h prior to centrifugation at 2500 g and 4 °C for 10 min. The resulting serum was shipped to the analytical lab and stored ≤−70 °C pending analysis. The pre-clinical study was conducted in accordance to the Guide for the Care and Use of Laboratory Animals and in compliance with the Novartis Animal Care and Use Committee, the Animal Welfare Act, and the Office of Laboratory Animal Welfare.

3.3.3.5 [^{3}H]-ADC1 extraction recovery determination

The total volume including the pipette tip was transferred at each sampling step into a 20 mL liquid scintillation counting vial (Perkin Elmer). The volume was evaporated to dryness at 60 °C to remove tritiated water. Afterwards, 500 µL of Solvable/isopropanol (2/1, v/v) was added to each sample and was incubated at 60 °C for 2 h. In a next step, the samples were neutralized with 200 µL of 2N hydrochloric acid and 15 mL of Ultima Gold XR scintillation cocktail was added to each vial. After short agitation, the samples were analyzed up to 5 min on a 2200CA Tri-Carb liquid scintillation counter (Perkin Elmer).

3.3.3.6 Magnetic bead preparation

For 35 samples, a volume of 1.3 mL of streptavidin-coated magnetic beads (10.0 mg/mL) was placed in a 2.0 mL Protein LoBind tube (Eppendorf) and was washed twice with 1.5 mL of PBS containing 0.05% Tween 20 (assay buffer). Afterwards, the beads were reconstituted in 1.7 mL of assay buffer and were incubated with an excess of biotinylated mouse anti-hIgG Fc capture antibody (62 µg/mg beads) for 2 h at room temperature using an end-over-end mixer. In a final step, magnetic beads were rinsed twice with 1.5 mL of assay buffer to remove unbound capture antibody followed by re-suspension in the initial volume. In case of additional samples, each volume was adapted accordingly.

3.3.3.7 Deglycosylation, IC, and elution

Rat serum sample (50 µL) was placed into a 500 µL Protein LoBind 96-well plate (Eppendorf) and was spiked with 10 µL of hIgG1 in PBS solution, resulting in a final hIgG1 concentration of 5.00 µg/mL. For blank samples, 10 µL of PBS was added as ISTD replacement. The samples were deglycosylated overnight on a ThermoMixer at 37 °C and 800 rpm using 4 µL of PNGase F/50 mM ammonium bicarbonate (1/4, v/v, 8 u/sample, pH≈7). The next day, capture antibody-containing magnetic bead solution (35 µL) was pipetted to each sample and was incubated at room temperature for additional 2 h on the ThermoMixer, while shaking at 900 rpm. After IC, four washing steps with 2 x 100 µL assay buffer or water were incorporated in the sample preparation prior to ADC and hIgG1 elution from the beads using 55 µL of 2% FA in 10% methanol for 15 min at 750 rpm. In a last step, the samples were transferred into a 200 µL ABgene V-bottom 96-well plate (Thermo Fisher Scientific) and were centrifuged at 1500 rpm for 5 min prior to LC-HRMS analysis.

3.3.3.8 LC-HRMS analysis

Forty microliters of sample were loaded onto a Waters MassPREP Micro Desalting Column (2.1 x 5 mm, 20 µm, 1000 Å), which was maintained at 40 °C. For chromatographic separation, acidified (0.1% FA) water and ACN were used as mobile phases A and B, respectively. The binary elution gradient program with a flow rate of 400 µL/min was set as follows: 0.0-2.0 min, 5% B; 2.0-3.5 min, 5-80% B; 3.5-5.0 min, 80% B; 5.0-5.5 min, 80-5% B; 5.5-10.0 min, 5% B. The ACQUITY UPLC I-Class system was hyphenated to a SYNAPT G2-Si QTOF HD high-resolution mass spectrometer (both from Waters), which operated in positive electrospray ionization mode. Full-scan MS spectra (*m/z* 500-5000) were acquired in sensitivity mode (resolution of 20 000) using a scan time of 1 s without any lock mass infusion. The remaining QTOF parameters were set as follows: capillary voltage 2.5 kV, source temperature 120 °C, sampling cone voltage 40 V, cone gas flow 0 L/h, desolvation temperature and gas flow at 150 °C and 600 L/h, respectively. The QTOF mass accuracy, achieved upon calibration with sodium iodide (*m/z* 400-4500), was below 5 ppm on each analysis day.

3.3.3.9 Data processing

In a first step, a 1.5 minutes-wide retention time window (3.0-4.5 min) was selected in the total ion chromatogram to extract full-scan MS spectra using MassLynx 4.1 (Waters). Afterwards, a 20th polynomial order background subtraction with a below the curve value of 1.0% and a tolerance of 0.1 was conducted. Next, the resulting MS spectrum was deconvoluted using the peaks between *m/z* 2400 to 4000. MS deconvolution was based on the maximum entropy analysis using the Maxent1 algorithm: the spectral peak width resolution and the uniform Gaussian width at half height were both set to 1.50 Da with an intensity ratio of minimum 40%. The deconvolution output range was restricted from 141 to 156 kDa and the iteration was completed upon full convergence. In the final step, each observed peak in the deconvoluted MS spectrum was centroid.

3.3.4 Results

3.3.4.1 General overview of the IC-LC-HRMS workflow for intact ADC analysis

A general overview of the developed generic IC-LC-HRMS-based workflow for combined qualitative and quantitative analysis of intact lysine-conjugated ADCs is illustrated in Figure 3.12. Briefly, a magnetic bead-based IC was favored due to the flexibility to increase the amount of capture antibody-containing magnetic beads added to the rat serum sample, whereas tip-based formats are limited to a fixed amount of streptavidin per tip (chapter 2.3 and 3.2). Moreover, a biotinylated mouse anti-hIgG Fc capture antibody was selected, allowing the co-extraction of the hIgG1 (ISTD) and the essential ADC D0 species for DLD/DAR assessment, besides the actual ADC drug load species (D1-Dx). This would not be possible with a biotinylated payload-targeting capture antibody (*i.e.* anti-maytansinoid). Furthermore, the strong binding affinity between the anti-maytansinoid capture antibody and the ADC payload represented another issue for intact ADC analysis, which is not present in LBA or IC-LC-MS/MS-based assays, employing primary detection antibodies or on-bead ADC digestion, respectively. By applying low-pH elution buffers such as 2% FA in 10% methanol (pH 2.3) or 0.4% TFA in water (pH 1.6), only 14.9 or 1.7% of immuno-captured ADC were released from the magnetic beads, respectively. In contrast, 90.0% of immuno-captured ADC was recovered from the mouse anti-hIgG Fc capture antibody with 2% FA in 10% methanol, which was selected as the elution solvent (ADC extraction is described in detail in section 3.3.4.4). In order to avoid peak broadening and MS signal dilution due to separation of individual ADC drug load species, a desalting cartridge was selected instead of an analytical column for LC-HRMS analysis. A single narrow chromatographic peak was obtained from which a 1.5 minutes-wide full-scan MS spectrum was extracted. In contrast to the intact hIgG1 quantification (chapter 3.2), the deconvolution approach was preferred for combined ADC assessment mainly due to two reasons: first, complex *m/z* assignment of different charge states for each known ADC drug load species in the full-scan MS spectrum and second, the lack of *a priori m/z* information, preventing the identification of potential metabolic or catabolic ADC species.
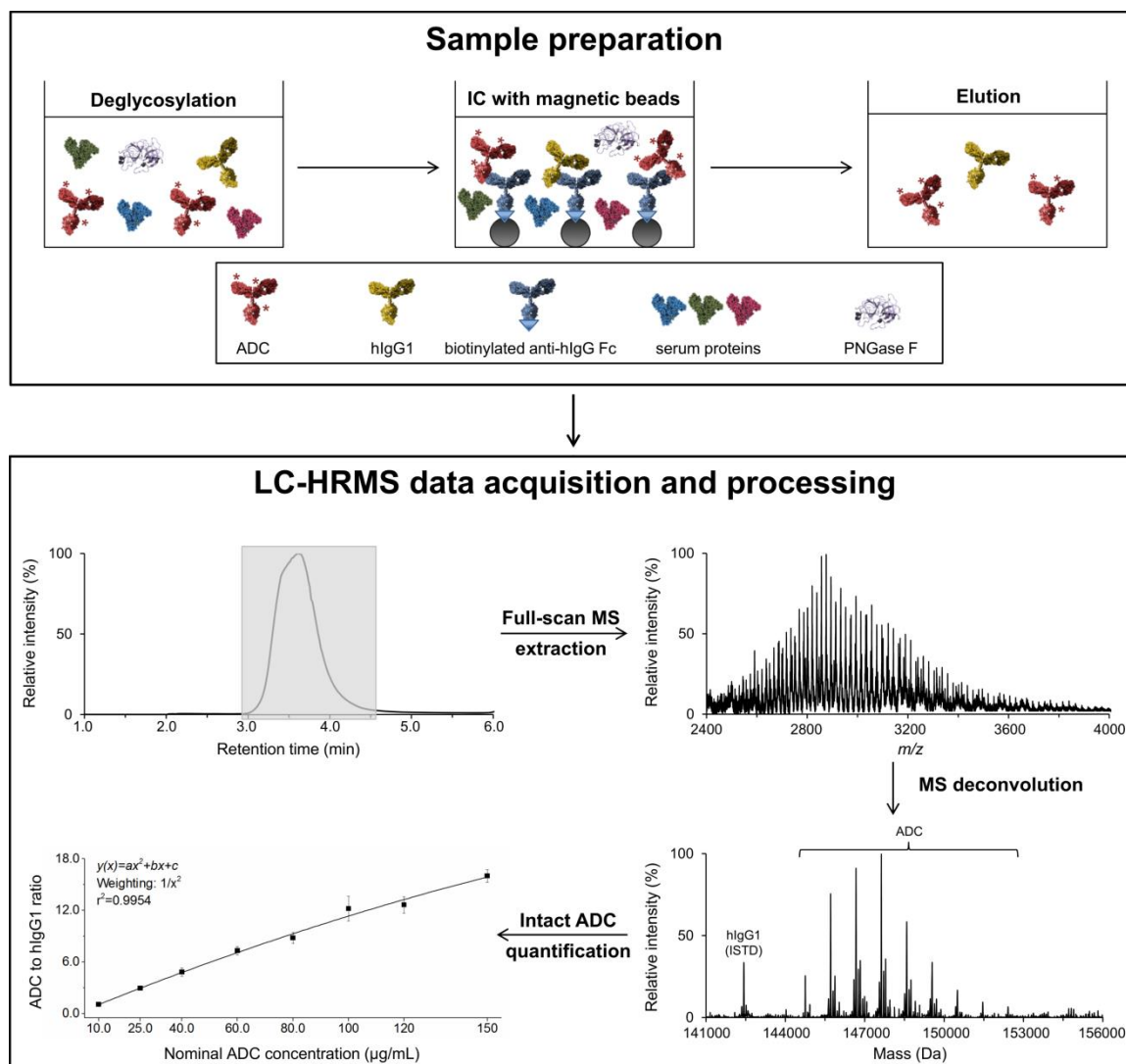
Figure 3.12 Overview of the generic IC-LC-HRMS workflow for a combined qualitative and quantitative analysis of intact lysine-conjugated ADCs in rat serum.

3.3.4.2 Glycosidase selection for ADC deglycosylation

As outlined in section 3.2.3.1, the employment of IgGZERO allows deglycosylation within less than one hour, whereas the use of PNGase F requires overnight sample processing. In addition, a chitin tag-containing version of PNGase F (Remove-It PNGase F) was additionally tested, enabling enzyme removal by a second IC step with chitin binding domain-coated magnetic beads prior to LC-HRMS analysis. The deconvoluted MS spectra after PNGase F and Remove-It PNGase F treatment were similar, detecting the ADC1 up to its D11 drug load species (Figure 3.13a+b). In contrast, the ADC1 could only be detected up to the D10 drug load species after IgGZERO treatment and the different N-glycan cleaving site caused a mass shift of the entire ADC1 intact mass envelope by 698±3.2 Da (Figure 3.13c). Unlike PNGase F, cleaving the N-glycans between the core GlcNac and asparagine residue, IgGZERO hydrolyzes the β1,4 glycosidic bond between both GlcNac residues. Hence, several species are present, containing

either two unconjugated GlcNac residues (one on each C_H2 domain), one unconjugated GlcNac on one domain and one fucosylated GlcNac on the other domain (monofucosylated), or one fucosylated GlcNac moiety on each domain (bifucosylated). This resulted in an increased complexity of the deconvoluted MS spectrum as exemplified with the ADC1 D3 drug load species (Figure 3.13d). After IgGZERO treatment, the monofucosylated (148180.5 Da) and bifucosylated (148321.5 Da) species were present besides the monoglycated bifucosylated (148482.0 Da) and biglycated bifucosylated (148626.0 Da) forms. In contrast, PNGase F treatment resulted only in the deglycosylated (147624.0 Da), monoglycated (147784.5 Da), and biglycated (147946.5 Da) species. Hence, PNGase F was selected due to a less complex deconvoluted MS spectrum.
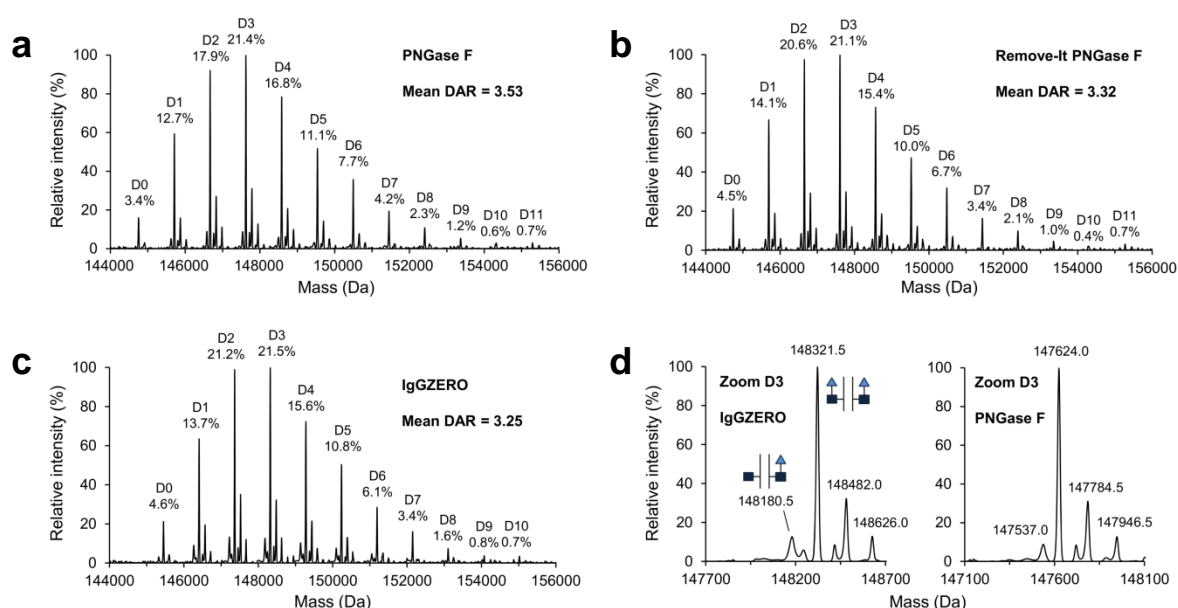
Figure 3.13 Deconvoluted MS spectra of ADC1 after (**a**) PNGase F, (**b**) Remove-It PNGase F, and (**c**) IgGZERO treatment. Panel (**d**) shows a zoomed view into the ADC1 D3 drug load species after IgGZERO or PNGase F treament. The deconvoluted MS spectra were obtained by injecting 2 µg of deglycosylated ADC1 without IC employed.

3.3.4.3 Order of sample preparation steps

Besides the general mAb heterogeneity, the diversity of different species is further increased with ADCs due to random conjugation of the payload/linker, which complicates the extraction from rat serum compared to unmodified hIgGs. Furthermore, the affinity of the capture antibody might differ between low and high-conjugated drug load species during ADC extraction. Ideally, the same DLD/DAR profile compared to the untreated ADC1 stock solution should be recovered after sample preparation including IC, elution (E), and deglycosylation (D) (Figure 3.14a). Experimental data indicated that the order of individual steps cannot be selected in an arbitrary manner. Unlike the IC-D-E protocol published by Xu K *et al.*, which utilizes a target specific antigen for IC,[557] on-bead deglycosylation failed (Figure 3.14b). The major mAb glycoforms could be identified besides
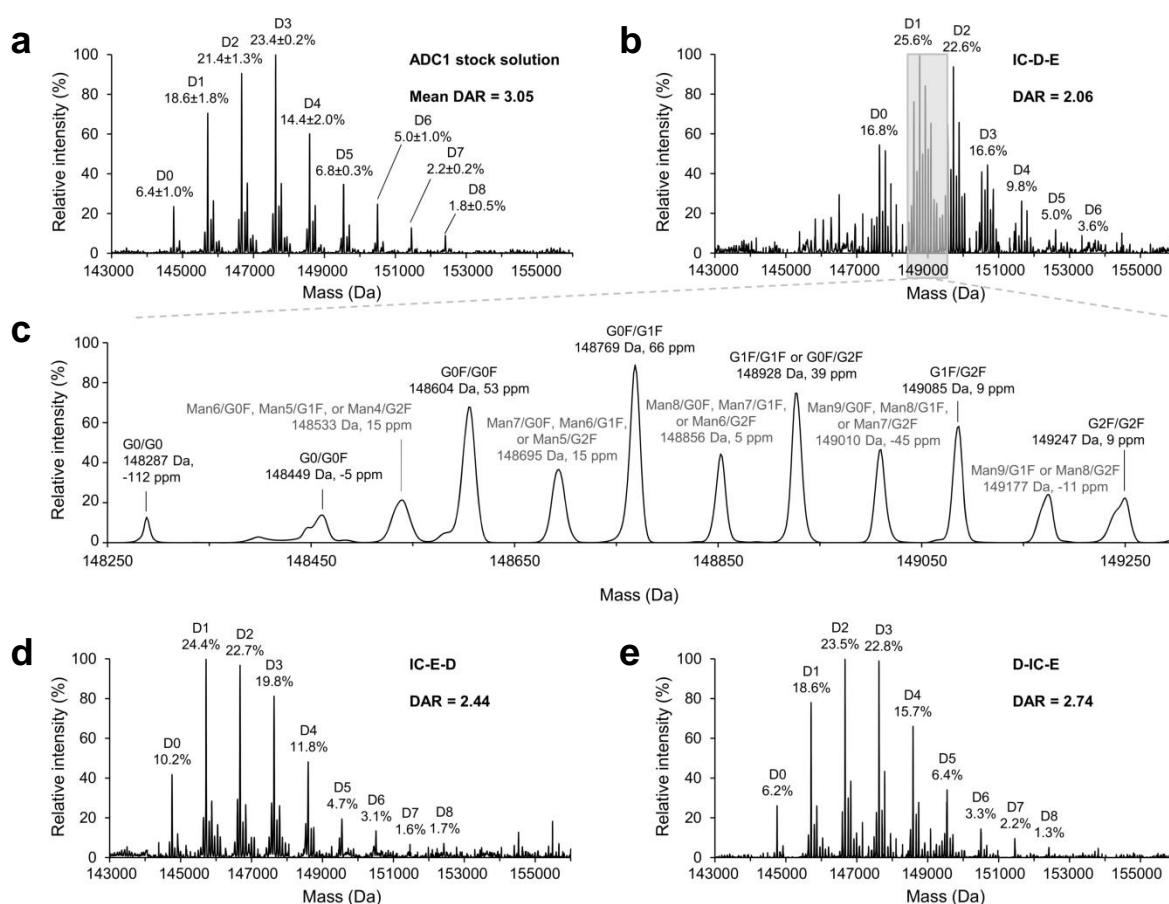
Figure 3.14 Comparison of sample preparation with different orders of immuno-capture (IC), overnight deglycosylation (D), and elution under acidic conditions (E). Expected DLD/DAR of (**a**) the ADC1 stock solution (n=3, 1 µg injected), (**b**) the IC-D-E protocol, (**c**) zoom into D1 species of the IC-D-E protocol showing unsuccessful on-bead deglycosylation, (**d**) the IC-E-D protocol resulting in a skewed DLD/DAR, and (**e**) the D-IC-E protocol, recovering the expected DLD/DAR best.

other mannose-containing glycans as exemplified with the D1 species (Figure 3.14c). This likely resulted from a sterically hindered release of sugar moieties by the PNGase F as the asparagine residue, carrying the mAb glycans, was in close proximity to the anti-hIgG Fc binding site. On the other hand, the glycans were successfully cleaved after IC and ADC elution from the magnetic beads (Figure 3.14d). Notwithstanding, a skewed DLD profile towards a lower DAR of 2.44 was obtained in comparison to the expected DLD of the ADC1 stock solution with a mean DAR of 3.05 (Figure 3.14a). The hypothesis that frequent pH changes within the IC-E-D protocol induced the shift in DLD *via* cleavage of the payload/linker from the mAb was withdrawn: a similar DLD/DAR compared to the stock solution was obtained by spiking ADC1 in elution buffer, adapting the pH for overnight deglycosylation, and quenching the enzyme activity the day after by lowering the pH (data not shown). Hence, the shift in DLD/DAR was most likely caused by different IC or elution profiles when the glycans were still attached. Nevertheless, glycan removal prior to IC and ADC elution (D-IC-E protocol) resulted in a similar DLD recovery compared to the ADC1 stock solution, indicating a comparable affinity and extraction capacity of the mouse anti-hIgG Fc for low and

high-conjugated ADC drug load species (Figure 3.14e). Since the less intense high-conjugated ADC1 drug load species (D6-D8) were slightly underestimated, the resultant DAR of 2.74 was slightly lower compared to the expected one of 3.05 (Figure 3.14a). In addition and in contrast to the IC-E-D protocol, the effect of ion suppression caused by excessive PNGase F was no longer present after ADC elution, likewise resulting in a two-fold increase in signal intensity for the D-IC-E protocol, which was selected for further investigations.

3.3.4.4 ADC1 extraction recovery

After selection of the most appropriate sample preparation strategy, the ADC1 extraction recovery from rat serum samples was investigated using the [³H]-ADC1 due to the sensitivity and simplicity associated with radioactivity measurement by liquid scintillation counting. On average, 92.7% of total radioactivity at two different QC levels (both n=3) was recovered during D-IC-E protocol application. The four washing steps after IC and the remaining radioactivity on the beads after ADC1 elution contributed to the radioactivity loss with 4.7±0.1 and 5.7±1.1%, respectively. Almost one third of total radioactivity (30.8±1.7%) remained in the rat serum sample after IC. Neither a reduction in sample viscosity by serum sample dilution with PBS, an increase of anti-hIgG Fc capture antibody-containing magnetic beads added to the sample, nor a prolongation of the incubation time resulted in any significant improvement of the ADC1 capture step (Figure 3.15). Since the [³H]-label was incorporated at the cytotoxic payload, the origin of detected radioactivity could be any possible construct carrying the labeled payload. In order to clarify if uncaptured intact ADC represented the remaining radioactivity after IC, a set of samples was prepared in surrogate matrix (PBS+0.5% BSA) and was subjected directly after IC for intact ADC analysis by LC-HRMS. However, no typical charge state envelope at the expected values (*m/z* 2400-4000) was observed for ADC1 in the full-scan MS spectrum, indicating that the remaining detected radioactivity signal was not originating from intact ADC1 (data not shown). Hence, the calculated total radioactivity recovery of 51.5±5.8% upon ADC1 elution might underestimate the absolute ADC1 extraction recovery.
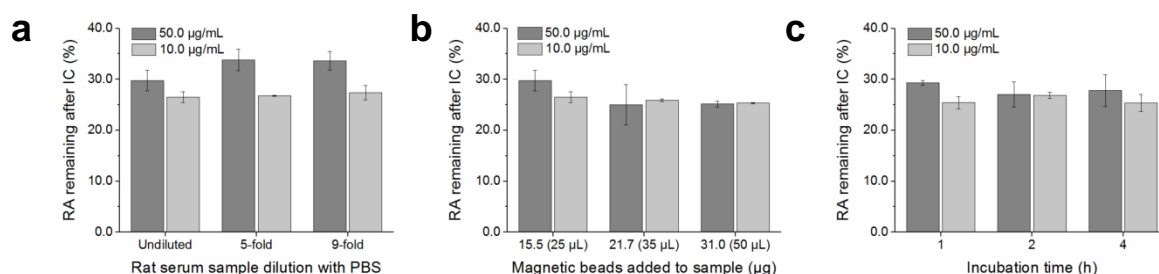
Figure 3.15 Efforts to improve [³H]-ADC1 extraction from rat serum including (**a**) sample dilution with PBS, (**b**) increase of anti-hIgG Fc capture antibody-containing magnetic beads added to the sample, and (**c**) prolongation of the incubation time. RA: radioactivity

3.3.4.5 Selectivity and principle for a combined qualitative and quantitative assay

The developed IC-LC-HRMS-based workflow was selective as no endogenous interfering protein was extracted from rat serum and present at the expected deglycosylated intact masses for the ADC1 and the hIgG1 (Figure 3.16a). The hIgG1 spiked into blank rat serum resulted in a decent signal at 142427.4 Da, deviating by 68 ppm from its expected theoretical intact mass based on its amino acid sequence (Figure 3.16b). The final ISTD concentration within the sample (5.00 µg/mL) had to be selected lower than the ADC1 LLOQ concentration (10.0 µg/mL) as the intact hIgG1 signal was concentrated only into one single species. In contrast, the ADC1 signal intensity was distributed and hence diluted over nine ADC1 drug load species (D0-D8). Of note, ADC1 drug load species >D8 could not be detected after sample preparation, but to a minor extent (≤1.2%) when 2 µg of the deglycosylated ADC1 stock solution were injected onto the desalting cartridge (Figure 3.13a). The ADC1-specific deglycosylated intact mass envelope, ranging from 144 to 153 kDa, was obtained until the D7 drug load species in the LLOQ sample (Figure 3.16c), whereas the D0-D8 drug load species were detected at the ULOQ of 150 µg/mL (Figure 3.16d). The mean mass accuracy between experimental and theoretical intact masses for each ADC1 drug load species at the LLOQ and ULOQ was 30 ppm. Moreover, the ADC1 DLD was consistent and in agreement with the expected DLD of the ADC1 stock solution (Figure 3.14a) throughout the whole calibration range, resulting in a mean DAR of 2.83±0.20 with a variability of 6.9%. Besides qualitative data (DLD/DAR), quantitative information can be derived in parallel from the same
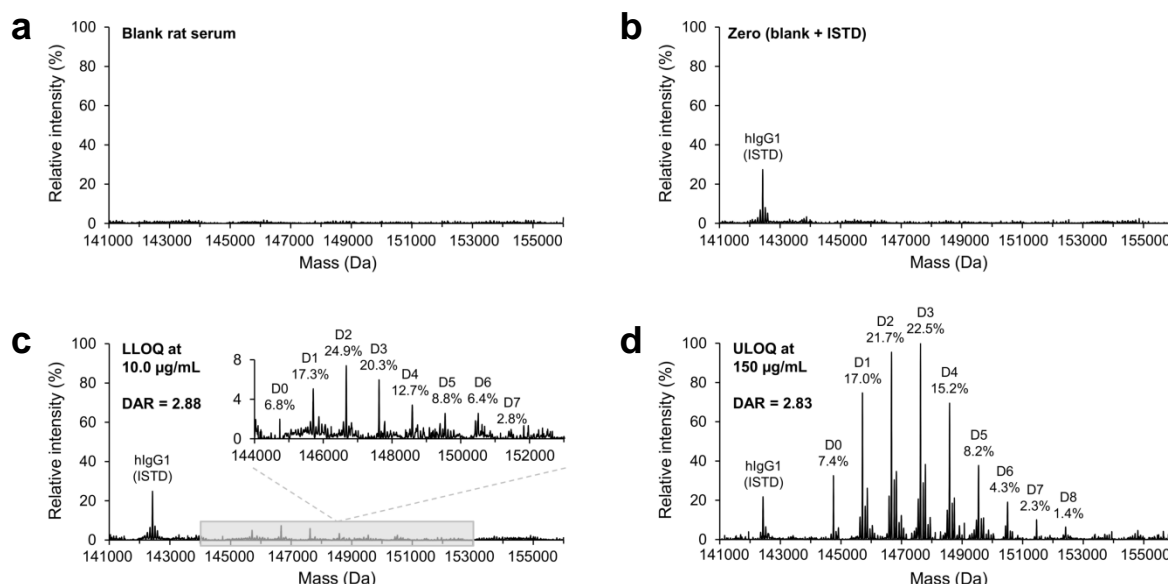
Figure 3.16 Selectivity of the developed IC-LC-HRMS-based workflow for a combined qualitative and quantitative analysis of an intact lysine-conjugated ADC (ADC1) in rat serum. Deconvoluted MS spectrum of (**a**) blank rat serum, (**b**) a zero sample (blank spiked with a hIgG1 used as ISTD), (**c**) the LLOQ sample at 10.0 µg/mL, and (**d**) the ULOQ sample at 150 µg/mL.

analysis. The peak height ratio between all apparent intact ADC masses after summation and the ISTD response plotted against the expected concentration represents the total mAb concentration (D0-Dx). In contrast, the exclusion of the D0 species corresponds to the total ADC concentration (D1-Dx). Based on the DLD of the ADC1 stock solution used for Cs/QCs preparation, the percentage of ADC1 without cytotoxic payload (D0) was 6.4±1.0%, whereas the remaining 93.6% of ADC1 carried at least one toxin (Figure 3.14a). Consequently, the expected total ADC1 concentration in the Cs/QCs had to be adapted accordingly by multiplying the initial spiked nominal concentrations (10.0-150 µg/mL) with a factor of 0.936, resulting in an adapted concentration range from 9.36 to 140 µg/mL. By applying this strategy, each individual ADC drug load species (Dx) could be quantified. Of note, a calibration curve for the D0 species was not necessary as its concentration could be derived from the difference between total mAb and total ADC determination.

3.3.4.6 Linearity, accuracy, and precision

The proposed intact ADC data processing strategy allowed to determine the concentration of the total mAb (D0-D8), total ADC1 (D1-D8), and individual ADC1 species (D1, D2, D3, D4) within one single analytical run. An example for each calibration curve is illustrated in Figure 3.17, whereby C1-C8 represent the expected concentrations after correction with the corresponding mean DLD value from the ADC1 stock solution used for Cs/QCs preparation (Figure 3.14a). The corresponding linearity of Cs, accuracy, and precision data obtained with four QC concentrations are summarized in Table 3.8.
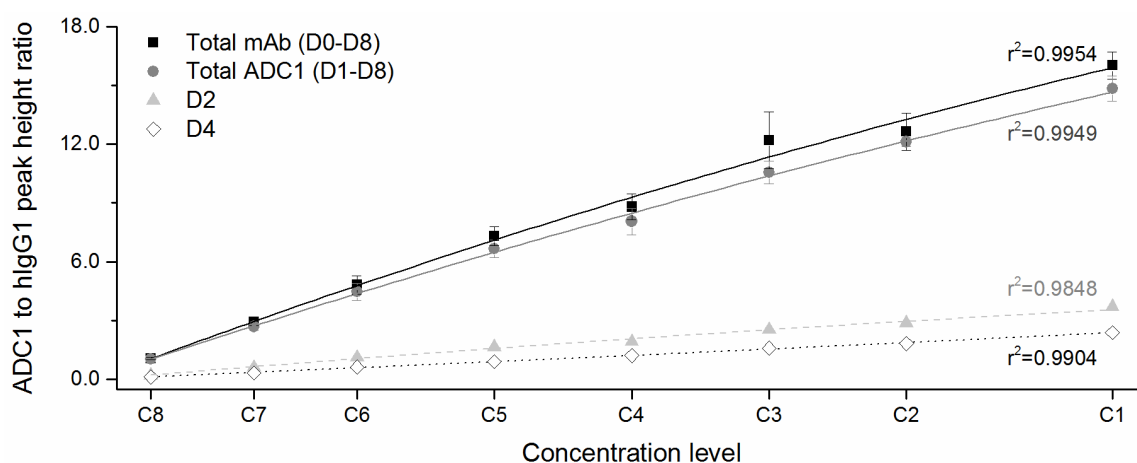
Figure 3.17 Example of obtained quadratic calibration curves with $1/x^2$ weighting for total mAb (D0-D8), total ADC1 (D1-D8), and two individual ADC1 drug load species (D2 and D4) by plotting the ADC1 to hIgG1 peak height ratio against the expected concentrations (C1-C8), which differed for each assay depending on the DLD value.

Table 3.8 Summary of linearity, accuracy, and precision data over three days obtained with ADC1 in rat serum. The linearity was determined with eight different non-zero Cs concentration levels ranging from 10.0-150 µg/mL, whereas the accuracy and precision was determined with four QC concentrations (nominal values: 10.0, 25.0, 75.0, and 125 µg/mL).

ADC species		Linearity		Accuracy (% bias)		Precision (% CV)	
Assay	DLD (n=3)	Range (µg/mL)	r^2-value (n=3)	Intra-day (n=3)	Inter-day (n=9)	Intra-day (n=3)	Inter-day (n=9)
Total mAb (D0-D8)	100%	10.0-150	0.9914±0.0034	-13.2 to 14.8	-0.9 to 3.3	0.9 to 16.6	7.6 to 14.5
Total ADC1 (D1-D8)	93.6%	9.36-140	0.9914±0.0033	-9.9 to 13.9	-2.1 to 4.5	0.6 to 18.4	8.9 to 11.5
D1	18.6%	1.86-27.9	0.9872±0.0064	-13.8 to 15.3	0.2 to 6.9	0.1 to 22.9[b]	5.9 to 14.7
D2	21.4%	2.14-32.1	0.9873±0.0028	-14.3 to 15.5	1.0 to 5.3	0.8 to 14.5	7.5 to 14.7
D3	23.4%	2.34-35.1	0.9897±0.0034	-20.3[a] to 9.6	-4.7 to 2.3	0.6 to 18.2	10.8 to 14.7
D4	14.4%	1.44-21.6	0.9896±0.0023	-17.4 to 18.0	-6.4 to 1.9	1.3 to 14.8	7.7 to 13.3

[a] At LLOQ QC with acceptance criterion of ±25.0% bias, [b] at LLOQ QC with acceptance criterion of ≤25.0% CV

3.3.4.7 ADC1 stability study

The applicability of the developed IC-LC-HRMS method for a combined qualitative and quantitative analysis of intact lysine-conjugated ADCs was first demonstrated in a small ADC1 stability study. As illustrated in Figure 3.18a, the concentration of intact ADC1 decreased by 96.9 and 62.2% during incubation over one week at 37 °C in rat serum batch 1 and 2, respectively. In contrast, a less significant decline of 49.0% was observed in PBS+0.5% BSA selected as surrogate matrix. A similar behavior was observed with the hIgG1 (Figure 3.18a). The concentration decline was delayed within the first 30 h, but equal endpoints were obtained following 168 h incubation as the initial intact hIgG1 concentration decreased by 89.7 and 61.6% in batch 1 and 2, respectively. Consequently, the decrease in concentration over time seemed to
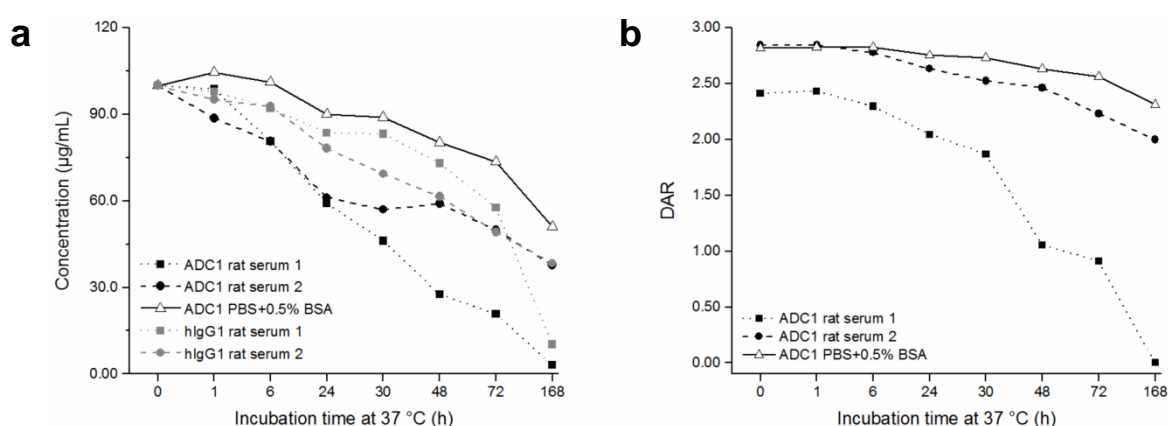
Figure 3.18 ADC1 stability data. (**a**) Concentration-time profile for ADC1 and hIgG1 (positive control) during one week incubated either in rat serum or surrogate matrix (PBS+0.5% BSA) at 37 °C and (**b**) evolution of DAR over time.

be dependent on the rat serum batch and does not necessarily indicate ADC1 instability. ADC1 stability was further supported by the absence of truncated ADC1 or any of its fragments in the full-scan or deconvoluted MS spectrum (data not shown). An explanation for the concentration decrease over time is a potential ADC1 or hIgG1 aggregation as well as conjugation to BSA or endogenous serum proteins, which likely result in a reduced extraction efficiency of the formed complexes. However, further experimental analysis (*e.g.* using size exclusion chromatography) would be required to confirm the presence of complexes and to investigate if the decrease of ADC concentration is actually not related to stability issues. Interestingly, an influence of the rat serum batch was also observed during DAR assessment (Figure 3.18b). The initial DAR value at time point 0 h was significantly lower with a DAR of 2.41 in rat serum batch 1 compared to a DAR of 2.83±0.01 for the surrogate matrix and the second batch of rat serum. A moderate decrease in the DAR value was recorded over time in rat serum batch 2 and surrogate matrix with endpoints at 2.00 and 2.31, respectively. This decrease in the DAR value over time was already reported,[558] resulting from retro-Michael reaction causing elimination of the maleimide linker from ADCs.[562,563] On the other hand, the DAR value of the ADC1 spiked in rat serum batch 1 declined to zero after 168 h of incubation, indicating a complete loss of the payload. A third batch-dependent effect was observed during the ADC1 stability assessment. The expected intact masses for ADC1 and the post-incubation spiked hIgG1 were obtained in rat serum batch 1 and 2 following 30 h incubation (Figure 3.19a+b). While equivalent results were obtained for rat serum batch 1 in all subsequent time points such as 48 h (Figure 3.19c), a mean mass shift of 698±6.0 Da for the ADC1 intact masses was observed in rat serum batch 2 for all samples after 30 h of incubation (Figure 3.19d). One hypothesis would be the formation of a reactive species in rat serum batch 2 at later time points of incubation, which is subsequently conjugated to the ADC. Since the same phenomenon
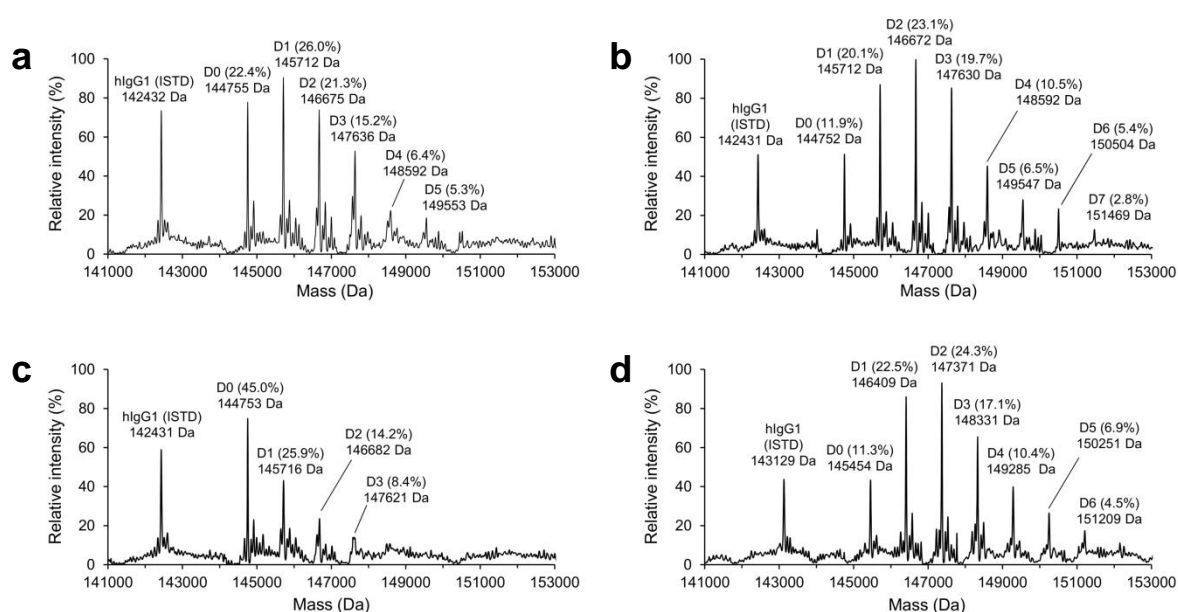
Figure 3.19 Deconvoluted MS spectra of ADC1 stability samples at (**a**) 30 h in rat serum batch 1, (**b**) 30 h in rat serum batch 2, (**c**) 48 h in rat serum batch 1, and (**d**) 48 h in rat serum batch 2.

was observed for the hIgG1, the conjugation must have been occurred on the mAb and not on the ADC payload/linker. At this stage, however, the entity and site of conjugation remains unknown, requiring further investigations (*e.g.* using middle-up or bottom-up approaches) for complete elucidation.

3.3.4.8 ADC2 *in vivo* PK samples from three rats

The concept of combined qualitative and quantitative analysis of intact lysine-conjugated ADCs by one single IC-LC-HRMS-based assay was subsequently demonstrated using *in vivo* PK samples from three individual rats, which were intravenously dosed with the ADC2 at 5.00 mg/kg on day 1 and 8. No ADC2 was detected in rat serum samples at pre-dose 1 (Figure 3.20a). In contrast, the typical ADC2 drug load species envelope, ranging from 143967.0 (D0) to 149731.5 Da (D6), was present besides the hIgG1 (ISTD) at 142431.0 Da in the 1 h post-dose 1 sample (Figure 3.20b). The percentage in DLD for the ADC2 D0 and D1 drug load species increased over time after the first dosing cycle, whereas D2 remained constant and the higher conjugated ADC2 species decreased as a result of higher clearance (Figure 3.20c).[564,565] The initial ADC2 DLD was recovered after the second dose, as illustrated by the 1 h post-dose 2 samples, which was in agreement with the DLD of the ADC2 stock solution. In addition, the same pattern (D0/D1 increase and D3-D6 decrease, while D2 remained constant over time) was also obtained in the second cycle (Figure 3.20c). The observed dynamics in DLD over the PK profile directly impacted the DAR value, which decreased from an initial value of 3.02 (ADC2 stock solution) to a maximum value of 2.45 (rat 1) and from 3.08±0.03 to 2.56±0.29 for the first and second dosing cycle, respectively (Figure 3.21a). Such a dynamic in DLD/DAR over the PK profile was in agreement with published results from other groups.[554,557,560] Since the ADC2 D0 drug load species
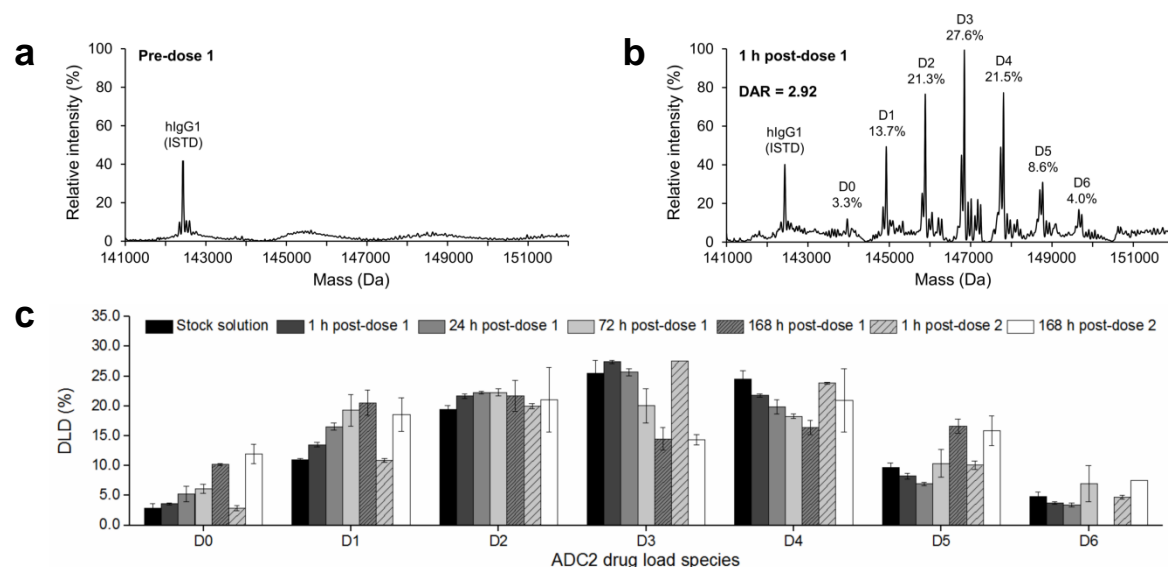
Figure 3.20 Deconvoluted MS spectrum of pre-clinical study samples from rat 2 at (**a**) pre-dose 1 and (**b**) 1 h post-dose 1 as well as (**c**) mean DLD of all three rats at different sampling time points after intravenous ADC2 administration (5.00 mg/kg) on day 1 and 8.

represented between 2.9±0.4% and 11.9±1.6% of the ADC2 DLD, the mean total mAb (D0-D6) and ADC2 (D1-D6) concentrations were overlapping throughout the PK profile for both dosing cycles (Figure 3.21b), indicating ADC2 stability in the systemic circulation system as no payload was released. In contrast to LBA or LC-MS/MS-based assays, *in vivo* concentration data of individual ADC2 drug load species such as D3 could be derived, ranging from 25.4±3.9 to 1.34±0.22 μg/mL and from 26.9±3.7 to 1.41±0.20 μg/mL for the first and second dosing cycle, respectively (Figure 3.21b).
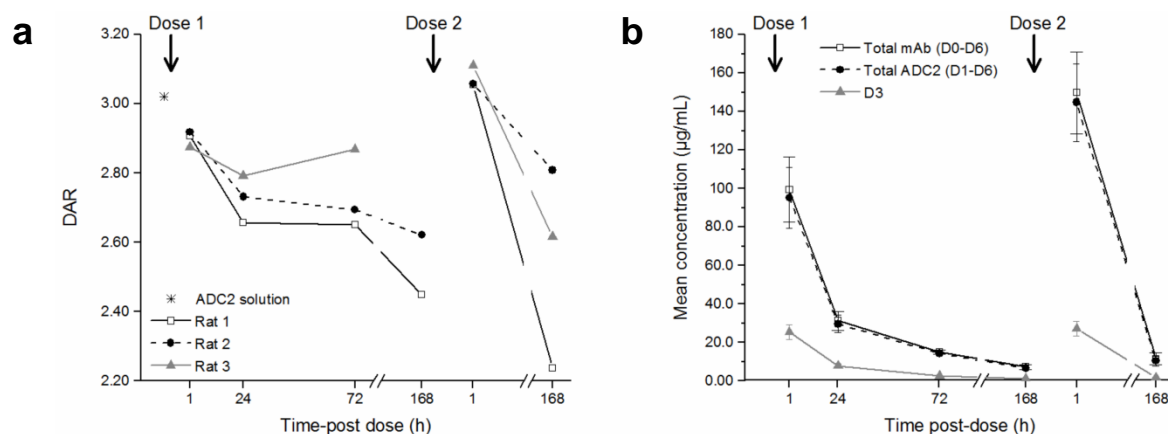
Figure 3.21 *In vivo* data from three individual rats dosed intravenously with ADC2 (5.00 mg/kg) on day 1 and 8 showing (**a**) individual DAR profiles and (**b**) mean concentration-time profile for total mAb (D0-D6), total ADC2 (D1-D6), and D3 drug load species.

3.3.5 Conclusions

By extending the developed concept of intact hIgG1 quantification by IC-LC-HRMS to more complex next-generation biotherapeutics, a combined qualitative and quantitative analysis of intact lysine-conjugated ADCs in rat serum using the deconvoluted MS spectrum was successfully implemented within this project. In terms of qualitative analysis, the dynamics of DLD/DAR could be investigated to study the ADC clearance *in vivo* or the payload/linker deconjugation from the mAb*,* while providing concentration data of the total mAb (D0-Dx), total ADC (D1-Dx), and major individual ADC drug load species (D1-D4). Further benefits of the developed IC-LC-HRMS assay for intact ADC analysis included the merging of three individual MS-based assays into a single HRMS methodology without the requirement for a second specific capture antibody (*i.e.* anti-payload) to distinguish between total mAb and total ADC concentration.

3.3.6 Scientific communication

The work described in this chapter is currently in progress of manuscript writing and submission to the *Journal of Analytical Chemistry*.

General conclusion and future perspectives

The **first part** of this thesis illustrated the potential of IgG-derived drugs for therapeutic applications and their market development over the last decade. On the other hand, the broad diversity of such modalities and the variety of assays required during the drug development process highlighted the associated analytical challenge and the demand for generic quantitative assays in order to support PK, PD, and IG assessments.

In this context, the doctoral work aimed to implement generic MS-based workflows and extend their application to the quantitative analysis of chimeric, humanized, and human IgGs as well as bsAbs and ADCs in pre-clinical species.

The development of generic LC-MS/MS-based methods and their versatility for bottom-up mAb-related therapeutic protein quantification in pre-clinical species was described in the **second part** of this thesis:

- It was shown that a generic MS-based assay, utilizing four conserved surrogate peptides, could be rapidly implemented for bottom-up mAb-related therapeutic protein quantification at the pre-clinical stage as no specific capture antibody was required. This pellet digestion-based generic LC-MS/MS workflow enables the support of total PK assessment of any type of mAb-related therapeutic protein, which is based on the hIgG1 or hIgG4 structural scaffold. Furthermore, the assay is both robust and versatile as (i) no exact matrix matching is necessary due to the incorporation of a SIL-hIgG1 ISTD and (ii) the ability to select the most appropriate generic surrogate peptide(s) for quantification enables analyte interchange. However, certain knowledge about potential mAb modifications is required when applying such an interchangeable concept to engineered mAb-related therapeutic proteins (*i.e.* stabilized IgGs, bsAbs, or ADCs). Consequently, the incorporation of at least two generic peptides from different parts of the constant region is recommended in order to gain additional confidence in the quantitative data and to enhance the method versatility.

- Both evaluated digestion kits enable a much faster, simplified, and standardized sample preparation, while providing equivalent quantitative data as compared to the pellet digestion-based approach. The employment of the kits requires minimal method development, digestion optimization, and fewer reagents. On the other hand, an enhanced deamidation process was observed with both asparagine-containing generic peptides due to an elevated digestion temperature of the SMART Digest Kit, which might affect assay sensitivity and robustness. Consequently, monitoring the digestion kinetics at different temperatures would be beneficial in order to minimize peptide deamidation. With respect to qualitative analysis, each kit can also serve as sample preparation for peptide mapping experiments in order to confirm the

primary amino acid sequence upon protein expression or to identify possible structural changes of mAb-related therapeutic proteins.

- The incorporation of a tip-based IC step in the sample preparation workflow significantly extended the application range of generic LC-MS/MS methods due to a 100-fold sensitivity enhancement. Great flexibility was also associated with the use of the generic hIgG Fc region-targeting capture antibody as any type of Fc region-containing modality could be extracted from pre-clinical serum samples. The elution process of the immuno-captured mAb-related therapeutic protein from the capture antibody remains the most critical step and requires extensive evaluation in order to achieve high extraction recoveries and hence good assay sensitivities. Moreover, the embedded IC step allows assay functionalization as the desired mAb species could selectively be extracted from serum samples. For instance, a generic LC-MS/MS assay for total ADC determination of any kind of maytansinoid-based ADC could be implemented by replacing the anti-hIgG Fc with an anti-maytansinoid capture antibody.

Overall, the presented generic LC-MS/MS workflows cover a wide calibration range over five orders of magnitude for bottom-up mAb-related therapeutic protein quantification, applying either direct serum digestion approaches (1.00-1000 µg/mL) or the IC strategy (10.0-1000 ng/mL). Since this dynamic range is sufficient for most pre-clinical dose range finding or toxicity studies, a combination of both generic LC-MS/MS assays would support the entire pre-clinical total PK assessment of a variety of mAb-related therapeutic proteins. Hence, the developed generic assays are conducive to externalization and implementation in open-access facilities. In order to extend the method applicability, generic peptides for the hIgG2 isotype subclass could be embedded. For this purpose, either a single generic tryptic peptide covering all therapeutic relevant IgG isotype subclasses (*e.g.* NQVSLTCLVK) or a hIgG2 isotype subclass-specific peptide (*e.g.* GLPAPIEK) could be incorporated. By applying the latter, multiplexing of co-administrated mAbs from different IgG isotype subclasses could be realized using one generic LC-MS/MS method, while simultaneous quantification of mAb-related therapeutic proteins from the same IgG isotype subclass would require the use of CDR peptides. In addition, the application of a generic LC-MS/MS-based assay is not necessarily limited to pre-clinical samples. "Fc-silenced" mAb-related therapeutic proteins exhibit common engineered Fc regions. As a result of specifically introduced mutations, peptides from engineered Fc regions exhibit altered amino acid sequences compared to endogenous IgGs. Hence, by utilizing those modified peptides, the presented approaches can be used to implement generic LC-MS/MS methods for "Fc-silenced" mAb-related therapeutic protein quantification, enabling the support of pre-clinical and clinical studies by a single assay.

The **third part** of this thesis demonstrated the potential of HRMS mass analyzers as an alternative to QqQ instruments, which are conventionally utilized for generic bottom-up mAb-related therapeutic protein quantification:

- Targeted acquisition modes of a QTOF instrument (*i.e.* TOF-MS/MS and TOF-MRM) displayed superior sensitivity in terms of S/N ratio compared to untargeted modes (*i.e.* TOF-MS) and hence were more suitable for quantitative purposes. In comparison to SRM-based approaches (QqQ instruments), the generic TOF-MRM-based method provided equivalent quantitative data over the same concentration range as successfully demonstrated with spiked serum samples and specimen from pre-clinical trial. Consequently, the latest generation of HRMS instruments can nowadays compete with conventional QqQ instruments. In some cases, HRMS offers certain advantages as its high mass resolution allows for removal of endogenous interferences, resulting in better selectivity and hence sensitivity for bottom-up mAb-related therapeutic protein quantification. Furthermore, the combination of IC-based sample preparation, targeted qHRMS approaches and finally ion mobility, which introduces drift time as an additional analytical dimension, would be a powerful approach to further increase the assay selectivity and sensitivity (S/N ratio). Based on these attributes, it is expected that targeted qHRMS approaches will be utilized more frequently in the future. On the other hand, even though quantification by TOF-MS is less sensitive, this untargeted approach is still valuable at early drug discovery stages, enabling data mining and retrospective quantification of additional analytes without the need of extra sample processing and data acquisition. Due to the nature of full-scan MS data acquisition, improvements in sensitivity could only be achieved through alternative sample preparation (*i.e.* IC) or chromatographic separation approaches (*i.e.* ultra-performance LC, multi-dimensional LC, or low-flow applications). Nevertheless, compliance-related issues in terms of data integrity and traceability have to be clarified before untargeted qHRMS approaches can be routinely be applied in a regulated environment.

- Combining HRMS mass analyzers with an IC-based sample preparation additionally provides the possibility to quantify simultaneously multiple intact mAb-related therapeutic proteins. Moreover, the developed generic tip-based IC-LC-HRMS workflow was identified as an orthogonal method to quantitative bottom-up LC-MS/MS analysis. Even though the latter is more sensitive, the level of provided information was markedly enhanced with the former approach. Consequently, a shift from bottom-up to intact hIgG quantification might occur as well in the future. In addition to the quantitative aspects, the multiplexing capability of the developed IC-LC-HRMS methodology could also serve as a screening tool. For instance, the appearance of additional intact masses in the deconvoluted MS spectrum might be an indication for the presence of *in vivo* generated metabolites or catabolites, ADA formation, or antigen binding. Hence, this approach provides better insights into the fate of mAb-related therapeutic proteins compared to peptide level analysis.

- By extending the concept of intact hIgG1 quantification to more complex next-generation biotherapeutics such as lysine-conjugated ADCs, three individual MS-based assays could be merged into a single one. This IC-LC-HRMS-based assay allows the study of time-dependent changes of the ADCs' DLD/DAR during stability and *in vivo* studies. In parallel, quantitative

information about the total mAb, total ADC, and major individual ADC drug load species, which was so far impossible with existing technologies, could be obtained within the same analytical run, reducing the overall sample volume required for analysis. Despite this successful first proof of concept study, a better understanding is required to clarify how the presented methodology can be applied to more dynamic systems in which additional ADC metabolites, catabolites, or other (protein)-conjugated ADC species are generated over time.

The results obtained in the third part of this thesis further demonstrate the relevance of HRMS-based approaches for the bioanalysis of mAb-related therapeutic proteins. Their implementation will provide new opportunities to support the drug development process of such modalities, while utilizing a single instrument for qualitative and quantitative assessments. Despite the promising features of HRMS, challenges for routine implementation still remain. First, appropriate local informatics systems are required to handle the significant amount of data that is generated per sample as long as no significant improvements with regard to data file reduction are available. Second, in particular for intact mAb quantification or HRMS analysis in combination with ion mobility, dedicated software including automated workflows would be desirable to manage the complexity of the acquired data and to avoid tedious manual data extraction/processing. Fortunately, processing workflows are being continuously developed by some MS vendors, which will facilitate complex data handling in the future.

In conclusion, the generic MS-based workflows developed in this thesis, significantly extend the number of available approaches for mAb-related therapeutic protein quantification in pre-clinical species. Furthermore, their applicability to drug development within the pharmaceutical industry was successfully demonstrated in several projects. Depending on the type of mAb-related therapeutic protein as well as the information level and the sensitivity requirements, the most appropriate generic MS-based assay can be selected from the "analytical tool box" presented herein.

References

1. Ladwig PM, Barnidge DR, Willrich MAV. Mass spectrometry approaches for identification and quantitation of therapeutic monoclonal antibodies in the clinical laboratory. *Clin Vaccine Immunol*, 2017, 24(5).

2. Litman GW, Rast JP, Fugmann SD. The origins of vertebrate adaptive immunity. *Nat Rev Immunol*, 2010, 10(8), 543-553.

3. Richter A, Eggenstein E, Skerra A. Anticalins: Exploiting a non-Ig scaffold with hypervariable loops for the engineering of binding proteins. *FEBS Letters*, 2014, 588(2), 213-218.

4. Murphy K, Travers P, Walport M, Janeway C. Janeway's immunobiology (Garland Science, New York; 2012).

5. Wang LD, Clark MR. B-cell antigen-receptor signalling in lymphocyte development. *Immunology*, 2003, 110(4), 411-420.

6. Treanor B. B-cell receptor: from resting state to activate. *Immunology*, 2012, 136(1), 21-27.

7. Panda S, Ding JL. Natural antibodies bridge innate and adaptive immunity. *J Immunol*, 2015, 194(1), 13-20.

8. Schroeder HW, Cavacini L. Structure and function of immunoglobulins. *J Allergy Clin Immunol*, 2010, 125(2 Suppl 2), S41-S52.

9. Sela-Culang I, Kunik V, Ofran Y. The structural basis of antibody-antigen recognition. *Front Immunol*, 2013, 4, 302.

10. Vidarsson G, Dekkers G, Rispens T. IgG subclasses and allotypes: from structure to effector functions. *Front Immunol*, 2014, 5(520).

11. Wingren C, Michaelsen TE, Magnusson CGM, Hansson UB. Comparison of surface properties of human IgA, IgE, IgG and IgM antibodies with identical and different specificities. *Scand J Immunol*, 1996, 44(5), 430-436.

12. Bloom JW, Madanat MS, Marriott D, Wong T, Chan SY. Intrachain disulfide bond in the core hinge region of human IgG4. *Protein Sci*, 1997, 6(2), 407-415.

13. Wypych J *et al*. Human IgG2 antibodies display disulfide-mediated structural isoforms. *J Biol Chem*, 2008, 283(23), 16194-16205.

14. Aalberse RC, Stapel SO, Schuurman J, Rispens T. Immunoglobulin G4: an odd antibody. *Clin Exp Allergy*, 2009, 39(4), 469-477.

15. Gaboriaud C *et al*. Structure and activation of the C1 complex of complement: unraveling the puzzle. *Trends Immunol*, 2004, 25(7), 368-373.

16. Rogers LM, Veeramani S, Weiner GJ. Complement in monoclonal antibody therapy of cancer. *Immunol Res*, 2014, 59(1-3), 203-210.

17. Shade K-TC, Anthony RM. Antibody glycosylation and inflammation. *Antibodies*, 2013, 2(3), 392-414.

18. Scanlan CN, Burton DR, Dwek RA. Making autoantibodies safe. *Proc Natl Acad Sci USA*, 2008, 105(11), 4081-4082.

19. Stewart R, Hammond SA, Oberst M, Wilkinson RW. The role of Fc gamma receptors in the activity of immunomodulatory antibodies for cancer. *J Immunother Cancer*, 2014, 2(1), 29.

20. Weiskopf K, Weissman IL. Macrophages are critical effectors of antibody therapies for cancer. *mAbs*, 2015, 7(2), 303-310.

21. Wang W, Wang EQ, Balthasar JP. Monoclonal antibody pharmacokinetics and pharmacodynamics. *Clin Pharm Ther*, 2008, 84(5), 548-558.

22. Kuo TT, Aveson VG. Neonatal Fc receptor and IgG-based therapeutics. *mAbs*, 2011, 3(5), 422-430.

23. Vugmeyster Y, Xu X, Theil FP, Khawli LA, Leach MW. Pharmacokinetics and toxicology of therapeutic proteins: advances and challenges. *World J Biol Chem*, 2012, 3(4), 73-92.

24. Irani V *et al.* Molecular properties of human IgG subclasses and their implications for designing therapeutic monoclonal antibodies against infectious diseases. *Mol Immunol*, 2015, 67(2, Pt A), 171-182.

25. West AP, Bjorkman PJ. Crystal structure and immunoglobulin G binding properties of the human major histocompatibility complex-related Fc receptor. *Biochemistry*, 2000, 39(32), 9698-9708.

26. Krapp S, Mimura Y, Jefferis R, Huber R, Sondermann P. Structural analysis of human IgG-Fc glycoforms reveals a correlation between glycosylation and structural integrity. *J Mol Biol*, 2003, 325(5), 979-989.

27. Zauner G *et al.* Glycoproteomic analysis of antibodies. *Mol Cell Proteomics*, 2013, 12(4), 856-865.

28. Ferrara C *et al.* Unique carbohydrate–carbohydrate interactions are required for high affinity binding between FcγRIII and antibodies lacking core fucose. *Proc Natl Acad Sci USA*, 2011, 108(31), 12669-12674.

29. Shields RL *et al.* Lack of fucose on human IgG1 N-linked oligosaccharide improves binding to human FcγRIII and antibody-dependent cellular toxicity. *J Biol Chem*, 2002, 277(30), 26733-26740.

30. Reusch D *et al.* High-throughput work flow for IgG Fc-glycosylation analysis of biotechnological samples. *Anal Biochem*, 2013, 432(2), 82-89.

31. Stadlmann J *et al*. A close look at human IgG sialylation and subclass distribution after lectin fractionation. *Proteomics*, 2009, 9(17), 4143-4153.

32. Scallon BJ, Tam SH, McCarthy SG, Cai AN, Raju TS. Higher levels of sialylated Fc glycans in immunoglobulin G molecules can adversely impact functionality. *Mol Immunol*, 2007, 44(7), 1524-1534.

33. Anthony RM *et al*. Recapitulation of IVIG anti-inflammatory activity with a recombinant IgG Fc. *Science*, 2008, 320(5874), 373-376.

34. Kaneko Y, Nimmerjahn F, Ravetch JV. Anti-inflammatory activity of immunoglobulin G resulting from Fc sialylation. *Science*, 2006, 313(5787), 670-673.

35. Chames P, Van Regenmortel M, Weiss E, Baty D. Therapeutic antibodies: successes, limitations and hopes for the future. *Bri J Pharmacol*, 2009, 157(2), 220-233.

36. Weiner LM, Surana R, Wang S. Antibodies and cancer therapy: versatile platforms for cancer immunotherapy. *Nat Rev Immunol*, 2010, 10(5), 317-327.

37. Adler MJ, Dimitrov DS. Therapeutic antibodies against cancer. *Hematol Oncol Clin North Am*, 2012, 26(3), 447-481.

38. Scott AM, Allison JP, Wolchok JD. Monoclonal antibodies in cancer therapy. *Cancer Immun*, 2012, 12, 14.

39. Scott AM, Wolchok JD, Old LJ. Antibody therapy of cancer. *Nat Rev Cancer*, 2012, 12(4), 278-287.

40. Kotsovilis S, Andreakos E. Human monoclonal antibodies: methods and protocols. 37-59 (Humana Press, Totowa, NJ; 2014).

41. Rider P, Carmi Y, Cohen I. Biologics for targeting inflammatory cytokines, clinical uses, and limitations. *Int J Cell Biol*, 2016, 2016, 9259646.

42. Shah B, Mayer L. Current status of monoclonal antibody therapy for the treatment of inflammatory bowel disease. *Expert Rev Clin Immunol*, 2010, 6(4), 607-620.

43. De Faire U, Frostegård J. Natural antibodies against phosphorylcholine in cardiovascular disease. *Ann N Y Acad Sci*, 2009, 1173(1), 292-300.

44. Frostegård J. Low level natural antibodies against phosphorylcholine: a novel risk marker and potential mechanism in atherosclerosis and cardiovascular disease. *Clin Immunol*, 2010, 134(1), 47-54.

45. Rosman Z, Shoenfeld Y, Zandman-Goddard G. Biologic therapy for autoimmune diseases: an update. *BMC Medicine*, 2013, 11, 88.

46. Ulmansky R, Naparstek Y. Protective antibodies against HSP60 for autoimmune inflammatory diseases. *Clin Immunol*, 2017, doi: 10.1016/j.clim.2017.07.016.

47. Kingwell K. Infectious diseases: Two-hit antibody tackles bacteria. *Nat Rev Drug Discov*, 2015, 14(1), 15.

48. Sparrow E, Friede M, Sheikh M, Torvaldsen S. Therapeutic antibodies for infectious diseases. *Bull World Health Organ*, 2017, 95(3), 235-237.

49. ter Meulen J. Monoclonal antibodies in infectious diseases: clinical pipeline in 2011. *Infect Dis Clin North Am*, 2011, 25(4), 789-802.

50. Chang AT, Platt JL. The role of antibodies in transplantation. *Transplant Rev*, 2009, 23(4), 191-198.

51. Platt JL. Antibodies in transplantation. *Discov Med*, 2010, 10(51), 125-133.

52. Zou Y, Stastny P, Süsal C, Döhler B, Opelz G. Antibodies against MICA antigens and kidney-transplant rejection. *N Eng J Med*, 2007, 357(13), 1293-1300.

53. Lipman NS, Jackson LR, Trudel LJ, Weis-Garcia F. Monoclonal versus polyclonal antibodies: distinguishing characteristics, applications, and information resources. *ILAR J*, 2005, 46(3), 258-268.

54. Kohler G, Milstein C. Continuous cultures of fused cells secreting antibody of predefined specificity. *Nature*, 1975, 256(5517), 495-497.

55. Hwang WYK, Foote J. Immunogenicity of engineered antibodies. *Methods*, 2005, 36(1), 3-10.

56. Newsome BW, Ernstoff MS. The clinical pharmacology of therapeutic monoclonal antibodies in the treatment of malignancy; have the magic bullets arrived? *Br J Clin Pharmacol*, 2008, 66(1), 6-19.

57. Lo BKC. Antibody engineering: methods and protocols. 135-159 (Humana Press, Totowa, NJ; 2004).

58. Golay J, Introna M. Mechanism of action of therapeutic monoclonal antibodies: promises and pitfalls of in vitro and in vivo assays. *Arch Biochem Biophys*, 2012, 526(2), 146-153.

59. Suzuki M, Kato C, Kato A. Therapeutic antibodies: their mechanisms of action and the pathological findings they induce in toxicity studies. *J Toxicol Pathol*, 2015, 28(3), 133-139.

60. Ellis LM. Mechanisms of action of bevacizumab as a component of therapy for metastatic colorectal cancer. *Semin Oncol*, 2006, 33(5 Suppl 10), S1-S7.

61. Lyseng-Williamson KA, Robinson DM. Spotlight on bevacizumab in advanced colorectal cancer, breast cancer, and non-small cell lung cancer. *BioDrugs*, 2006, 20(3), 193-195.

62. Goldstein NI, Prewett M, Zuklys K, Rockwell P, Mendelsohn J. Biological efficacy of a chimeric antibody to the epidermal growth factor receptor in a human tumor xenograft model. *Clin Cancer Res*, 1995, 1(11), 1311-1318.

63. Byrd JC *et al*. The mechanism of tumor cell clearance by rituximab in vivo in patients with B-cell chronic lymphocytic leukemia: evidence of caspase activation and apoptosis induction. *Blood*, 2002, 99(3), 1038-1043.

64. Abulayha A, Bredan A, El Enshasy H, Daniels I. Rituximab: modes of action, remaining dispute and future perspective. *Future Oncol*, 2014, 10(15), 2481-2492.

65. Einarsdottir H *et al*. H435-containing immunoglobulin G3 allotypes are transported efficiently across the human placenta: implications for alloantibody-mediated diseases of the newborn. *Transfusion*, 2014, 54(3), 665-671.

66. Natsume A, Niwa R, Satoh M. Improving effector functions of antibodies for cancer treatment: enhancing ADCC and CDC. *Drug Des Devel Ther*, 2009, 3, 7-16.

67. Robbie GJ *et al*. A novel investigational Fc-modified humanized monoclonal antibody, motavizumab-YTE, has an extended half-life in healthy adults. *Antimicrob Agents Chemother*, 2013, 57(12), 6147-6153.

68. Borrok MJ *et al*. An "Fc-Silenced" IgG1 format with extended half-life designed for improved stability. *J Pharm Sci*, 2017, 106(4), 1008-1017.

69. Schlothauer T *et al*. Novel human IgG1 and IgG4 Fc-engineered antibodies with completely abolished immune effector functions. *Protein Eng Des Sel*, 2016, 29(10), 457-466.

70. Chen *et al*. ^{131}I-labeled monoclonal antibody targeting neuropilin receptor type-2 for tumor SPECT imaging. *Int J Oncol*, 2017, 50(2), 649-659.

71. Hu PH *et al*. ([125])I-labeled anti-bFGF monoclonal antibody inhibits growth of hepatocellular carcinoma. *World J Gastroenterol*, 2016, 22(21), 5033-5041.

72. Shusterman S *et al*. Antitumor activity of Hu14.18-IL2 in patients with relapsed/refractory neuroblastoma: a children's oncology group (COG) phase II study. *J Clin Oncol*, 2010, 28(33), 4969-4975.

73. Yu AL *et al*. Anti-GD2 antibody with GM-CSF, interleukin-2, and isotretinoin for neuroblastoma. *New Engl J Med*, 2010, 363(14), 1324-1334.

74. Sommer A *et al*. Preclinical efficacy of the auristatin-based antibody–drug conjugate BAY 1187982 for the treatment of FGFR2-positive solid tumors. *Cancer Res*, 2016, 76(21), 6331-6339.

75. Willuda J *et al*. Preclinical antitumor efficacy of BAY 1129980—a novel auristatin-based anti-C4.4A (LYPD3) antibody–drug conjugate for the treatment of non–small cell lung cancer. *Mol Cancer Ther*, 2017, 16(5), 893-904.

76. Yu SF *et al*. A novel anti-CD22 anthracycline-based antibody–drug conjugate (ADC) that overcomes resistance to auristatin-based ADCs. *Clin Cancer Res*, 2015, 21(14), 3298-3306.

77. Bialucha CU *et al.* Discovery and optimization of HKT288, a cadherin-6–targeting ADC for the treatment of ovarian and renal cancers. *Cancer Discov*, 2017, 7(9), 1030-1045.

78. Hong EE *et al.* Design of coltuximab ravtansine, a CD19-targeting antibody-drug conjugate (ADC) for the treatment of B-cell malignancies: structure-activity relationships and preclinical evaluation. *Mol Pharm*, 2015, 12(6), 1703-1716.

79. Poon KA *et al.* Preclinical safety profile of trastuzumab emtansine (T-DM1): mechanism of action of its cytotoxic component retained with improved tolerability. *Toxicol Appl Pharmacol*, 2013, 273(2), 298-313.

80. Beck A, Goetsch L, Dumontet C, Corvaia N. Strategies and challenges for the next generation of antibody-drug conjugates. *Nat Rev Drug Discov*, 2017, 16(5), 315-337.

81. Strebhardt K, Ullrich A. Paul Ehrlich's magic bullet concept: 100 years of progress. *Nat Rev Cancer*, 2008, 8(6), 473-480.

82. Kim EG, Kim KM. Strategies and advancement in antibody-drug conjugate optimization for targeted cancer therapeutics. *Biomol Ther*, 2015, 23(6), 493-509.

83. Lewis Phillips GD *et al.* Targeting HER2-positive breast cancer with trastuzumab-DM1, an antibody–cytotoxic drug conjugate. *Cancer Res*, 2008, 68(22), 9280-9290.

84. Li JY *et al.* A biparatopic HER2-targeting antibody-drug conjugate induces tumor regression in primary models refractory to or ineligible for HER2-targeted therapy. *Cancer Cell*, 2016, 29(1), 117-129.

85. Peters C, Brown S. Antibody-drug conjugates as novel anti-cancer chemotherapeutics. *Biosci Rep*, 2015, 35(4), pii: e00225.

86. Bouchard H, Viskov C, Garcia-Echeverria C. Antibody-drug conjugates-a new wave of cancer drugs. *Bioorg Med Chem Lett*, 2014, 24(23), 5357-5363.

87. Beck A *et al.* Cutting-edge mass spectrometry methods for the multi-level structural characterization of antibody-drug conjugates. *Expert Rev Proteomics*, 2016, 13(2), 157-183.

88. Junutula JR *et al.* Site-specific conjugation of a cytotoxic drug to an antibody improves the therapeutic index. *Nat Biotech*, 2008, 26(8), 925-932.

89. Axup JY *et al.* Synthesis of site-specific antibody-drug conjugates using unnatural amino acids. *Proc Natl Acad Sci USA*, 2012, 109(40), 16101-16106.

90. Schumacher D *et al.* Versatile and efficient site-specific protein functionalization by tubulin tyrosine ligase. *Angew Chem Int Ed Engl*, 2015, 54(46), 13787-13791.

91. Zhou Q *et al.* Site-specific antibody-drug conjugation through glycoengineering. *Bioconjug Chem*, 2014, 25(3), 510-520.

92. Jain N, Smith SW, Ghone S, Tomczuk B. Current ADC linker chemistry. *Pharm Res*, 2015, 32(11), 3526-3540.

93. Han TH, Zhao B. Absorption, distribution, metabolism, and excretion considerations for the development of antibody-drug conjugates. *Drug Metab Dispos*, 2014, 42(11), 1914-1920.

94. Diamantis N, Banerji U. Antibody-drug conjugates-an emerging class of cancer treatment. *Br J Cancer*, 2016, 114(4), 362-367.

95. Wagner-Rousset E *et al*. Antibody-drug conjugate model fast characterization by LC-MS following IdeS proteolytic digestion. *mAbs*, 2014, 6(1), 173-184.

96. Erickson HK *et al*. Antibody-maytansinoid conjugates are activated in targeted cancer cells by lysosomal degradation and linker-dependent intracellular processing. *Cancer Res*, 2006, 66(8), 4426-4433.

97. Walles M *et al*. New insights in tissue distribution, metabolism, and excretion of [^{3}H]-labeled antibody maytansinoid conjugates in female tumor-bearing nude rats. *Drug Metab Dispos*, 2016, 44(7), 897-910.

98. Junttila TT, Li G, Parsons K, Phillips GL, Sliwkowski MX. Trastuzumab-DM1 (T-DM1) retains all the mechanisms of action of trastuzumab and efficiently inhibits growth of lapatinib insensitive breast cancer. *Breast Cancer Res Treat*, 2011, 128(2), 347-356.

99. Jain N, Smith SW, Ghone S, Tomczuk B. Current ADC linker chemistry. *Pharm Res,* 2015, 32(11), 3526-3540.

100. Teicher BA, Chari RVJ. Antibody conjugate therapeutics: challenges and potential. *Clin Cancer Res*, 2011, 17(20), 6389-6397.

101. Sau S, Alsaab HO, Kashaw SK, Tatiparti K, Iyer AK. Advances in antibody–drug conjugates: A new era of targeted cancer therapy. *Drug Discov Today*, 2017, 22(10), 1547-1556.

102. Regales L *et al*. Dual targeting of EGFR can overcome a major drug resistance mutation in mouse models of EGFR mutant lung cancer. *J Clin Invest*, 2009, 119(10), 3000-3010.

103. Seimetz D, Lindhofer H, Bokemeyer C. Development and approval of the trifunctional antibody catumaxomab (anti-EpCAM×anti-CD3) as a targeted cancer immunotherapy. *Cancer Treat Rev*, 2010, 36(6), 458-467.

104. Fitzgerald JB *et al*. MM-141, an IGF-IR–and ErbB3-directed bispecific antibody, overcomes network adaptations that limit activity of IGF-IR inhibitors. *Mol Cancer Ther*, 2014, 13(2), 410-425.

105. Sheikhi Mehrabadi F *et al*. Bispecific antibodies for targeted delivery of dendritic polyglycerol (dPG) prodrug conjugates. *Curr Cancer Drug Targets*, 2016, 16(7), 639-649.

106. Kitazawa T *et al*. A bispecific antibody to factors IXa and X restores factor VIII hemostatic activity in a hemophilia A model. *Nat Med*, 2012, 18(10), 1570-1574.

107. Fan G, Wang Z, Hao M, Li J. Bispecific antibodies and their applications. *J Hematol Oncol*, 2015, 8, 130.

108. Kontermann RE, Brinkmann U. Bispecific antibodies. *Drug Discov Today*, 2015, 20(7), 838-847.

109. Spiess C, Zhai Q, Carter PJ. Alternative molecular formats and therapeutic applications for bispecific antibodies. *Mol Immunol*, 2015, 67, 95-106.

110. Staerz UD, Bevan MJ. Hybrid hybridoma producing a bispecific monoclonal antibody that can focus effector T-cell activity. *Proc Natl Acad Sci USA*, 1986, 83(5), 1453-1457.

111. Schaefer W *et al*. Heavy and light chain pairing of bivalent quadroma and knobs-into-holes antibodies analyzed by UHR-ESI-QTOF mass spectrometry. *mAbs*, 2016, 8(1), 49-55.

112. Xu Y *et al.* Production of bispecific antibodies in "knobs-into-holes" using a cell-free expression system. *mAbs*, 2015, 7(1), 231-242.

113. Hassanzadeh-Ghassabeh G, Devoogdt N, De Pauw P, Vincke C, Muyldermans S. Nanobodies and their potential applications. *Nanomedicine*, 2013, 8(6), 1013-1026.

114. Nelson AL. Antibody fragments: Hope and hype. *mAbs*, 2010, 2(1), 77-83.

115. Beck A, Reichert JM. Therapeutic Fc-fusion proteins and peptides as successful alternatives to antibodies. *mAbs*, 2011, 3(5), 415-416.

116. Frenzel A, Hust M, Schirrmann T. Expression of recombinant antibodies. *Front Immunol*, 2013, 4, 217.

117. Holliger P, Hudson PJ. Engineered antibody fragments and the rise of single domains. *Nat Biotechnol*, 2005, 23(9), 1126.

118. Oyen D, Srinivasan V, Steyaert J, Barlow JN. Constraining enzyme conformational cange by an antibody leads to hyperbolic inhibition. *J Mol Biol*, 2011, 407(1), 138-148.

119. Skottrup PD *et al*. Diagnostic evaluation of a nanobody with picomolar affinity toward the protease RgpB from Porphyromonas gingivalis. *Anal Biochem*, 2011, 415(2), 158-167.

120. Yokota T, Milenic DE, Whitlow M, Schlom J. Rapid tumor penetration of a single-chain Fv and comparison with other immunoglobulin forms. *Cancer Res*, 1992, 52(12), 3402-3408.

121. van der Linden RHJ *et al*. Comparison of physical chemical properties of llama VHH antibody fragments and mouse monoclonal antibodies. *Biochim Biophys Acta*, 1999, 1431(1), 37-46.

122. Holland MC *et al*. Autoantibodies to variable heavy (VH) chain Ig sequences in humans impact the safety and clinical pharmacology of a VH domain antibody antagonist of TNF-α receptor 1. *J Clin Immunol*, 2013, 33(7), 1192-1203.

123. Papadopoulos KP *et al*. Unexpected hepatotoxicity in a phase I study of TAS266, a novel tetravalent agonistic Nanobody® targeting the DR5 receptor. *Cancer Chemother Pharmacol*, 2015, 75(5), 887-895.

124. Gorovits B *et al*. Pre-existing antibody: biotherapeutic modality-based review. *AAPS J*, 2016, 18(2), 311-320.

125. Pabst TM *et al*. Camelid VHH affinity ligands enable separation of closely related biopharmaceuticals. *Biotech J*, 2017, 12(2), doi: 10.1002/biot.201600357.

126. Verheesen P, ten Haaft MR, Lindner N, Verrips CT, de Haard JJW. Beneficial properties of single-domain antibody fragments for application in immunoaffinity purification and immuno-perfusion chromatography. *Biochim Biophys Acta*, 2003, 1624(1), 21-28.

127. Romer T, Leonhardt H, Rothbauer U. Engineering antibodies and proteins for molecular in vivo imaging. *Curr Opin Biotechnol*, 2011, 22(6), 882-887.

128. Xavier C *et al*. ^{18}F-nanobody for PET imaging of HER2 overexpressing tumors. *Nucl Med Biol*, 2016, 43(4), 247-252.

129. Šenolt L, Vencovský J, Pavelka K, Ospelt C, Gay S. Prospective new biological therapies for rheumatoid arthritis. *Autoimmun Rev*, 2009, 9(2), 102-107.

130. Kantarjian H *et al*. Blinatumomab versus chemotherapy for advanced acute lymphoblastic leukemia. *N Engl J Med*, 2017, 376(9), 836-847.

131. Lasoff DR, Ruha AM, Curry SC, Koh C, Clark RF. A new F(ab')2 antivenom for the treatment of crotaline envenomation in children. *Am J Emerg Med*, 2016, 34(10), 2003-2006.

132. Pucca MB *et al*. Serrumab: A novel human single chain-fragment antibody with multiple scorpion toxin-neutralizing capacities. *J Immunotoxicol*, 2014, 11(2), 133-140.

133. Kinch MS, Haynesworth A, Kinch SL, Hoyer D. An overview of FDA-approved new molecular entities: 1827–2013. *Drug Discovery Today*, 2014, 19(8), 1033-1039.

134. Mullard A. 2016 EMA drug approval recommendations. *Nat Rev Drug Discov*, 2017, 16(2), 77.

135. U.S. Food and Drug Administration - Center for Drug Evaluation and Research. 2016 Novel Drug Summary. Jan 2017 https://www.fda.gov.

136. Reichert JM. Antibodies to watch in 2017. *mAbs*, 2017, 9(2), 167-181.

137. La Merie Publishing. 2016 Sales of Recombinant Therapeutic Antibodies & Proteins. Mar 2017 http://www.pipelinereview.com.

138. Ecker DM, Jones SD, Levine HL. The therapeutic monoclonal antibody market. *mAbs*, 2015, 7(1), 9-14.

139. Elvin JG, Couston RG, van der Walle CF. Therapeutic antibodies: Market considerations, disease targets and bioprocessing. *Int J Pharm*, 2013, 440(1), 83-98.

140. Loke J, Khan JN, Wilson JS, Craddock C, Wheatley K. Mylotarg has potent anti-leukaemic effect: a systematic review and meta-analysis of anti-CD33 antibody treatment in acute myeloid leukaemia. *Ann Hematol*, 2015, 94, 361-373.

141. Beck A, Reichert JM. Approval of the first biosimilar antibodies in Europe. *mAbs*, 2013, 5(5), 621-623.

142. Chow S. Quantitative evaluation of bioequivalence/biosimilarity. *J Bioequiv Availab*, 2011, 1, 1-8.

143. Hyland E *et al*. Comparison of the pharmacokinetics, safety, and immunogenicity of MSB11022, a biosimilar of adalimumab, with Humira(®) in healthy subjects. *Br J Clin Pharmac*ol, 2016, 82(4), 983-993.

144. Upda N, Million R. Monoclonal antibody biosimilars. *Nat Rev Drug Discov*, 2016, 15(1), 13-14.

145. Mullard A. Bracing for the biosimilar wave. *Nat Rev Drug Discov*, 2017, 16(3), 152-154.

146. Blackstone EA, Joseph PF. The economics of biosimilars. *Am Health Drug Benefits*, 2013, 6(8), 469-478.

147. Dimitrov DS. Therapeutic proteins: methods and protocols. *Methods Mol Biol*, 2012, 899, 1-26.

148. La Merie Publishing. Top 20 Biologics-2008 Sales of Antibodies & Proteins Mar 2009 http://www.pipelinereview.com.

149. La Merie Publishing. 2015 Sales of Recombinant Therapeutic Antibodies & Proteins. Mar 2016 http://www.pipelinereview.com.

150. Walsh G. Biopharmaceutical benchmarks 2010. *Nat Biotech*, 2010, 28(9), 917-924.

151. Saxena A, Wu D. Advances in therapeutic Fc engineering - modulation of IgG-associated effector functions and serum half-life. *Front Immunol*, 2016, 7, 580.

152. Carter PJ. Potent antibody therapeutics by design. *Nat Rev Immunol*, 2006, 6(5), 343-357.

153. Reichert JM. Antibodies to watch in 2016. *mAbs*, 2015, 8(2), 1-8.

154. TechNavio. Global Biologic Therapeutics Market 2015-2019. Oct 2015 https://www.technavio.com.

155. Beck A *et al*. Cutting-edge mass spectrometry characterization of originator, biosimilar and biobetter antibodies. *J Mass Spectrom*, 2015, 50(2), 285-297.

156. Beck A, Wagner-Rousset E, Ayoub D, Van Dorsselaer A, Sanglier-Cianférani S. Characterization of therapeutic antibodies and related products. *Anal Chem*, 2013, 85(2), 715-736.

157. Masson GR, Jenkins ML, Burke JE. An overview of hydrogen deuterium exchange mass spectrometry (HDX-MS) in drug discovery. *Expert Opin Drug Discov*, 2017, 12(10), 981-994.

158. Mistarz UH, Brown JM, Haselmann KF, Rand KD. Probing the binding interfaces of protein complexes using gas-phase H/D exchange mass spectrometry. *Structure*, 2016, 24(2), 310-318.

159. Huber C. Higher order mass spectrometry techniques applied to biopharmaceuticals. *LCGC Europe*, 2015, Special Issues, 31-36.

160. Botzanowski T *et al*. Insights from native mass spectrometry approaches for top- and middle-level characterization of site-specific antibody-drug conjugates. *mAbs*, 2017, 9(5), 801-811.

161. Olinares PDB *et al*. A robust workflow for native mass spectrometric analysis of affinity-isolated endogenous protein assemblies. *Anal Chem*, 2016, 88(5), 2799-2807.

162. Yang Y, Wang G, Song T, Lebrilla CB, Heck AJR. Resolving the micro-heterogeneity and structural integrity of monoclonal antibodies by hybrid mass spectrometric approaches. *mAbs*, 2017, 9(4), 638-645.

163. Debaene F *et al*. Time resolved native ion-mobility mass spectrometry to monitor dynamics of IgG4 Fab arm exchange and "bispecific" monoclonal antibody formation. *Anal Chem*, 2013, 85(20), 9785-9792.

164. Marcoux J *et al*. Native mass spectrometry and ion mobility characterization of trastuzumab emtansine, a lysine-linked antibody drug conjugate. *Protein Sci*, 2015, 24(8), 1210-1223.

165. Stojko J *et al*. Ion mobility coupled to native mass spectrometry as a relevant tool to investigate extremely small ligand-induced conformational changes. *Analyst*, 2015, 140(21), 7234-7245.

166. Terral G, Beck A, Cianférani S. Insights from native mass spectrometry and ion mobility-mass spectrometry for antibody and antibody-based product characterization. *J Chromatogr B*, 2016, 1032, 79-90.

167. Aich U, Lakbub J, Liu A. State of the art technologies for rapid and high-throughput sample preparation and analysis of n-glycans from antibodies. *Electrophoresis*, 2016, 37(11), 1468-1488.

168. Tran BQ *et al*. Glycosylation characterization of therapeutic mAbs by top- and middle-down mass spectrometry. *Data Brief*, 2016, 6, 68-76.

169. Forstenlehner IC, Holzmann J, Toll H, Huber CG. Site-specific characterization and absolute quantification of pegfilgrastim oxidation by top-down high-performance liquid chromatography-mass spectrometry. *Anal Chem*, 2015, 87(18), 9336-9343.

170. Biacchi M, Said N, Beck A, Leize-Wagner E, François Y-N. Top-down and middle-down approach by fraction collection enrichment using off-line capillary electrophoresis-mass spectrometry coupling: Application to monoclonal antibody Fc/2 charge variants. *J Chromatogr A*, 2017, 1498, 120-127.

171. Griaud F *et al*. Unbiased in-depth characterization of CEX fractions from a stressed monoclonal antibody by mass spectrometry. *mAbs*, 2017, 9(5), 820-830.

172. Wagner-Rousset E *et al*. Development of a fast workflow to screen the charge variants of therapeutic antibodies. *J Chromatogr A*, 2017, 1498, 147-154.

173. Xu CF, Zang L, Weiskopf A. Size-exclusion chromatography-mass spectrometry with m-nitrobenzyl alcohol as post-column additive for direct characterization of size variants of monoclonal antibodies. *J Chromatogr B*, 2014, 960, 230-238.

174. Chen J, Yin S, Wu Y, Ouyang J. Development of a native nanoelectrospray mass spectrometry method for determination of the drug-to-antibody ratio of antibody-drug conjugates. *Anal Chem*, 2013, 85(3), 1699-1704.

175. Debaene F *et al*. Innovative native MS methodologies for antibody drug conjugate characterization: high resolution native MS and IM-MS for average DAR and DAR distribution assessment. *Anal Chem*, 2014, 86(21), 10674-10683.

176. Redman EA, Mellors JS, Starkey JA, Ramsey JM. Characterization of intact antibody drug conjugate variants using microfluidic capillary electrophoresis-mass spectrometry. *Anal Chem*, 2016, 88(4), 2220-2226.

177. Janin-Bussat MC, Dillenbourg M, Corvaia N, Beck A, Klinguer-Hamour C. Characterization of antibody drug conjugate positional isomers at cysteine residues by peptide mapping LC-MS analysis. *J Chromatogr B*, 2015, 981-982, 9-13.

178. Beck A *et al*. Characterization by liquid chromatography combined with mass spectrometry of monoclonal anti-IGF-1 receptor antibodies produced in CHO and NS0 cells. *J Chromatogr B*, 2005, 819(2), 203-218.

179. Chen L *et al*. In-depth structural characterization of Kadcyla® (ado-trastuzumab emtansine) and its biosimilar candidate. *mAbs*, 2016, 8(7), 1210-1223.

180. Gautier V, Boumeester AJ, Lössl P, Heck AJR. Lysine conjugation properties in human IgGs studied by integrating high-resolution native mass spectrometry and bottom-up proteomics. *Proteomics*, 2015, 15(16), 2756-2765.

181. Wang Y *et al*. Simultaneous monitoring of oxidation, deamidation, isomerization, and glycosylation of monoclonal antibodies by liquid chromatography-mass spectrometry method with ultrafast tryptic digestion. *mAbs*, 2016, 8(8), 1477-1486.

182. Xie H, Gilar M, Gebler JC. Characterization of protein impurities and site-specific modifications using peptide mapping with liquid chromatography and data independent acquisition mass spectrometry. *Anal Chem*, 2009, 81(14), 5699-5708.

183. Zhang YT *et al*. Characterization of asparagine 330 deamidation in an Fc-fragment of IgG1 using cation exchange chromatography and peptide mapping. *J Chromatogr B*, 2014, 965, 65-71.

184. Tholey A, Toll H, Huber CG. Separation and detection of phosphorylated and nonphosphorylated peptides in liquid chromatography-mass spectrometry using monolithic columns and acidic or alkaline mobile phases. *Anal Chem*, 2005, 77(14), 4618-4625.

185. Tsubaki M, Terashima I, Kamata K, Koga A. C-terminal modification of monoclonal antibody drugs: Amidated species as a general product-related substance. *Int J Biol Macromol*, 2013, 52, 139-147.

186. Regl C, Wohlschlager T, Holzmann J, Huber CG. A generic HPLC method for absolute quantification of oxidation in monoclonal antibodies and Fc-fusion proteins using UV and MS detection. *Anal Chem*, 2017, 89(16), 8391-8398.

187. Lee JW *et al*. Bioanalytical approaches to quantify "total" and "free" therapeutic antibodies and their targets: technical challenges and PK/PD applications over the course of drug development. *AAPS J*, 2011, 13(1), 99-110.

188. Pritchard JF *et al*. Making better drugs: decision gates in non-clinical drug revelopment. *Nat Rev Drug Discov*, 2003, 2(7), 542-553.

189. International Council for Harmonisation. Guidance for Industry: S6 Preclinical Safety Evaluation of Biotechnology-derived Pharmaceuticals. Jul 1997 http://www.ich.org/.

190. Kuang B, King L, Wang HF. Therapeutic monoclonal antibody concentration monitoring: free or total? *Bioanalysis*, 2010, 2(6), 1125-1140.

191. Andersen CY. Possible new mechanism of cortisol action in female reproductive organs: physiological implications of the free hormone hypothesis. *J Endocrinol*, 2002, 173(2), 211-217.

192. Mendel CM. The free hormone hypothesis: a physiologically based mathematical model. *Endocr Rev*, 1989, 10(3), 232-274.

193. Smith A *et al*. Unraveling the effect of immunogenicity on the PK/PD, efficacy, and safety of therapeutic proteins. *J Immunol Res*, 2016, 2016, 2342187.

194. Myler H *et al*. An integrated multiplatform bioanalytical strategy for antibody-drug conjugates: a novel case study. *Bioanalysis*, 2015, 7(13), 1569-1582.

195. Barrette RW, Urbonas J, Silbart LK. Quantifying specific antibody concentrations by enzyme-linked immunosorbent assay using slope correction. *Clin Vaccine Immunol*, 2006, 13(7), 802-805.

196. Kelley M *et al*. Theoretical considerations and practical approaches to address the effect of anti-drug antibody (ADA) on quantification of biotherapeutics in circulation. *AAPS J*, 2013, 15(3), 646-658.

197. Ezan E, Bitsch F. Critical comparison of MS and immunoassays for the bioanalysis of therapeutic antibodies. *Bioanalysis*, 2009, 1(8), 1375-1388.

198. Findlay JWA *et al*. Validation of immunoassays for bioanalysis: a pharmaceutical industry perspective. *J Pharm Biomed Anal*, 2000, 21(6), 1249-1273.

199. Lee JW, Kelley M. Quality assessment of bioanalytical quantification of monoclonal antibody drugs. *Ther Deliv*, 2011, 2(3), 383-396.

200. Qu M *et al*. Qualitative and quantitative characterization of protein biotherapeutics with liquid chromatography mass spectrometry. *Mass Spectrom Rev*, 2017, 36(6), 734-754.

201. Zheng J, Mehl J, Zhu Y, Xin B, Olah T. Application and challenges in using LC-MS assays for absolute quantitative analysis of therapeutic proteins in drug discovery. *Bioanalysis*, 2014, 6(6), 859-879.

202. An B, Zhang M, Qu J. Toward sensitive and accurate analysis of antibody biotherapeutics by liquid chromatography coupled with mass spectrometry. *Drug Metab Dispos*, 2014, 42(11), 1858-1866.

203. O'Hara DM *et al*. Ligand binding assays in the 21st century laboratory: recommendations for characterization and supply of critical reagents. *AAPS J*, 2012, 14(2), 316-328.

204. Savoie N *et al*. 2010 white paper on recent issues in regulated bioanalysis & global harmonization of bioanalytical guidance. *Bioanalysis*, 2010, 2(12), 1945-1960.

205. Pendley C, Shankar G. Bioanalytical interferences in immunoassays for antibody biotherapeutics. *Bioanalysis*, 2011, 3(7), 703-706.

206. Pandya K *et al*. Strategies to minimize variability and bias associated with manual pipetting in ligand binding assays to assure data quality of protein therapeutic quantification. *J Pharm Biomed Anal*, 2010, 53(3), 623-630.

207. Budhraja R *et al*. LC-MS/MS validation analysis of trastuzumab using dSIL approach for evaluating pharmacokinetics. *Molecules*, 2016, 21(11), 1464.

208. Shi J *et al*. Reagent-free LC-MS/MS-based pharmacokinetic quantification of polyhistidine-tagged therapeutic proteins. *Bioanalysis*, 2017, 9(3), 251-264.

209. Szapacs ME *et al.* Absolute quantification of a therapeutic domain antibody using ultra-performance liquid chromatography-mass spectrometry and immunoassay. *Bioanalysis*, 2010, 2(9), 1597-1608.

210. Xu L, Packer LE, Li C, Abdul-Hadi K, Veiby P. A generic approach for simultaneous measurements of total antibody and cleavable antibody-conjugated drug by LC/MS/MS. *Anal Biochem*, 2017, 537, 33-36.

211. Wang Y, Roth JD, Taylor SW. Simultaneous quantification of the glucagon-like peptide-1 (GLP-1) and cholecystokinin (CCK) receptor agonists in rodent plasma by on-line solid phase extraction and LC-MS/MS. *J Chromatogr B*, 2014, 957, 24-29.

212. Bielohuby M *et al.* Validation of serum IGF-I as a biomarker to monitor the bioactivity of exogenous growth hormone agonists and antagonists in rabbits. *Dis Model Mech*, 2014, 7(11), 1263-1273.

213. Whiteaker JR *et al.* Peptide immunoaffinity enrichment and targeted mass spectrometry enables multiplex, quantitative pharmacodynamic studies of phospho-signaling. *Mol Cell Proteomics*, 2015, 14(8), 2261-2273.

214. Zhang YJ, Olah TV, Zeng J. The integration of ligand binding and LC-MS-based assays into bioanalytical strategies for protein analysis. *Bioanalysis*, 2014, 6(13), 1827-1841.

215. Chen LZ, Roos D, Philip E. Development of immunocapture-LC/MS assay for simultaneous ADA isotyping and semiquantitation. *J Immunol Res*, 2016, 2016, 14.

216. Jiang H *et al.* Innovative use of LC-MS/MS for simultaneous quantitation of neutralizing antibody, residual drug, and human immunoglobulin G in immunogenicity assay development. *Anal Chem*, 2014, 86(5), 2673-2680.

217. Neubert H, Grace C, Rumpel K, James I. Assessing immunogenicity in the presence of excess protein therapeutic using immunoprecipation and quantitative mass spectrometry. *Anal Chem*, 2008, 80(18), 6907-6914.

218. van den Broek I, Niessen WM, van Dongen WD. Bioanalytical LC-MS/MS of protein-based biopharmaceuticals. *J Chromatogr B*, 2013, 929, 161-179.

219. Dupré M *et al.* Multiplex quantification of protein toxins in human biofluids and food matrices using immunoextraction and high-resolution targeted mass spectrometry. *Anal Chem*, 2015, 87(16), 8473-8480.

220. Gilquin B *et al.* Multiplex and accurate quantification of acute kidney injury biomarker candidates in urine using Protein Standard Absolute Quantification (PSAQ) and targeted proteomics. *Talanta*, 2017, 164, 77-84.

221. Lebert D *et al.* Absolute and multiplex quantification of antibodies in serum using PSAQ™ standards and LC-MS/MS. *Bioanalysis*, 2015, 7(10), 1237-1251.

222. Zhu Y *et al*. LC-MS/MS multiplexed assay for the quantitation of a therapeutic protein BMS-986089 and the target protein myostatin. *Bioanalysis*, 2016, 8(3), 193-204.

223. Compton PD, Zamdborg L, Thomas PM, Kelleher NL. On the scalability and requirements of whole protein mass spectrometry. *Anal Chem*, 2011, 83(17), 6868-6874.

224. Hopfgartner G, Lesur A, Varesio E. Analysis of biopharmaceutical proteins in biological matrices by LC-MS/MS II. LC-MS/MS analysis. *Trends Analyt Chem*, 2013, 48, 52-61.

225. Gallien S, Duriez E, Domon B. Selected reaction monitoring applied to proteomics. *J Mass Spectrom*, 2011, 46(3), 298-312.

226. MacLean B *et al*. Skyline: an open source document editor for creating and analyzing targeted proteomics experiments. *Bioinformatics*, 2010, 26(7), 966-968.

227. Mead JA *et al*. MRMaid, the web-based tool for designing multiple reaction monitoring (MRM) transitions. *Mol Cell Proteomics*, 2009, 8(4), 696-705.

228. Deutsch EW, Lam H, Aebersold R. PeptideAtlas: a resource for target selection for emerging targeted proteomics workflows. *EMBO Reports*, 2008, 9(5), 429-434.

229. Mallick P *et al*. Computational prediction of proteotypic peptides for quantitative proteomics. *Nat Biotech*, 2007, 25(1), 125-131.

230. Martin DB *et al*. MRMer, an interactive open source and cross-platform system for data extraction and visualization of multiple reaction monitoring experiments. *Mol Cell Proteomics*, 2008, 7(11), 2270-2278.

231. Sherwood CA *et al*. MaRiMba: A software application for spectral lbrary-based MRM transition list assembly. *J Proteome Res*, 2009, 8(10), 4396-4405.

232. van den Steen P, Rudd PM, Dwek RA, Opdenakker G. Concepts and principles of O-linked glycosylation. *Crit Rev Biochem Mol Biol*, 1998, 33(3), 151-208.

233. Mellquist JL, Kasturi L, Spitalnik SL, Shakin-Eshleman SH. The amino acid following an Asn-X-Ser/Thr sequon is an important determinant of N-linked core glycosylation efficiency. *Biochemistry*, 1998, 37(19), 6833-6837.

234. Krieg J *et al*. Recognition signal for C-mannosylation of Trp-7 in RNase 2 consists of sequence Trp-x-x-Trp. *Mol Biol Cell*, 1998, 9(2), 301-309.

235. Pan Y *et al*. Human germline and pan-cancer variomes and their distinct functional profiles. *Nucleic Acids Res*, 2014, 42(18), 11570-11588.

236. Mount DW. Using the basic local alignment search tool (BLAST). CSH Prot, 2007, 2007(7), pdb.top17.

237. Hagman C *et al*. Absolute quantification of monoclonal antibodies in biofluids by liquid chromatography-tandem mass spectrometry. *Anal Chem*, 2008, 80(4), 1290-1296.

238. Heudi O *et al*. Towards absolute quantification of therapeutic monoclonal antibody in serum by LC-MS/MS using isotope-labeled antibody standard and protein cleavage isotope dilution mass spectrometry. *Anal Chem*, 2008, 80(11), 4200-4207.

239. Furlong MT *et al*. A universal surrogate peptide to enable LC-MS/MS bioanalysis of a diversity of human monoclonal antibody and human Fc-fusion protein drug candidates in pre-clinical animal studies. *Biomed Chromatogr*, 2012, 26(8), 1024-1032.

240. Li H *et al*. General LC-MS/MS method approach to quantify therapeutic monoclonal antibodies using a common whole antibody internal standard with application to preclinical studies. *Anal Chem*, 2012, 84(3), 1267-1273.

241. Furlong MT *et al*. Dual universal peptide approach to bioanalysis of human monoclonal antibody protein drug candidates in animal studies. *Bioanalysis*, 2013, 5(11), 1363-1376.

242. Law WS *et al*. Use of generic LC–MS/MS assays to characterize atypical PK profile of a biotherapeutic monoclonal antibody. *Bioanalysis*, 2014, 6(23), 3225-3235.

243. Zhang Q *et al*. Generic automated method for liquid chromatography-multiple reaction monitoring mass spectrometry based monoclonal antibody quantitation for preclinical pharmacokinetic studies. *Anal Chem*, 2014, 86(17), 8776-8784.

244. Kaur S *et al*. Validation of a biotherapeutic immunoaffinity-LC-MS/MS assay in monkey serum: 'plug-and-play' across seven molecules. *Bioanalysis*, 2016, 8(15), 1565-1577.

245. Kuzyk MA *et al*. Multiple reaction monitoring-based, multiplexed, absolute quantitation of 45 proteins in human plasma. *Mol Cell Proteomics*, 2009, 8(8), 1860-1877.

246. Percy AJ, Chambers AG, Yang J, Hardie DB, Borchers CH. Advances in multiplexed MRM-based protein biomarker quantitation toward clinical utility. *Biochim Biophys Acta*, 2014, 1844(5), 917-926.

247. Shi T *et al*. Antibody-free, targeted mass-spectrometric approach for quantification of proteins at low picogram per milliliter levels in human plasma/serum. *Proc Natl Acad Sci USA*, 2012, 109(38), 15395-15400.

248. Wilffert D, Bischoff R, van de Merbel NC. Antibody-free workflows for protein quantification by LC-MS/MS. *Bioanalysis*, 2015, 7(6), 763-779.

249. Bischoff R, Bronsema KJ, van de Merbel NC. Analysis of biopharmaceutical proteins in biological matrices by LC-MS/MS I. Sample preparation. *Trends Analyt Chem*, 2013, 48, 41-51.

250. Furey A, Moriarty M, Bane V, Kinsella B, Lehane M. Ion suppression; a critical review on causes, evaluation, prevention and applications. *Talanta*, 2013, 115, 104-122.

251. Barnidge DR, Goodmanson MK, Klee GG, Muddiman DC. Absolute quantification of the model biomarker prostate-specific antigen in serum by LC-MS/MS using protein cleavage and isotope dilution mass spectrometry. *J Proteome Res*, 2004, 3(3), 644-652.

252. Seegmiller JC *et al*. Quantification of urinary albumin by using protein cleavage and LC-MS/MS. *Clin Chem*, 2009, 55(6), 1100-1107.

253. Anderson NL *et al*. Mass spectrometric quantitation of peptides and proteins using Stable Isotope Standards and Capture by Anti-Peptide Antibodies (SISCAPA). *J Proteome Res*, 2004, 3(2), 235-244.

254. Razavi M, Leigh Anderson N, Pope ME, Yip R, Pearson TW. High precision quantification of human plasma proteins using the automated SISCAPA immuno-MS workflow. *N Biotechnol*, 2016, 33(5 Pt A), 494-502.

255. van den Broek I *et al*. Quantification of serum apolipoproteins A-I and B-100 in clinical samples using an automated SISCAPA-MALDI-TOF-MS workflow. *Methods*, 2015, 81, 74-85.

256. Choi E, Loo D, Dennis JW, O'Leary CA, Hill MM. High-throughput lectin magnetic bead array-coupled tandem mass spectrometry for glycoprotein biomarker discovery. *Electrophoresis*, 2011, 32(24), 3564-3575.

257. Gao X *et al*. Quantitative analysis of factor P (properdin) in monkey serum using immunoaffinity capturing in combination with LC-MS/MS. *Bioanalysis*, 2016, 8(5), 425-438.

258. Smits NE *et al*. Monolith immuno-affinity enrichment liquid chromatography tandem mass spectrometry for quantitative protein analysis of recombinant bovine somatotropin in serum. *Anal Bioanal Chem*, 2015, 407(20), 6041-6050.

259. Ueda K *et al*. Antibody-coupled monolithic silica microtips for highthroughput molecular profiling of circulating exosomes. *Sci Rep*, 2014, 4, 6232.

260. Yu Y, Xu J, Liu Y, Chen Y. Quantification of human serum transferrin using liquid chromatography-tandem mass spectrometry based targeted proteomics. *J Chromatogr B*, 2012, 902, 10-15.

261. Yang Z, Ke J, Hayes M, Bryant M, Tse FL. A sensitive and high-throughput LC-MS/MS method for the quantification of pegylated-interferon-alpha2a in human serum using monolithic C18 solid phase extraction for enrichment. *J Chromatogr B*, 2009, 877(18-19), 1737-1742.

262. Proc JL *et al*. A quantitative study of the effects of chaotropic agents, surfactants, and solvents on the digestion efficiency of human plasma proteins by trypsin. *J Proteome Res*, 2010, 9(10), 5422-5437.

263. Mandal P, Molla AR, Mandal DK. Denaturation of bovine spleen galectin-1 in guanidine hydrochloride and fluoroalcohols: structural characterization and implications for protein folding. *J Biochem*, 2013, 154(6), 531-540.

264. Wu ST, Ouyang Z, Olah TV, Jemal M. A strategy for liquid chromatography/tandem mass spectrometry based quantitation of pegylated protein drugs in plasma using plasma

protein precipitation with water-miscible organic solvents and subsequent trypsin digestion to generate surrogate peptides for detection. *Rapid Commun Mass Spectrom*, 2011, 25(2), 281-290.

265. Duan X, Abuqayyas L, Dai L, Balthasar JP, Qu J. High-throughput method development for sensitive, accurate, and reproducible quantification of therapeutic monoclonal antibodies in tissues using orthogonal array optimization and nano liquid chromatography/selected reaction monitoring mass spectrometry. *Anal Chem*, 2012, 84(10), 4373-4382.

266. Heudi O, Barteau S, Picard F, Kretz O. Quantitative analysis of maytansinoid (DM1) in human serum by on-line solid phase extraction coupled with liquid chromatography tandem mass spectrometry - method validation and its application to clinical samples. *J Pharm Biomed Anal*, 2016, 120, 322-332.

267. Sturm R *et al*. Absolute quantification of prion protein (90–231) using stable isotope-labeled chymotryptic peptide standards in a LC-MRM AQUA workflow. *J Am Soc Mass Spectrom*, 2012, 23(9), 1522-1533.

268. van den Broek I, Sparidans RW, Schellens JH, Beijnen JH. Enzymatic digestion as a tool for the LC-MS/MS quantification of large peptides in biological matrices: measurement of chymotryptic fragments from the HIV-1 fusion inhibitor enfuvirtide and its metabolite M-20 in human plasma. *J Chromatogr B*, 2007, 854(1), 245-259.

269. Glatter T *et al*. Large-scale quantitative assessment of different in-solution protein digestion protocols reveals superior cleavage efficiency of tandem Lys-C/trypsin proteolysis over trypsin digestion. *J Proteome Res*, 2012, 11(11), 5145-5156.

270. Kehler J, Akella N, Citerone D, Szapacs M. Application of DBS for the quantitative assessment of a protein biologic using on-card digestion LC-MS/MS or immunoassay. *Bioanalysis*, 2011, 3(20), 2283-2290.

271. Ye H, Hill J, Kauffman J, Gryniewicz C, Han X. Detection of protein modifications and counterfeit protein pharmaceuticals using isotope tags for relative and absolute quantification and matrix-assisted laser desorption/ionization tandem time-of-flight mass spectrometry: studies of insulins. *Anal Biochem*, 2008, 379(2), 182-191.

272. Yu L *et al*. Identification and quantification of Fc fusion peptibody degradations by limited proteolysis method. *Anal Biochem*, 2012, 428(2), 137-142.

273. Wang H *et al*. Quantification of mutant SPOP proteins in prostate cancer using mass spectrometry-based targeted proteomics. *J Transl Med*, 2017, 15(1), 175.

274. de Kock SS, Rodgers JP, Swanepoel BC. Growth hormone abuse in the horse: preliminary assessment of a mass spectrometric procedure for IGF-1 identification and quantitation. *Rapid Commun Mass Spectrom*, 2001, 15(14), 1191-1197.

275. Nie S *et al*. Isobaric protein-level labeling strategy for serum glycoprotein quantification analysis by liquid chromatography-tandem mass spectrometry. *Anal Chem*, 2013, 85(11), 5353-5357.

276. Cingöz A, Hugon-Chapuis F, Pichon V. Total on-line analysis of a target protein from plasma by immunoextraction, digestion and liquid chromatography-mass spectrometry. *J Chromatogr B*, 2010, 878(2), 213-221.

277. Sporty JLS *et al*. Immunomagnetic separation and quantification of butyrylcholinesterase nerve agent adducts in human serum. *Anal Chem*, 2010, 82(15), 6593-6600.

278. Cappiello A *et al*. Overcoming matrix effects in liquid chromatography-mass spectrometry. *Anal Chem*, 2008, 80(23), 9343-9348.

279. Taylor PJ. Matrix effects: the Achilles heel of quantitative high-performance liquid chromatography-electrospray-tandem mass spectrometry. *Clin Biochem*, 2005, 38(4), 328-334.

280. Bronsema KJ, Bischoff R, van de Merbel NC. High-sensitivity LC-MS/MS quantification of peptides and proteins in complex biological samples: the impact of enzymatic digestion and internal standard selection on method performance. *Anal Chem*, 2013, 85(20), 9528-9535.

281. Lanckmans K, Sarre S, Smolders I, Michotte Y. Use of a structural analogue versus a stable isotope labeled internal standard for the quantification of angiotensin IV in rat brain dialysates using nano-liquid chromatography/tandem mass spectrometry. *Rapid Commun Mass Spectrom*, 2007, 21(7), 1187-1195.

282. Nouri-Nigjeh E *et al*. Effects of calibration approaches on the accuracy for LC-MS targeted quantification of therapeutic protein. *Anal Chem*, 2014, 86(7), 3575-3584.

283. Bronsema KJ, Bischoff R, van de Merbel NC. Internal standards in the quantitative determination of protein biopharmaceuticals using liquid chromatography coupled to mass spectrometry. *J Chromatogr B*, 2012, 893-894, 1-14.

284. Aguiar M, Masse R, Gibbs BF. Mass spectrometric quantitation of C-reactive protein using labeled tryptic peptides. *Anal Biochem*, 2006, 354(2), 175-181.

285. Kirkpatrick DS, Gerber SA, Gygi SP. The absolute quantification strategy: a general procedure for the quantification of proteins and post-translational modifications. *Methods*, 2005, 35(3), 265-273.

286. Picotti P, Bodenmiller B, Mueller LN, Domon B, Aebersold R. Full dynamic range proteome analysis of S. cerevisiae by targeted proteomics. *Cell*, 2009, 138(4), 795-806.

287. Ji C, Sadagopan N, Zhang Y, Lepsy C. A universal strategy for development of a method for absolute quantification of therapeutic monoclonal antibodies in biological matrices using

differential dimethyl labeling coupled with ultra performance liquid chromatography-tandem mass spectrometry. *Anal Chem*, 2009, 81(22), 9321-9328.

288. Callipo L *et al*. Immunoprecipitation on magnetic beads and liquid chromatography-tandem mass spectrometry for carbonic anhydrase II quantification in human serum. *Anal Biochem*, 2010, 400(2), 195-202.

289. Li YC *et al*. Quantification of endostar in rat plasma by LC-MS/MS and its application in a pharmacokinetic study. *J Pharm Biomed Anal*, 2012, 70, 505-511.

290. Remily-Wood ER, Koomen JM. Evaluation of protein quantification using standard peptides containing single conservative amino acid replacements. *J Mass Spectrom*, 2012, 47(2), 188-194.

291. Faria M *et al*. Comparison of a stable isotope labeled (SIL) peptide and an extended SIL peptide as internal standards to track digestion variability of an unstable signature peptide during quantification of a cancer biomarker, human osteopontin, from plasma using capillary microflow LC-MS/MS. *J Chromatogr B*, 2015, 1001, 156-168.

292. Lai S *et al*. A combined tryptic peptide and winged peptide internal standard approach for the determination of α-lactalbumin in dairy products by ultra high performance liquid chromatography with tandem mass spectrometry. *J Sep Sci*, 2015, 38(10), 1800-1806.

293. Neubert H *et al*. Sequential protein and peptide immunoaffinity capture for mass spectrometry-based quantification of total human β-nerve growth factor. *Anal Chem*, 2013, 85(3), 1719-1726.

294. Beynon RJ, Doherty MK, Pratt JM, Gaskell SJ. Multiplexed absolute quantification in proteomics using artificial QCAT proteins of concatenated signature peptides. *Nat Methods*, 2005, 2(8), 587.

295. Scott KB, Turko IV, Phinney KW. Methods in enzymology, 566. 289-303 (Academic Press, 2016).

296. Smith DGS, Gingras G, Aubin Y, Cyr TD. Design and expression of a QconCAT protein to validate Hi3 protein quantification of influenza vaccine antigens. *J Proteomics*, 2016, 146, 133-140.

297. Bennett RJ *et al*. DOSCATs: double standards for protein quantification. *Sci Rep*, 2017, 7, 45570.

298. Al-Majdoub ZM, Carroll KM, Gaskell SJ, Barber J. Quantification of the proteins of the bacterial ribosome using QconCAT technology. *J Proteome Res*, 2014, 13(3), 1211-1222.

299. Pratt JM *et al*. Multiplexed absolute quantification for proteomics using concatenated signature peptides encoded by QconCAT genes. *Nat Protocols*, 2006, 1(2), 1029.

300. Simpson DM, Beynon RJ. QconCATs: design and expression of concatenated protein standards for multiplexed protein quantification. *Anal Bioanal Chem*, 2012, 404(4), 977-989.

301. Dubois M *et al*. Immunopurification and mass spectrometric quantification of the active form of a chimeric therapeutic antibody in human serum. *Anal Chem*, 2008, 80(5), 1737-1745.

302. Halquist MS, Karnes HT. Quantification of alefacept, an immunosuppressive fusion protein in human plasma using a protein analogue internal standard, trypsin cleaved signature peptides and liquid chromatography tandem mass spectrometry. *J Chromatogr B*, 2011, 879(11-12), 789-798.

303. Yang Z *et al*. LC-MS/MS approach for quantification of therapeutic proteins in plasma using a protein internal standard and 2D-solid-phase extraction cleanup. *Anal Chem*, 2007, 79(24), 9294-9301.

304. Adrait A *et al*. Development of a protein standard absolute quantification (PSAQ™) assay for the quantification of staphylococcus aureus enterotoxin A in serum. *J Proteomics*, 2012, 75(10), 3041-3049.

305. Brun V *et al*. Isotope-labeled protein standards: toward absolute quantitative proteomics. *Mol Cell Proteomics*, 2007, 6(12), 2139-2149.

306. Huillet C *et al*. Accurate quantification of cardiovascular biomarkers in serum using protein standard absolute quantification (PSAQ™) and selected reaction monitoring. *Mol Cell Proteomics*, 2012, 11(2), M111.008235.

307. Lebert D, Dupuis A, Garin J, Bruley C, Brun V. Gel-free proteomics: methods and protocols. 93-115 (Humana Press, Totowa, NJ; 2011).

308. Picard G *et al*. PSAQ™ standards for accurate MS-based quantification of proteins: from the concept to biomedical applications. *J Mass Spectrom*, 2012, 47(10), 1353-1363.

309. Amsler P *et al*. Production and application of high quality stable isotope-labeled human immunoglobulin G1 for mass spectrometry analysis. *J Labelled Comp Radiopharm*, 2017, 60, 160-167.

310. Ong SE *et al*. Stable isotope labeling by amino acids in cell culture, SILAC, as a simple and accurate approach to expression proteomics. *Mol Cell Proteomics*, 2002, 1(5), 376-386.

311. Liu H, Manuilov AV, Chumsae C, Babineau ML, Tarcsa E. Quantitation of a recombinant monoclonal antibody in monkey serum by liquid chromatography-mass spectrometry. *Anal Biochem*, 2011, 414(1), 147-153.

312. Li W, Lin H, Fu Y, Flarakos J. LC-MS/MS determination of a human mAb drug candidate in rat serum using an isotopically labeled universal mAb internal standard. *J Chromatogr B*, 2017, 1044, 166-176.

313. Martínez Bueno MJ *et al*. Application of liquid chromatography/quadrupole-linear ion trap mass spectrometry and time-of-flight mass spectrometry to the determination of pharmaceuticals and related contaminants in wastewater. *Anal Chem*, 2007, 79(24), 9372-9384.

314. Sandra K, Devreese B, Van Beeumen J, Stals I, Claeyssens M. The Q-Trap mass spectrometer, a novel tool in the study of protein glycosylation. *J Am Soc Mass Spectrom*, 2004, 15(3), 413-423.

315. Lange V, Picotti P, Domon B, Aebersold R. Selected reaction monitoring for quantitative proteomics: a tutorial. *Mol Syst Biol*, 2008, 4, 222-222.

316. Du Z, Douglas D, Konenkov N. Elemental analysis with quadrupole mass filters operated in higher stability regions. *J Anal At Spectrom*, 1999, 14(8), 1111-1119.

317. Henchman M, Steel C. Understanding the quadrupole mass filter through computer simulation. *J Chem Educ*, 1998, 75(8), 1049.

318. Niessen WMA. Liquid chromatography-mass spectrometry, third edition. (CRC Press, 2006).

319. Liebler DC, Zimmerman LJ. Targeted quantitation of proteins by mass spectrometry. *Biochemistry*, 2013, 52(22), 3797-3806.

320. Colangelo CM, Chung L, Bruce C, Cheung KH. Review of software tools for design and analysis of large scale MRM proteomic datasets. *Methods*, 2013, 61(3), 287-298.

321. Bose N, Zee T, Kapahi P, Stoller ML. Mass spectrometry-based in vitro assay to identify drugs that influence cystine solubility. *Bio Protoc*, 2017, 7(14), pii: e2417.

322. Gosetti F, Mazzucco E, Gennaro MC, Marengo E. Simultaneous determination of sixteen underivatized biogenic amines in human urine by HPLC-MS/MS. *Anal Bioanal Chem*, 2013, 405(2), 907-916.

323. Picotti P, Aebersold R. Selected reaction monitoring-based proteomics: workflows, potential, pitfalls and future directions. *Nat Meth*, 2012, 9(6), 555-566.

324. Gallien S, Domon B. Advances in high-resolution quantitative proteomics: implications for clinical applications. *Expert Rev Proteomics*, 2015, 1-10.

325. Maes P *et al*. Introducing plasma/serum glycodepletion for the targeted proteomics analysis of cytolysis biomarkers. *Talanta*, 2017, 170, 473-480.

326. Mohr J, Swart R, Samonig M, Böhm G, Huber CG. High-efficiency nano- and micro-HPLC-high-resolution orbitrap-MS platform for top-down proteomics. *Proteomics*, 2010, 10(20), 3598-3609.

327. Ramus C *et al*. Spiked proteomic standard dataset for testing label-free quantitative software and statistical methods. *Data in brief*, 2016, 6, 286-294.

328. Ke M *et al*. Differential proteomic analysis of white adipose tissues from T2D KKAy mice by LC-ESI-QTOF. *Proteomics*, 2017, 17(5), doi: 10.1002/pmic.201600219.

329. Lu W, Liu J, Gao B, Lv X, Yu L. Technical note: nontargeted detection of adulterated plant proteins in raw milk by UPLC-quadrupole time-of-flight mass spectrometric proteomics combined with chemometrics. *J Dairy Sci*, 2017, 100(9), 6980-6986.

330. Fedorova G, Randak T, Lindberg RH, Grabic R. Comparison of the quantitative performance of a Q-Exactive high-resolution mass spectrometer with that of a triple quadrupole tandem mass spectrometer for the analysis of illicit drugs in wastewater. *Rapid Commun Mass Spectrom*, 2013, 27(15), 1751-1762.

331. Grund B, Marvin L, Rochat B. Quantitative performance of a quadrupole-orbitrap-MS in targeted LC-MS determinations of small molecules. *J Pharm Biomed Anal*, 2016, 124, 48-56.

332. Zhang NR *et al*. Quantitation of small molecules using high-resolution accurate mass spectrometers - a different approach for analysis of biological samples. *Rapid Commun Mass Spectrom*, 2009, 23(7), 1085-1094.

333. Michalski A *et al*. Mass spectrometry-based proteomics using Q Exactive, a high-performance benchtop quadrupole orbitrap mass spectrometer. *Mol Cell Proteomics*, 2011, 10(9), doi: 10.1074/mcp.M111.011015.

334. Kumar P *et al*. Targeted analysis with benchtop quadrupole-orbitrap hybrid mass spectrometer: application to determination of synthetic hormones in animal urine. *Anal Chim Acta*, 2013, 780, 65-73.

335. Peterson AC, Russell JD, Bailey DJ, Westphall MS, Coon JJ. Parallel reaction monitoring for high resolution and high mass accuracy quantitative, targeted proteomics. *Mol Cell Proteomics*, 2012, 11(11), 1475-1488.

336. Zhou J *et al*. Development and evaluation of a parallel reaction monitoring strategy for large-scale targeted metabolomics quantification. *Anal Chem*, 2016, 88(8), 4478-4486.

337. Hu Q *et al*. The orbitrap: a new mass spectrometer. *J Mass Spectrom*, 2005, 40(4), 430-443.

338. Makarov A. Electrostatic axially harmonic orbital trapping: a high-performance technique of mass analysis. *Anal Chem*, 2000, 72(6), 1156-1162.

339. Perry RH, Cooks RG, Noll RJ. Orbitrap mass spectrometry: instrumentation, ion motion and applications. *Mass Spectrom Rev*, 2008, 27(6), 661-699.

340. Scigelova M, Hornshaw M, Giannakopulos A, Makarov A. Fourier transform mass spectrometry. *Mol Cell Proteomics*, 2011, 10(7), M111.009431.

341. Gallien S *et al*. Targeted proteomic quantification on quadrupole-orbitrap mass spectrometer. *Mol Cell Proteomics*, 2012, 11(12), 1709-1723.

342. Rauniyar N. Parallel reaction monitoring: a targeted experiment performed using high resolution and high mass accuracy mass spectrometry. *I J Mol Sci*, 2015, 16(12), 28566-28581.

343. Tsuchiya H, Tanaka K, Saeki Y. The parallel reaction monitoring method contributes to a highly sensitive polyubiquitin chain quantification. *Biochem Biophys Res Commun*, 2013, 436(2), 223-229.

344. Luo Y *et al*. Quantification and confirmation of flunixin in equine plasma by liquid chromatography-quadrupole time-of-flight tandem mass spectrometry. *J Chromatogr B*, 2004, 801(2), 173-184.

345. Paul D, Allakonda L, Satheeshkumar N. A validated UHPLC-QTOF-MS method for quantification of metformin and teneligliptin in rat plasma: application to pharmacokinetic interaction study. *J Pharm Biomed Anal*, 2017, 143, 1-8.

346. Fachi MM, Cerqueira LB, Leonart LP, de Francisco TMG, Pontarolo R. Simultaneous quantification of antidiabetic agents in human plasma by a UPLC-QToF-MS method. *PloS one*, 2016, 11(12), e0167107.

347. Balcerzak M. An overview of analytical applications of time of flight-mass spectrometric (TOF-MS) analyzers and an inductively coupled plasma-TOF-MS technique. *Anal Sci*, 2003, 19(7), 979-989.

348. Standing KG, Ens W. Encyclopedia of spectroscopy and spectrometry (third edition). 458-462 (Academic Press, Oxford; 2017).

349. Chernushevich IV. Duty cycle improvement for a quadrupole-time-of-flight mass spectrometer and its use for precursor ion scans. *Eur J Mass Spectrom*, 2000, 6(6), 471-480.

350. Helm D *et al*. Ion mobility tandem mass spectrometry enhances performance of bottom-up proteomics. *Mol Cell Proteomics*, 2014, 13(12), 3709-3715.

351. Jenkins R *et al*. Recommendations for validation of LC-MS/MS bioanalytical methods for protein biotherapeutics. *AAPS J*, 2015, 17(1), 1-16.

352. U.S. Food and Drug Administration. Guidance for Industry: Bioanalytical Method Validation. May 2001 http://www.fda.gov.

353. European Medicine Agency. Guideline on Bioanalytical Method Validation. Jul 2011 http://www.ema.europa.eu.

354. Becher F *et al*. A simple and rapid LC-MS/MS method for therapeutic drug monitoring of cetuximab: a GPCO-UNICANCER proof of concept study in head-and-neck cancer patients. *Sci Rep*, 2017, 7, 2714.

355. Ouyang Z *et al.* Pellet digestion: a simple and efficient sample preparation technique for LC-MS/MS quantification of large therapeutic proteins in plasma. Bioanalysis, 2011, 4(1), 17-28.

356. Duan X *et al.* A straightforward and highly efficient precipitation/on-pellet digestion procedure coupled with a long gradient nano-LC separation and orbitrap mass spectrometry for label-free expression profiling of the swine heart mitochondrial proteome. *J Proteome Res*, 2009, 8(6), 2838-2850.

357. Yuan L, Arnold ME, Aubry AF, Ji QC. Simple and efficient digestion of a monoclonal antibody in serum using pellet digestion: comparison with traditional digestion methods in LC-MS/MS bioanalysis. *Bioanalysis*, 2012, 4(24), 2887-2896.

358. Gong C, Zheng N, Zeng J, Aubry AF, Arnold ME. Post-pellet-digestion precipitation and solid phase extraction: A practical and efficient workflow to extract surrogate peptides for ultra-high performance liquid chromatography-tandem mass spectrometry bioanalysis of a therapeutic antibody in the low ng/mL range. *J Chromatogr A*, 2015, 1424, 27-36.

359. Mehl JT *et al.* Quantification of in vivo site-specific Asp isomerization and Asn deamidation of mAbs in animal serum using IP-LC-MS. *Bioanalysis*, 2016, 8(15), 1611-1622.

360. Robinson N *et al.* Structure-dependent nonenzymatic deamidation of glutaminyl and asparaginyl pentapeptides. *J Pept Res*, 2004, 63(5), 426-436.

361. Timm V, Gruber P, Wasiliu M, Lindhofer H, Chelius D. Identification and characterization of oxidation and deamidation sites in monoclonal rat/mouse hybrid antibodies. *J Chromatogr B*, 2010, 878(9-10), 777-784.

362. Wakankar AA, Borchardt RT. Formulation considerations for proteins susceptible to asparagine deamidation and aspartate isomerization. *J Pharm Sci*, 2006, 95(11), 2321-2336.

363. Ewles M, Goodwin L. Bioanalytical approaches to analyzing peptides and proteins by LC-MS/MS. *Bioanalysis*, 2011, 3(12), 1379-1397.

364. Yuan L, Aubry AF, Arnold ME, Ji QC. Systematic investigation of orthogonal SPE sample preparation for the LC-MS/MS bioanalysis of a monoclonal antibody after pellet digestion. *Bioanalysis*, 2013, 5(19), 2379-2391.

365. Merrell K *et al.* Analysis of low-abundance, low-molecular-weight serum proteins using mass spectrometry. *J Biomol Tech*, 2004, 15(4), 238-248.

366. Chen X *et al.* Compound property optimization in drug discovery using quantitative surface sampling micro liquid chromatography with tandem mass spectrometry. *Anal Chem*, 2016, 88(23), 11813-11820.

367. Jones BR, Schultz GA, Eckstein JA, Ackermann BL. Surrogate matrix and surrogate analyte approaches for definitive quantitation of endogenous biomolecules. *Bioanalysis*, 2012, 4(19), 2343-2356.

368. Lee JW *et al*. Method validation and measurement of biomarkers in nonclinical and clinical samples in drug development: a conference report. *Pharm Res*, 2005, 22(4), 499-511.

369. Labrijn AF *et al*. Therapeutic IgG4 antibodies engage in Fab-arm exchange with endogenous human IgG4 in vivo. *Nat Biotech*, 2009, 27(8), 767-771.

370. Silva JP, Vetterlein O, Jose J, Peters S, Kirby H. The S228P mutation prevents in vivo and in vitro IgG4 Fab-arm exchange as demonstrated using a combination of novel quantitative immunoassays and physiological matrix preparation. *J Biol Chem*, 2015, 290(9), 5462-5469.

371. Yang H, Lame M, Naughton S, Chambers E. Quantification of the antibody drug conjugate, trastuzumab emtansine, and the monocolonal antibody, trastuzumab in plasma using a generic kit-based approach. Application Note 720005619EN www.waters.com, 2016.

372. Kirmaier A, Diehl W, Johnson WE. Acquisition and processing of nonhuman primate samples for genetic and phylogenetic analyses. *Methods*, 2009, 49(1), 5-10.

373. Li F, Fast D, Michael S. Absolute quantitation of protein therapeutics in biological matrices by enzymatic digestion and LC-MS. *Bioanalysis*, 2011, 3(21), 2459-2480.

374. Switzar L, Giera M, Niessen WMA. Protein digestion: an overview of the available techniques and recent developments. *J Proteome Res*, 2013, 12(3), 1067-1077.

375. Burkhart JM, Schumbrutzki C, Wortelkamp S, Sickmann A, Zahedi RP. Systematic and quantitative comparison of digest efficiency and specificity reveals the impact of trypsin quality on MS-based proteomics. *J Proteomics*, 2012, 75(4), 1454-1462.

376. Norrgran J *et al*. Optimization of digestion parameters for protein quantification. *Anal Biochem*, 2009, 393(1), 48-55.

377. Switzar L, Giera M, Lingeman H, Irth H, Niessen WMA. Protein digestion optimization for characterization of drug-protein adducts using response surface modeling. *J Chromatogr A*, 2011, 1218(13), 1715-1723.

378. Hu Z *et al*. The on-bead digestion of protein corona on nanoparticles by trypsin immobilized on the magnetic nanoparticle. *J Chromatogr A*, 2014, 1334, 55-63.

379. Jiang S, Zhang Z, Li L. A one-step preparation method of monolithic enzyme reactor for highly efficient sample preparation coupled to mass spectrometry-based proteomics studies. *J Chromatogr A*, 2015, 1412, 75-81.

380. Naldi M, Černigoj U, Štrancar A, Bartolini M. Towards automation in protein digestion: development of a monolithic trypsin immobilized reactor for highly efficient on-line digestion and analysis. *Talanta*, 2017, 167, 143-157.

381. Ning W, Bruening ML. Rapid protein digestion and purification with membranes attached to pipet tips. *Anal Chem*, 2015, 87(24), 11984-11989.

382. Regnier FE, Kim J. Accelerating trypsin digestion: the immobilized enzyme reactor. *Bioanalysis*, 2014, 6(19), 2685-2698.

383. Priego-Capote F, de Castro L. Ultrasound-assisted digestion: a useful alternative in sample preparation. *J Biochem Biophys Methods*, 2007, 70(2), 299-310.

384. Wang S, Zhang L, Yang P, Chen G. Infrared-assisted tryptic proteolysis for peptide mapping. *Proteomics*, 2008, 8(13), 2579-2582.

385. Bark SJ, Muster N, Yates JR, Siuzdak G. High-temperature protein mass mapping using a thermophilic protease. *J Am Chem Soc*, 2001, 123(8), 1774-1775.

386. Lesur A, Varesio E, Hopfgartner G. Accelerated tryptic digestion for the analysis of biopharmaceutical monoclonal antibodies in plasma by liquid chromatography with tandem mass spectrometric detection. *J Chromatogr A*, 2010, 1217(1), 57-64.

387. Park ZY, Russell DH. Thermal denaturation: a useful technique in peptide mass mapping. *Anal Chem*, 2000, 72(11), 2667-2670.

388. Li F, Schmerberg CM, Ji QC. Accelerated tryptic digestion of proteins in plasma for absolute quantitation using a protein internal standard by liquid chromatography/tandem mass spectrometry. *Rapid Commun Mass Spectrom*, 2009, 23(5), 729-732.

389. Russell WK, Park ZY, Russell DH. Proteolysis in mixed organic-aqueous solvent systems: applications for peptide mass mapping using mass spectrometry. *Anal Chem*, 2001, 73(11), 2682-2685.

390. Strader MB, Tabb DL, Hervey WJ, Pan C, Hurst GB. Efficient and specific trypsin digestion of microgram to nanogram quantities of proteins in organic-aqueous solvent systems. *Anal Chem*, 2006, 78(1), 125-134.

391. Chan AC, Carter PJ. Therapeutic antibodies for autoimmunity and inflammation. *Nat Rev Immunol*, 2010, 10(5), 301-316.

392. Fellner RC, Terryah ST, Tarran R. Inhaled protein/peptide-based therapies for respiratory disease. *Mol Cell Pediatr*, 2016, 3(1), 16.

393. Guilleminault L *et al*. Fate of inhaled monoclonal antibodies after the deposition of aerosolized particles in the respiratory system. *J Control Release*, 2014, 196, 344-354.

394. McDonald TA, Zepeda ML, Tomlinson MJ, Bee WH, Ivens IA. Subcutaneous administration of biotherapeutics: current experience in animal models. *Curr Opin Mol Ther*, 2010, 12(4), 461-470.

395. Respaud R, Vecellio L, Diot P, Heuzé-Vourc'h N. Nebulization as a delivery method for mAbs in respiratory diseases. *Expert Opin Drug Deliv*, 2015, 12(6), 1027-1039.

396. Richter WF, Bhansali SG, Morris ME. Mechanistic determinants of biotherapeutics absorption following SC administration. *AAPS J*, 2012, 14(3), 559-570.

397. Richter WF, Jacobsen B. Subcutaneous absorption of biotherapeutics: knowns and unknowns. *Drug Metab Dispos*, 2014, 42(11), 1881-1889.

398. Neubert H *et al*. Tissue bioanalysis of biotherapeutics and drug targets to support PK/PD. *Bioanalysis*, 2012, 4(21), 2589-2604.

399. Ezan E, Dubois M, Becher F. Bioanalysis of recombinant proteins and antibodies by mass spectrometry. *Analyst*, 2009, 134(5), 825-834.

400. Anderson NL, Anderson NG. The human plasma proteome: history, character, and diagnostic prospects. *Mol Cell Proteomics*, 2002, 1(11), 845-867.

401. Anderson NL *et al*. The human plasma proteome: a nonredundant list developed by combination of four separate sources. *Mol Cell Proteomics*, 2004, 3(4), 311-326.

402. Boichenko AP, Govorukhina N, van der Zee AGJ, Bischoff R. Multidimensional separation of tryptic peptides from human serum proteins using reversed-phase, strong cation exchange, weak anion exchange, and fused-core fluorinated stationary phases. *J Sep Sci*, 2013, 36(21-22), 3463-3470.

403. Cook DW, Rutan SC, Stoll DR, Carr PW. Two dimensional assisted liquid chromatography - a chemometric approach to improve accuracy and precision of quantitation in liquid chromatography using 2D separation, dual detectors, and multivariate curve resolution. *Anal Chim Acta*, 2015, 859, 87-95.

404. Shen Y *et al*. Online 2D-LC-MS/MS assay to quantify therapeutic protein in human serum in the presence of pre-existing antidrug antibodies. *Anal Chem*, 2015, 87(16), 8555-8563.

405. Simpkins SW *et al*. Targeted three-dimensional liquid chromatography: a versatile tool for quantitative trace analysis in complex matrices. *J Chromatogr A*, 2010, 1217(49), 7648-7660.

406. Spicer V *et al*. 3D HPLC-MS with reversed-phase separation functionality in all three dimensions for large-scale bottom-up proteomics and peptide retention data collection. *Anal Chem*, 2016, 88(5), 2847-2855.

407. Stoll DR, Carr PW. Two-dimensional liquid chromatography: a state of the art tutorial. *Anal Chem*, 2017, 89(1), 519-531.

408. Stoll DR *et al*. Direct identification of rituximab main isoforms and subunit analysis by online selective comprehensive two-dimensional liquid chromatography-mass spectrometry. *Anal Chem*, 2015, 87(16), 8307-8315.

409. Vonk RJ *et al*. Comprehensive two-dimensional liquid chromatography with stationary-phase-assisted modulation coupled to high-resolution mass spectrometry applied to proteome analysis of saccharomyces cerevisiae. *Anal Chem*, 2015, 87(10), 5387-5394.

410. Fortin T *et al.* Multiple reaction monitoring cubed for protein quantification at the low nanogram/milliliter level in nondepleted human serum. *Anal Chem*, 2009, 81(22), 9343-9352.

411. Jaffuel A *et al.* Optimization of liquid chromatography-multiple reaction monitoring cubed mass spectrometry assay for protein quantification: application to aquaporin-2 water channel in human urine. *J Chromatogr A*, 2013, 1301, 122-130.

412. Jeudy J *et al.* Overcoming biofluid protein complexity during targeted mass spectrometry detection and quantification of protein biomarkers by MRM cubed (MRM3). *Anal Bioanal Chem*, 2014, 406(4), 1193-1200.

413. Sidibé J, Varesio E, Hopfgartner G. Quantification of ghrelin and des-acyl ghrelin in human plasma by using cubic-selected reaction-monitoring LCMS. *Bioanalysis*, 2014, 6(10), 1373-1383.

414. Bohrer BC, Merenbloom SI, Koeniger SL, Hilderbrand AE, Clemmer DE. Biomolecule analysis by ion mobility spectrometry. *Annu Rev Anal Chem*, 2008, 1, 293-327.

415. Doneanu CE *et al.* Enhanced detection of low-abundance host cell protein impurities in high-purity monoclonal antibodies down to 1 ppm using ion mobility mass spectrometry coupled with multidimensional liquid chromatography. *Anal Chem*, 2015, 87(20), 10283-10291.

416. Pfammatter S, Bonneil E, Thibault P. Improvement of quantitative measurements in multiplex proteomics using high-field asymmetric waveform spectrometry. *J Proteome Res*, 2016, 15(12), 4653-4665.

417. Swearingen KE *et al* Nanospray FAIMS fractionation provides significant increases in proteome coverage of unfractionated complex protein digests. *Mol Cell Proteomics*, 2012, 11(4), M111.014985.

418. Christianson CC, Johnson CJL, Needham SR. The advantages of microflow LC-MS/MS compared with conventional HPLC-MS/MS for the analysis of methotrexate from human plasma. *Bioanalysis*, 2013, 5(11), 1387-1396.

419. Schmidt A, Karas M, Dülcks T. Effect of different solution flow rates on analyte ion signals in nano-ESI MS, or: when does ESI turn into nano-ESI? *J Am Soc Mass Spectrom*, 2003, 14(5), 492-500.

420. Tang K, Page JS, Smith RD. Charge competition and the linear dynamic range of detection in electrospray ionization mass spectrometry. *J Am Soc Mass Spectrom*, 2004, 15(10), 1416-1423.

421. Lassman ME, Fernandez-Metzler C. Applications of low-flow LC–SRM for the analysis of large molecules in pharmaceutical R&D. *Bioanalysis*, 2014, 6(13), 1859-1867.

422. Batycka M *et al*. Ultra-fast tandem mass spectrometry scanning combined with monolithic column liquid chromatography increases throughput in proteomic analysis. *Rapid Commun Mass Spectrom*, 2006, 20(14), 2074-2080.

423. Kocher T, Pichler P, Swart R, Mechtler K. Analysis of protein mixtures from whole-cell extracts by single-run nanoLC-MS/MS using ultralong gradients. *Nat Protoc*, 2012, 7(5), 882-890.

424. Schley C, Swart R, Huber CG. Capillary scale monolithic trap column for desalting and preconcentration of peptides and proteins in one- and two-dimensional separations. *J Chromatogr A*, 2006, 1136(2), 210-220.

425. Shen X *et al*. An IonStar experimental strategy for MS1 ion current-based quantification using ultrahigh-field orbitrap: reproducible, in-depth, and accurate protein measurement in large cohorts. *J Proteome Res*, 2017, 16(7), 2445-2456.

426. Kleinnijenhuis AJ, Ingola M, Toersche JH, van Holthoon FL, van Dongen WD. Quantitative bottom up analysis of infliximab in serum using protein A purification and integrated µLC-electrospray chip IonKey MS/MS technology. *Bioanalysis*, 2016, 8(9), 891-904.

427. Ladwig PM, Barnidge DR, Willrich MAV. Quantification of the IgG2/4 kappa monoclonal therapeutic eculizumab from serum using isotype specific affinity purification and microflow LC-ESI-Q-TOF mass spectrometry. *J Am Soc Mass Spectrom*, 2016, 28(5), 811-817.

428. Lee AYH *et al*. Multiplexed quantification of proglucagon-derived peptides by immunoaffinity enrichment and tandem mass spectrometry after a meal tolerance test. *Clin Chem*, 2016, 62(1), 227-235.

429. Anderson L, Hunter CL. Quantitative mass spectrometric multiple reaction monitoring assays for major plasma proteins. *Mol Cell Proteomics*, 2006, 5(4), 573-588.

430. Liu G *et al*. A novel and cost effective method of removing excess albumin from plasma/serum samples and its impacts on LC-MS/MS bioanalysis of therapeutic proteins. *Anal Chem*, 2014, 86(16), 8336-8343.

431. Shi T *et al*. IgY14 and SuperMix immunoaffinity separations coupled with liquid chromatography-mass spectrometry for human plasma proteomics biomarker discovery. *Methods*, 2012, 56(2), 246-253.

432. Bronsema KJ, Bischoff R, Bouche MP, Mortier K, van de Merbel NC. High-sensitivity quantitation of a Nanobody® in plasma by single-cartridge multidimensional SPE and ultra-performance LC-MS/MS. *Bioanalysis*, 2015, 7(1), 53-64.

433. Mesmin C, Domon B. Improvement of the performance of targeted LC-MS assays through enrichment of histidine-containing peptides. *J Proteome Res*, 2014, 13(12), 6160-6168.

434. Shi T *et al.* Sensitive targeted quantification of ERK phosphorylation dynamics and stoichiometry in human cells without affinity enrichment. *Anal Chem*, 2015, 87(2), 1103-1110.

435. Kushnir MM *et al.* Measurement of thyroglobulin by liquid chromatography-tandem mass spectrometry in serum and plasma in the presence of antithyroglobulin autoantibodies. *Clin Chem*, 2013, 59(6), 982-990.

436. Neubert H *et al.* Sequential protein and peptide immunoaffinity capture for mass spectrometry-based quantification of total human β-nerve growth factor. *Anal Chem*, 2012, 85(3), 1719-1726.

437. Chappell DL *et al.* An ultrasensitive method for the quantitation of active and inactive GLP-1 in human plasma via immunoaffinity LC-MS/MS. *Bioanalysis*, 2014, 6(1), 33-42.

438. Fernandez Ocana M *et al.* Clinical pharmacokinetic assessment of an anti-MAdCAM monoclonal antibody therapeutic by LC-MS/MS. *Anal Chem*, 2012, 84(14), 5959-5967.

439. Onami I, Ayabe M, Murao N, Ishigai M. A versatile method for protein-based antigen bioanalysis in non-clinical pharmacokinetics studies of a human monoclonal antibody drug by an immunoaffinity liquid chromatography-tandem mass spectrometry. *J Chromatogr A*, 2014, 1334, 64-71.

440. Yang W, Kernstock R, Simmons N, Alak A. ELISA microplate: a viable immunocapture platform over magnetic beads for immunoaffinity-LC-MS/MS quantitation of protein therapeutics? *Bioanalysis*, 2015, 7(3), 307-318.

441. Encinas L *et al.* Encoded library technology as a source of hits for the discovery and lead optimization of a potent and selective class of bactericidal direct inhibitors of mycobacterium tuberculosis InhA. *J Med Chem*, 2014, 57(4), 1276-1288.

442. Smith C. Striving for purity: advances in protein purification. *Nat Methods*, 2005, 2(1), 71-77.

443. Szigeti M *et al.* Rapid N-glycan release from glycoproteins using immobilized PNGase F microcolumns. *J Chromatogr B*, 2016, 1032, 139-143.

444. Ippoliti PJ *et al.* Automated microchromatography enables multiplexing of immunoaffinity enrichment of peptides to greater than 150 for targeted MS-based assays. *Anal Chem*, 2016, 88(15), 7548-7555.

445. Popp R *et al.* An automated assay for the clinical measurement of plasma renin activity by immuno-MALDI (iMALDI). *Biochim Biophys Acta,* 2015, 1854(6), 547-558.

446. Ruelcke JE, Loo D, Hill MM. Reducing the cost of semi-automated in-gel tryptic digestion and GeLC sample preparation for high-throughput proteomics. *J Proteomics*, 2016, 149, 3-6.

447. Krastins B *et al*. Rapid development of sensitive, high-throughput, quantitative and highly selective mass spectrometric targeted immunoassays for clinically important proteins in human plasma and serum. *Clin Biochem*, 2013, 46(6), 399-410.

448. Kumar V *et al*. Quantification of serum 1-84 parathyroid hormone in patients with hyperparathyroidism by immunocapture in situ digestion liquid chromatography-tandem mass spectrometry. *Clin Chem*, 2010, 56(2), 306-313.

449. Lopez MF *et al*. Proteomic signatures of serum albumin-bound proteins from stroke patients with and without endovascular closure of PFO are significantly different and suggest a novel mechanism for cholesterol efflux. *Clin Proteomics*, 2015, 12(1), 2.

450. Nelson R, Krone J, Bieber A. Mass-spectrometric immunoassay. *Anal Chem*, 1995, 67, 1153-1158.

451. Prakash A *et al*. Interlaboratory reproducibility of selective reaction monitoring assays using multiple upfront analyte enrichment strategies. *J Proteome Res*, 2012, 11(8), 3986-3995.

452. Thermo Fisher Scientific. Application Notes MSIA 1004 - Thermo Scientific MSIA Streptavidin D.A.R.T.'S: Robust immunoenrichment process and reproducibility across multiple labs. 2013 http://www.thermofisher.com.

453. Ouyang J. Antibody-drug conjugates. 275-283 (Humana Press, Totowa, NJ; 2013).

454. Green NM. Avidin and streptavidin. *Methods Enzymol*, 1990, 184, 51-67.

455. Weber PC, Ohlendorf D, Wendoloski J, Salemme F. Structural origins of high-affinity biotin binding to streptavidin. *Science*, 1989, 243(4887), 85.

456. Lopez MF *et al*. Selected reaction monitoring-mass spectrometric immunoassay responsive to parathyroid hormone and related variants. *Clin Chem*, 2010, 56(2), 281-290.

457. Niederkofler EE, Tubbs KA, Kiernan UA, Nedelkov D, Nelson RW. Novel mass spectrometric immunoassays for the rapid structural characterization of plasma apolipoproteins. *J Lipid Res*, 2003, 44(3), 630-639.

458. Sherma ND *et al*. Mass spectrometric immunoassay for the qualitative and quantitative analysis of the cytokine macrophage migration inhibitory factor (MIF). *Proteome Sci*, 2014, 12(1), 52.

459. Smits NE *et al*. Monolith immuno-affinity enrichment liquid chromatography tandem mass spectrometry for quantitative protein analysis of recombinant bovine somatotropin in serum. *Anal Bioanal Chem*, 2015, 407(20), 6041-6050.

460. Beck A, Sanglier-Cianférani S, Van Dorsselaer A. Biosimilar, biobetter, and next generation antibody characterization by mass spectrometry. *Anal Chem*, (84)11, 4637-4646.

461. Fekete S, Dong MW, Zhang T, Guillarme D. High resolution reversed phase analysis of recombinant monoclonal antibodies by ultra-high pressure liquid chromatography column coupling. *J Pharm Biomed Anal*, 2013, 83, 273-278.

462. Gahoual R, Beck A, Leize-Wagner E, François YN. Cutting-edge capillary electrophoresis characterization of monoclonal antibodies and related products. *J Chromatogr B*, 2016, 1032, 61-78.

463. He J *et al*. High-resolution accurate-mass mass spectrometry enables in-depth characterization of in vivo biotransformations for intact antibody-drug conjugates. *Anal Chem*, 2017, 89(10), 5476-5483.

464. Wrona M, Mauriala T, Bateman KP, Mortishire-Smith RJ, O'Connor D. 'All-in-One' analysis for metabolite identification using liquid chromatography/hybrid quadrupole time-of-flight mass spectrometry with collision energy switching. *Rapid Commun Mass Spectrom*, 2005, 19(18), 2597-2602.

465. Xing J, Zang M, Zhang H, Zhu M. The application of high-resolution mass spectrometry-based data-mining tools in tandem to metabolite profiling of a triple drug combination in humans. *Anal Chim Acta*, 2015, 897, 34-44.

466. Yang A, Zang M, Liu H, Fan P, Xing J. Metabolite identification of the antimalarial piperaquine in vivo using liquid chromatography-high-resolution mass spectrometry in combination with multiple data-mining tools in tandem. *Biomed Chromatogr*, 2016, 30(8), 1324-1330.

467. Mekhssian K, Mess JN, Garofolo F. Application of high-resolution MS in the quantification of a therapeutic monoclonal antibody in human plasma. *Bioanalysis*, 2014, 6(13), 1767-1779.

468. Sturm RM, Jones BR, Mulvana DE, Lowes S. HRMS using a Q-Exactive series mass spectrometer for regulated quantitative bioanalysis: how, when, and why to implement. *Bioanalysis*, 2016, 8(16), 1709-1721.

469. Dillen L *et al*. Comparison of triple quadrupole and high-resolution TOF-MS for quantification of peptides. *Bioanalysis*, 2012, 4(5), 565-579.

470. Morin LP, Mess JN, Garofolo F. Large-molecule quantification: sensitivity and selectivity head-to-head comparison of triple quadrupole with Q-TOF. *Bioanalysis*, 2013, 5(10), 1181-1193.

471. Ramagiri S, Garofolo F. Large molecule bioanalysis using Q-TOF without predigestion and its data processing challenges. *Bioanalysis*, 2012, 4(5), 529-540.

472. Niessen WMA, Falck D. Analyzing biomolecular interactions by mass spectrometry 1-54 (Wiley-VCH Verlag GmbH & Co. KGaA, 2015).

473. Nikolaev EN, Jertz R, Grigoryev A, Baykut G. Fine structure in isotopic peak distributions measured using a dynamically harmonized Fourier transform ion cyclotron resonance cell at 7 T. *Anal Chem*, 2012, 84(5), 2275-2283.

474. Scigelova M, Makarov A. Orbitrap mass analyzer - overview and applications in proteomics. *Proteomics*, 2006, 6, 16-21.

475. Kellie JF, Kehler JR, Szapacs ME. Application of high-resolution MS for development of peptide and large-molecule drug candidates. *Bioanalysis*, 2016, 8(3), 169-177.

476. Plumb RS *et al*. Comparison of the quantification of a therapeutic protein using nominal and accurate mass MS/MS. *Bioanalysis*, 2012, 4(5), 605-615.

477. Jiwan JLH, Wallemacq P, Hérent MF. HPLC-high resolution mass spectrometry in clinical laboratory? *Clin Biochem*, 2011, 44(1), 136-147.

478. Korfmacher W. High-resolution mass spectrometry will dramatically change our drug-discovery bioanalysis procedures. *Bioanalysis*, 2011, 3(11), 1169-1171.

479. Korfmacher W, Ramanathan R. HRMS in DMPK. *Bioanalysis*, 2016, 8(16), 1635-1637.

480. Ramanathan DM. Looking beyond the SRM to high-resolution MS paradigm shift for DMPK studies. *Bioanalysis*, 2013, 5(10), 1141-1143.

481. Ramanathan R *et al*. It is time for a paradigm shift in drug discovery bioanalysis: from SRM to HRMS. *J Mass Spectrom*, 2011, 46(6), 595-601.

482. Geib T, Sleno L, Hall RA, Stokes CS, Volmer DA. Triple quadrupole versus high resolution quadrupole-time-of-flight mass spectrometry for quantitative LC-MS/MS analysis of 25-hydroxyvitamin D in human serum. *J Am Soc Mass Spectrom*, 2016, 27(8), 1404-1410.

483. Zheng Y *et al*. Identification and quantitative analysis of physalin D and its metabolites in rat urine and feces by liquid chromatography with triple quadrupole time-of-flight mass spectrometry. *J Sep Sci*, 2017, 40(11), 2355-2365.

484. Zhou J *et al*. Workflow development for targeted lipidomic quantification using parallel reaction monitoring on a quadrupole-time of flight mass spectrometry. *Anal Chim Acta*, 2017, 972, 62-72.

485. Ciccimaro E *et al.* Strategy to improve the quantitative LC-MS analysis of molecular ions resistant to gas-phase collision induced dissociation: application to disulfide-rich cyclic peptides. *Anal Chem*, 2014, 86(23), 11523-11527.

486. Gallien S, Domon B. Advances in high-resolution quantitative proteomics: implications for clinical applications. *Expert Rev Proteomics*, 2015, 12(5), 489-498.

487. Murphy K, Bennett PK, Duczak N. High-throughput quantitation of large molecules using multiplexed chromatography and high-resolution/accurate mass LC–MS. *Bioanalysis*, 2012, 4(9), 1013-1024.

488. Huang MQ, Lin ZJ, Weng N. Applications of high-resolution MS in bioanalysis. *Bioanalysis*, 2013, 5(10), 1269-1276.

489. Fung EN *et al*. Full-scan high resolution accurate mass spectrometry (HRMS) in regulated bioanalysis: LC-HRMS for the quantitation of prednisone and prednisolone in human plasma. *J Chromatogr B*, 2011, 879(27), 2919-2927.

490. Tonoli D, Varesio E, Hopfgartner G. Quantification of acetaminophen and two of its metabolites in human plasma by ultra-high performance liquid chromatography-low and high resolution tandem mass spectrometry. *J Chromatogr B*, 2012, 904, 42-50.

491. Qu L, Qian J, Ma P, Yin Z. Utilizing online-dual-SPE-LC with HRMS for the simultaneous quantification of amphotericin B, fluconazole, and fluorocytosine in human plasma and cerebrospinal fluid. *Talanta*, 2017, 165, 449-457.

492. de Sain-van der Velden MGM *et al*. Quantification of metabolites in dried blood spots by direct infusion high resolution mass spectrometry. *Anal Chim Acta*, 2017, 979, 45-50.

493. Lawson G, Cocks E, Tanna S. Quantitative determination of atenolol in dried blood spot samples by LC-HRMS: A potential method for assessing medication adherence. *J Chromatogr B*, 2012, 897, 72-79.

494. Oliveira RV, Henion J, Wickremsinhe E. Fully-automated approach for online dried blood spot extraction and bioanalysis by two-dimensional-liquid chromatography coupled with high-resolution quadrupole time-of-flight mass spectrometry. *Anal Chem*, 2014, 86(2), 1246-1253.

495. Thomas A *et al*. Sensitive determination of prohibited drugs in dried blood spots (DBS) for doping controls by means of a benchtop quadrupole/orbitrap mass spectrometer. *Anal Bioanal Chem*, 2012, 403(5), 1279-1289.

496. Glicksberg L, Bryand K, Kerrigan S. Identification and quantification of synthetic cathinones in blood and urine using liquid chromatography-quadrupole/time of flight (LC-Q/TOF) mass spectrometry. *J Chromatogr B*, 2016, 1035, 91-103.

497. Lu H *et al*. Optimized ultra performance liquid chromatography tandem high resolution mass spectrometry method for the quantification of paraquat in plasma and urine. *J Chromatogr B, 2016*, 1027, 96-102.

498. Yao W, Fan Z, Zhang S. Poly(N-vinylcarbazole-co-divinylbenzene) monolith microextraction coupled to liquid chromatography-high resolution orbitrap mass spectrometry to analyse benzodiazepines in beer and urine. *J Chromatogr A*, 2016, 1465, 55-62.

499. Cox JM *et al*. Characterization and quantification of oxyntomodulin in human and rat plasma using high-resolution accurate mass LC-MS. *Bioanalysis*, 2016, 8(15), 1579-1595.

500. Zheng N *et al*. Quantitation of a PEGylated protein in monkey serum by UHPLC-HRMS using a surrogate disulfide-containing peptide: a new approach to bioanalysis and in vivo

stability evaluation of disulfide-rich protein therapeutics. *Anal Chim Acta*, 2016, 916, 42-51.

501. Henry H *et al.* Comparison between a high-resolution single-stage orbitrap and a triple quadrupole mass spectrometer for quantitative analyses of drugs. *Rapid Commun Mass Spectrom*, 2012, 26(5), 499-509.

502. Li X, Cournoyer JJ, Lin C, O'Connor PB. Use of ^{18}O labels to monitor deamidation during protein and peptide sample processing. *J Am Soc Mass Spectrom*, 2008, 19(6), 855-864.

503. Pace AL, Wong RL, Zhang YT, Kao YH, Wang YJ. Asparagine deamidation dependence on buffer type, pH, and temperature. J Pharm Sci, 2013, 102(6), 1712-1723.

504. Shimura K *et al.* Estimation of the deamidation rates of major deamidation sites in a Fab fragment of mouse IgG1-kappa by capillary isoelectric focusing of mutated Fab fragments. *Anal Chem*, 2013, 85(3), 1705-1710.

505. Sinha S *et al.* Effect of protein structure on deamidation rate in the Fc fragment of an IgG1 monoclonal antibody. *Protein Sci*, 2009, 18(8), 1573-1584.

506. Song Y, Schowen RL, Borchardt RT, Topp EM. Effect of 'pH' on the rate of asparagine deamidation in polymeric formulations: 'pH'-rate profile. *J Pharm Sci*, 2001, 90(2), 141-156.

507. Stroop SD. A modified peptide mapping strategy for quantifying site-specific deamidation by electrospray time-of-flight mass spectrometry. *Rapid Commun Mass Spectrom*, 2007, 21(6), 830-836.

508. Bults P, Bischoff R, Bakker H, Gietema JA, van de Merbel NC. LC-MS/MS-based monitoring of in vivo protein biotransformation: quantitative determination of trastuzumab and its deamidation products in human plasma. *Anal Chem*, 2016, 88(3), 1871-1877.

509. Powell BS *et al.* Multiple asparagine deamidation of Bacillus anthracis protective antigen causes charge isoforms whose complexity correlates with reduced biological activity. *Proteins*, 2007, 68(2), 458-479.

510. Tran JC *et al.* Automated affinity capture and on-tip digestion to accurately quantitate in vivo deamidation of therapeutic antibodies. *Anal Chem*, 2016, 88(23), 11521-11526.

511. Vlasak J *et al.* Identification and characterization of asparagine deamidation in the light chain CDR1 of a humanized IgG1 antibody. *Anal Biochem*, 2009, 392(2), 145-154.

512. Yan B *et al.* Succinimide formation at Asn 55 in the complementarity determining region of a recombinant monoclonal antibody IgG1 heavy chain. *J Pharm Sci*, 2009, 98(10), 3509-3521.

513. Doyle HA, Gee RJ, Mamula MJ. A failure to repair self-proteins leads to T cell hyperproliferation and autoantibody production. *J Immunol*, 2003, 171(6), 2840-2847.

514. Verma A *et al*. Use of site-directed mutagenesis to model the effects of spontaneous deamidation on the immunogenicity of bacillus anthracis protective antigen. *Infect Immun*, 2013, 81(1), 278-284.

515. Chelius D, Rehder DS, Bondarenko PV. Identification and characterization of deamidation sites in the conserved regions of human immunoglobulin gamma antibodies. *Anal Chem*, 2005, 77(18), 6004-6011.

516. Ren D *et al*. An improved trypsin digestion method minimizes digestion-induced modifications on proteins. *Anal Biochem*, 2009, 392(1), 12-21.

517. Wei C, Grace JE, Zvyaga TA, Drexler DM. Utility of high-resolution accurate MS to eliminate interferences in the bioanalysis of ribavirin and its phosphate metabolites. *Bioanalysis*, 2012, 4(15), 1895-1905.

518. Herrero P *et al*. Comparison of triple quadrupole mass spectrometry and orbitrap high-resolution mass spectrometry in ultrahigh performance liquid chromatography for the determination of veterinary drugs in sewage: benefits and drawbacks. *J Mass Spectrom*, 2014, 49(7), 585-596.

519. Bereman MS, MacLean B, Tomazela DM, Liebler DC, MacCoss MJ. The development of selected reaction monitoring methods for targeted proteomics via empirical refinement. *Proteomics*, 2012, 12(8), 1134-1141.

520. Shuford CM, Sederoff RR, Chiang VL, Muddiman DC. Peptide production and decay rates affect the quantitative accuracy of protein cleavage isotope dilution mass spectrometry (PC-IDMS). *Mol Cell Proteomics*, 2012, 11(9), 814-823.

521. van den Broek I, van Dongen WD. LC-MS-based quantification of intact proteins: perspective for clinical and bioanalytical applications. *Bioanalysis*, 2015, 7(15), 1943-1958.

522. van den Broek I *et al*. Quantifying protein measurands by peptide measurements: where do errors arise? *J Proteome Res*, 2015, 14(2), 928-942.

523. Bogdanov B, Smith RD. Proteomics by FTICR mass spectrometry: top down and bottom up. *Mass Spectrom Rev*, 2005, 24(2), 168-200.

524. Kang L *et al*. Simultaneous catabolite identification and quantitation of large therapeutic protein at the intact level by immunoaffinity capture liquid chromatography-high-resolution mass spectrometry. *Anal Chem*, 2017, 89(11), 6065-6075.

525. Kellie JF, Kehler JR, Mencken TJ, Snell RJ, Hottenstein CS. A whole-molecule immunocapture LC-MS approach for the in vivo quantitation of biotherapeutics. *Bioanalysis*, 2016, 8(20), 2103-2114.

526. Ezan E. Pharmacokinetic studies of protein drugs: past, present and future. *Adv Drug Deliv Rev*, 2013, 65(8), 1065-1073.

527. Jian W, Kang L, Burton L, Weng N. A workflow for absolute quantitation of large therapeutic proteins in biological samples at intact level using LC-HRMS. *Bioanalysis*, 2016, 8(16), 1679-1691.

528. Ruan Q, Ji QC, Arnold ME, Humphreys WG, Zhu M. Strategy and its implications of protein bioanalysis utilizing high-resolution mass spectrometric detection of intact protein. *Anal Chem*, 2011, 83(23), 8937-8944.

529. Chambers EE, Legido-Quigley C, Smith N, Fountain KJ. Development of a fast method for direct analysis of intact synthetic insulins in human plasma: the large peptide challenge. *Bioanalysis*, 2013, 5(1), 65-81.

530. Darby SM, Miller ML, Allen RO, LeBeau M. A mass spectrometric method for quantitation of intact insulin in blood samples. *J Anal Toxicol*, 2001, 25(1), 8-14.

531. Kim YJ *et al*. Quantification of SAA1 and SAA2 in lung cancer plasma using the isotype-specific PRM assays. *Proteomics*, 2015, 15(18), 3116-3125.

532. Fang H *et al*. Intact protein quantitation using pseudoisobaric dimethyl labeling. *Anal Chem*, 2016, 88(14), 7198-7205.

533. Wang EH, Appulage DK, McAllister EA, Schug KA. Investigation of ion transmission effects on intact protein quantification in a triple quadrupole mass spectrometer. *J Am Soc Mass Spectrom*, 2017, 28(9), 1977-1986.

534. Wang EH, Combe PC, Schug KA. Multiple reaction monitoring for direct quantitation of intact proteins using a triple quadrupole mass spectrometer. *J Am Soc Mass Spectrom*, 2016, 27(5), 886-896.

535. Wang Y, Heilig JS. Differentiation and quantification of endogenous and recombinant-methionyl human leptin in clinical plasma samples by immunocapture/mass spectrometry. *J Pharm Biomed Anal*, 2012, 70, 440-446.

536. Gucinski AC, Boyne MT, II. Evaluation of intact mass spectrometry for the quantitative analysis of protein therapeutics. *Anal Chem*, 2012, 84(18), 8045-8051.

537. Acosta-Martin AE *et al*. Quantitative mass spectrometry analysis of intact hemoglobin A2 by precursor ion isolation and detection. *Anal Chem*, 2013, 85(16), 7971-7975.

538. Becher F, Pruvost A, Clement G, Tabet JC, Ezan E. Quantification of small therapeutic proteins in plasma by liquid chromatography-tandem mass spectrometry: application to an elastase inhibitor EPI-hNE4. *Anal Chem*, 2006, 78(7), 2306-2313.

539. Bredehoft M, Schanzer W, Thevis M. Quantification of human insulin-like growth factor-1 and qualitative detection of its analogues in plasma using liquid chromatography/electrospray ionisation tandem mass spectrometry. *Rapid Commun Mass Spectrom*, 2008, 22(4), 477-485.

540. Dubois M, Becher F, Herbet A, Ezan E. Immuno-mass spectrometry assay of EPI-HNE4, a recombinant protein inhibitor of human elastase. *Rapid Commun Mass Spectrom*, 2007, 21(3), 352-358.

541. Ji QC, Rodila R, Gage EM, El-Shourbagy TA. A strategy of plasma protein quantitation by selective reaction monitoring of an intact protein. *Anal Chem*, 2003, 75(24), 7008-7014.

542. Bystrom CE, Sheng S, Clarke NJ. Narrow mass extraction of time-of-flight data for quantitative analysis of proteins: determination of insulin-like growth factor-1. *Anal Chem*, 2011, 83(23), 9005-9010.

543. Calderón-Celis F *et al*. Elemental mass spectrometry for absolute intact protein quantification without protein-specific standards: application to snake venomics. *Anal Chem*, 2016, 88(19), 9699-9706.

544. Jian W, Edom RW, Wang D, Weng N, Zhang S. Relative quantitation of glycoisoforms of intact apolipoprotein C3 in human plasma by liquid chromatography-high-resolution mass spectrometry. *Anal Chem*, 2013, 85(5), 2867-2874.

545. Peterman S *et al*. An automated, high-throughput method for targeted quantification of intact insulin and its therapeutic analogs in human serum or plasma coupling mass spectrometric immunoassay with high resolution and accurate mass detection (MSIA-HR/AM). *Proteomics*, 2014, 14(12), 1445-1456.

546. Roman GT, Murphy JP. Improving sensitivity and linear dynamic range of intact protein analysis using a robust and easy to use microfluidic device. *Analyst*, 2017, 142(7), 1073-1083.

547. Bobály B, Beck A, Fekete J, Guillarme D, Fekete S. Systematic evaluation of mobile phase additives for the LC-MS characterization of therapeutic proteins. *Talanta*, 2015, 136, 60-67.

548. Heck AJR. Native mass spectrometry: a bridge between interactomics and structural biology. *Nat Meth*, 2008, 5(11), 927-933.

549. Savaryn JP *et al*. Targeted analysis of recombinant NF kappa B (RelA/p65) by denaturing and native top down mass spectrometry. *J Proteomics*, 2016, 134, 76-84.

550. Campbell JL, Le Blanc JCY. Targeted ion parking for the quantitation of biotherapeutic proteins: concepts and preliminary data. *J Am Soc Mass Spectrom*, 2010, 21(12), 2011-2022.

551. Buscher B, Toersche J, van Holthoon F, Kleinnijenhuis A. Comparison of triple quadrupole and orbitrap mass spectrometry for quantitative bioanalysis of intact proteins. *J Res Anal*, 2015, 1(1), 3-10.

552. Macchi FD *et al*. Absolute quantitation of intact recombinant antibody product variants using mass spectrometry. *Anal Chem*, 2015, 87(20), 10475-10482.

553. Yin Y *et al*. Precise quantification of mixtures of bispecific IgG produced in single host cells by liquid chromatography-orbitrap high-resolution mass spectrometry. *mAbs*, 2016, 8(8), 1467-1476.

554. Grafmuller L *et al*. Unconjugated payload quantification and DAR characterization of antibody-drug conjugates using high-resolution MS. *Bioanalysis*, 2016, 8(16), 1663-1678.

555. Shen BQ *et al*. Conjugation site modulates the in vivo stability and therapeutic activity of antibody-drug conjugates. *Nat Biotech*, 2012, 30(2), 184-189.

556. Su D *et al*. Custom-designed affinity capture LC-MS F(ab′)2 assay for biotransformation assessment of site-specific antibody drug conjugates. *Anal Chem*, 2016, 88(23), 11340-11346.

557. Xu K *et al*. Characterization of intact antibody-drug conjugates from plasma/serum in vivo by affinity capture capillary liquid chromatography-mass spectrometry. *Anal Biochem*, 2011, 412(1), 56-66.

558. Excoffier M *et al*. A new anti-human Fc method to capture and analyze ADCs for characterization of drug distribution and the drug-to-antibody ratio in serum from pre-clinical species. *J Chromatogr B*, 2016, 1032, 149-154.

559. Hengel SM *et al*. Measurement of in vivo drug load distribution of cysteine-linked antibody-drug conjugates using microscale liquid chromatography mass spectrometry. *Anal Chem*, 2014, 86(7), 3420-3425.

560. Liu A *et al*. Quantitative bioanalysis of antibody-conjugated payload in monkey plasma using a hybrid immuno-capture LC-MS/MS approach: assay development, validation, and a case study. *J Chromatogr B*, 2015, 1002, 54-62.

561. Kaur S, Xu K, Saad OM, Dere RC, Carrasco-Triguero M. Bioanalytical assay strategies for the development of antibody-drug conjugate biotherapeutics. *Bioanalysis*, 2013, 5(2), 201-226.

562. Fontaine SD, Reid R, Robinson L, Ashley GW, Santi DV. Long-term stabilization of maleimide–thiol conjugates. *Bioconjug Chem*, 2015, 26(1), 145-152.

563. Lyon RP *et al*. Self-hydrolyzing maleimides improve the stability and pharmacological properties of antibody-drug conjugates. *Nat Biotech*, 2014, 32(10), 1059-1062.

564. Dere R *et al*. PK assays for antibody-drug conjugates: case study with ado-trastuzumab emtansine. *Bioanalysis*, 2013, 5(9), 1025-1040.

565. Hamblett KJ *et al*. Effects of drug loading on the antitumor activity of a monoclonal antibody drug conjugate. *Clin Cancer Res*, 2004, 10(20), 7063-7070.

Christian LANSHOEFT

Développement de nouvelles approches génériques de spectrométrie de masse pour la quantification de protéines thérapeutiques dans des études précliniques

Résumé

Ce travail de thèse s'est focalisé sur le développement des approches génériques de spectrométrie de masse (MS) pour la quantification des anticorps monoclonaux (mAbs) et de leurs produits dérivés dans des études précliniques.

Premièrement, le développement des protocoles de préparation d'échantillons basée sur la digestion directe à partir de sérum ou comportant une étape d'immuno-précipitation spécifique par anticorps a permis la quantification des mAbs couvrant une large gamme d'étalonnage de cinq ordres de grandeur. En outre, l'emploi de peptides provenant de la région constante du mAb a démontré la polyvalence de telles approches génériques de chromatographie liquide en tandem MS (LC-MS/MS).

Deuxièmement, les instruments de MS à haute résolution (HRMS) ont étés évalués dans le cadre de cette thèse en tant qu'alternative aux spectromètres de masse de type triple quadripôle traditionnellement utilisés pour l'analyse bottom-up quantitative. L'avantage majeur de l'intégration des analyseurs de HRMS a été associé à la possibilité de l'analyse quantitative simultanée des mAbs et leurs produits associés directement au niveau de la protéine fournissant un niveau d'informations bien au-delà de celui obtenu avec des approches bottom-up. Par conséquent, l'apport essentiel de la HRMS pour les analyses qualitative et quantitative des protéines thérapeutiques de type mAbs et produits associés a été démontré dans cette thèse.

Mots-clés: Spectrométrie de masse, quantification des anticorps, études précliniques

Résumé en anglais

This PhD thesis focused on the development of generic mass spectrometry (MS)-based workflows for monoclonal antibody (mAb)-related therapeutic protein quantification in pre-clinical species.

First, the development of bottom-up sample preparation protocols either based on direct serum digestion or immuno-capture allowed mAb-related therapeutic protein quantification over five orders of magnitude whereas the employment of peptides from the constant region of the mAb demonstrated the versatility of such generic liquid chromatography tandem MS (LC-MS/MS)-based approaches.

Second, high-resolution MS (HRMS) instruments were evaluated as an alternative to triple quadrupole mass analyzers, traditionally utilized for bottom-up mAb quantification by LC-MS/MS. The major benefit of HRMS incorporation into the workflow was associated with the possibility to quantify simultaneously mAb-related therapeutic proteins directly at an intact level, providing an information level far beyond the one obtained with bottom-up LC-MS/MS methodologies. Hence, the pivotal role of HRMS for the qualitative and quantitative analyses of mAb-related therapeutic proteins was further outlined throughout this doctoral work.

Keywords: Mass Spectrometry, antibody quantification, pre-clinical studies